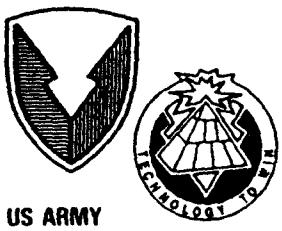

US ARMY
LABORATORY COMMAND
MATERIALS TECHNOLOGY LABORATORY

MTL TR 92-29

SMART MATERIALS FOR ARMY STRUCTURES

April 1992

SUBRAMANIAM RAMAMURTHY, MUKESH V. GANDHI, and
BRIAN S. THOMPSON

Quantum Consultants, Inc.
Hannah Technology and Research Center
East Lansing, MI 48823

FINAL REPORT

Contract DAAL04-91-C-0033

Prepared for

U.S. ARMY MATERIALS TECHNOLOGY LABORATORY
Watertown, Massachusetts 02172-0001

The findings in this report are not to be construed as an official Department of the Army position, unless so designated by other authorized documents.

Mention of any trade names or manufacturers in this report shall not be construed as advertising nor as an official indorsement or approval of such products or companies by the United States Government.

DISPOSITION INSTRUCTIONS

Destroy this report when it is no longer needed.
Do not return it to the originator.

UNCLASSIFIED

SECURITY CLASSIFICATION OF THIS PAGE (When Data Entered)

REPORT DOCUMENTATION PAGE		READ INSTRUCTIONS BEFORE COMPLETING FORM
1. REPORT NUMBER MTL TR 92-29	2. GOVT ACCESSION NO.	3. RECIPIENT'S CATALOG NUMBER
4. TITLE (and Subtitle) SMART MATERIALS FOR ARMY STRUCTURES		5. TYPE OF REPORT & PERIOD COVERED Final Report - July 1991 to February 1992
		6. PERFORMING ORG. REPORT NUMBER
7. AUTHOR(s) Subramaniam Ramamurthy, Mukesh V. Gandhi, and Brian S. Thompson		8. CONTRACT OR GRANT NUMBER(s) DAAL04-91-C-0033
9. PERFORMING ORGANIZATION NAME AND ADDRESS Quantum Consultants, Inc., Hannah Technology and Research Center East Lansing, Michigan 48823		10. PROGRAM ELEMENT, PROJECT, TASK AREA & WORK UNIT NUMBERS
11. CONTROLLING OFFICE NAME AND ADDRESS U.S. Army Materials Technology Laboratory Watertown, Massachusetts 02172-0001 ATTN: SLCMT-PR		12. REPORT DATE April 1992 13. NUMBER OF PAGES 197
14. MONITORING AGENCY NAME & ADDRESS(if different from Controlling Office)		15. SECURITY CLASS. (of this report) Unclassified 15a. DECLASSIFICATION/DOWNGRADING SCHEDULE

16. DISTRIBUTION STATEMENT (of this Report)

Approved for public release; distribution unlimited

17. DISTRIBUTION STATEMENT (of the abstract entered in Block 20, if different from Report)

18. SUPPLEMENTARY NOTES

Panagiotis Blanas (COR)

19. KEY WORDS (Continue on reverse side if necessary and identify by block number)

Composite materials
Smart materials
Electrorheological fluids
Fiber optic sensors
Vibration
Piezoelectric materials

20. ABSTRACT (Continue on reverse side if necessary and identify by block number)

(See Reverse Side)

DD FORM 1 JAN 73 1473 EDITION OF 1 NOV 65 IS OBSOLETE

UNCLASSIFIED

SECURITY CLASSIFICATION OF THIS PAGE (When Data Entered)

Block No. 20

ABSTRACT

This final report documents the results of the research and development activities focused on the development of a new generation of smart structures incorporating embedded hybrid multiple actuation systems which capitalize on the diverse strengths of both electrorheological fluids and piezoelectric materials, and employ fiber-optic sensing systems. A state-of-the-art review of smart materials and structures technologies has been undertaken, and an in-depth critique of the current generation of actuators and sensors for smart structures applications has also been presented. An in-depth review of analytical, computational and experimental investigations on controlling the vibrational characteristics of beams, plates and a variety of prototype structural systems has also been undertaken. Furthermore, variational formulations for predicting the performance characteristics of smart structures featuring hybrid embedded piezoelectric and electrorheological domains have been successfully developed. These formulations will form viable bases for the development of finite element design tools for Phase II.

A comprehensive library of smart structures and articulating mechanical systems applications has been developed and documented. The principal research findings distilled from these comprehensive set of investigations clearly indicate that it is possible to significantly tailor the vibrational and aeroelastic characteristics of structural and mechanical systems for US Army applications. Phase II will, therefore, be focused on the development of a US Army smart rotorcraft demonstrator system which will have the ability to autonomously tailor its vibrational and aeroelastic characteristics in response to variable service conditions while operating in unstructured environments. The rotorcraft system will also feature capabilities to detect and appropriately respond to routine service damage and/or battlefield damage by employing state-of-the-art optronic systems. Preliminary concepts for the design, development, fabrication, and testing of a smart US Army rotorcraft demonstrator have also been presented.

SUMMARY

- A state-of-the-art review of smart materials and structures technologies has been undertaken.

- An in-depth critique of the current generation of actuators and sensors for smart structures applications has been developed.

- Variational formulations for predicting the performance characteristics of smart structures featuring embedded piezoelectric and electrorheological domains have been successfully developed. These formulations will form viable bases for the development of finite element design tools for Phase II of the program.

- The development of a new generation of hybrid smart structures has been discussed extensively.

- The application of artificial intelligence strategies and the deployment of neural networks to smart structures applications have been enunciated.

- An in-depth review of analytical, computational and experimental investigations on controlling the vibrational characteristics of beams, plates and a variety of prototype structural systems has also been undertaken.

- Innovative ideas pertaining to the aeroelastic tailoring of airfoils in order to tailor their aerodynamic characteristics have also been presented.

- A comprehensive library of smart structures applications have been developed and documented.

- The principal research findings distilled from these comprehensive set of investigations are:

    1) It is possible to significantly tailor the vibrational characteristics of structural and mechanical systems for US Army applications.

    2) The appropriate mathematical tools for predicting the elastodynamic characteristics and developing the relevant control strategies for deploying smart structures and mechanical systems in battlefield environments have been developed. These tools will serve as viable basis for undertaking Phase II of the program.

3) Fiber-optic technologies are mature enough to be successfully employed for the cure sensing, health monitoring and damage detection of macroscopically smart composite structures.

- Phase II will be focused on the development of a US Army smart rotorcraft demonstrator system which will have the ability to autonomously tailor its vibrational and aeroelastic characteristics in response to variable service conditions while operating in unstructured environments. The rotorcraft system will also feature capabilities to detect and appropriately respond to routine service damage and/or battlefield damage by employing state-of-the-art optronic systems. Preliminary concepts for the design, development, fabrication, and testing of a smart US Army rotorcraft demonstrator have also been presented.

TABLE OF CONTENTS

SUMMARY iii

TABLE OF CONTENTS v

I INTRODUCTION 1

1.1 Background 1
1.2 Synopsis of the Report 2

II SMART MATERIALS FOR ARMY STRUCTURES 5

III ACTUATORS FOR SMART MATERIALS 17

3.1 Electrorheological Fluids 17

3.1.1 Analytical and Experimental Investigations of the Constitutive Characteristics of Electrorheological Fluids 18

3.2 Piezoelectric Materials 21

3.2.1 Characterization of Piezoelectric Materials for Smart Structures 21

3.3 Shape-Memory-Materials 22
3.4 Thermally-Active Materials 26
3.5 Magnetostrictive Materials 26
3.6 Electrostrictive Materials 27

IV SENSORS FOR SMART MATERIALS 28

4.1 Fiber-optic Sensors 29

4.1.1 Influence of Embedded Optical Fibers on the Structural Integrity of Composite Materials 30
4.1.2 Michelson Fiber-Optic Sensor 31
4.1.3 Polarimetric Fiber-Optic Sensor 31

V MATHEMATICAL FORMULATIONS FOR TWO CLASSES OF SMART STRUCTURES 41

5.1 Variational Theorem: Smart Structures Incorporating Piezoelectric Actuator Domains 41
5.2 Variational Theorem: Smart Structures Incorporating Electrorheological Fluid Domains 54

VI HYBRID SMART STRUCTURES 65

VII DAMAGE DETECTION STRATEGIES FOR SMART STRUCTURES 72

7.1 Fiber-Optic Detection of Acoustic Emission Associated with Composite Damage 72
7.2 Fundamentals of Composite Damage Detected with Embedded Optical Fibers 72
7.3 Growth of Composite Damage Detected with Embedded Optical Fibers 73
7.4 Aircraft Wing Leading Edge Fiber-Optic Damage Assessment System 74
7.5 Damage Detection Algorithms 74

VIII ARTIFICIAL INTELLIGENCE STRATEGIES FOR SMART STRUCTURES 77

IX NEURAL NETWORKS FOR SMART STRUCTURES 80

X VIBRATION CHARACTERISTICS OF SMART STRUCTURES 82

10.1 Development of a Mathematical Capability to Predict and Control the Vibration Characteristics of Smart Structures Featuring Embedded Electrorheological Fluids and Piezoelectric Materials 104

XI CONTROL STRATEGIES FOR SMART STRUCTURES 120

11.1 Controller Design 125

XII PROOF-OF-CONCEPT INVESTIGATIONS OF ARTICULATING MECHANICAL SYSTEMS 128

XIII AEROELASTIC TAILORING OF AIRFOILS 133

13.1 Steady-State Airfoil Performance 141
13.2 Suppression of Autorotation 141
13.3 Transient Effects 142

XIV SMART STRUCTURES APPLICATIONS FOR THE US ARMY 143

14.1 Aircraft 143
14.2 Helicopters 145
14.3 Defense Industry 147
14.4 Military Vehicle Applications 149
14.5 Biomedical Devices 149
14.6 Advanced Machinery Applications 150
14.7 Highways, Buildings and Bridges 150
14.8 Impact on Other Consumer Products and Sporting Goods 151
14.9 High Precision Instruments, Electronic PCB's and Packaging 151

XV RESEARCH FINDINGS AND RECOMMENDATIONS 152

15.1 Research Findings 152

15.1.1 Electrorheological Fluids 152
15.1.2 Piezoelectric Materials 152
15.1.3 Fiber-Optic Sensing Systems 153
15.1.4 Smart Structures and Articulating Mechanical Systems 154

15.2 Recommendations 155

XVI PHASE II : PRELIMINARY CONCEPTS FOR THE DESIGN DEVELOPMENT, FABRICATION, AND TESTING OF A SMART U.S. ARMY ROTORCRAFT DEMONSTRATOR 156

16.1 Introduction 157

XVII BIBLIOGRAPHY 164

XVIII DISTRIBUTION LIST 194

XIX ABSTRACT CARDS 196

I INTRODUCTION

This final report formally documents the accomplishments of a research and development program which was funded by an SBIR Phase I Award entitled "Smart Materials for Army Structures". This SBIR award was financially supported by the Department of the Army, Materials Technology Laboratory in Watertown, Massachusetts under Contract Number DAAL4-91-C-0033 for the time-period July 10, 1991 to January 9, 1992. The principal objective of the research and development program is to develop appropriate tools for synthesizing new generations of revolutionary smart composite structures by, for example, incorporating embedded hybrid multiple actuation systems which capitalize on the diverse strengths of both electro-rheological fluids and piezoelectric materials, in addition to employing fiber-optic sensing systems.

The goal of this Phase I program is to evaluate the state-of-the-art in the field of smart materials, and to explore the feasibility of exploiting these materials to develop a new generation of Army vehicles and rotorcraft systems, large-scale structures and machinery. It is anticipated that this new generation of smart Army systems will feature tremendous capabilities to reduce shock and vibration, and sense battle-field damage, while simultaneously demonstrating effective maintenance and life-prediction capabilities. The research results will also significantly benefit several national defense programs and also substantially impact the commercial sector.

1.1 BACKGROUND

Human civilization has been so profoundly influenced by materials technologies that historians have defined distinct time periods by the materials that were dominant during these eras. Thus as humankind embarked upon the continual quest for superior products and weaponry fabricated from superior materials, terms such as the *Stone Age*, the *Bronze Age*, and the *Iron Age* have entered the vocabulary. The current *Synthetic Materials Age* featuring plastics and fibrous composites is providing a viable precursor to the dawn of a new era, the *Smart Materials Age*, which will capitalize on these synthetic materials in order to exploit several eclectic emerging technologies for the synthesis of smart materials exhibiting nervous systems, brains, and muscular capabilities. The degree of sophistication displayed by this new generation of materials will depend mostly on the individual application, however, it is anticipated that these innovative material methodologies and

technologies will eventually be utilized in several diverse fields of science, such as nanotechnology, biomimetics, neural networking, artificial intelligence, materials science, and molecular electronics, for example, as depicted in Figure I.1.

This new generation of smart materials will significantly impact civilization and the defence sciences. For example, some classes of materials will be able to select and execute specific functions autonomously in response to changing environmental stimuli, others will only feature embedded sensory capabilities in order that a structural member is manufactured to comply with the quality control specifications. Self-repair, self-diagnosis, self-multiplication and self-degradation are also some of the characteristics anticipated to be a feature of the supreme classes of smart materials. It is clearly evident upon reviewing the capabilities of these smart, or intelligent, materials in an engineering context that all aspects of civilization will be influenced by these new generations of innovative materials as designers capitalize on their unique capabilities in industries as diverse as aerospace, manufacturing, automotive, sporting goods, medicine, and civil engineering.

1.2 SYNOPSIS OF THE REPORT

This report formally documents a state-of-the-art evaluation of the embryonic field of smart materials by discussing and highlighting the salient features of the principal sub-fields. Subsequently this knowledge-base provides the necessary conditions for addressing how this new generation of materials will impact upon the U. S. Army's military systems at the end of the twentieth century.

Chapter II provides an introduction to the field of smart materials. The anatomy is documented and the relationships between the sub-disciplines is enunciated. Chapters III and IV include discussions on the principal actuation technologies and the principal sensing technologies. Subsequently Chapter V presents mathematical formulations for two classes of smart structures with different types of actuation systems. The fact that there is no single type of actuators or sensor which can satisfy all of the criteria imposed upon smart structural systems, motivates the philosophy proposed in Chapter VI that hybrid systems should be established which exploit the capabilities of several types of actuators and several types of sensors. Chapter VII addresses the crucial military field of damage detection in structures which is particularly relevant to smart structures fabricated from polymeric composite materials. Chapter VIII and IX discuss the impact on smart structures of two very embryonic, but potentially very powerful technologies of artificial intelligence and neural networking. Chapter X presents experimental results for different classes of smart structure within the context of the static response, the transient vibrational response and the forced response of both structures and also mechanical systems. Chapter XI builds upon this theme by discussing the ability to control these static and dynamical responses by utilizing classical algorithms from the field of automatic control theory.

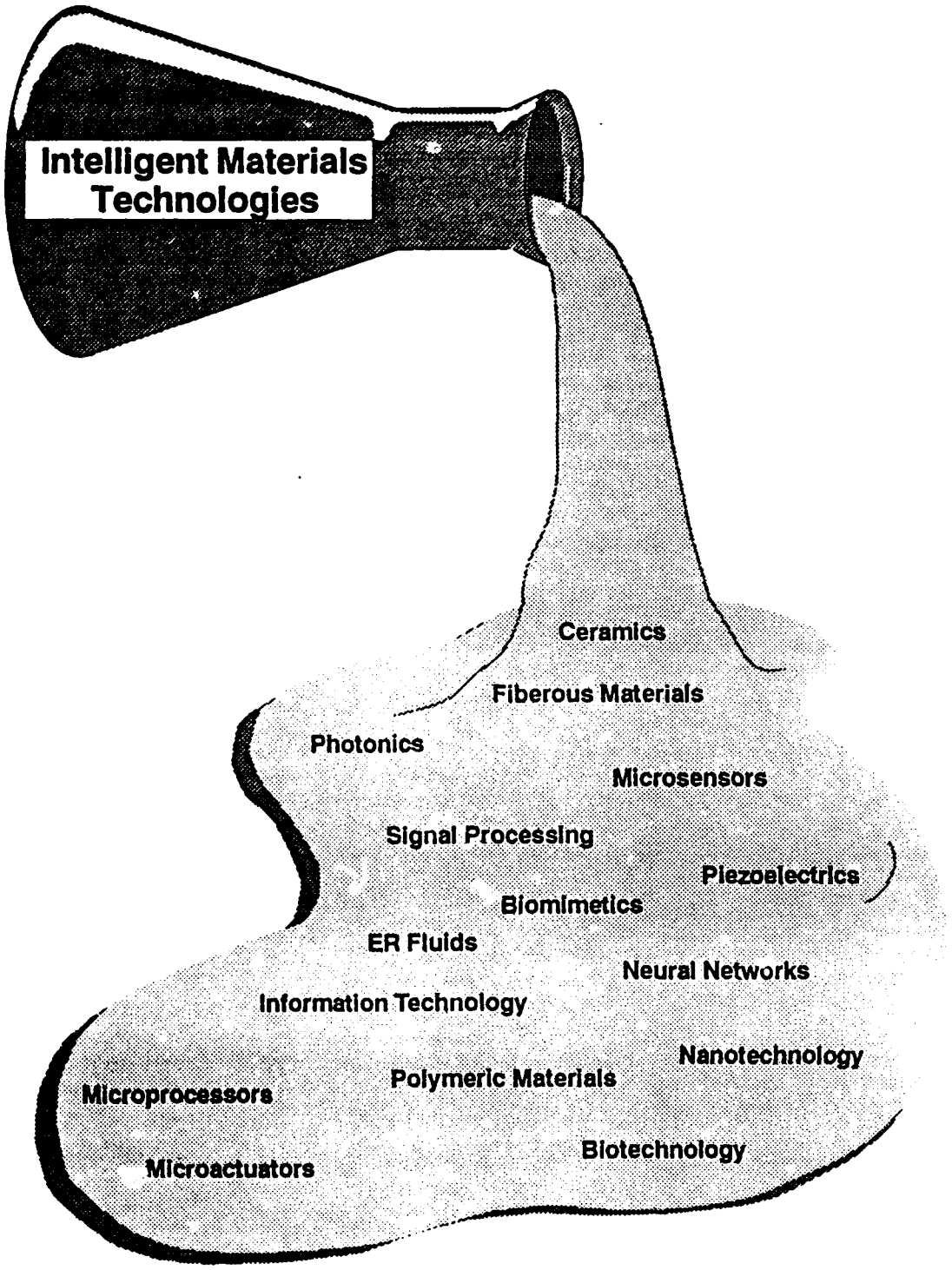

Fig. I.1 The diverse areas of intelligent materials.

The previous chapters have focused upon a diverse range of somewhat generic research issues involving smart materials and structures. The remaining chapters transition away from generic concepts to the more applied development issues of feasibility. Chapter XII presents results from a number of proof-of-concept investigations involving both smart structures and also mechanical systems featuring smart structural members. Chapter XIII continues this theme by providing an exposition on tailoring the aeroelastic characteristics of airfoils for superior performance. Chapter XIV provides an exposition on the impact of smart materials technologies on US Army systems. These systems range from aircraft and helicopters, through vehicles and machinery, to civil engineering applications. Chapter XV formally documents the research findings, the results, and the recommendations of this SBIR Phase I award. Chapter XVI presents some preliminary concepts for a Phase II award involving the design, development, fabrication and testing of a smart system demonstrator for the US Army. Chapter XVII conclude this final report by furnishing a comprehensive bibliography.

II SMART MATERIALS FOR ARMY STRUCTURES

The innovative research program on 'Smart Materials for Army Structures' is focused on a class of biomimetic intelligent materials for military systems that must operate in unstructured environments where the relevant intelligent functions include self-diagnosis, damage assessment and self-repair, in addition to high reliability. As the field of smart materials and structures matures, greater emphasis will be placed upon the creation of new synthetic materials requiring the synthesis of compounds with inherent functional properties. The intelligent characteristics associated with this activity include numerous autonomous functions such as self-degradation, self-learning, and regeneration. Other functions could include the ability to recognize and subsequently discriminate, redundancy at the most primitive level of computational, sensory, and actuation functions, hierarchical control functions and the ability to predict the future based upon sensory date prior to developing an appropriate response.

These diverse attributes of intelligence are dependent upon a more basic set of properties which include homeostasis, the tendency of an organism to maintain normal internal stability by a coordinated response of systems that autonomously compensate for environmental changes, appropriate feedback mechanisms, and also the ability to respond to an external stimulus in an appropriate time-frame and in an appropriate manner. Examples of these latter traits include materials that can evaluate current trends and circumstances in order to predict future conditions. Another classification includes materials that possess time-dependent properties which enable these materials to autonomously respond to stimuli imposed by the external environment. Thus, for example, a material which has been damaged and is undergoing a self-repair process may reduce its level of performance from a superior performance category to an adequate performance category in order to survive.

Smart materials will have the capacity to select and execute specific functions intelligently in response to changes in environment stimuli. This ability may be complemented by several other capabilities that are characteristic of intelligent systems, mentioned above. Furthermore, these features may be augmented by capabilities for anticipating future challenges and missions, and the ability to recognize and discriminate.

The current generation of smart materials incorporate at the global level material functions associated with structural, actuation and sensing properties. Thus, for example, a current generation smart structure might feature a load-bearing graphite-epoxy fibrous polymeric structural material in which are embedded piezoelectric discs for sensing purposes and

embedded shape-memory-alloy wires for actuation purposes. Research is currently being prosecuted on embedding these material functions of sensor, actuator, and structure at a much more local level. For example, carbon fibers may be coated with piezo-electric materials in order to synthesize a smart composite material which has distributed actuator and structural properties at length scales comparable to the diameter of the fiber. Similarly, electro-rheological fluids may be embedded within hollow fibers which may be employed in the structure for reinforcement or sensing, for example.

In the future, the current methodology of large scale macroscopic and mesoscopic integration of structural, sensory, and actuator materials will be replaced by the integration of the microstructural properties at the atomic scale in order to synthesize somewhat more homogeneous substances as shown in Figure II.1.

Typically these techniques will be employed at regions with dimensions that are too large to be considered to be at the inter-atomic level but too small to be considered at the solid-state level. This concept has been referred to by several scientific terms such as *micro-composite materials, mesoscopic materials, hybrid materials, structurally-controlled materials, and engineered materials*. When this technology has been perfected, the materials scientist will be able to synthesize, design and create three-dimensional atomic arrangements which will render obsolete the categorization of materials into such groups as insulators, metals, polymeric materials and biomaterials, for example.

A cursory review of the history of materials science will certainly reveal the profound influence of this scientific discipline upon the evolution of civilization during the millennia. Thus, it is therefore inevitable that the new generation of smart materials and structures technologies featuring at the most sophisticated level a network of sensors and actuators, real-time control capabilities, computational capabilities and a host structural material, as presented in Figure II.2, will not only have a tremendous impact upon the design, development, and manufacture of the next generation of products in diverse industries but also the economic climate in the international marketplace.

In the context of intelligent materials there is considerable focus on sensors and actuators which are of course discrete materials with discrete functional properties. With the development of techniques for designing and manufacturing materials at the atomic level these terms will again become somewhat obsolete. After all, the basic unit of life in biomaterials, the cells, monolithically unite all of the structural, sensory and actuator functions in a truly integrated system.

The current generation of smart materials and structures incorporate one or more of the following features:

- *Sensors* which are either embedded within a structural materials or else bonded to surface of that material. Alternatively the sensing function can be performed by a

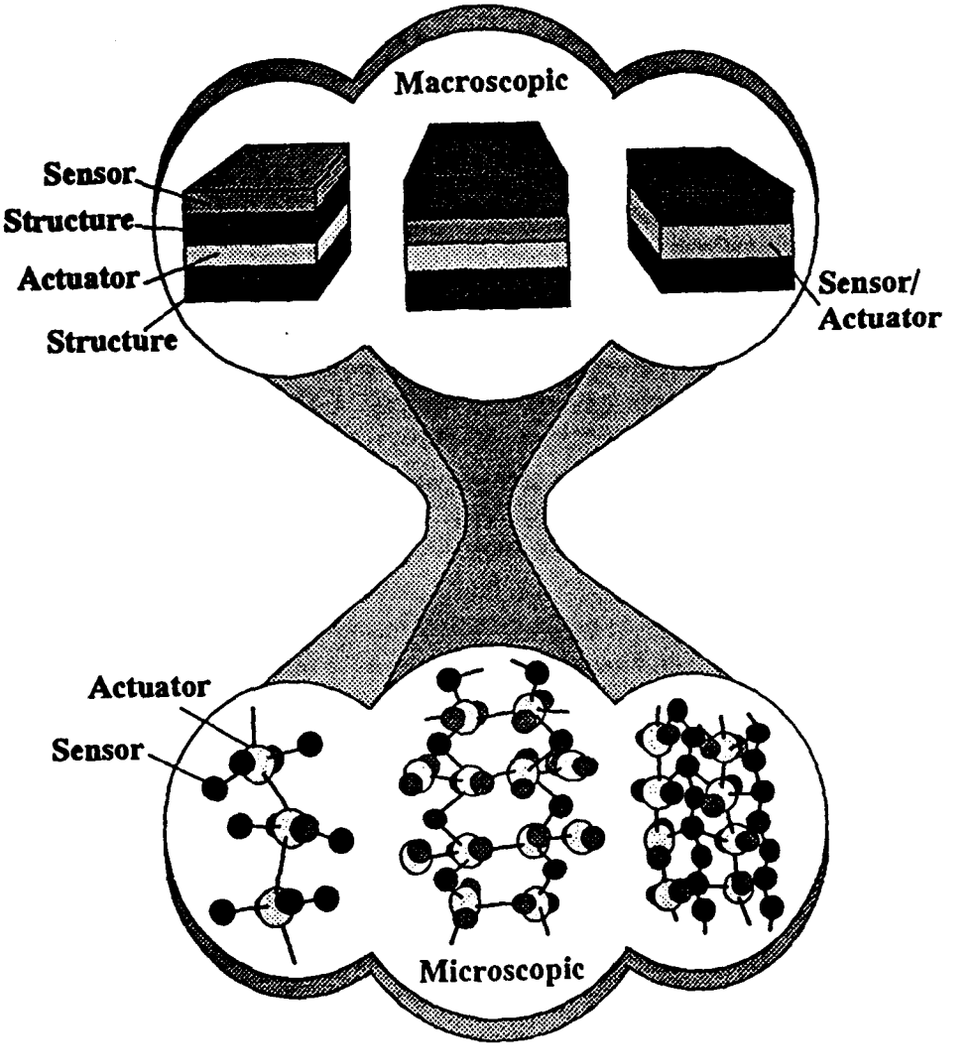

Fig. II.1 Synthesis of macroscopic and microscopic substructures.

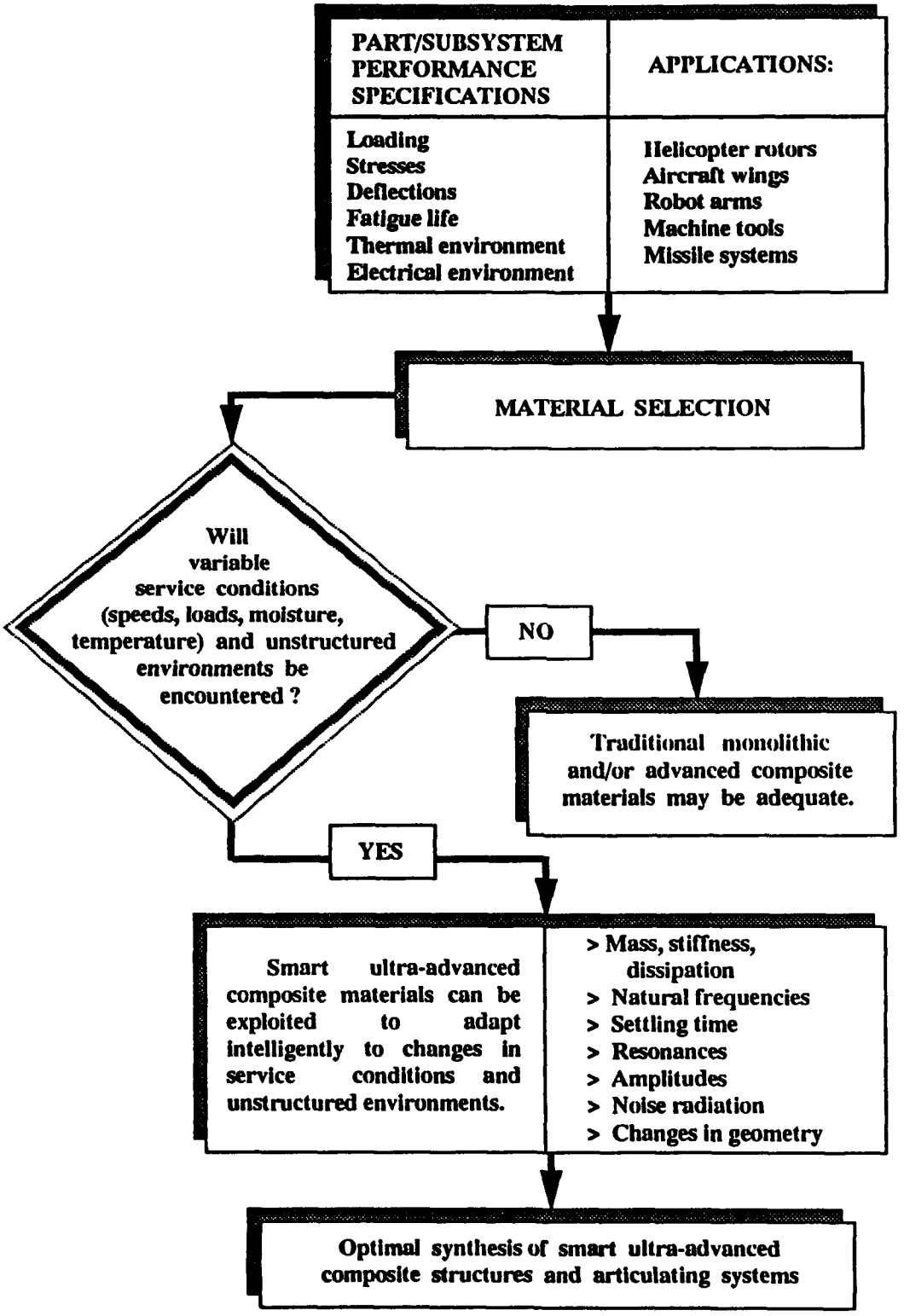

Fig. II.2 A decision-making algorithm for material selection.

functional materials which, for example, measures the intensity of the stimulus associated with stress, strain, electrical, thermal, radiative, or chemical phenomena.

- *Actuators* which are embedded within a structural material or else bonded to surface of the material. These actuators are typically excited by an external stimulus, such as electricity in order to either change their geometrical configuration or else change their stiffness and energy dissipation properties in controlled manner. Alternatively, the actuator function can be performed by a hybrid material which serves as both a structural material and also as a functional material.

- *Control capabilities* which permit the behavior of the material to respond to an external stimulus according to a prescribed functional relationship or control algorithm. These capabilities typically involve one or more microprocessors and data transmission links which are based upon the utilization of an automatic control theory.

The applications for these new generations of smart materials and structures will be diverse, but a common denominator for the development of the most sophisticated class of systems featuring actuators, sensors, and microprocessors will probably be the unstructured environment in which a system must operate. Thus the uncertainty associated with the behavior of the relevant external stimuli which govern the system response relative to prescribed design criteria will largely dictate the deployment of smart materials and structures. The decision-making algorithm is presented in Figure II.2 from which it is evident that the necessity for synthesizing materials and structures with autonomous self-adapting, self-correcting characteristics is governed by the desire to achieve optimal performance at all times under variable service conditions and while operating in unstructured environments. There are several characteristics of these smart materials and structures which have been the foci of research activities, and these include changing the mass-distribution, the stiffness, and the energy distribution characteristics for vibration-control purposes.

These smart systems are typically synthesized from a range of off-the-shelf materials and discrete devices whose properties are well known, rather than fabricate systems with new materials synthesized at the microscopic level. Thus each discrete material in the current generation of smart materials and structures satisfies a discrete functional requirement of the overall system in order to provide sensing, actuation or structural properties. The current generation of smart materials and structures generally exploit the actuation characteristics offered by electrorheological(ER) fluids, piezoelectric materials, shape-memory-alloys(SMAs), magnetostrictive materials and ferro-electric materials, for example, but there are a variety of actuator candidates, and the characteristics of some of these actuator materials are documented in Figure II.3.

Several sensing technologies can be incorporated into the current generation of smart materials and structures, and some leading candidates for undertaking strain measurement,

Actuator / Char-acteristics	Electro-Strictive Materials	Electro-Rheological Fluids	Magneto-Strictive Materials	Nitinol Shape Memory Alloy	Piezoelectric Ceramic
Cost	Moderate	Moderate	Moderate	Low	Moderate
Technical Maturity	Fair	Fair	Fair	Good	Good
Networkable	Yes	Yes	Yes	Yes	Yes
Embedability	Good	Fair	Good	Excellent	Excellent
Linearity	Fair	Fair	Good	Good	Good
Response (Hz)	1-20,000	0-12,000	1-20,000	DC-5	1-20,000
Maximum Microstrain	200	———	200	5000	200
Maximum Temperature (°C)	300	300	400	300	300

Fig. II.3 Actuator Candidates for Smart Structures

which is a common requirement for many smart materials applications, are presented in Figure II.4.

These sensors have diverse characteristics, such as thermal operating range and dynamic response, consequently each class of actuator and each class of sensor have distinct advantages and disadvantages. Nevertheless, by judicious selection, the smart-materials designer can synthesize numerous classes of actuators and sensors to satisfy a broad range of performance specifications.

Consider the smart-structural system whose desired actuation and sensing characteristics are schematically shown in Figure II.5. This illustrative example features a structure which must be controlled over a broad bandwidth from low frequencies to high frequencies. Typical requirements include vibration control at the high frequencies through the tailoring of damping, natural frequencies, and the amplitude of dynamic behavior of the structure; while at low frequencies a shape or geometrical control requirement is imposed upon the structure. Since these requirements are extremely diverse, a hybrid smart material is proposed featuring two types of actuators and two types of sensors. Thus, for example, while the high frequency actuator is able to provide actuation capabilities at high frequencies, and the low-frequency actuator is able to provide appropriate actuation capabilities at low frequencies, the domain of applicability for these actuation systems overlap in mid-frequency range whereupon either actuator, or alternatively both actuators, may be activated.

In order to satisfy the low-frequency requirements, shape-memory-alloy actuators may be employed in conjunction with embedded fiber-optic sensors to satisfy the shape control specification, while the high-frequency requirements may be satisfied by employing an array of piezoelectric actuators which are interfaced with an array of piezopolymeric sensors. A review of the actuator and sensor candidates suggests that some functional materials may be employed as either an actuator or a sensor, while others are only able to perform one of these functions, as indicated in Figure II.6. The dual versatility of these materials could be exploited in some smart materials and structures applications by employing the same material as a sensor and/or as an actuator during service. Thus, for example, a material serving as a sensor could continuously monitor the vibrational response of a structure, prior to becoming an actuator when the amplitude of vibration becomes excessive in order to alleviate this dynamical behavior.

Smart materials and structures in the foreseeable future will in the most general sense comprise an integrated set of discrete subsystems featuring structural materials, sensors, actuators, and microprocessing capabilities as indicated in Figure II.7. The design philosophy presented in Figure II.7 contains a very large multi-parameter search domain because of the very large number of decisions and design parameters associated with the properties and characteristics of sensors, structures, and actuators. Furthermore, the designer seeking a global optimal solution in the synthesis of an appropriate smart material for a particular application must also address other crucial decisions concerning computational capabilities, networking issues, and appropriate control strategies.

Sensor / Char-acteristics	Fiber Optic Interferometer	Nitinol Shape Memory Alloy	Piezoelectric Ceramic	Strain Gauge
Cost	Moderate	Low	Moderate	Low
Technical Maturity	Good	Good	Good	Good
Networkable	Yes	Yes	Yes	Yes
Embedability	Excellent	Excellent	Excellent	Good
Linearity	Good	Good	Good	Good
Response (Hz)	1-10,000	0-10,000	1-20,000	0-500,000
Sensivity (Microstrain)	0.11 per fiber	0.1-1.0	0.001-0.01	2
Maximum Microstrain	3000	5000	550	10,000
Maximum Temperature (°C)	300	300	200	300

Fig. II.4 Sensor Candidates for Strain Measurement

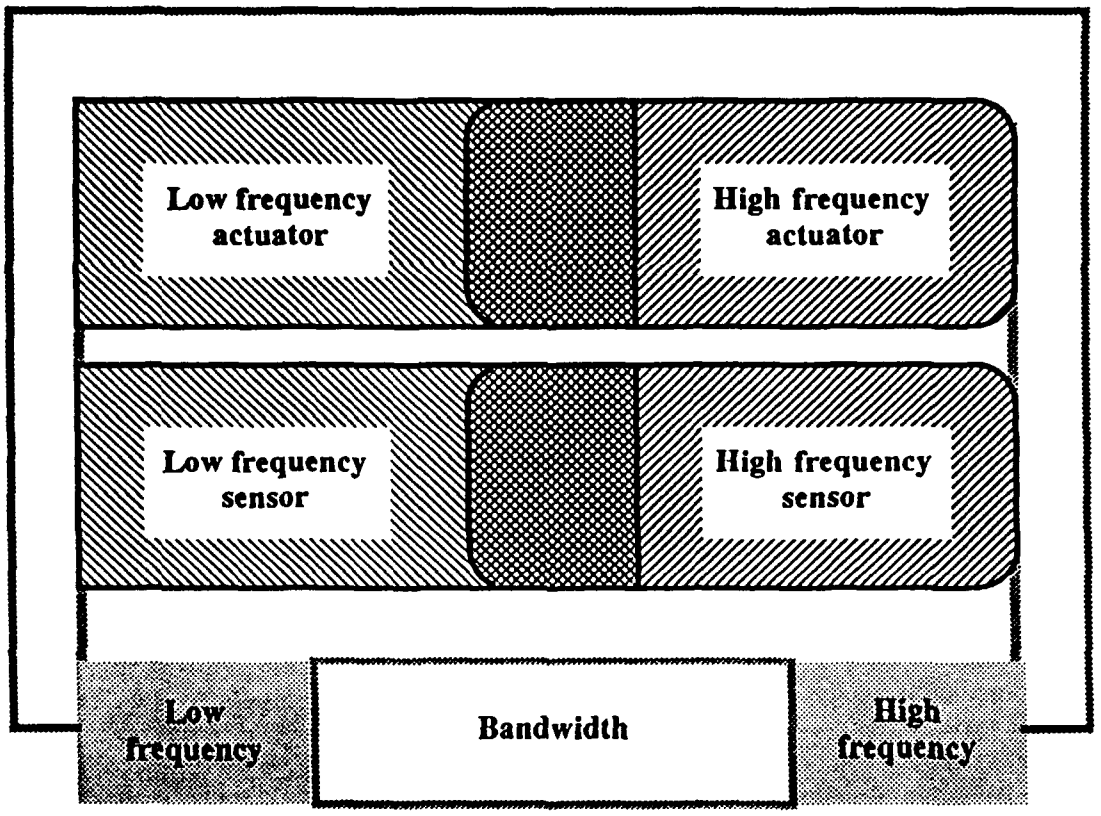

Fig. II.5 Smart structures featuring hybrid actuation and sensing capabilities.

	Actuators	Sensors
Acoustical Devices		X
Capacitive Devices		X
Electro-rheological Fluids	X	
Electrostrictive Materials	X	
Fiber Optics Devices		X
Magnetostrictive Materials	X	X
Piezoelectric Materials	X	X
Shape Memory Alloys	X	X
Strain Gauges		X
X-ray Devices		X

Fig. II.6 Actuator and sensor capabilities for smart materials and structures applications

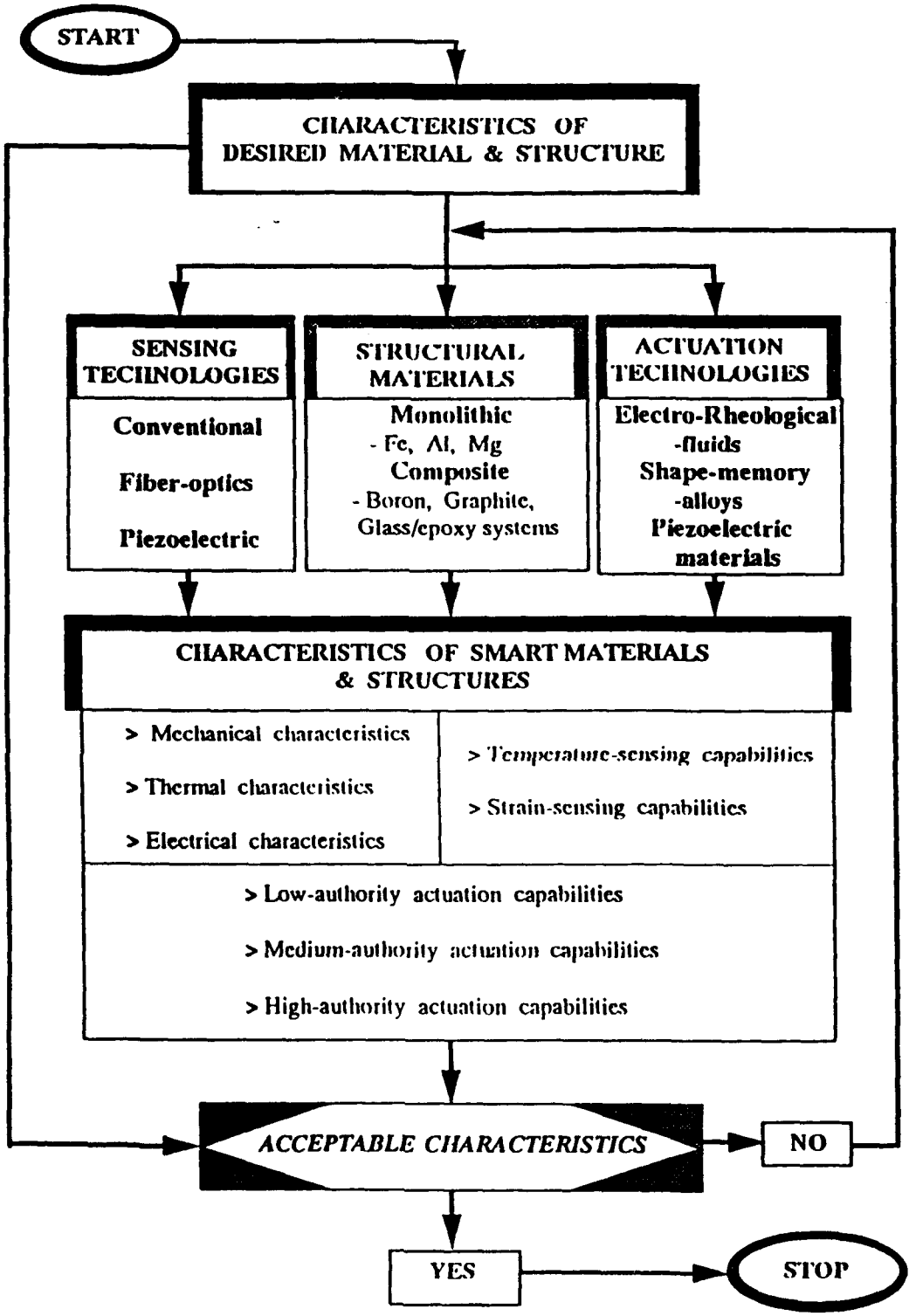

Fig. II.7 An algorithm for synthesizing a smart material featuring structural materials, actuation technologies, and sensing technologies.

The establishment of a set of viable analytical tools for predicting the behavior of smart material and structures featuring embedded actuator materials, the characteristics of structural materials, and also the characteristics of the interface regions and the characteristics of the piezo-electric actuators is a prerequisite for hybrid optimal control strategies for smart mechanical and structural systems featuring multi-functional smart actuation and sensing capabilities. Since these materials will typically be employed in engineering practice to satisfy various performance specifications, the tailoring of the structural characteristics by employing hybrid optimal control strategies is a crucial step in the development of the knowledge-base in this area.

III ACTUATORS FOR SMART MATERIALS

Actuator materials are one of the principal ingredients of several important classes of smart materials and structures. These actuator materials are typically employed to dynamically tune the global mechanical properties of the structure, or else to dynamically tailor the shape of the structure in an orchestrated manner. The subsequent pages document synoptic qualitative descriptions of the current generation of candidate actuator materials.

3.1 ELECTRORHEOLOGICAL FLUIDS

Electrorheological (ER) fluids are typically suspensions of micron-sized hydrophilic particles suspended in suitable hydrophobic carrier liquids, that undergo significant instantaneous reversible changes in their mechanical properties, such as their mass distribution, and energy-dissipation characteristics, when subjected to electric fields. When these fluids are embedded in voids in structural materials, the imposition of an appropriate electrical field on each voidal domain permits the mechanical properties of the embedded fluid to be actively controlled, which enables the global properties of the structure containing the ER fluid domains to be controlled. The voltages required to activate the phase-change in ER fluids are typically in the order of 1 to 4 kV/mm of fluid thickness, but since current densities are in the order of 10 mA/cm^2, the total power required to change the fluid properties is quite low. Furthermore, the response-time of ER fluids to an electrical stimulus is typically less than one millisecond.

However, other significant activities in the field of ER fluids can be decomposed into two parts; namely the development of new classes of ER fluids, and the engineering and development of discrete devices such as valves, engine mounts, and finite-degree-of-freedom vibration isolation systems. All ER fluids comprise solid particulates dispersed within an insulating liquid phase. When an electric field is applied the rheological changes are precipitated by the rearrangement of the solid dispersed phase within the liquid medium. Since the liquid must be electrically non-conducting, organic oils are often used. However, it must be emphasized that many ER-active compositions are not well characterized chemically and a variety of different formulations have been shown to exhibit ER behavior. Furthermore, it is apparent that all compositions involve dispersed polarizable or conducting particles within the insulating oil. If the dispersed phase is not, or is only weakly, polarizable or conducting then the addition of various reagents can cause or enhance

ER-activity. These additives become absorbed on the surface of the dispersed solid. Although the presence of some water was once considered essential for ER-activity, some anhydrous systems have been developed. Two examples are aluminosilicates dispersed in a hydrocarbon oil and semiconducting polymeric quinones dispersed in hydrocarbon or silicone oil. Other examples of solids used as the particulate phase include metal oxides, clays and other aluminosilicates, silica, carbon, polyaccharides, and several polymeric organics. Typically, particulates vary in size between 40nm and 50,000nm and the polymers employed have typically been characterized by molecular weights above 1,000,000. The liquid phase is most often a hydrocarbon or silicone oil or one of the halogenated or polyhalogenated derivatives. It is clearly evident, therefore, that the rheological characteristics of ER fluids are derivatives of the physical chemistry of the fluid suspension.

Smart structures exploit the dynamically-tunable characteristics of electrorheological fluids by embedding these fluids in host structural materials, which are fabricated in either conventional materials or advanced composite materials. By controlling the voltages imposed on the fluid domains in the structure, the properties of the fluids are controlled and hence the properties of the smart structure are also controlled.

In order to determine the feasibility of exploiting this class of smart structures for U.S. Army applications analytical and experimental investigations of the constitutive characteristics of electrorheological fluids were undertaken prior to the development of a mathematical capability for predicting the constitutive characteristics of smart structures featuring embedded electrorheological fluids.

3.1.1 Analytical and Experimental Investigations of the Constitutive Characteristics of Electrorheological Fluids

The steady-state rheological characteristics of a variety of electrorheological fluids subjected to static electrical fields of different intensities were determined experimentally and subsequently evaluated. The investigation involved a coherent combination of analytical and experimental work. One of the experimental results is presented in the figure below, Figure 3.1, from which it is evident that the constitutive behavior is of a non-Newtonian form. The reported results indicate that this class of electrorheological fluids has a constitutive equation dependent upon the rate of strain and also the yield stress, which are both dependent upon the magnitude of the applied voltage. This observation permits a constitutive equation of the following form to be proposed,

$$\tau = \alpha E^{x_o} \qquad \text{for } \gamma \le \gamma_c$$

and

$$\tau = \alpha E^{x_o} + \eta \gamma(E) \qquad \text{for } \gamma > \gamma_c$$

where α, η and x_0 are material constants, γ_c is a critical strain rate, and E is the electrical field intensity.

The mathematical models for describing the electrical-field dependent non-Newtonian rheological characteristics of ER fluids, and also the magnetic field dependent characteristics of magnetostrictive materials discussed in section 3.5, will be, typically, similar to those exhibited by Bingham bodies and BKZ fluids, for example. These mathematical models will account for the electrical field-dependence of the rheological characteristics of ER fluids, and also the dependence of the constitutive characteristics of magnetostrictive material upon the imposed magnetic field.

A typical representation for a BKZ-type constitutive model for describing the properties of field-dependent ER fluids is anticipated to take the following qualitative form:

$$\sigma[E(x,t)] = -pI + q\,[\int_{-\infty}^{t}\{U_i C_t^{-1}(\zeta) - U_2 C_t(\zeta)\}d\zeta]$$

where σ are the components of the stress tensor for the ER fluid, p is an indeterminate scalar, q is a function, and U_i and C_t are defined as follows:

$$U_i = \frac{dU}{dI_i}\,,\ i = 1,2$$

where U(E(x,t)), is the electrical field-dependent strain energy potential of the ER fluid, and I_1 and I_2 are the first and second invariants of the right relative Cauchy-Green deformation tensor

$$C_t(\zeta) = F_t^T(\zeta)F_t(\zeta)$$

where F_t are the components of the relative deformation gradient tensor. Clearly the electrical field E(x,t) imposed upon the ER fluid would be a function of the geometry of the electrodes, their distribution in space and the potential difference, and can be determined from the classical theory of electro-magnetism. Similar mathematical developments are also proposed for magnetostrictive actuator materials.

The research results distilled from this experimental and analytical investigation are summarized succinctly below:

1. Electrorheological fluids are characterized by non-Newtonian constitutive behavior.

2. Electrorheological fluids sometimes exhibit shear thinning.

3. There is a large change in the non-Newtonian viscosity in the presence of an electric field for a prescribed shear rate.

4. As the concentration of the particulate phase of an electrorheological fluid decreases, the electrorheological effect also decreases.

5. The yield stress of electrorheological fluids increases monotonically with the magnitude of the electrical field intensity.

6. A first-order model for electrorheological fluids has been proposed.

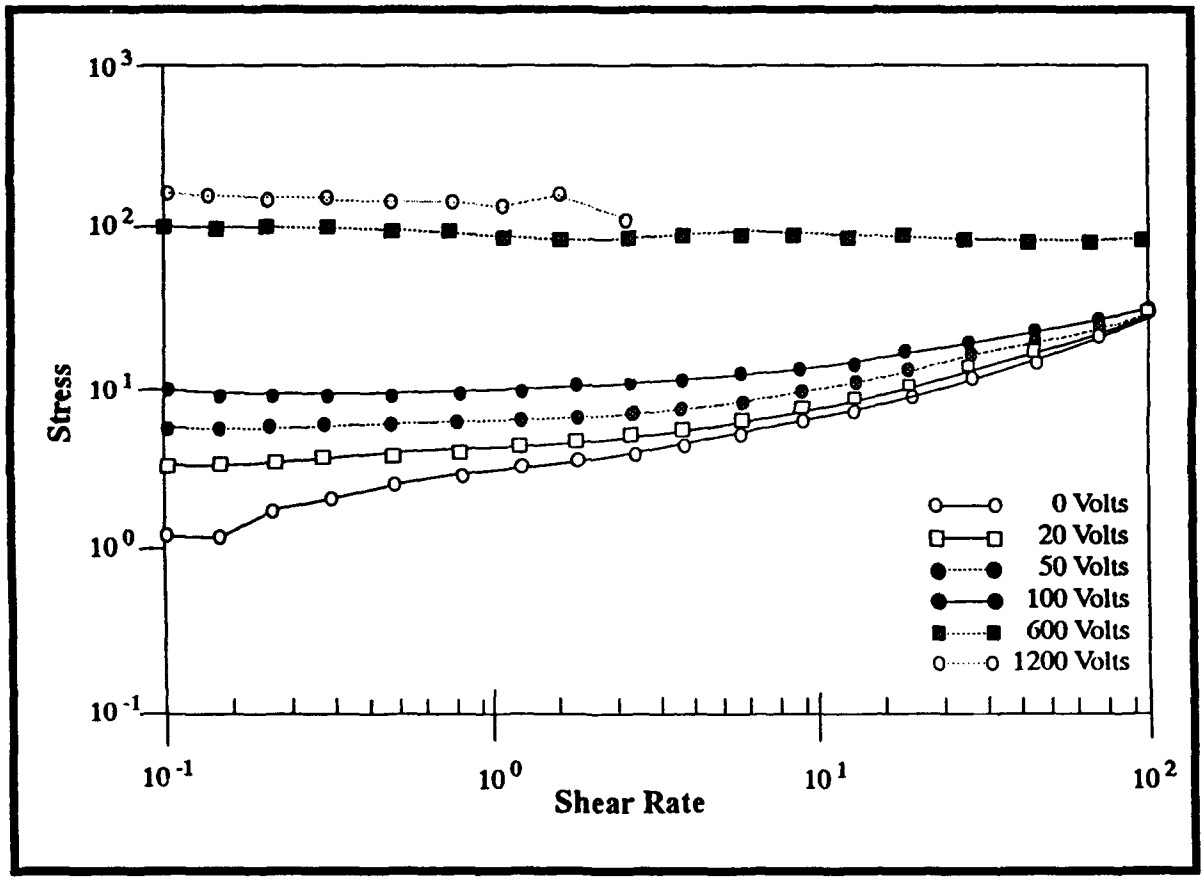

Fig. III.1 Experimentally determined stress versus shear-rate characteristics measured at different voltages for a hydrous electro-rheological fluid comprising of 45 percent corn starch and 55 percent silicone oil.

3.2 PIEZOELECTRIC MATERIALS

Piezoelectric materials are solids which generate a change in their latent electrical potential difference in response to a mechanical deformation, or alternatively they develop mechanical deformation when subjected to an electrical field. These properties enable this class of functional materials to be employed as either actuators or sensors in the development of smart structures.

Piezoelectric ceramic materials are typically employed as actuators while polymeric piezoelectric materials are typically employed as sensors for tactile sensing, temperature sensing, and strain sensing. Typically piezoceramics are the lead zirconate titanates (PZTs) while typical piezopolymers are the polyvinylidene fluorides (PVDF).

3.2.1 Characterization of Piezoelectric Materials for Smart Structures

The constitutive characteristics of a variety of piezoelectric materials subjected to a variety of electrical fields were evaluated, and a linear constitutive equation was proposed for predicting the behavior of these functional materials. This equation relating the mechanical and electrical behavior of the material naturally incorporates a term representing the intensity of the electrical field. This equation is given by:

$$\tau_{ij} = C_{ijkl}\,\gamma_{kl} - d_{kij}\,E_k$$

$$D_i = d_{ijk}\,\gamma_{jk} + \epsilon_{ij}\,E_j$$

where τ_{ij} are the components of stress, C_{ijkl} are the components of the tensor of elastic constants, γ_{kl} are the components of the Lagrangian strain tensor, d_{kij} is the piezoelectric strain constant, E_k is the electric field strength, D_i is the electric displacement, and ϵ_{ij} is the dielectric permittivity of the piezoelectric material.

The research results distilled from this experimental and analytical investigation are summarized succinctly below:

1. The constitutive characteristics of commercially available piezoelectric ceramics and polymers are adequately modeled by linear constitutive relations.

2. Distinct classes of piezoelectric ceramic (PZTs) materials are more appropriate for actuators while piezoelectric polymeric materials (PVDF) are more appropriate for sensors in smart material applications.

3. Piezoelectric actuators have capabilities superior to the electrorheological fluids for imposing higher magnitude bending moments and other classes of loading characteristics on smart structures.

4. The response characteristics of piezoelectric actuators are infinitely variable through the selection of appropriate excitation voltages which permit amplitudes and frequencies of smart structures to be controlled in real-time. Non-harmonic and harmonic excitation voltages can also be employed to tailor the response characteristics of this class of smart structures.

3.3 Shape-Memory-Materials

Shape-memory-alloys are metals which, when plastically deformed at one temperature, will completely recover their original undeformed state upon raising their temperature above an alloy-specific transformation temperature. A characteristics of these alloys is that the crystal structure undergoes a phase-transformation into, and out of, a martensitic-phase when subjected to either prescribed mechanical loads or temperature. During the shape-recovery process, these alloys can be engineered to develop prescribed forces or displacements. The transformation temperature of these materials can be selectively-tuned over a broad temperature range to suit each application, and plastic strains as high as six percent can be completely recovered by subjecting them to heat. Shape-memory-metals have been employed as both actuators and sensors in smart materials and structures applications. Typical materials which exhibit the shape-memory effect include the copper alloy systems of Cu-Zn, Cu-Zn-Al, Cu-Zn-Ga, Cu-Zn-Sn, Cu-Zn-Si, Cu-Zn-Ni, Cu-Au-Zn, Cu-Sn, and the alloys of Au-Cd, Ni-Al, and Fe-Pt. Nitinol, a nickel-titanium alloy, is the most common of the SMAs or transformation metals.

Nickel-titanium alloys (Nitinol, NiTi) acquire their name from Ni (Nickel)-Ti(Titanium)-NOL (Naval Ordnance Laboratory). NiTi alloys, featuring a near-equiatomic composition, can be plastically deformed in their low temperature martensitic phase and then be restored to the original shape by heating them above the characteristic transition temperature. Typically plastic strains as high as 6% to 8% can be completely recovered by heating the Nitinol in order to transform it to the austenitic phase, and constraining it from regaining the memory shape can result in stresses of 100 000 psi, for example. The yield strength of martensitic Nitinol is approximately 12 000 psi.

There is a substantial database on the thermal, electrical, magnetic, and mechanical characteristics of Nitinol, however, the influence of residual stresses and high temperatures

associated with the fabrication and processing of Nitinol-based composites, for example, is not well understood. Furthermore, the extent, duration and repeatability of the shape -memory effect as well as the dynamic actuator and sensing characteristics of Nitinol are also not understood. Shape-memory effects in alloys and metals are characterized by deformation mechanisms which are associated with shape changes due to martensitic transformations. Therefore a thorough understanding of martensitic transformations is an important prerequisite to the understanding of the shape-memory effect in alloys and metals.

The transformation of steel in a high-temperature austenitic phase to a low temperature martensitic phase was first observed by the German metallurgist Adolf Martens. The extremely fine structure observed in the martensitic phase results from a lattice transformation without atomic diffusion. The face-centered cubic austenite transforms into body-centered cubic lattices or body-centered tetragonal lattices. These diffusion-free martensitic transformations manifest themselves in a variety of alloys and metals.

Martensitic transformations fundamentally involve a lattice transformation featuring shear deformation and a coordinated atomic movement, which maintains a one-to-one lattice correspondence between the lattice points in the parent phase and the transformed phase. The martensitic phase is a substitutional or interstitial solid solution. The transformation is diffusion-free which yields the same concentration of solute atoms dissolved in the martensitic phase as in the parent phase. Martensitic transformations are typically characterized by well-defined shape changes or surface reliefs.

Mathematical models need to be developed to predict the stiffness and dissipative thermo-mechanical behavior of shape-memory alloys. These models must feature the capability to predict the behavior of shape-memory materials, where changes in loads and temperature significantly alter martensitic and austenitic phases. A basis for such an activity is provided by an energy density function based on a model for a constrained elastic crystal which is governed by the expression

$$W(C,\theta) = b(\theta)J + c(\theta)K + d(\theta)J^2$$

where C is the right Cauchy-Green tensor, θ is the temperature, $b(\theta)$, $c(\theta)$ and $d(\theta)$ are the constitutive coefficients which must be based on experimental data, and J and K are deformation measures. This energy density function will have the ability to predict that the austenitic phase will be stable when the temperature is greater than the critical temperature, and martensitic phase will be stable when the temperature is less than the critical temperature, and the two phases will be able to co-exist in the neighborhood of the critical temperature.

The entire subject of martensitic phase transformations (MPTs) is one of considerable technological and scientific interest. In recent years, theoretical understanding of the basic physical properties of these systems has developed along two parallel tracks; one by applying

finite element techniques to solve continuum elastic models for cubic to tetragonal phase transitions and the other by considering simple atomistic model Hamiltonians which incorporate the essential ingredients of a martensitic system and solving them using several theoretical tools. There have also been some attempts to construct phenomenological Hamiltonians which incorporate the basic underlying physical characteristics of MPTs and solve these models using Monte Carlo and molecular dynamics techniques. In fact it is now believed that the MPTs are basically *first order displacive structural phase transitions*. Such phase transitions have been of great interest to physicists in the area of structural phase transitions in solids. The *Quantum* research team has worked extensively in the area of structural phase transitions in molecular solids,some of which show first order cubic to orthorhombic phase transitions with large pre-transitional elastic anomalies in the so-called plastic phase, and order-disorder transitions in intercalation systems.

The fundamental physical but technologically important questions which are addressed in this proposal include (i) the dynamical response of a martensitic alloy both above and below MPT temperature, (ii) the effect of finite geometry on the thermodynamics and dynamics in thin films of martensitic alloys, (iii) the effect of impurities on the phase transition and hence on the pseudo-elastic and thermo-elastic response both in the bulk and film systems. These issues are extremely important for the future application of shape-memory alloys in small-scale integrated smart structures. It is now possible to quantitatively predict some of the important characteristics of shape-memory alloys starting from an *atomistic microscopic theory*. This can be achieved by calculating the fundamental Landau parameters appearing in a continuum (long length-scale description of MPT) model in terms of atomic correlation functions, an approach which was highly successful in understanding the MPT's and elastic response in molecular solids. This is essential if a fundamental understanding of shape-memory alloys is to be developed in the context of probing the effects of finite size and impurities.

A variety of shape-memory-plastics are currently being developed. Norsorex, for example, is the trade name of the polynorbornene polymer manufactured by Norsler in France. Norsorex has excellent shape recovery properties at shape memory temperatures of over 35° C. However, Norsorex has several characteristics which have impeded its commercialization in engineering applications. Norsorex is characterized by a super high molecular weight of over 3 000 000. Furthermore, the shape recovery temperature of Norsorex cannot be changed easily. For commercial applications shape-memory-plastics must be easily processible and feature a wide temperature range in which the shape recovery temperature can be changed. Other considerations, such as strength, durability, environmental resistance, etc. are also significant.

Zeon Shable is a relatively new shape-memory-plastic which addresses several requirements for commercialization. Zeon Shable yields itself to easy processing by injection molding, extrusion, and blow molding, for example. The plastic is available in five different grades which feature five different shape recovery temperatures ranging from 40° C to 80° C, which

are 10° C apart for each grade of the material. Zeon Shable features very good strength properties, and good environmental and chemical resistance.

In the injection molding process, the plastic is initially heated, melted and injected into a mold, which is maintained at a specified temperature. Upon cooling, a hard molded plastic is obtained as a result of the primary molding operation. When the molded plastic is heated up to the shape recovery temperature the product manifests itself in a soft rubbery state. In this soft state, the product can be easily subjected to large deformations by the application of appropriate force fields. The deformed product in the rubbery state can be cooled in order to retain the same geometric configuration even in the absence of the applied force field. This process is usually referred to as secondary molding. When it is heated again to the shape recovery temperature, the secondary molded product becomes rubbery and recovers the geometric configuration attained by primary molding. This is accomplished by the release of the residual strain energy. When the product in this state is cooled to room temperature, the recovered product solidifies while maintaining its geometric shape, thereby returning to its shape after the primary molding.

It is clearly obvious from this discussion that shape-memory-plastics can memorize the shape corresponding to the completion of the primary molding process. By employing an external stimulus, such as heat, the primary molded product can be easily deformed by secondary molding and its new shape fixed by cooling. By employing external stimuli, it is possible to reversibly transform the product from its primary molded shape to its secondary molded shape, and vice versa.

The shape-memory property involves several processes which enable the material to:

1. Memorize the shape of the primary structure.
2. Fix the shape of the secondary molding.

The processes involved in memorizing the shape of the primary structure include:

a) entanglement of the polymer chains,
b) cross-linking,
c) crystallization,
d) formation of domain structure.

The shape of the secondary molded product is fixed by:

a) heating the material over the glass transition temperature and cooling,
b) melting and re-crystallization of the crystalline phase,
c) melting and reformation of the domain structure.

The secondary molded shape is fixed mainly by physical structural changes, whereas the primary molded shape is chemically and physically memorized.

Shape-memory-plastics (SMP) have several distinct advantages as compared with SMAs. These advantages include the characteristic of being lightweight, freedom from rust, the ability to impact color to products fabricated from SMP's, and the ability to print on these products. Furthermore, SMP products can undergo substantially larger deformations, they are easier to mold, process, and impart memory in addition to lower price.

3.4 Thermally-Active Materials

Distributed thermal actuators exploiting the Peltier effect, which characterizes certain classes of semiconductor materials, have been employed to generate thermal gradients for controlling the dynamic response of flexible structures. These semiconductors act as heat pumps when a voltage is applied to them and this excitation is responsible for the development of a temperature gradient and hence deformation of the material. There are a number of environmentally-responsive polymers that are commercially-available, and some of the materials generate a mechanical deformation in response to a thermal excitation.

3.5 Magnetostrictive Materials

Magnetostrictive materials are solids which typically develop large mechanical deformations when subjected to an external magnetic field. This magnetostrictive phenomenon is attributed to the rotations of small magnetic domains which are randomly-orientated when the material is not exposed to a magnetic field. The orienting of these small domains by the imposition of the magnetic field results in the development of a strain field. As the intensity of the magnetic field is increased, more and more magnetic domains orientate themselves so that their principal axes of anisotropy are collinear with the magnetic field in each region and finally saturation is achieved. Terbium-iron alloys are typical magnetostricitive materials.

"Terfenol-D" is a commercially available magnetostrictive material marketed by Edge Technologies Inc. which incorporates the rare-earth element dysprosium. This material offers strains up to 0.002, which is an order of magnitude superior to the current generation of piezoceramic materials. However, this class of mechano-magnetic materials do suffer from some disadvantages which must be carefully considered when synthesizing smart structural materials. These include the technological challenges of delivering a controlled magnetic field to a magnetostrictive actuator embedded within a host structural material; furthermore, the material generates a much greater response when it is subjected to compressive loads; and the power requirements for this class of actuators are greater then those for piezoelectric materials.

3.6 Electrostrictive Materials

Electrostrictive materials are analogous to magnetostrictive materials since these materials develop mechanical deformations when they are subjected to an external electrical field. The electrostrictive phenomenon is attributed to the rotation of small electrical domains in the material when an external electrical field is imposed upon them. In the absence of this field, the domains are randomly orientated. The alignment of these electrical domains parallel to the electrical field results in the development of a deformation field in the electrostrictive material.

The ceramic compound lead-magnesium-niobate, PMN, exhibits a thermo-electrostrictive effect and the quadratic electrostrictive phenomenon is dependent upon the ambient temperature. This type of material, while exhibiting less hysteresis losses than piezoceramics, features a nonlinear constitutive relationship requiring some biasing in practice to achieve a normally linear relationship over a limited range of excitation.

IV SENSORS FOR SMART MATERIALS

The diverse range of off-the-shelf sensors available in the market place must be evaluated within the context of smart material applications. The principal criteria for evaluating these sensors are documented below, and these criteria are applied to the list of sensors presented in the tabulated synopsis of the current generation of sensors documented in Section II

- Accuracy: the minimum sensitivity required for the actuator/sensor
- Dynamic Range: the desired maximum range of the actuator authority or the sensed measurand
- Frequency Response: the bandwidth of the actuator or sensor
- Linearity: the expected non-linear behavior of the actuator or sensor throughout the required bandwidth and dynamic range. This non-linearity is typically evidenced in hysteresis, saturation, etc.
- Noise Rejection: the sensitivity of the actuator or sensor to interference from electronic noise and EMI signals
- Embeddability: the ability of the actuator or sensor to withstand the processing environment of the composite material
- Health Monitoring Capability: the ability of sensors to measure parameters required to detect structural damage
- Networkability: the ability of an actuator or sensor to be integrated into a distributed control system or health monitoring system
- Cost: the cost of the actuator or sensor and the associated ancillary opto-electronic equipment, for example

- Survivability: the ability of the actuator or sensor to function in a diverse range of environments
- Technical maturity: the technical ability to commercially deploy the actuator or sensor with minimum development cost and/or time

In addition to the conventional structure/sensor architectures, there is an increasing need for "smart materials" in US Army structures as well as in airframe applications. Such materials would contain sensors and control elements as integral parts of their structures to provide detection, and perhaps prevention or correction, of imminent failure or misalignment. One such possible approach is the *in situ* formation of piezoelectric thin films on the surface of existing light-weight structural materials such as aluminum alloys. Piezoelectric material is a natural electromechanical transducer. When an electric field is applied to such a material, a strain is produced in it. Conversely, if the material is stressed mechanically, an electric field is generated.

Polymeric materials with piezoelectric properties such as polyvinylidene fluoride (PVDF) that can be deposited as thin films are potential candidates for such materials. However, polymer materials typically have limited lifetimes in the radiation and vacuum environment of space for example. In contrast, ceramic piezoelectric materials have much greater stability. However, they are less easily formed into thin films, particularly on existing large structures. Recently, significant advances have been made in using organic precursors such as alkoxides to produce a variety of piezoelectric ceramics such as barium titanate.

Fiber-optics can also be employed by embedding a fault tolerant fiber-optic network into the structure and using fault tolerant networking techniques to detect and isolate structural damage. In such a fault tolerant to assess the state of smart structures networking environment, there are several available routing algorithms to detect and isolate the malfunctioning nodes and paths for a given network topology. In addition, it is possible to measure physical variables of interest in structural applications using optic fibers. For instance, measurements of both static and dynamic strain have been reported using optical fibers embedded in composite materials.

Other potential sensors for damage detection in smart structures include computer vision. This involves the development of a TV-based vision system for the detection of structural damage using, for instance, edge detection algorithms.

4.1 FIBER-OPTIC SENSORS

The health management of smart structures is a philosophy involving the utilization of sensors embedded in a structure to monitor the state of relevant governing parameters.

These sensors must typically be very small in order not to adversely affect the structural integrity of the structure. Fiber-optic sensors satisfy this criteria. Research involving Kevlar-epoxy fibrous materials has demonstrated that the embedded optical fibers do not reduce the tensile or compressive strength of the host structural material, nor the interlamina fracture toughness (see claus et.al and Measures et.al, Bibliography: B5). These results need to be generalized, and further work undertaken to study the long-term effects on the fatigue life of these structures. Damage detection in this class of smart structural material can also be determined using a simple technique whereby optical fibers are fractured with the attendant disruption in their transmitted light. Furthermore, fiber-optic strain rosettes, involving Michelson interferometry, permit the principal strains in a local domain to be calculated for smart structural applications.

In terms of smart structures, strain, deformation and vibration measurements are often the most important. Fiber-optic strain sensors offer several distinct advantages over their electrical counter parts, such as resistive strain gauges for this class of applications. These advantages include:

- They can be embedded within composite materials
- They do not generate electrical interference
- They require no electrical isolation
- They do not heat the structure
- They can provide fine spatial resolution
- They can make integrated strain measurements over larger distances

Moreover, since optical fibers are dielectric in nature they are compatible with composites and when embedded avoid creating electrical pathways within the structure. This will become more important as composites are used increasingly in aircraft that fly in the vicinity of thunderstorms.

4.1.1 Influence of Embedded Optical Fibers on the Structural Integrity of Composite Materials

A fundamental issue that must be addressed if optical fibers are to be embedded within composite materials as a routine industrial practice concerns their potential to compromise the strength and damage vulnerability of the material. It has been previously shown that neither the tensile nor compressive strength of Kevlar/epoxy appears to be reduced by the presence of the embedded optical fibers. Initial investigations of the influence of the embedded optical fibers upon the interlamina fracture toughness have been undertaken and the results of this work indicate that if anything the critical energy release rate is increased by the presence of the embedded optical fibers. This experimental evidence suggests that the presence of optical fibers has no adverse effect upon the structural integrity of fibrous polymeric composite materials.

Indeed, they marginally improve the damage resistance of the material. These preliminary results have been for Kevlar/epoxy materials and need to be generalized. A further study of the long-term effects of embedded optical fibers on the fatigue life of composite materials also needs to be undertaken before total confidence in these results can be obtained.

4.1.2 Michelson Fiber-Optic Sensor

The differential Michelson interferometric fiber-optic sensor uses two closely spaced single mode optical fibers, and one of these optical fiber serves as a reference. The sensing region is localized between the mirrored ends of the two optical fibers, and interference associated with changes in the strain or temperature of the structure modulates the intensity of light incident on the detector. The coupler mixes the light from the two optical fibers. Some of the advantages offered by this sensor in terms of its use as a strain gauge are: high sensitivity, well-defined directionality, and excellent localization. This enables it to be especially effective as a pointer sensor. A number of fiber-optic Michelson strain gauges have been built and a series of experiments designed to characterize their performance capabilities have been undertaken.

The ultimate goal of a fiber-optic strain sensor is the measurement of an arbitrary state of strain consequently there has been considerable research on the development of a fiber-optic strain rosette. Current approaches are focused on the development of the Michelson fiber-optic sensor because this leads to a simpler and more sensitive optical strain rosette than the polarization based-system developed previously.

4.1.3 Polarimetric Fiber-Optic Sensor

One of the problems associated with the philosophy associated with the Michelson fiber-optic sensor is the difficulty of maintaining the intimate mechanical bond between the two fibers needed for the common mode rejection necessary to achieve lead-in/lead-out insensitivity. Even when the two arms of the interferometer are adequately bonded together, in-plane bending will subject one to tension and the other to compression making lead-in/lead-out insensitivity difficult to attain. On the other hand, a polarimetric fiber-optic sensor relies on a single optical fiber making it much easier to obtain lead-in/lead-out insensitivity. Although the strain sensitivity of a polarimetric fiber-optic sensor is close to two orders of magnitude less than it's interferometric counterpart, this feature is useful if long sensor lengths are desired. Another significant advantage of this type of sensor is that it can be used with a laser of small coherence length. Localization of the sensing region is typically accomplished in a polarimetric

fiber-optic sensor by use of either dual 45 degree splices or a single 45 degree splice and a mirrored end face.

A structurally integrated optical microsensor system for assessing the state of a structure has been termed a Type I passive smart structure. Typically the smart structure comprises a fibrous polymeric composite material in which is embedded an optical microsensor system. This embryonic field requires the integration of diverse technological disciplines ranging from materials science and composites manufacturing, through networks and artificial intelligence to microelectronics and fiber-optics. With these basic raw ingredients, several different recipes exist for producing different classes of baked goods.

The first class of products involve the manufacture of fibrous polymeric composite parts which are typically cooked in an autoclave where the part is simultaneously subjected to both pressure and temperature in order to cure the matrix system. Currently, this manufacturing process is undertaken using an open--loop control philosophy, where the heat and pressure profiles of the autoclave are prescribed by the manufacturer of the resin or polymeric material. Consequently, if the curing process is incomplete during manufacture, then the resulting mechanical properties of the part, such as the strength and the stiffness characteristics, will not comply with the design specifications for that part.

The curing process is by no means a simple straight-forward undertaking. For example, the degree of cure can vary dramatically in a large fibrous polymeric part because of the thermal characteristics of the autoclave; the exothermic phenomena associated with the curing of the matrix; the thermal diffusivity of the part material; which typically depends upon the layup and the fiber volume fraction, and also the geometry of the part. Variations in the batch properties of prepreg materials and also the period of time that the prepreg remains outside the cold-storage facility, may also be contributing factors. Since an incomplete state of cure in a region of a part will typically result in the part failing to comply with the design specifications, critical parts are typically subjected to cure cycles that are longer than the optimal duration in order to develop a state of overcure. This philosophy is clearly expensive.

A closed-loop control philosophy may be invoked for the manufacture of autoclave parts by embedding fiber-optic sensors involving a network of thin optical fibers in the composite part. This processing philosophy enables the state of cure throughout the part to be continually assessed by a microcomputer-based control system, connected to the autoclave controller prior to tailoring the characteristics of the external stimuli imposed on the part by the autoclave, in a localized region of the part in order to achieve the desired state of cure. Figure IV.1 presents a schematic diagram of the system. This embryonic technology has broad ramifications for the fabrication of parts with complex shapes, and also high-performance composite parts where quality is of paramount importance. The technology would naturally impact all of the diverse industrial and

commercial products that are currently exploiting the superior properties of polymeric fibrous composite materials.

In some situations the objective of the smart structure may be to simply ensure that a critical part for an aerospace system is manufactured to specification in an optimal fashion. The embedded sensors could monitor the state of cure, the magnitudes of the residual stresses, and also provide information on the size and location of defects. Thus, the part is only smart during the manufacturing cycle since it becomes dumb once the optical fibers are severed where they emerge from the composite structure.

In sharp contrast to this class of products featuring smart capabilities only during the manufacturing process, a second class of products would continuously employ this class of *in situ* photonic sensors throughout the processes employed to manufacture the part and also throughout the service life of the part. Thus, as depicted in Figure IV.2, the embedded sensing system would initially be employed to monitor the state of cure during the fabrication of a smart component featuring fibrous polymeric materials, in order to ensure that the part is processed correctly. Subsequently, the embedded sensing system would be employed to continuously monitor a number of critical parameters within the part during service, as illustrated by the dynamic stress characteristics of robot arm shown in Figure IV.3 due to the loading generated by the end-effector tooling. If these stresses exceed prescribed criteria, for example, then the associated signals would be fed to the robot controller and the resultant mode of operation would be modified in order to restore the system characteristics to the prescribed work envelope. Finally, the embedded sensing system would be employed to monitor the structural integrity of the component. As shown in Figure IV.4, the embedded sensing system could be employed to monitor the structural integrity of structural members, such as aircraft wings, for example, by detecting cracks and monitoring the propagation of these defects. Such a capability will be an invaluable tool for inspection and maintenance personnel.

This notion of employing sensors embedded within a structural member in order to monitor the properties of the part has resulted in the coining of the term "health-monitoring,' and the relevant scenarios are depicted in Figure IV.5 Other terms include the cradle-through-grave philosophy. These terms are derived from the continual health-monitoring activities of *homo sapiens* and they build upon notions of biomimetics. This field is a principal ingredient of many smart materials technologies. Prior to birth, human beings are often subjected to non-invasive techniques to monitor the status of the fetus prior to embarking upon corrective courses of treatment. These medical practices often continue through the birth process. Subsequently, throughout life the health of human beings is monitored in response to external stimuli of various forms prior to being subjected to corrective treatments. Finally, as depicted in Figure IV.2 in the scene involving the emergency care vehicle, the sensing systems can be employed to monitor the vital signs and record the failure of the principal organs such as the heart, liver, and kidneys.

It is clear, therefore, that the most sophisticated classes of smart structures will embody health monitoring capabilities as engineers endeavor to replicate biological systems. Products featuring health-monitoring capabilities would typically include pressure vessels and piping in industrial, military, and aerospace systems where the focus of attention would be the structural integrity of these shell-like structures in high pressure systems, or leakage in low pressure systems containing hazardous chemicals. The fuselages and wings of both commercial and military aircraft where structural integrity and vibration phenomena would also feature health-monitoring technologies. There are, of course, numerous other engineering situations involving components being subjected to fatigue environments, other classes of hostile environments, and other scenarios involving unstructured external stimuli, where this technology is also relevant.

The cost of installing a passive smart structure featuring a structurally integrated microsensing system must be carefully weighed, relative to the cost of part failure and subsequent loss of performance of the overall system containing the smart structural part. For example, consider a scenario in which a critical articulating member of a piece of military machinery, is being subjected to a variety of unstructured external dynamic stimuli that are prematurely precipitating a fatigue failure of the part with the consequential loss of capabilities in the battlefield. The deployment of this embryonic technology would provide a diagnostic tool whereby the status of fatigue cracks in the part could be monitored, and upon attaining a specific threshold, planned-maintenance procedures could then be initiated in order to replace the part at a convenient time, in order to avoid the subsequent loss of battlefield capabilities associated with the previous generation of production machines.

A variety of fiber-optic materials and sensing strategies for several applications were comprehensively evaluated (see Bibliography: B5, for example). The research results are highlighted below.

1. Fiber-optic sensing systems are able to monitor the state of cure during the manufacture of a composite structural component and this information can provide the basis for on-line closed loop control during manufacture in an autoclave process, for example.

2. Fiber-optic sensing systems possess the ability to rapidly transfer high volumes of data, and in addition photonic phenomena permit a diverse group of parameters to be measured such as pressure, force, strain, magnetic fields, damage, and temperature, for example.

3. Typical fiber-optic systems are Mach-Zehnder interferometers, Michelson interferometers and several polarimetric devices.

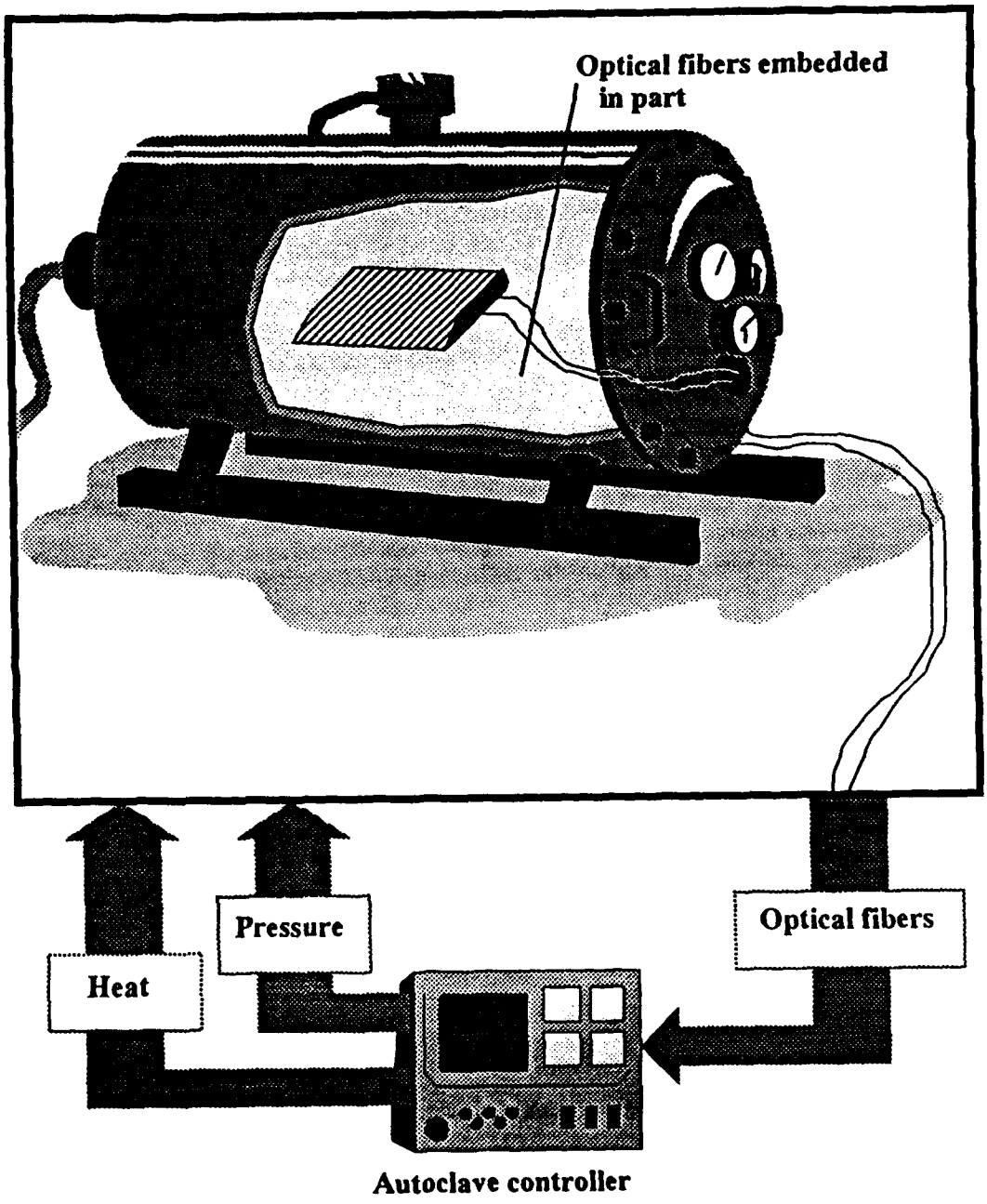

Fig. IV.1 Optical fibers embedded for autoclave cure monitoring.

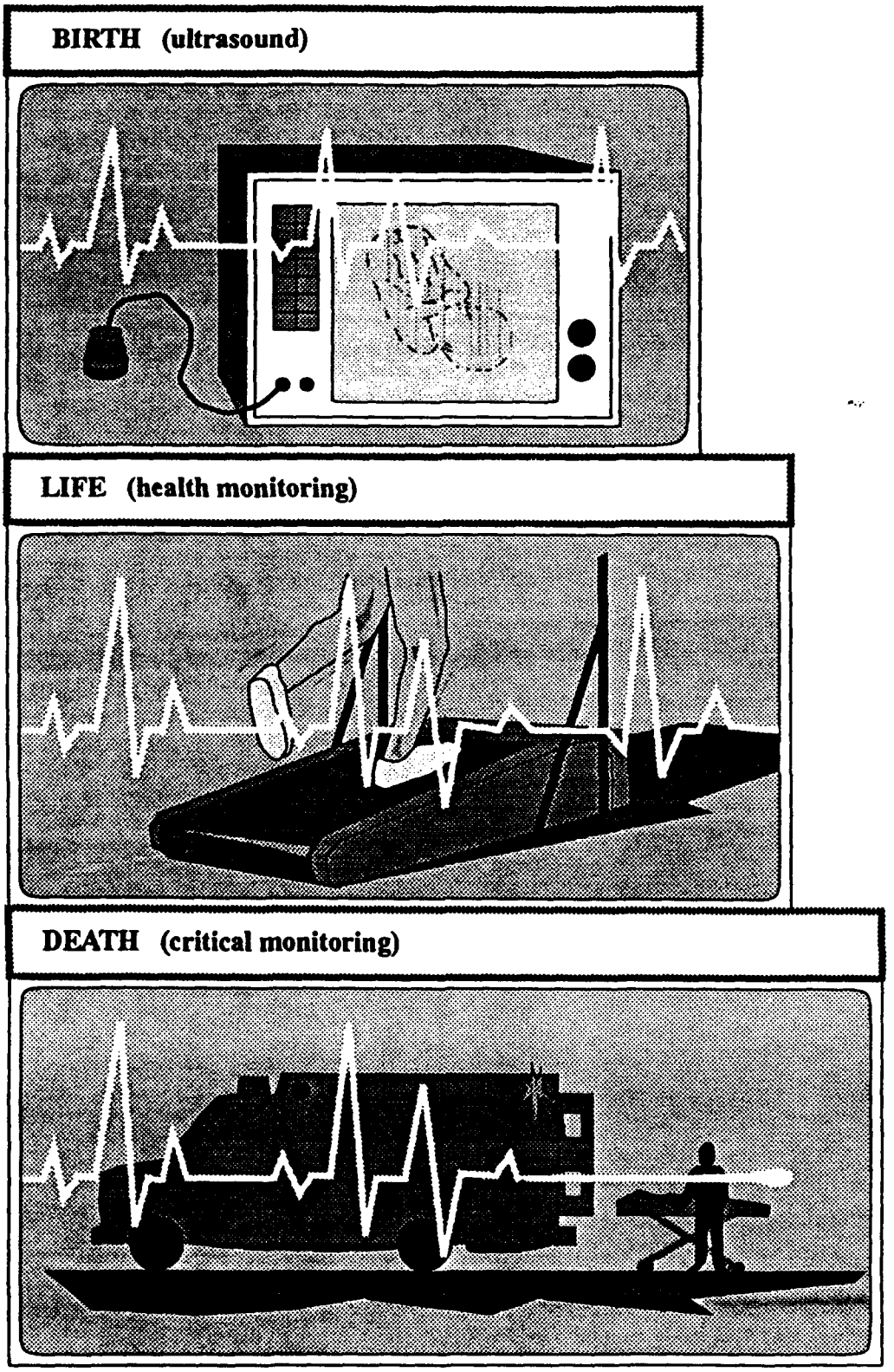

Fig. IV.2 The health-monitoring of *Homo sapiens*

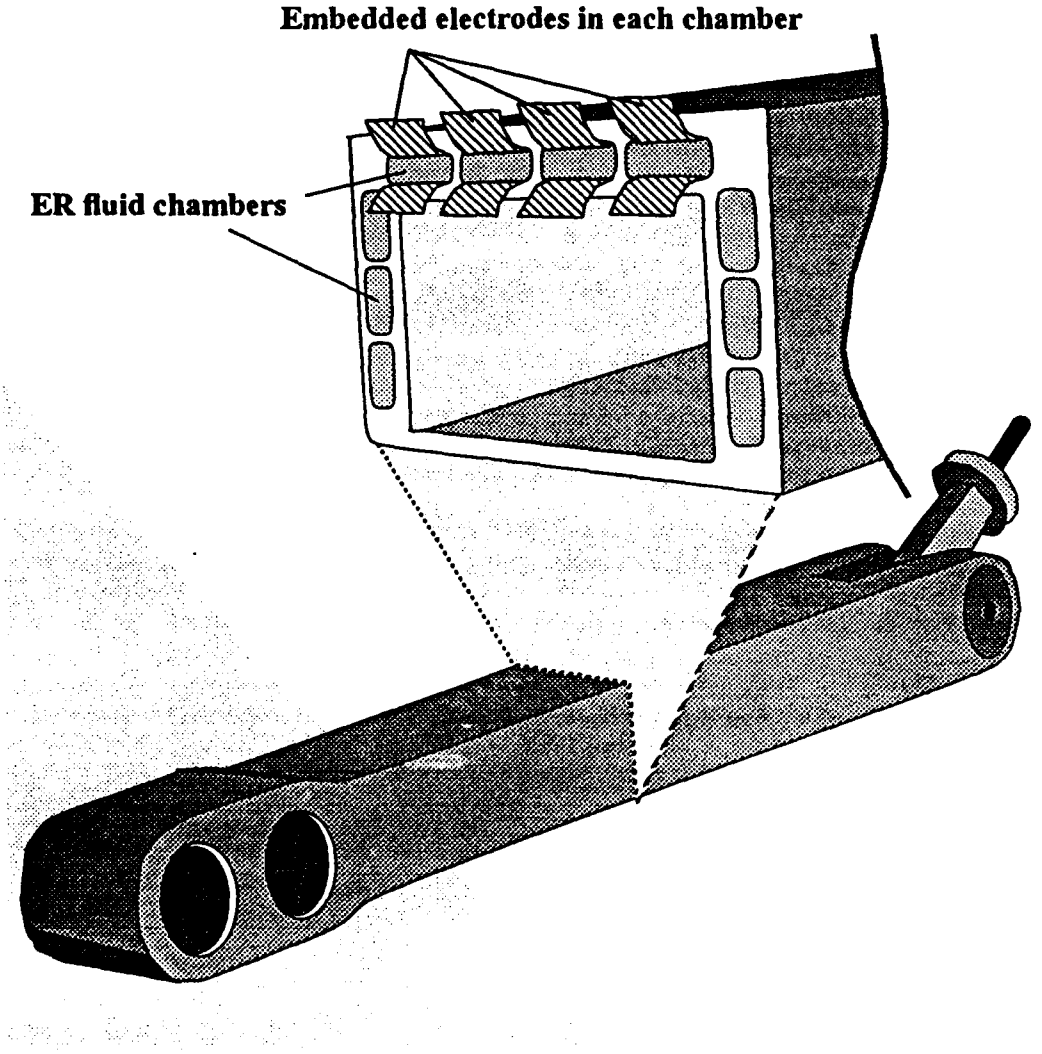

Fig. IV.3 An ER fluid-enhanced robot arm.

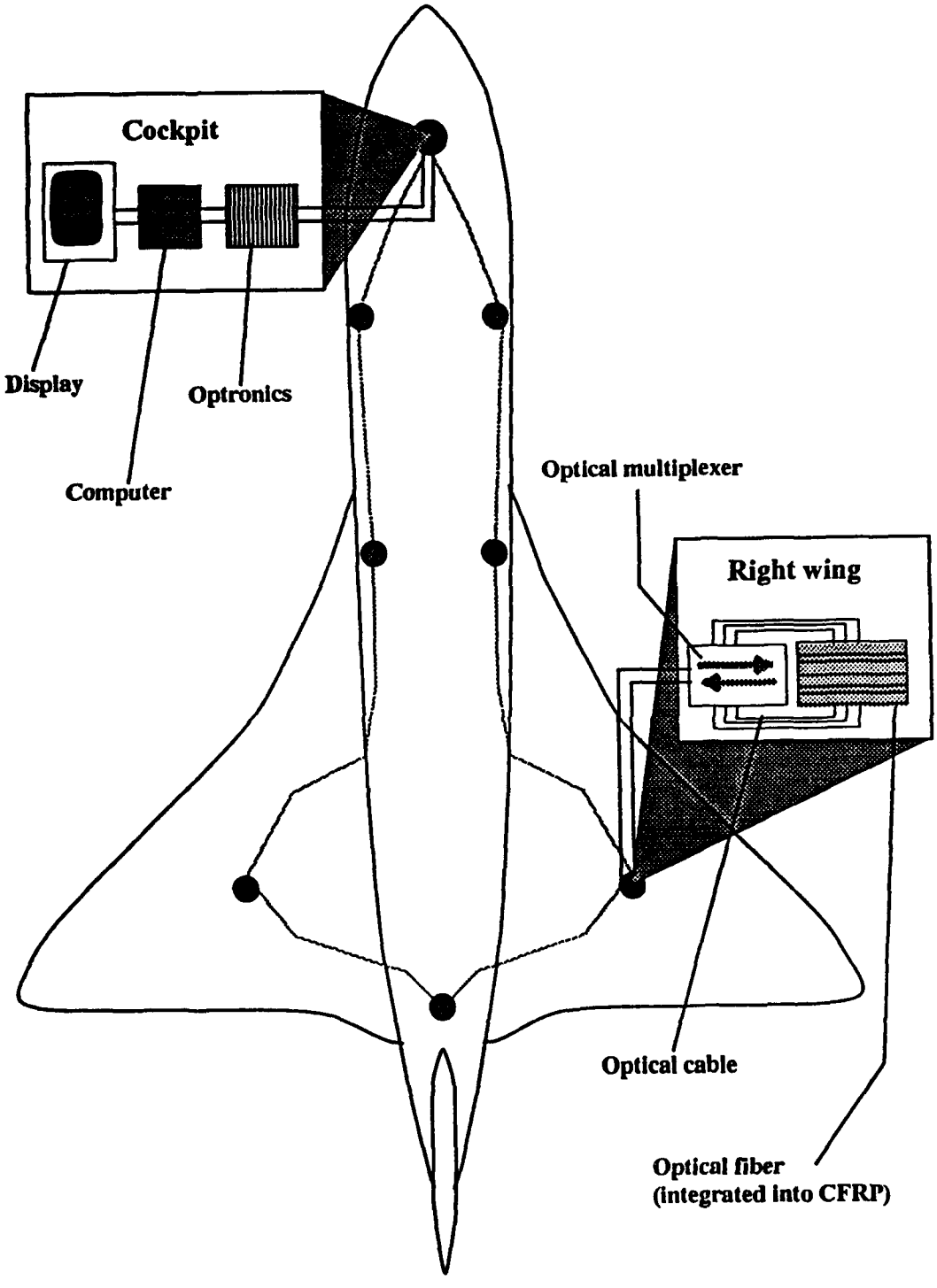

Fig. IV.4 In-flight structure surveillance would require fiber-optic nervous system (FONS) channels in key structural regions of a plane.

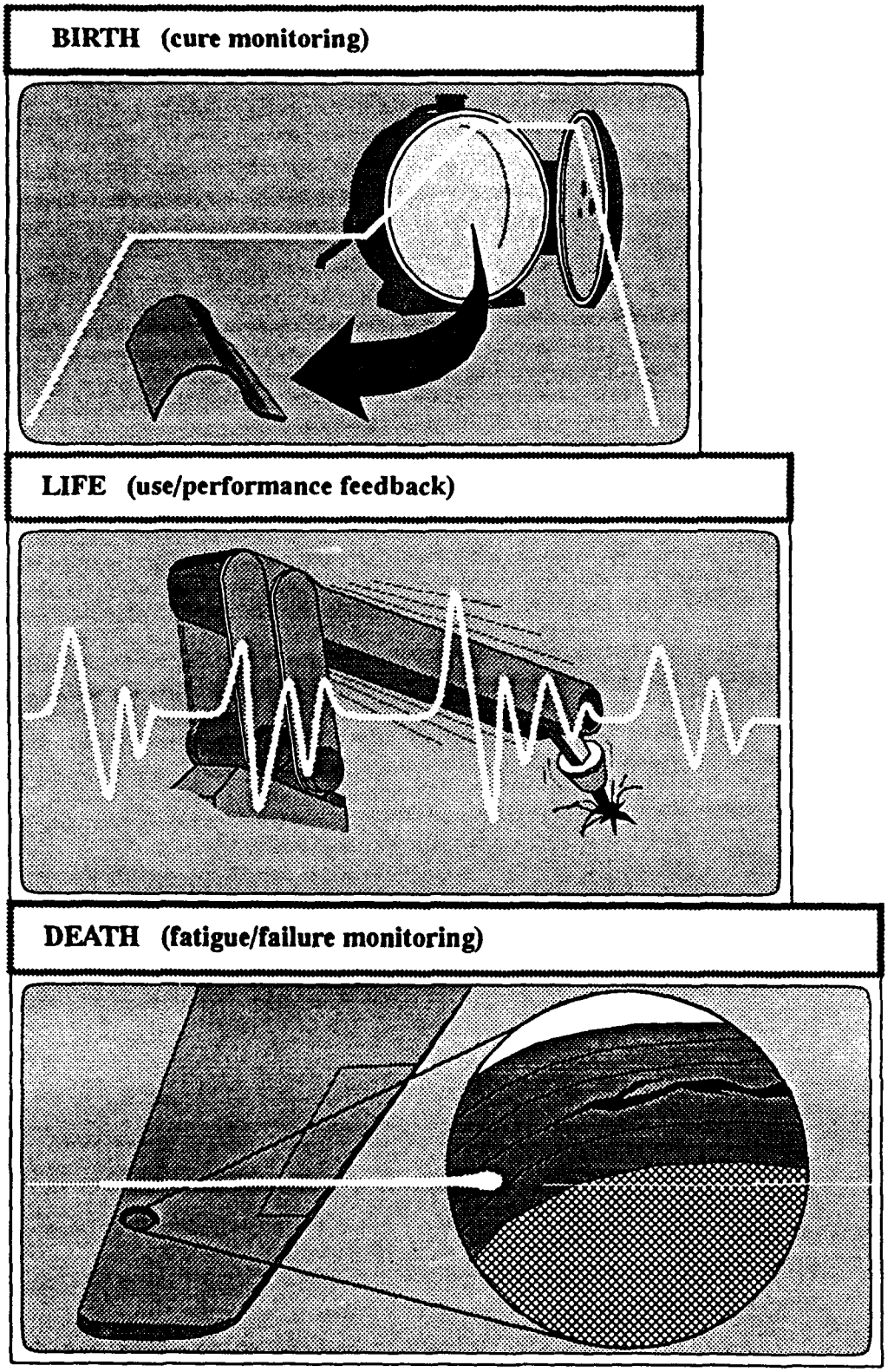

Fig. IV.5 The health-monitoring of parts utilizing embedded sensors.

4. Fiber-optic strain sensors have been developed for measuring strain at a point and they have also been employed for damage detection associated with impact and delamination phenomena.

5. The embedding of optical fibers in polymeric laminates does *not* adversely affect the interlaminar toughness of the structure, or the strength of the structure provided empirical guidelines are complied with.

6. Damage detection in polymeric composites can be accomplished by the utilization of an array of optical wave guides that are severed by cracks propagating through the structure, thereby severing the optical path and reducing the intensity of light at the photodetector.

V MATHEMATICAL FORMULATION FOR TWO CLASSES OF SMART STRUCTURES

Design tools for smart materials and structures applications will typically involve the integration of concepts from continuum mechanics, such as field equations and boundary conditions, and computational techniques such as finite element methods. In order to develop these computational tools, two variational theorems are established herein for smart structures featuring firstly an elastic body with piezoelectric properties; and secondly for an elastic body with embedded electrorheological fluid domains. Subsequently, finite element formulations are systematically developed for these two classes of smart structural systems.

5.1 VARIATIONAl THEOREM : SMART STRUCTURES INCORPORATING PIEZOELECTRIC ACTUATOR DOMAINS

A variational formulation for an elastic body with piezoelectric properties is established herein. OXYZ are Lagrangian coordinates fixed in the body in an undeformed reference state. Using an indicial notation (i = x,y,z), at time t, a general point P in the continuum has the position vector

$$r_i = r_{oi} + r_{Ri} + u_i$$

where r_{oi} are the components measured in the oxyz frame of the position vector of the origin of the body axes relative to the origin of the inertial frame. Similarly, r_{Ri} represents the position vector of point P in the reference state relative to the origin of the body axes and u_i is the deformation displacement vector. The velocity associated with the time rate of change of r_i is written as p_i. By using the Lagrange multiplier, the functional governing this response may be written

$$J = \int_{t_0}^{t_1} \left\{ \iint_V \left\{ (T-H) + X_i r_i + \frac{1}{2} \gamma_{ij} \left(\tau_{ij} - C_{ijkl}\gamma_{kl} + d_{kij}E_k \right) \right.\right.$$

$$- \frac{1}{2} E_i (D_i - d_{ijk}\gamma_{jk} - \epsilon_{ij}E_j) + \tau_{ij}(\gamma_{ij} - \frac{1}{2}(u_{i,j}+u_{j,i}))$$

$$\left.\left. -D_i(E_i+\phi_{,i}) - \rho p_i (p_i - (\overset{*}{r}_{oi} + \overset{*}{u}_i + e_{ijk}\dot{\psi}_j (r_{ok}+r_{Rk}+u_k))) \right\} dV \right.$$

$$\left. + \int_{S_1} \bar{g}_i r_i dS - \int_{S_2} g_i (\bar{u}_i - u_i)\, dS + \int_{S_3} \phi(\sigma) dS \right\} dt \qquad (1)$$

where the kinetic energy density $T = \frac{1}{2} \rho\, p_i p_i$, and electric enthalpy density $H = \frac{1}{2} \tau_{ij}\, \gamma_{ij} - \frac{1}{2} E_i D_i$. In this functional, X_i is the body force and g_i is the surface traction on region S_2. C_{ijkl} represents the tensor of elastic constants from the generalized Hooke's Law, and this tensor interrelates the Langrangian stress tensor τ_{ij} and the strain tensor γ_{ij}. Components of the angular velocity of the moving coordinates are represented by ψ_i, while e_{ijk} is the alternating tensor. The electric potential and electric field strength generated by the applied surface charge σ are represented by ϕ and E_i respectively, while D_i is the electric displacement. The piezoelectric strain constant is given by d_{ijk} and ϵ_{ij} represents the dielectric permittivity of the piezoelectric material. Three differential notations are used in this expression: $(\overset{*}{})$ is the time rate of change with respect to the moving frame oxyz; $(\dot{})$ is the absolute rate of change and $(,)$ represents the spatial differentation. In equation (1), an overbar denotes a prescribed quantity. The sum of S_1, S_2, S_3 defines the total surface area S of the continuum which has a volume V. The first variation of the functional J can be written as

$$\delta J = 0 = \int_{t_0}^{t_1} \Big\{ \iint_V \frac{1}{2}\,\delta\gamma_{ij}\,(\tau_{ij} - C_{ijkl}\gamma_{kl} + d_{kij}E_k)\,dV$$

$$+ \int_V \delta\tau_{ij}\,(\gamma_{ij} - \tfrac{1}{2}\,(u_{i,j} + u_{j,i}))\,dV$$

$$- \int_V \rho\,\delta p_i\,(p_i - (\overset{*}{r}_{oi} + \overset{*}{u}_i + e_{ijk}\dot{\psi}_j\,(r_{ok} + r_{Rk} + u_k)))\,dV$$

$$+ \int_V \delta u_i\,(X_i + \tau_{ij,j} - \rho\,\dot{p}_i)\,dV$$

$$+ \int_V \delta\phi\; D_{i,i}\,dV$$

$$- \frac{1}{2}\int_V \delta E_i\,(D_i - d_{ijk}\gamma_{jk} - \epsilon_{ij}E_j)\,dV$$

$$- \int_V \delta D_i\,(E_i + \phi_{,i})\,dV$$

$$+ \int_{S_1} \delta u_i(\bar{g}_i - g_i)\,dS - \int_{S_2} \delta g_i(\bar{u}_i - u_i)\,dS + \int_{S_3} \delta\phi\,(\bar{\sigma} - D_i n_i)\,dS$$

$$+ \delta r_{oi}\Big\{\iint_V X_i\,dV + \int_{S_1} \bar{g}_i\,dS - \int_V \rho\,\dot{p}_i\,dV\Big\}$$

$$+ \delta\psi_j\Big\{\iint_V e_{ijk}\,X_i\,(r_{ok} + r_{Rk} + u_k)\,dV + \int_{S_1} e_{ijk}\,\bar{g}_i\,(r_{ok} + r_{Rk} + u_k)\,dS$$

$$- \int_V e_{ijk}\rho\,\dot{p}_i\,(r_{ok} + r_{Rk} + u_k)\,dV\Big\}\Big\}\,dt \qquad (2)$$

In equation 2, n_i represents the component of the unit vector of the outward normal from the surface S. By permitting arbitrary independent variations of the system parameters γ_{ij}, τ_{ij}, p_i, u_i, ϕ, E_i, D_i, r_{oi}, ψ_i in equation (2), the field equations and associated boundary conditions can be established for a diverse class of engineering situations where flexible piezo-electric members are describing general planar motions relative to an inertial reference frame.

Upon prescribing the boundary conditions and the initial conditions for a specific member, then the solution of the field equations provides the basis for establishing a viable design tool for this class of problems. Since closed-form solutions are not realizable in practice, herein, a finite element formulation will be established in order to yield approximate solutions.

FINITE ELEMENT FORMULATION

In the finite element method, discrete quantities are employed to represent continuous functions, consequently all equations written for a continuous medium must be reformulated as matrix equation using discrete quantities. Since equation (2) was written for a continuum model and it is to be the basis for determining the finite element equations, this expression must now be modified.

A simple displacement model for the deformations of a component will be adopted, herein. The response of the link will be obtained by superimposing the nodal displacements on the gross rigid-body motion of the member. This assumption is considered to be appropriate and realistic since a linear theory of elasticity has been invoked and the subsequent investigation is restricted to the analysis of slender links in their lower modes of vibration.

The general displacement vector at any point in an element is related to the nodal displacement vector $\{U^e\}$ by

$$\{u^e\} = [N]\{U^e\}$$

where [N] is the matrix containing the shape functions, and superscript e denotes the parameter in element level. The electric potential vector at any point in an element can be assumed to have the following spatial distribution

$$\{\phi^e\} = [N_e]\ \{\Phi^e\}.$$

where $[N_e]$ contains the interpolation functions for the electric potential and $\{\Phi\}$ is the nodal potential vector. Assuming the velocity at any point within an element, p , is related to the nodal velocities (P) by the expression

$$\{p^e\} = [N]\ \{P^e\}\ ,$$

where [N] contains the same interpolation functions used to describe the spatial distribution of displacement u, then the third expression in (2) may be rewritten

$$-\int_{V^e} \rho\ (\delta P^e)^T [N]^T [N]\ (\{P^e\} - \{P_R^e\} - \{\dot{U}^e\})\ dV$$

The velocity field associated with the rigid-body motion of the link is approximated by $[N]\ \{P_R^e\}$ and implicitly contains the equation of closure of the mechanism.

Using matrix notation, the variational equation of motion for a single finite element may be written

$$\delta J^e = 0 = \int_{t_o}^{t_1} \Big\{ \frac{1}{2} \int_{V^e} (\delta\gamma)^T \left((\tau) - [C](\gamma) + [d](E) \right) dV$$

$$+ \int_{V^e} (\delta\tau)^T \left((\gamma) - [L_1][N](U) \right) dV$$

$$- \int_{V^e} \rho (\delta P)^T [N]^T [N] \left((P) - (P_R) - (\dot{U}) \right) dV$$

$$+ (\delta U)^T \Big[\int_{V^e} [N]^T \left((X) + [L_2](\tau) - \rho [N](\dot{P}) \right) dV + \int_{S_1^e \cap S_1} [N]^T \left((\bar{g}) - (g) \right) dS \Big]$$

$$+ \int_{V^e} (\delta\Phi)^T [N_e]^T [L_3](D) \, dV$$

$$- \int_{V^e} \frac{1}{2} (\delta E)^T \left((D) - [\bar{d}]^T (\gamma) - [\epsilon](E) \right) dV$$

$$- \int_{V^e} (\delta D)^T \left((E) + [L_3][N_e](\Phi) \right) dV$$

$$+ \int_{S_2^e \cap S_2} (\delta g)^T [N] \left((\bar{U}) - (U) \right) dS - \int_{S^e \cap S} (\delta\Phi)^T [N_e]^T \left(\bar{\sigma} - (D)^T (n) \right) dS$$

$$+ (\delta r_o)^T \Big(\int_{V^e} (X) dV + \int_{S_1^e \cap S_1} (\bar{g}) dS - \int_{V^e} \rho \, [N](\dot{P}) \, dV \Big)$$

$$+ \delta\psi \cdot \Big(\int_{V^e} (r \times X) dV + \int_{S_1^e \cap S_1} (r \times \bar{g}) dS - \int_{V^e} (r \times \rho \, \dot{p}) \, dV \Big) \Big\} \, dt \qquad (3)$$

where the bolded parameters denote vector quantities. The differential operators $[L_1]$, $[L_2]$ and $[L_3]$ and definitions of the (τ), (γ), $[d]$, $[\epsilon]$ are given in the Appendix. Integrating by parts the second term in the fourth

integral and the fifth integral respectively, and using the following notations,

$$[K] = \int_{V^e} ([L_2][N])^T[\tilde{C}]([L_2][N])\, dV$$

$$[K_c] = \int_{V^e} ([L_2][N])^T\, [d]([L_3][N_e])\, dV$$

$$[M] = \int_{V^e} \rho\, [N]^T[N]\, dV$$

$$[R] = \int_{V^e} ([L_3][N_e])^T[\epsilon]\, ([L_3][N_e])\, dV$$

$$[R_c] = \int_{V^e} ([L_3][N_e])^T[\tilde{d}]^T([L_1][N])\, dV$$

the variational equation of motion becomes

$$\delta J^e = 0 = \int_{t_0}^{t_1} \Big(\iint_{V^e} \frac{1}{2}\, (\delta\gamma)^T((\tau) - [C](\gamma) + [d](E))\, dV$$

$$+ \int_{V^e} (\delta\tau)^T\, ((\gamma) - [L_1][N](U))\, dV$$

$$- \int_{V^e} \rho\, (\delta P)^T[N]^T[N]\, ((P) - (P_R) - (\dot{U}))\, dV$$

$$+(\delta U)^T(-[K](U) - [K_c](\Phi) - [M](\dot{P}) + \int_V [N]^T(X)\, dV + \int_{S_1^e \cap S_1} [N]^T(\bar{g})\, dS)$$

$$+ (\delta\Phi)^T(-[R](\Phi) + [R_e](U) + \int_{S^e \cap S} [N_e]^T\, \bar{\sigma}\, dS)$$

$$- \int_{V^e} \frac{1}{2} (\delta E)^T ((D) - [d](\gamma) - [\epsilon](E)) \, dV$$

$$- \int_{S_2^e \cap S_2} (\delta g)^T [N]((\bar{U}) - (U)) \, dS$$

$$+ (\delta r_o)^T \left(\int_{V^e} (X) dV + \int_{S_1^e \cap S_1} (\bar{g}) dS - \int_{V^e} \rho [N] (\ddot{P}) \, dV \right)$$

$$+ \delta \psi \cdot \left(\int_{V^e} (r \times X) \, dV + \int_{S_1^e \cap S_1} (r \times \bar{g}) \, dS - \int_{V^e} (r \times \rho \, \ddot{p}) \, dV \right) \Big\} \, dt \qquad (4)$$

From equation (4) the governing equations governing the displacement vector (U) and electric potential (Φ) can be written as

$$[K](U) + [K_c](\Phi) + [M](\ddot{U}) = (F) \qquad (5)$$

$$[R](\Phi) - [R_c](U) = (Q) \qquad (6)$$

where

$$(F) = \int_{V^e} [N]^T (X) \, dV + \int_{S_1^e \cap S_1} [N]^T (\bar{g}) \, dS - [M](\ddot{P}_R)$$

$$(Q) = \int_{S^e \cap S} [N_e]^T \bar{\sigma} \, dS$$

It can be seen that equations (5) and (6) couple the displacement field and electric field. The aforementioned element equations can be assembled to

develop the system equations. For brevity, the same notation will be used for the system equations.

The governing equations governing the response of a member macroscopically consisting of two materials in different regions, one being the usual structural material and the other being the piezoelectric material, can be developed by first considering each material independently prior to utilizing the compatibility condition on the interface. Thus,

(i) the piezoelectric part

$$[K^p](U^p) + [K_c](\Phi) + [M^p](U^p) = (F^p) + (F_i)$$

$$[R](\Phi) - [R_c](U^p) = (Q)$$

(ii) the structural part

$$[K^s](U^s) + [M^s](U^s) = (F^s) - (F_i)$$

(iii) the displacement compatibility

$$(U_i^p) = (U_i^s) = (U_i)$$

where superscripts, p and s are used to distinguish the piezoelectric and structural parts respectively, and subscript i denotes the quantity on the interface. By combining these equations, the global equation can be written in a matrix form

$$
\begin{bmatrix} M_{11}^{p} & M_{12}^{p} & 0 & 0 \\ M_{21}^{p} & M_{22}^{p}+M_{22}^{s} & M_{21}^{s} & 0 \\ 0 & M_{12}^{s} & M_{11}^{s} & 0 \\ 0 & 0 & 0 & 0 \end{bmatrix} \begin{Bmatrix} \ddot{U}_1^{p} \\ \ddot{U}_i \\ \ddot{U}_1^{s} \\ \ddot{\Phi} \end{Bmatrix} + \begin{bmatrix} K_{11}^{p} & K_{12}^{p} & 0 & K_{c1} \\ K_{21}^{p} & K_{22}^{p}+K_{22}^{s} & K_{21}^{s} & K_{c2} \\ 0 & K_{12}^{s} & K_{22}^{s} & 0 \\ -R_{c1} & -R_{c2} & 0 & R \end{bmatrix} \begin{Bmatrix} U_1^{p} \\ U_i \\ U^{s} \\ \Phi \end{Bmatrix} = \begin{Bmatrix} F_1^{p} \\ F_2^{p}+F_2^{s} \\ F_1^{s} \\ Q \end{Bmatrix}
$$

where the submatrix and subvector are discretized by the location of those quantities described.

In the case that the piezoelectric material acts as an actuator. The electric potential Φ is the control variable. The equation can then be written

$$
\begin{bmatrix} M_{11}^{p} & M_{12}^{p} & 0 \\ M_{21}^{p} & M_{22}^{p}+M_{22}^{s} & M_{21}^{s} \\ 0 & M_{12}^{s} & M_{11}^{s} \end{bmatrix} \begin{Bmatrix} \ddot{U}^{p} \\ \ddot{U}_i \\ \ddot{U}^{s} \end{Bmatrix} + \begin{bmatrix} K_{11}^{p} & K_{12}^{p} & 0 \\ K_{21}^{p} & K_{22}^{p}+K_{22}^{s} & K_{21}^{s} \\ 0 & K_{12}^{s} & K_{22}^{s} \end{bmatrix} \begin{Bmatrix} U_1^{p} \\ U_i \\ U^{s} \end{Bmatrix} = \begin{Bmatrix} F_1^{p} \\ F_2^{p}+F_2^{s} \\ F_1^{s} \end{Bmatrix} + \begin{Bmatrix} [K_{c1}](\Phi) \\ [K_{c2}](\Phi) \\ 0 \end{Bmatrix}
$$

or in a compact form

$$
[M](\ddot{U}) + [K](U) = (f_e) + (f_c) \qquad (7)
$$

where $\{f_e\}$ and $\{f_c\}$ are the external force vector and the control force vector respectively. If a proportional damping matrix is introduced for the structural material, the equation (7) can be augmented and written

$$[M]\{\ddot{U}\} + [C]\{\dot{U}\} + [K]\{U\} = \{f_e\} + \{f_c\} \qquad (8)$$

where the damping matrix is written

$$[C] = \alpha[M] + \beta[K] \qquad (9)$$

The following vector and matrix notations are used in equation (3),

Stress vector

$$\{\tau\} = \begin{Bmatrix} \tau_{11} \\ \tau_{22} \\ \tau_{33} \\ \tau_{23} \\ \tau_{13} \\ \tau_{12} \end{Bmatrix}$$

Strain vector

$$\{\gamma\} = \begin{Bmatrix} \gamma_{11} \\ \gamma_{22} \\ \gamma_{33} \\ \gamma_{23} \\ \gamma_{13} \\ \gamma_{12} \end{Bmatrix}$$

Electric field

$$\{E\} = \begin{Bmatrix} E_1 \\ E_2 \\ E_3 \end{Bmatrix}$$

Electric displacement

$$\{D\} = \begin{Bmatrix} D_1 \\ D_2 \\ D_3 \end{Bmatrix}$$

Piezoelectric strain constant

$$[d] = \begin{bmatrix} d_{111} & d_{211} & d_{311} \\ d_{122} & d_{222} & d_{322} \\ d_{133} & d_{233} & d_{333} \\ d_{123} & d_{223} & d_{323} \\ d_{113} & d_{213} & d_{313} \\ d_{112} & d_{212} & d_{312} \end{bmatrix}$$

$$[\bar{d}] = \begin{bmatrix} d_{111} & d_{211} & d_{311} \\ d_{122} & d_{222} & d_{322} \\ d_{133} & d_{233} & d_{333} \\ 2d_{123} & 2d_{223} & 2d_{323} \\ 2d_{113} & 2d_{213} & 2d_{313} \\ 2d_{112} & 2d_{212} & 2d_{312} \end{bmatrix}$$

Dielectric permittivity

$$[\epsilon] = \begin{bmatrix} \epsilon_{11} & \epsilon_{12} & \epsilon_{13} \\ \epsilon_{21} & \epsilon_{22} & \epsilon_{23} \\ \epsilon_{31} & \epsilon_{32} & \epsilon_{33} \end{bmatrix}$$

Elastic constant (orthotropic)

$$[C] = \begin{bmatrix} C_{11} & C_{12} & C_{13} & 0 & 0 & 0 \\ C_{21} & C_{22} & C_{23} & 0 & 0 & 0 \\ C_{31} & C_{32} & C_{33} & 0 & 0 & 0 \\ 0 & 0 & 0 & C_{44} & 0 & 0 \\ 0 & 0 & 0 & 0 & C_{55} & 0 \\ 0 & 0 & 0 & 0 & 0 & C_{66} \end{bmatrix}, \quad [\bar{C}] = \begin{bmatrix} C_{11} & C_{12} & C_{13} & 0 & 0 & 0 \\ C_{21} & C_{22} & C_{23} & 0 & 0 & 0 \\ C_{31} & C_{32} & C_{33} & 0 & 0 & 0 \\ 0 & 0 & 0 & \frac{C_{44}}{2} & 0 & 0 \\ 0 & 0 & 0 & 0 & \frac{C_{55}}{2} & 0 \\ 0 & 0 & 0 & 0 & 0 & \frac{C_{66}}{2} \end{bmatrix}$$

Where $[\bar{C}]$ is used for the symmetric expression of [K] while $[\tilde{d}]$ is used for the equalities: $\gamma_{12} = \gamma_{21}$, $\gamma_{13} = \gamma_{31}$ and $\gamma_{23} = \gamma_{32}$.

and the differential operators,

$$[L_1] = \begin{bmatrix} \frac{\partial}{\partial x_1} & 0 & 0 \\ 0 & \frac{\partial}{\partial x_2} & 0 \\ 0 & 0 & \frac{\partial}{\partial x_3} \\ 0 & \frac{1}{2}\frac{\partial}{\partial x_3} & \frac{1}{2}\frac{\partial}{\partial x_2} \\ \frac{1}{2}\frac{\partial}{\partial x_3} & 0 & \frac{1}{2}\frac{\partial}{\partial x_1} \\ \frac{1}{2}\frac{\partial}{\partial x_2} & \frac{1}{2}\frac{\partial}{\partial x_1} & 0 \end{bmatrix}$$

$$[L_2] = \begin{bmatrix} \frac{\partial}{\partial x_1} & 0 & 0 \\ 0 & \frac{\partial}{\partial x_2} & 0 \\ 0 & 0 & \frac{\partial}{\partial x_3} \\ 0 & \frac{\partial}{\partial x_3} & \frac{\partial}{\partial x_2} \\ \frac{\partial}{\partial x_3} & 0 & \frac{\partial}{\partial x_1} \\ \frac{\partial}{\partial x_2} & \frac{\partial}{\partial x_1} & 0 \end{bmatrix}$$

$$[L_3] = \left(\frac{\partial}{\partial x_1} \quad \frac{\partial}{\partial x_2} \quad \frac{\partial}{\partial x_3} \right)^T$$

5.2 VARIATIONAL THEOREM : SMART STRUCTURES INCORPORATING ElectrorheoLOGICAL FLUID DOMAINS

The static response of a given structure subjected to a prescribed loading regime is governed by the stiffness of the structure. The dynamic response, however, is largely governed by the mass, stiffness and energy dissipation characteristics of the structure and also the nature of dynamic excitation. Thus in order to control the static and dynamic behavior of a structure, the structure must in general possess the innate ability to change, upon command, the mass, stiffness and energy-dissipation characteristics. Since ER fluids possess electrically-dependent mechanical characteristics when subjected to static or dynamic electrical signals, then if these ER fluids are embedded within an electrically conductive solid medium, as shown in Figure V.1, the ability then exists to control the global properties of this material.

The task of modeling the dynamic response of a viscoelastic body comprising both a solid and a fluid domain is accomplished herein by developing a variational principle which governs the motion of a viscoelastic body of volume V, with an embedded Lagrangian reference frame oxyz, describing a general spatial motion relative to an inertial frame of reference frame OXYZ.

At time, t, a general point P in a viscoelastic continuum may be defined by the position vector r

$$r_i = r_{0i} + r_{Ri} + u_i \qquad (1)$$

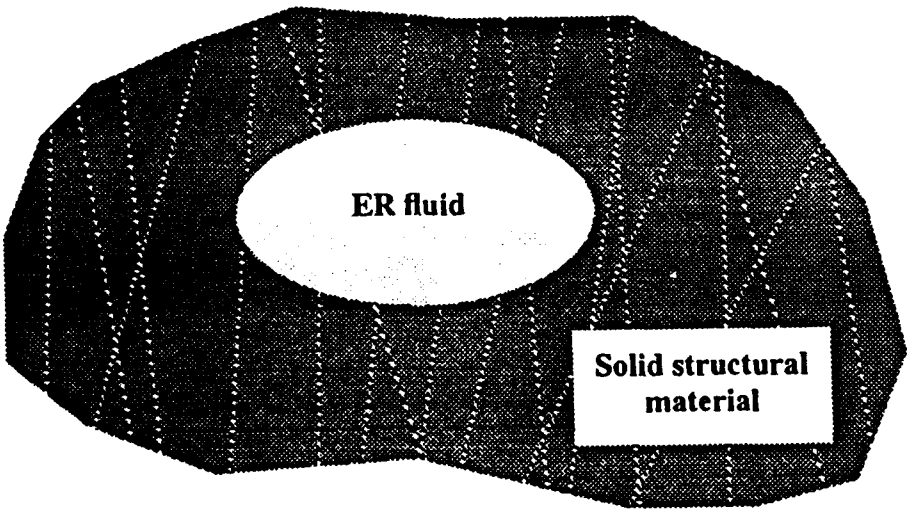

Fig. V.1 The generic idea of an electrorheological fluid embedded in a deformable solid.

When the continuum is subjected to an isothermal process during the time interval $t_1 = 0$ to $t_1 = t$, the principle of virtual work requires the stationary conditions of the following functional to be determined

$$J_1 = \int_V \int_o^t \left\{ \frac{\partial T}{\partial \tau} + \frac{\partial A}{\partial \tau} + \Lambda - X_i \frac{\partial r_i}{\partial \tau} \right\} d\tau dV$$

$$- \int_{S_1} \int_o^t \bar{g}_i \frac{\partial r_i}{\partial \tau} d\tau dS_1 \quad . \tag{2}$$

The equations governing this class of dynamic linear-viscoelastic problems are the field equations throughout the volume, the boundary conditions and also the initial conditions. The first two classes of equations may be established by seeking the stationary conditions of the functional J_1 subject to the following constraints throughout the continuum,

$$e_{ij} = \frac{1}{2} (u_{i,j} + u_{j,i}) \tag{3}$$

$$\epsilon_{ijk}\omega_k = - \frac{1}{2}(u_{i,j} - u_{j,i}) \tag{4}$$

$$p_i = \overset{*}{r}_{0i} + \overset{*}{r}_{Ri} + \epsilon_{ijk}\phi_j(r_{0k} + r_{Rk} + u_k) \tag{5}$$

and on the surface region S_2

$$\bar{u}_i = u_i . \tag{6}$$

A free variational problem may be constructed by incorporating the constraint equations (3), (4), (5) and (6) into the functional J_1 using

Lagrange multipliers to formulate a functional J. Upon taking the first variation of the functional J and setting it equal to zero, these undetermined multipliers may be expressed as functions of the system variables.

Expressions for A and Λ in equation (2) need to be established before the above task may be addressed. This is accomplished by combining the local equation for conservation of energy and the entropy production inequality under isothermal conditions [16]. Thus,

$$-\dot{A}(t) + \sigma_{ij}(t)\dot{e}_{ij}(t) \geq 0 \tag{7}$$

Now, assuming that

$$A(t) = \frac{1}{2}\int_0^t\int_0^t G_{ijk\ell}(2t - \tau - \eta)\,\frac{\partial e_{ij}}{\partial \tau}^{(\tau)} \cdot \frac{\partial e_{k\ell}}{\partial \eta}^{(\eta)}\, d\tau d\eta \tag{8}$$

where $G_{ijk\ell}(t)$ are the isothermal relaxation functions of the viscoelastic body, and upon substituting (8) into (7) and requiring the resulting form to be valid for arbitrary values of the current strain rate $\dot{e}_{ij}(t)$, then the following hereditary stress-strain relation

$$\sigma_{ij}(t) = \int_0^t G_{ijk\ell}(t - \tau)\,\frac{\partial e_{k\ell}}{\partial \tau}^{(\tau)}\, d\tau \tag{9}$$

is obtained. Equation (7) now becomes

$$\Lambda(t) \geq 0 \tag{10}$$

where

$$\Lambda(t) = -\frac{1}{2}\int_0^t\int_0^t \frac{\partial}{\partial t} G_{ijk\ell}(2t - \tau - \eta)\,\frac{\partial e_{ij}^{(\tau)}}{\partial \tau}\,\frac{\partial e_{k\ell}^{(\eta)}}{\partial \eta}\,d\tau d\eta \qquad (11)$$

which states that the rate of dissipation of energy must be non-negative.

In this work, attention is focussed on ultra-advanced composites which are structurally alternating layers of two different species of materials. One set of layers is assumed to be either a monolithic material, or a traditional composite material, whereas the second set of layers is assumed to be an electro-rheological fluid. The constitutive model for this class of ultra-advanced composite materials is based upon the concept of geometrically-weighted averages.

In this variational theorem, the effective mass density $\tilde{\rho}$ of the ultra-advanced composite material consisting of $\hat{S}_1$ layers of a structural material and $\hat{S}_2$ layers of an electro-rheological fluid is defined by

$$\tilde{\rho} = \left[\sum_{m=1}^{\hat{S}_1} \rho_1^{(m)} \frac{\hat{t}^{(m)}}{h_1}\right] \nu_1 + \left[\sum_{n=1}^{\hat{S}_2} \rho_2^{(n)} \frac{\hat{t}^{(n)}}{h_2}\right] \nu_1 \qquad (12)$$

where, the volume fractions of the solid and fluid components of the material are related by the volume additivity constraint,

$$\nu_1 + \nu_2 = 1, \qquad (13)$$

and the total thickness h of the ultra-advanced composite material is defined by,

$$h_1 + h_2 = h \tag{14}$$

In equation (1), $\rho_1^{(m)}$ and $\rho_2^{(n)}$ are the densities of the mth layer of the traditional composite material and the nth layer of the ER fluid respectively. Similarly $\hat{t}^{(m)}$ and $\hat{t}^{(n)}$ represent the thickness of the mth layer of the traditional composite material and the nth layer of the ER fluid, respectively.

The effective relaxation function $\tilde{G}_{ijk\ell}(\hat{V}^{(n)})$ of the ultra-advanced composite material is defined by

$$\tilde{G}_{ijk\ell}(\hat{V}^{(n)}) = \left[\sum_{m=1}^{\hat{S}_1} G_{ijk\ell}^{(m)} \frac{\hat{t}^{(m)}}{h_1} \right] \nu_1 + \left[\sum_{n=1}^{\hat{S}_2} G_{ijk\ell}^{(n)}(\hat{V}^{(n)}) \frac{\hat{t}^{(n)}}{h_2} \right] \nu_2 \tag{15}$$

where $G_{ijk\ell}^{(m)}$ represent the components of the tensor for the mth layer of the traditional composite material. The corresponding relaxation function of the nth layer of the ER material $\hat{G}_{ijk\ell}^{(n)}(\hat{V})^{(n)}$ is a function of the applied voltage $\hat{V}^{(n)}$. Clearly when the applied voltage in a given layer of the ER fluid induces a fluid-like state, the contribution to the overall relaxation function may be minimal depending on the fluidic properties.

Upon substituting equations (8) and (11)-(15) into equation (2), and also incorporating equations (3), (4), (5) and (6) into (2) after each equation in this latter group is first premultiplied by a Lagrange multiplier, the following variational equation is obtained by the standard rules of the variational calculus,

$$\delta J = 0 = \int_V \int_o^t (\delta\sigma_{(ij)} [-\dot{e}_{ij} + \frac{1}{2}(\dot{u}_{j,i} + \dot{u}_{i,j})]$$

$$+ \delta\sigma_{[ij]}[\epsilon_{ijk}\dot{\omega}_k + \tfrac{1}{2}(\dot{u}_{i,j} - \dot{u}_{j,i})] + \delta\dot{\omega}_k\sigma_{ji}\epsilon_{ijk}$$

$$+ \delta\dot{e}_{ij}\left[-\sigma_{ij} + \int_o^r \left\{ \sum_{m=1}^{\hat{S}_1} G^{(m)}_{ijk\ell}(t-\eta)\frac{\hat{t}^{(m)}}{h_1}\nu_1 + \sum_{n=1}^{\hat{S}_2} G^{(n)}_{ijk\ell}(t-\eta)\frac{\hat{t}^{(n)}}{h_2}\nu_2 \right\} \frac{\partial e_{kl}}{\partial \eta}^{(\eta)} d\eta\right]$$

$$+ \bar{\rho}\delta\dot{p}_i\left[-p_i + (\overset{*}{r}_{0i} + \overset{*}{r}_{Ri} + \epsilon_{ijk}\dot{\phi}_j(r_{0k} + r_{Rk} + u_k))\right]$$

$$+ \delta\dot{u}_i\left[\sigma_{ij,j} + X_i - \left\{ \sum_{m=1}^{\hat{S}_1} \rho_1^{(m)}\frac{\hat{t}^{(m)}}{h_1}\nu_1 + \sum_{n=1}^{\hat{S}_2} \rho_2^{(n)}\frac{\hat{t}^{(n)}}{h_2}\nu_2 \right\} \dot{p}_i\right]\right) d\tau dV$$

$$+ \int_{S_1}\int_o^t \delta\dot{u}_i(\bar{g}_i - g_i)d\tau dS_1 - \int_{S_2}\int_o^t \delta g_i(\bar{u}_i - \dot{u}_i)\, d\tau dS_2 \qquad (16)$$

$$+ \int_o^t \delta\dot{r}_{0i}\left\{\int_V X_i dV + \int_{S_1}\bar{g}_i\, dS_1 - \int_V \left\{ \sum_{m=1}^{\hat{S}_1} \rho_1^{(m)}\frac{\hat{t}^{(m)}}{h_1}\nu_1 + \sum_{n=1}^{\hat{S}_2} \rho_2^{(n)}\frac{\hat{t}^{(n)}}{h_2}\nu_2 \right\} \dot{p}_i dV\right\} d\tau$$

$$+ \int_o^t \delta\dot{\phi}_j\left(\int_V \epsilon_{ijk}X_i\,(r_{0k} + r_{Rk} + u_k)dV + \int_{S_1}\epsilon_{ijk}\bar{g}_i(r_{0k} + r_{Rk} + u_k)\, dS_1\right.$$

$$\left. - \int_V \epsilon_{ijk}\dot{p}_i \left\{ \sum_{m=1}^{\hat{S}_1} \rho_1^{(m)}\frac{\hat{t}^{(m)}}{h_1}\nu_1 + \sum_{n=1}^{\hat{S}_2} \rho_2^{(n)}\frac{\hat{t}^{(n)}}{h_2}\nu_2 \right\} (r_{0k} + r_{Rk} + u_k)dV\right) d\tau$$

If independent arbitrary variations of the system parameters p_i, u_i, r_{0i}, r_{Ri}, e_{ij}, ω_k, ϕ_j, $\sigma_{[ij]}$, $\sigma_{(ij)}$ and g_i in equation (5) are permitted, the characteristic equations for this class of dynamic linear-viscoelastic problem follow. They are the balance of linear and angular momentum for the

complete continuum, the field equations defining the stress-strain constitutive relations, the strain-displacement expression, the rotation-displacement equations, the requirement that the stress tensor be symmetric, the velocity-rate-of-change-of-position statement and the equations of equilibrium. These expressions are subject to the boundary conditions for prescribed tractions and deformation displacements.

By taking arbitrary independent variations in equation (5) the equations governing the response of flexible multi-bodied articulating systems fabricated in monolithic or multi-constituent materials are obtained. Exact solutions to these equations are not possible for a broad class of physical problems, therefore, herein, approximate finite element solutions have been developed. For illustration purposes, a General Electric P-50 robot retrofitted with an arm incorporating an ER fluid is considered. The constitutive behavior of both the structural material and the ER fluid is assumed to be viscoelastic.

FINITE ELEMENT FORMULATION

The variational equation of motion (16), provides the basis for developing a variety of mixed, hybrid, equilibrium or displacement finite element models for plate, shell or beam-like articulating structures. Herein, a finite element formulation for the predicting the elastodynamic response of flexible multi-bodied articulating beam-shaped robotic systems is developed by assuming that the deflections are governed by the Euler-Bernoulli beam theory. The transverse and axial deflections are assumed to be of the form

$$u(x,t) = [N_x](W_x) \quad \text{and} \quad w(x,t) = [N_z](W_z) \quad \text{or} \quad \begin{Bmatrix} u \\ w \end{Bmatrix} = [N](W) \qquad (17)$$

where [N] is the row vector containing the shape functions, (') represents the spatial derivative with respect to the axial variable, x, and z is the spatial variable perpendicular to the beam section in the plane of the mechanical linkage of the robot. The absolute acceleration field $\dot{p}(x,t)$ which may be decomposed into two components $\dot{p}_x$ and $\dot{p}_z$ is assumed to the related to the nodal values of the discretized field by the expression

$$\{\dot{p}\} = [N_R]\{\dot{P}_R\} + [N]\{\ddot{W}\} + 2\dot{\phi}\begin{bmatrix} 0 & | & N_z \\ -N_x' & | & 0 \end{bmatrix}\{\dot{W}\}$$

$$+ \begin{bmatrix} -\dot{\phi}^2 N_x & | & \ddot{\phi} N_z \\ -\ddot{\phi} N_x & | & -\dot{\phi}^2 N_z \end{bmatrix}\{W\} \qquad (18)$$

Using the standard formulation for a Kelvin solid [17], namely a spring and dashpot in parallel, the constitutive equation for the ultra advanced-composite material may be written as

$$\{\sigma(\hat{V})\} = [\bar{C}(\hat{V})]\{\gamma\} + [\bar{C}_1(\hat{V})]\{\dot{\gamma}\} \qquad (19)$$

where $\{\sigma\}$ and $\{\gamma\}$ are the stress and strain vectors respectively, $[\bar{C}(\hat{V})]$ is the matrix of elastic constants and $[\bar{C}_1(\hat{V})]$ is a damping matrix. Both of these matrices are assumed to model material characteristics which are functions of the applied voltage $\hat{V}$. This latter matrix models material damping stresses which are assumed to be proportional to the strain velocity. This damping matrix, which may be defined as a function of the

matrix of elastic constants is dependent upon the voltage applied to each layer of the ER fluid. Hence

$$[\bar{C}_1(V)] - \beta(\bar{\zeta})\ [\bar{C}(\hat{V}^{(n)})] \tag{20}$$

where the effective damping ratio $\bar{\zeta}$ of the laminate is defined by

$$\bar{\zeta}(\hat{V}^{(n)}) - \left[\sum_{m=1}^{S_1} \zeta_1^{(m)} \frac{t^{(m)}}{h} \right] \nu_1 + \left[\sum_{n=1}^{S_2} \zeta_2^{(n)}(\hat{V}^{(n)}) \frac{\hat{t}^{(n)}}{h_2} \right] \nu_2 \tag{21}$$

where $\zeta_1^{(m)}$ and $\zeta_2^{(n)}$ are the damping ratios of the nth layer of the traditional material and the nth layer of the ER fluid. In equation (20), β is an experimentally determined factor which is a function of the natural frequencies and the damping ratio of the laminate. An approach for experimentally determining this factor is presented in the subsequent section of the manuscript. This semi-empirical approach permits a simple descriptive mathematical model to be established for describing the complex phenomenological behavior of composite materials with a liquid phase and a solid phase.

A finite element formulation for the dynamic analysis of flexible robots fabricated in ultra-advanced composite-ER materials may be established by transforming equation (16) from a cartesian tensor expression in to a statement in linear algebra. Upon incorporating the assumptions of equations (17) - (21) into equation (16), and also exercising the option of taking the arbitrary independent variations in $\dot{r}_{0i}$, $\dot{\phi}_j$ and $\dot{\omega}_k$ to be zero, the resulting variational equation of motion for one finite element becomes

$$\delta J = 0 = \int_0^t \Bigg\{ \int_V (\delta\sigma)^T((\dot{\gamma}) - [B](\dot{W}))dV$$

$$+ \int_V (\delta\dot{\gamma})^T(-(\sigma) + [\bar{C}](\gamma) + [\bar{C}_1](\dot{\gamma}))dV$$

$$+ \int_V \tilde{\rho}\ (\delta\dot{P})^T(-(P) + [N_R](P_R) + [N](\dot{W}))dV$$

$$+ (\delta\dot{W})^T([K]+[M_{IC}])(W) + ([C]+[M_{COR}])(\dot{W}) + [M_R](\dot{P}_R)+[M](\ddot{W})$$

$$- \int_V [N]^T(X)dV - \int_{S_1} [N]^T(\bar{g})dS_1)$$

$$+ \int_{S_2} [N]^T(\delta g)((\dot{\bar{W}}) - (\dot{W}))dS_2 \Bigg\}\ dt \qquad (22)$$

where,

$$[K] = \int_V [B]^T[\bar{C}(\hat{V})][B]dV$$

$$[C] = \beta[K] \qquad (23)$$

$$[M] = \int_V \tilde{\rho}\ [N]^T[N]dV$$

$$[M_R] = \int_V \tilde{\rho}[N]^T[N_R]dV$$

$$[M_{IC}] = \int_V \tilde{\rho} \begin{bmatrix} N_x & 0 \\ 0 & N_z \end{bmatrix}^T \begin{bmatrix} -\dot{\phi}^2 N_x & -\ddot{\phi} N_z \\ -\ddot{\phi} N_x & -\dot{\phi}^2 N_z \end{bmatrix} dV$$

$$[M_{COR}] = \int_V 2\dot{\phi}\tilde{\rho} \begin{bmatrix} N_x & 0 \\ 0 & N_z \end{bmatrix}^T \begin{bmatrix} 0 & N_z \\ N_x & 0 \end{bmatrix} dV$$

are the local stiffness matrix, damping matrix, mass matrix coupling the discretized deformation and rigid-body fields, the inertial coupling matrix and the Coriolis' acceleration matrix, respectively. The strain transformation matrix is written as [B], where

$$[B]^T = \left[-\frac{1}{L} \quad \frac{1}{L} \quad \left(-\frac{6x}{L^2} + \frac{6x^2}{L^2}\right) \quad \left(\frac{6x}{L^2} - \frac{6x^2}{L^3}\right) \quad L\left(\frac{1}{L} - \frac{4x}{L^2} + \frac{3x^2}{L^3}\right) \quad L\left(-\frac{2x}{L^2} - \frac{3x^2}{L^3}\right)\right]$$

$$[N]^T = \begin{bmatrix} \left(1-\frac{x}{L}\right) & \frac{x}{L} & 0 & 0 & 0 & 0 \\ 0 & 0 & \left(1 - \frac{3x^2}{L^2} + \frac{2x^3}{L^3}\right) & \left(\frac{3x^2}{L^2} - \frac{2x^3}{L^3}\right) & \left(x - \frac{2x^2}{L} + \frac{x^3}{L^2}\right) & \left(\frac{x^3}{L^2} - \frac{x^2}{L}\right) \end{bmatrix}$$

(24)

$$[N_R]^T = \begin{bmatrix} \left(1 - \frac{x}{L}\right) & \frac{x}{L} & 0 & 0 & 0 & 0 \\ 0 & 0 & \left(1 - \frac{x}{L}\right) & \frac{x}{L} & 1 & 1 \end{bmatrix}$$

where L is the element length.

This completes the development of the mathematical apparatus necessary for analyzing an articulating assemblage of flexible bodies fabricated with ultra-advanced composite materials incorporating ER fluids.

VI HYBRID SMART STRUCTURES

The above muscular systems and sensory systems feature diverse characteristics, such as thermal operating range and dynamic response, consequently, each class of actuator and each class of sensor have distinct advantages and disadvantages. Nevertheless, by judicious selection, the smart-materials designer can synthesize numerous classes of hybrid actuator systems and sensor systems featuring several different classes of actuators and sensors to satisfy a broad range of performance specifications as shown in Figures II.3 and II.4).

Consider the smart-structural system whose desired actuation and sensing characteristics are schematically shown in Figure VI.1. This illustrative example features a structure which must be controlled over a broad bandwidth from low frequencies to high frequencies. Typical requirements include vibration control at the high frequencies through the tailoring of damping, natural frequencies, and the amplitude of the dynamic behavior of the structure, while at the low frequencies a shape or geometrical control requirement is imposed upon the structure. Since these requirements are extremely diverse, a hybrid smart material is proposed featuring two types of actuators and two types of sensors. Thus, for example, while the high frequency actuator is able to provide actuation capabilities at high frequencies, and the low-frequency actuator is able to provide appropriate actuation capabilities at low frequencies, the domain of applicability for these actuation systems overlap in the mid-frequency range whereupon either actuator, or alternatively both actuators, can be activated.

In order to satisfy the low-frequency requirements, shape-memory-alloy actuators can be employed in conjunction with embedded fiber-optic sensors in order to satisfy the shape control specification; while the high-frequency requirements may be satisfied by employing an array of piezoceramic actuators which are interfaced with an array of piezopolymeric sensors. A review of the actuator and sensor candidates suggests that some functional materials may be employed as either an actuator or as a sensor, while others are only able to perform one of these functions, as indicated in Figure II.6. The dual versatility of these materials could be exploited in some smart materials and structures applications by employing the same material as a sensor and/or as an actuator during service depending upon the environment and conditions under which the material is operating. Thus, for example, a material serving as a sensor could continuously monitor the vibrational response of a structure, prior to becoming an actuator when the amplitude of vibration becomes excessive in order to alleviate this dynamical behavior.

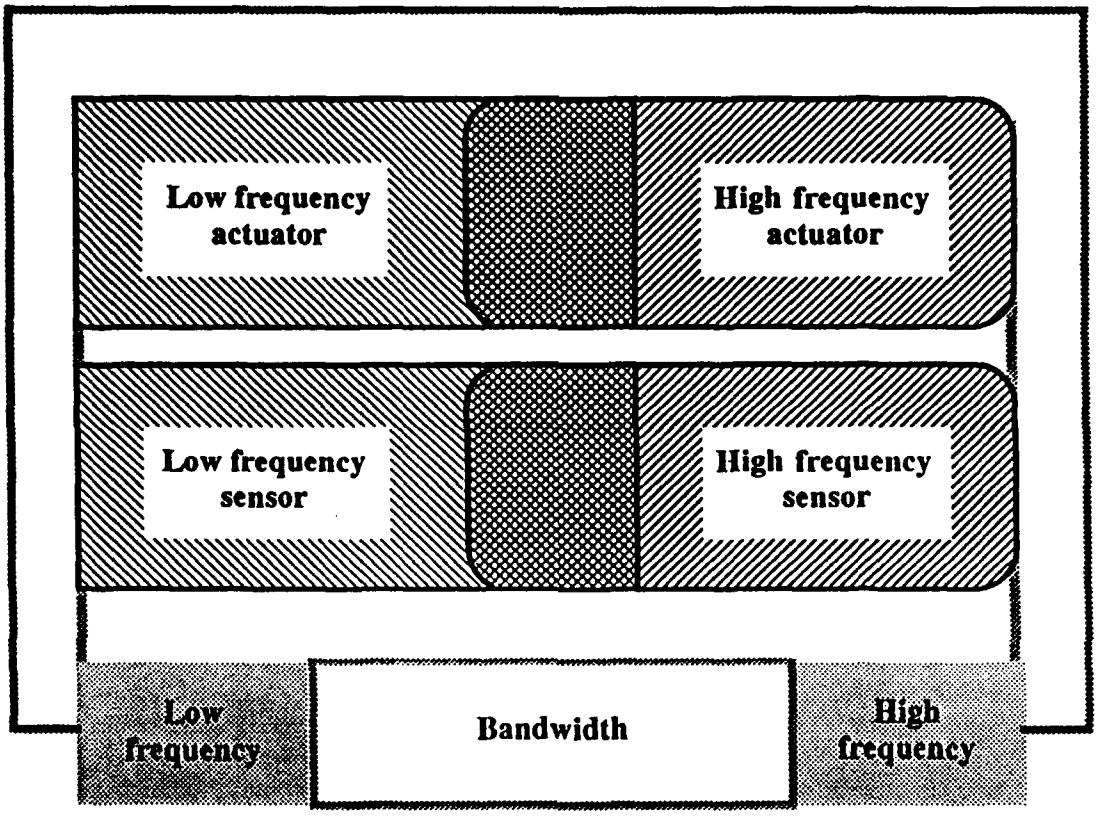

Fig. VI.1 Smart structures featuring hybrid actuation and sensing capabilities.

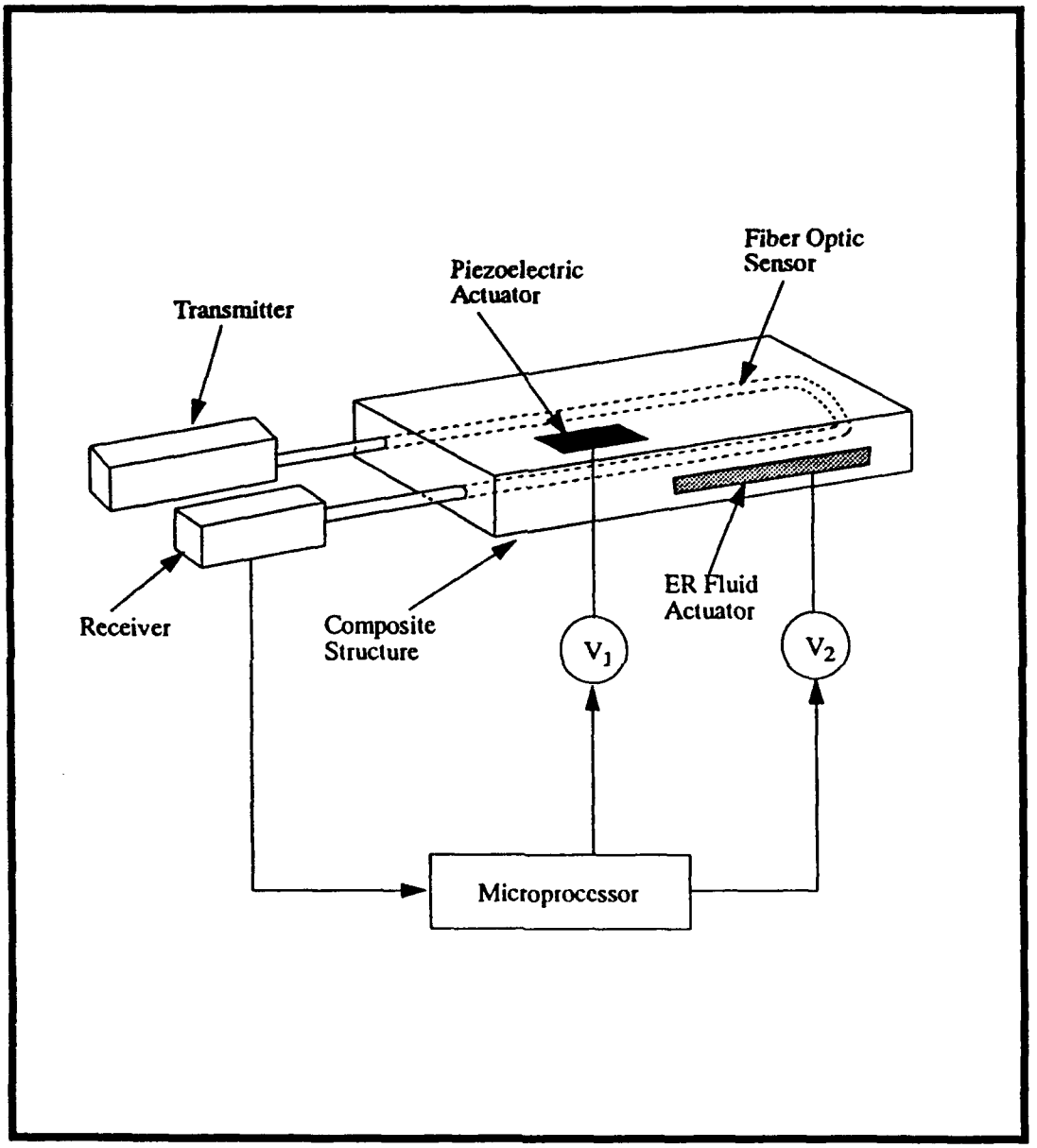

Fig. VI.2 Smart beam featuring a hybrid actuation and sensing system.

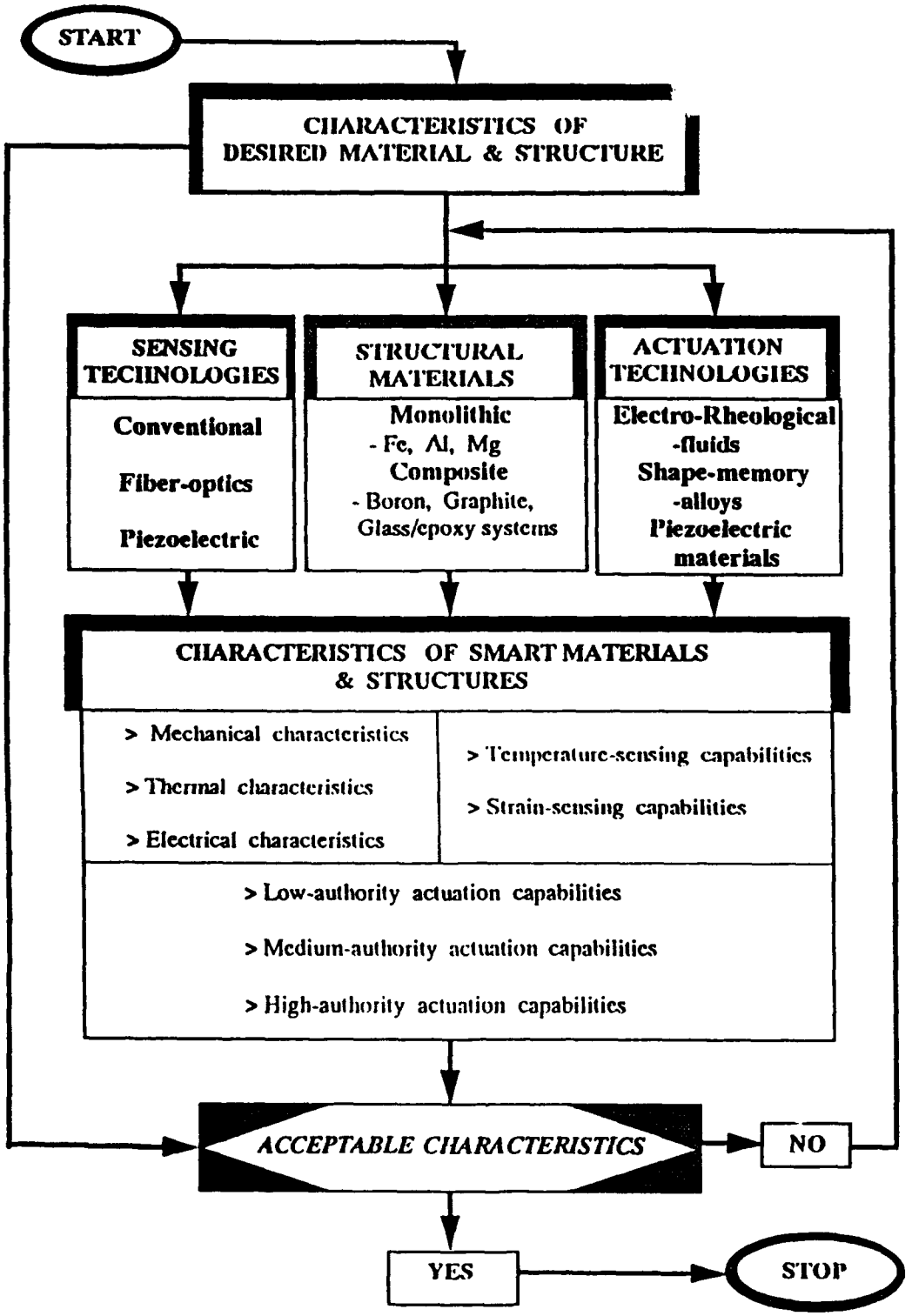

Fig. VI.3 An algorithm for synthesizing a smart material featuring structural materials, actuation technologies, and sensing technologies.

Smart materials and structures in the foreseeable future will in the most general sense comprise an integrated set of discrete subsystems featuring structural materials, sensors, actuators, and microprocessing capabilities as indicated in Figure VI.2. The design philosophy presented in Figure VI.3 contains a very large multi-parameter search domain because of the very large number of decisions and design parameters associated with the properties and characteristics of sensors, structures, and actuators. Typical experimental results for a hybrid beam featuring ER fluid and piezoelectric actuators are presented in Figure VI.4. Furthermore, the designer seeking a global optimal solution in the synthesis of an appropriate smart material for a particular application also must address other crucial decisions concerning computational capabilities, networking issues, and appropriate control strategies.

The establishment of a set of viable analytical tools for predicting the behavior of smart materials and structures featuring embedded actuator materials, the characteristics of the structural materials, and also the characteristics of the interface regions and the characteristics of the piezo-electric actuators, is a prerequisite for hybrid optimal control strategies for smart mechanical and structural systems, featuring multi-functional smart actuation and sensing capabilities. Since these materials will typically be employed in engineering practice to satisfy various performance specifications, the tailoring of the structural characteristics by employing hybrid optimal control strategies is a crucial step in the development of the knowledge-base in this area.

Consider, for example, the task of controlling the vibrational response of a smart structure featuring embedded hybrid electrorheological and piezo-electric actuators. By incorporating suitable simplifying assumptions, the governing equations can be formulated as

$$\dot{\mathbf{x}} = \mathbf{A}\,\mathbf{x} + \mathbf{B}\,\mathbf{U} + \mathbf{B}_1\,\mathbf{V}_1 + \mathbf{B}_2\,\mathbf{V}_2$$
$$\mathbf{y} = \mathbf{C}\,\mathbf{x}$$

where $\mathbf{y}$ is the output vector and $\mathbf{x}$ is the state variable vector, where $\mathbf{A}$ is the plant matrix, $\mathbf{B}$ is the input matrix associated with the electrorheological actuator, while, $\mathbf{B}_2$ is the input matrix associated with the piezo-electric actuator. Vectors $\mathbf{U}$, $\mathbf{V}_1$, and $\mathbf{V}_2$ provide the system inputs associated with the conventional, electrorheological and piezo-electric actuators, respectively.

In the context of this mathematical framework attention may by focused on optimal hybrid control strategies for the following problem of finding the optimal location of distributed actuators incorporating electrorheological fluids and piezo-electric materials which maximize the control influence matrices $\mathbf{B}_1$ and $\mathbf{B}_2$. For the matrix $\mathbf{B}_2$ associated with the piezo-electric actuator find the optimal location which maximizes the difference of the modal slope coefficients of the actuator segment, for example. This problem may be summarized as follows:

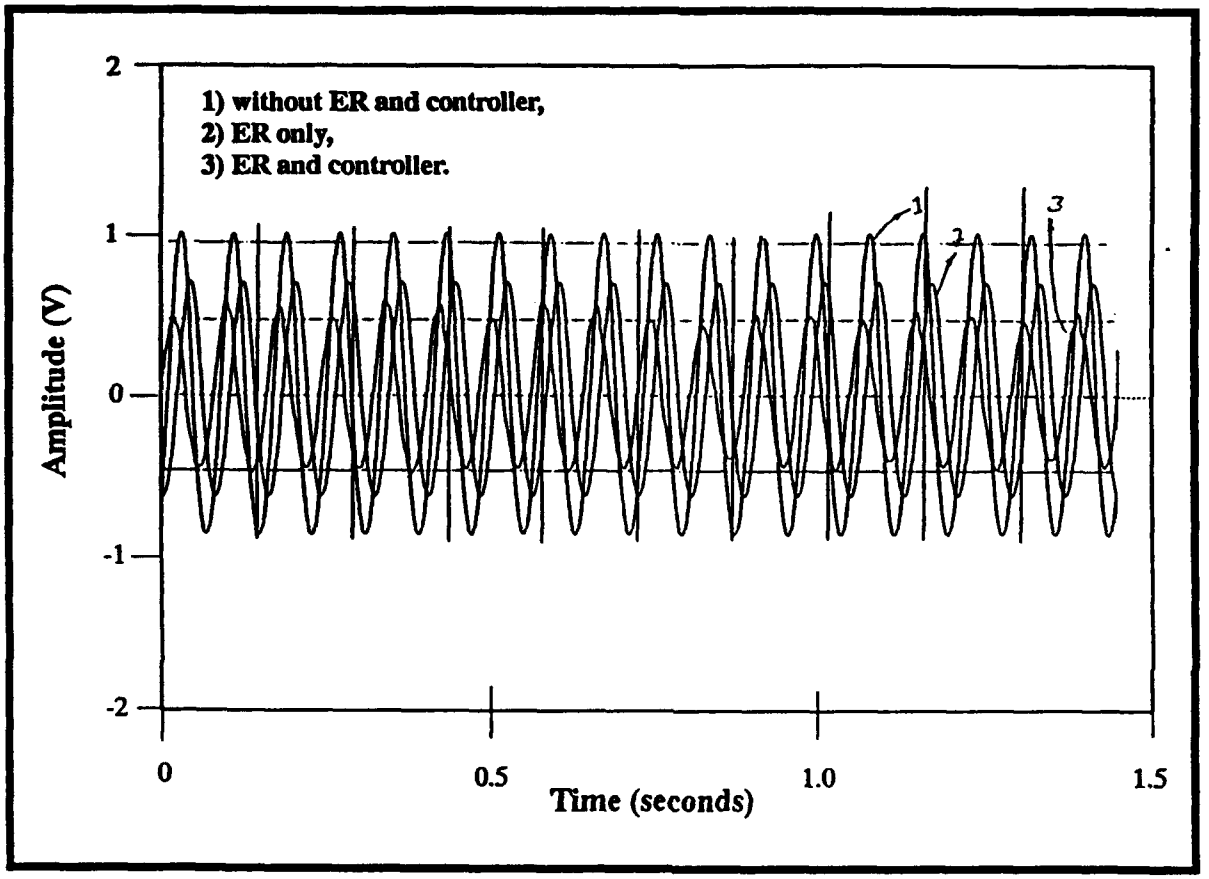

Fig. VI.4 The elastodynamic response characteristics of a hybrid beam featuring an ER fluid and piezoelectric actuators.

$$Maximize \left(\frac{d\phi_i}{dx}(x_i^1) - \frac{d\phi_i}{dx}(x_i^2)\right)$$

subjected to geometrical and material constraints.

Similarly, for minimizing rise time, the problem reduces to the design of the controller inputs **U** and $\mathbf{V_1}$ which minimize the performance index

$$J = \int (x^T Q x + U^T R_1 U + U_1^T R_2 U_1)dt$$

with state weighting matrix,

Q which is partitioned into a matrix $\mathbf{Q_1}$ and a matrix ϵ **I**,
I is the identity matrix,
$\mathbf{Q_1}$ is associated with velocity state,
ϵ **I** is associated with displacement state,
$\mathbf{R_1}$ and $\mathbf{R_2}$ are the control weighting matrices.

Clearly, the optimal hybrid control strategies for minimizing settling time, rise time, overshoot time and tailoring the aeroelastic characteristics in the presence of external disturbances and bounded uncertainties, can be formulated in the analogous manner for a variety of actuator materials including magnetostrictive materials and shape-memory-alloys, for example.

VII DAMAGE DETECTION STRATEGIES FOR SMART STRUCTURES

The defense industry is increasingly fabricating structures with composite materials. Consequently the development of a *built-in* damage assessment system that could constantly monitor the structural integrity of each critical component in a system would greatly alleviate concerns over the introduction of composite materials, as well as substantially reduce the cost of their deployment in rotorcraft systems, for example caused by a reduction in down-time for inspection. For composite materials a built-in monitoring system can be based on a grid of optical fibers imbedded within the structure at the time of manufacture.

7.1 FIBER-OPTIC DETECTION OF ACOUSTIC EMISSION ASSOCIATED WITH COMPOSITE DAMAGE

One approach to fiber-optic damage assessment employs the high sensitivity of an interferometric based system to detect acoustic energy released as a result of matrix cracking, fiber breakage or interlamina debonding (delamination) within composite materials. An embedded Michelson fiber-optic strain gauge can detect delaminations caused by out-of-plane loading of Kevlar/epoxy laminate panels. Image enhanced backlighting has been used to confirm the creation of the delamination association with the acoustic signal. Although these results are somewhat preliminary, they represent the first direct confirmation of the feasibility of detecting a specific form of composite damage with embedded optical fiber sensors. Indeed research results suggest that the different modes of damage within composites can be discerned from their acoustic emission signals

7.2 FUNDAMENTALS OF COMPOSITE DAMAGE DETECTED WITH EMBEDDED OPTICAL FIBERS

Fracture of optical fibers, with the attendant disruption in their transmitted light, represents the simplest technique for damage detection. Optical fibers imbedded within carbon/epoxy composite materials were shown to detect severe impact damage

sometimes inflicted on submarine acoustic domes. This concept was then extended to damage detection in composite structures of relevance to aircraft.

In the case of Kevlar/epoxy panels, experimental studies have shown that the imbedded optical fibers fracture only when they were in the immediate impact zone, and then only if substantial damage was inflicted. A special treatment of optical fibers has been devised for reducing the strength of these optical waveguides and thereby control their damage sensitivity. A combination of optical bleeding and image enhanced backlighting was used in an extensive analysis of the dependence of the sensitivity to fracture of the treated optical fibers with respect to: their orientation relative to the material reinforcing fibers in the adjacent plies and their depth location within the structure. The greatest sensitivity to damage arises when the optical fibers are embedded as close to the surface of maximum tensile strain as possible and sandwiched orthogonally between a pair of collinear plies. When this is not possible, the orientation leading to the best damage response for optical fibers embedded between a given pair of plies is determined by the most likely direction for transverse matrix crack propagation. This in turn depends upon the overall layup and the direction of the applied load. This observation is consistent with the premise that through-the-thickness matrix cracks constitute the principal fracture mechanism for embedded optical fibers.

In general the optical fibers should be configured perpendicular to the reinforcing fibers in the ply that separates the optical fibers from the region of damage to be sensed. This arrangement would, however, be unsatisfactory if it lead to the optical fibers being aligned with one of the ply directions. Under these circumstances it would be better to orient the optical fibers so that they bisect the larger angle between the plies.

7.3 GROWTH OF COMPOSITE DAMAGE DETECTED WITH EMBEDDED OPTICAL FIBERS

Research investigations have shown that imbedded optical fibers can detect load induced growth of a region of damage in a fibrous composite structure. In this research various fiber-optic instrumented multi-ply Kevlar/epoxy panels were simply supported on all four edges and subjected to a central force that caused out-of-plane deformation. In between successive deformations the panel was examined by backlighting to assess the formation of delaminations and the embedded optical fibers were interrogated by laser radiation to determine where they had fractured.

These results are fairly representative of many experiments and this work is very encouraging since it strongly indicates the viability of using embedded optical fibers to assess the growth of a region of delamination. Further work, suggests that optical fibers are able to sense the presence of delaminations between lamina that are located several

plies away provided they are able to communicate with the optical fibers by means of through-the-thickness matrix cracks.

7.4 AIRCRAFT WING LEADING EDGE FIBER-OPTIC DAMAGE ASSESSMENT SYSTEM

The University of Toronto Institute for Aerospace Studies have just completed the fabrication of the world's first aircraft composite leading edge containing a build-in fiber-optic damage assessment system with the assistance and collaboration of Boeing - de Havilland Division. This is the culmination of a study that involved undertaking a substantial series of impact experiments on planar versions of the leading edge, to determine the minimum number of optical fiber arrays and their optimum placement and orientation. This work resulted in the conclusion that it was necessary to employ three arrays of damage-sensitized optical fibers embedded within three separate lamina.

Although the visual inspection of the light transmitted through the optical fibers can be used to assess damage, a photodiode array that is butt fitted against the optical fiber output port is more a reliable approach. The output from the photodiode array will be interpreted by a computer and a display of the predicted region of damage will be presented on a monitor.

7.5 DAMAGE DETECTION ALGORITHMS

The analytic redundancy approach to failure detection and isolation problems in dynamic systems uses the analytic relationships between various sensor outputs arising from a knowledge of the underlying system dynamics. Analytic redundancy can be either in the form of algebraic redundancy involving the instantaneous relationship between sensor outputs, or dynamic redundancy involving the relationship between the time histories of sensor outputs. The term "analytic redundancy" was coined in the early seventies to differentiate this technique from the traditional hardware redundancy approach in which the outputs of like sensors are compared for failure detection. Analytic redundancy comes about from the common estimation capability of various sensor groups. Sensor failure detection and isolation algorithms make use of this inherent analytic redundancy by considering different sensor subsets. Hence, the analytic redundancy approach offers the capability of comparing dissimilar instrument outputs for failure detection and thus, allows the design of reliable systems with reduced hardware duplication requirements.

During the past twenty years, or so, several failure detection and isolation algorithms applicable to damage detection problems for smart structures have been developed based on dynamic system descriptions. Such analytic redundancy research culminated in

the development of aircraft sensor fault tolerant digital flight control systems, engine sensor failure detection systems, strapped down navigation systems with skewed sensor arrays, sensor fault tolerant integrated flight control and navigation systems, and more recently in reconfiguration strategies for aircraft subjected to actuator failure/surface damage.

General failure detection and isolation methods for dynamic systems can be divided into the following groups: a) parity techniques; b) failure sensitive filters; c) jump parameter formulations; d) multiple model methods; e) innovations signature analysis. Parity techniques encompass the standard voting techniques for systems with parallel hardware redundancy and their generalizations to systems with algebraic redundancy . Failure sensitive filters exploit output decoupling concepts are used to make failures manifest themselves in a fixed direction within the measurement space. In jump parameter formulations, failures are modeled as jumps in system parameters. Multiple model methods are based on constructing a different model for each failure mode. Innovations signature analysis techniques include performing statistical tests on measurement innovations.

Recent work has concentrated on extending the signature analysis methods to non-linear dynamic systems with modelling uncertainties. For instance, the research by Cagayan and Rahnamai resulted in a hierarchical actuator failure/surface damage detection and isolation system based on the modification of the multiple hypothesis test to account for modelling errors in aircraft dynamics. In this approach, isolation thresholds are introduced in addition to detection thresholds so that the algorithm first declares a detection decision with a partial isolation decision, and a full isolation decision only when a certain distinguishability criterion is met. The performance of this developed actuator failure/surface damage detection and isolation system has been demonstrated using the non-linear AFTI F16 and Combat Reconfigurable Control Aircraft dynamic simulators.

The advantages to using analytic redundancy in reliability improvement will be more pronounced in developing damage detection algorithms for large space structures (LSS). Due to weight limitations, these structures will be very flexible and, therefore, the suppression of the structural vibrations by active control will be necessary for the critical substructures. Furthermore, the proposed functional uses will dictate stringent design specifications for shape control and pointing accuracy. Consequently, the overall reliability design of the control hardware deployed in LSS will be critical in satisfying the vibration suppression, shape control and pointing accuracy specifications. These requirements, along with the weight and the volume limitations of the sensors and actuators which can be transported into space, will necessitate the use of analytic redundancy in the design of fault tolerant control systems for LSS. The automated diagnostics capability provided by the analytic redundancy approach will be especially important in unmanned structures such as the large flexible antennas. In addition, the reliability provided by an analytic redundancy based scheme would be indispensable in

an application where the accuracy requirement is critical, e.g., the pointing accuracy of a microwave energy transmitter.

The current failure detection and isolation technology developed for the conventional rigid aircraft will not be directly applicable to large space structures. First, these structures have infinite dimensionality since they are distributed parameter systems. In practice, their description will be approximated, through modal truncation, by a large dimensional linear system. Therefore, current methods for low order systems will be unsuitable for LSS due to the increased system order. The second challenge in LSS will be the inadequacy of the modal used for the system description, due both to truncation and to a lack of knowledge about the parameters of the truncated model. For instance, the application of the generalized parity technique to a simple flexible beam problem has shown that this approach is very sensitive to system parameter errors. Again, the current methods which may be adequate for low dimensional systems with fairly known parameters, e.g. a conventional rigid body aircraft will prove unsuitable for LSS due to large false alarms caused by the parameter modeling errors. Since on-earth-testing for LSS will be extremely limited, these limitations should be incorporated into the design.

VIII ARTIFICIAL INTELLIGENCE STRATEGIES FOR SMART STRUCTURES

The recent success of expert systems technology, a subfield of artificial intelligence, in diagnosis and monitoring problems in certain application domains has initiated similar efforts in onboard flight monitoring and diagnosis as well. Successful expert system applications such as SOPHIE in computer assisted instruction, MYCIN in medical diagnosis, PROSPECTOR in oil exploration, DENDRAL in biology initiated onboard real-time expert system developments such as Experimental Expert Flight Status Monitor (EEFSM) in flight control systems monitoring, FAULTFINDER in onboard aircraft diagnostics, and expert systems for self-repairing flight control system maintenance diagnostic.

An expert system is a computer program that can perform a task normally requiring the reasoning ability of a human expert. Expert systems are highly specialized according to their application domains. Although any program solving a particular problem may be considered to exhibit expert behavior such as computer programs implementing the damage detection algorithms described in the last section, expert systems are differentiated form other programs according to the manner in which the application domain specific knowledge is structured within a program. In particular, expert system programs partition their knowledge into the following three block: Data Base, Rule Base, and Inference Engine.

In other words, the knowledge about the application domain is compartmentalized rather than distributed throughout the program. The Data Base contains the facts about the application domain. The Rule Base contains the set of rules specifying how facts in the Data Base can be combined to generate new facts and form conclusions. The Inference Engine determines the construct of reasoning in the application of the rules. For instance, the diagnostic system MYCIN starts from the symptom facts in order to find the conditions causing the symptom. This manner of reasoning is called "backward chaining". In contrast, "forward chaining" inference starts with the established facts to find a set of consistent conclusions. The partitioning of application domain knowledge in expert systems allow the incremental addition of rules to the Rule Base without major revisions to the program. Moreover, the expert system can explain the reasoning chain by recording the rules as they are applied.

While expert systems have been traditionally built using collections of rules based on empirical associations, interest has grown recently in *knowledge-based expert systems*

which perform reasoning from representations of structure and function knowledge. For instance, an expert system for digital electronic systems troubleshooting is developed by using a structural and behavioral description of digital circuits. Qualitative process (Q^P) theory is another approach allowing the representation of causal behavior based on a qualitative representation of numerical knowledge using predicate calculus.

Q^P theory is a first-order predicate calculus defined on objects parameterized by a quantity consisting of two parts: an amount and a derivative, each represented by a sign and magnitude. In qualitative Process theory, physical systems are described in terms of a collection of objects, their properties, and the relationships among them within a framework of a first order predicate calculus.

In applying Q^P theory to physical dynamic systems such as structural damage detection problems, the bottoms-up approach in getting the qualitative rules from low levels of elemental descriptions can possibly yield erroneous results at higher levels. In contrast, finding qualitative rules at high levels using a complete knowledge of the system via reduced order modelling would not be susceptible to such problems.

For fault diagnosis in digital circuit applications, some researchers have advocated reasoning from first principles starting with simple hypotheses, keep track of simplifying assumptions made, and using multiple representations (e.g., both physical and functional representation of a digital circuit). The multiple representation approach is analogous to hierarchical knowledge representation at several levels of abstraction used in modelling human problem solving strategies for complex systems.

This hierarchical knowledge representation introduces an abstraction hierarchy in modelling human fault diagnostic strategies. This hierarchy is two dimensional. The first is the functional layers of abstraction for the physical system: functional purpose, abstract function, generalized function, and physical form. The second is the structural layers of abstraction for the physical system: system, subsystem, module, submodule, component. Using a qualitative approximation method based on a simplified version of such a functional hierarchy, a training system for marine engineers of a steam power plant has been developed.

The aerospace flight and space application domain introduce the attribute of dynamics not encountered in early applications of expert systems. This has necessitated the inclusion of a dynamics knowledge into expert systems implementations. Current commercially available expert system building tools (shells) are not generally applicable to building expert systems for onboard fault diagnosis applications due to the following reasons: 1) the shells are not fast enough; 2) the shells have insufficient facilities for temporal reasoning; 3) the shells are not easily embeddable into conventional high level programming languages and most cannot run on numeric microprocessors used for embedded applications; 4) the shells have insufficient facilities for devoting attention to significant events; 5) the shells are not designed to accept onboard sensor data; 6) the

shells have no integration with a real-time clock and do not handle hardware interrupts; 7) the shells cannot provide guaranteed response times.

As discussed previously, most interpretive expert system shells spend 90% of their time in matching the current facts against the antecedent of rules in their rule base. Hence, an expert system development approach where the interpretive processing is performed off-line would offer a substantial execution time improvement. Similarly, the execution efficiency is a strong function of knowledge representation facilities employed in the expert system shell. For instance, an approach based on multiple hierarchical representations of a physical system and using forward chaining would have a linear execution time complexity as compared to a rule based system with forward chaining having exponential time complexity.

For ease of integration into conventional high level programs, programming language of the expert system shell is an important choice. For instance, the choice of a programming language commonly used for embedded application such as Ada or C would be advantageous from an integration viewpoint. Moreover, such an expert system would be easily portable to microprocessors commonly used for embedded applications (e.g., 1750A, 80386, 68020). Moreover, the language constructs for handling real-time issues (tasking, interrupt servicing, exception handling) would be available to such an expert system development tool.

There are two formal definitions for real-time expert systems: the expert system is said to exhibit real-time performance if a) it is predictably fast enough for the process being served, or b) if it can provide a response within a given time limit.

For real-time fault diagnosis applications, even if an expert system satisfies both of these premises, it would still not be sufficient for inclusion in an embedded application since the quality of the response would determine its inclusion in an onboard time-critical system. We believe that the following is an appropriate criterion for real-time expert systems for embedded applications: an expert system is said to exhibit real-time performance if the execution speed of a stand alone compiled version of the expert system for a fixed application is comparable to the speed of a real-time conventional program written to solve the specific application at hand.

The integration of expert systems technology into time-critical applications presents new challenges due to the unique attributes of these applications. For instance, most expert systems have usually been implemented as stand alone computer programs that presuppose a high degree of human interaction will be available during the problem solving process. While this approach is quite satisfactory for many naturally interactive applications, immediate human interaction is neither available nor desirable in time-critical smart structure applications. Similarly, the powerful explanation feature of the inference mechanism in expert systems is also neither required nor desirable during on-line execution in these applications.

IX NEURAL NETWORKS FOR SMART STRUCTURES

Neural networks represent a non-algorithmic class of information processing which employ massively parallel distributed processing architectures. Stimulated by the efforts directed at understanding the interconnection of neurons in the human brain. These neural networks allow the storage, retrieval, and processing of complex data. Research during the last 25 years in artificial neural systems has produced solutions to complex problems in visual pattern recognition, combinatorial search, and adaptive signal processing.

The most common artificial neural net structure is a network of processing elements (neurons) connected with each other through interconnects (information links). Each processing element can have multiple inputs and only one output. The input/output relationship is described by a first-order differential equation. Specifically, a weighted sum of the nonlinear transformations of the multiple inputs along with a nonlinear transformation of the current neuron's state are the driving functions of this first-order differential equation. The weighing coefficients also satisfy a first-order differential equation driven by a nonlinear transformation of multiple inputs and the weighing coefficients associated with the input links. These two first-order differential equations (also called the update and learning rules) and a specific network topology provide a complete neural network specification.

Artificial neural networks produce a nearest-neighbor classifier. Since the weighing coefficients change in an unpredictable manner, the global stability of the neural network description is an important consideration. The strongest theoretical result to date shows that the neural net converges to one of the finite set of equilibrium points corresponding to local minima of the energy function under certain restrictive conditions (e.g., symmetric, positive weighing coefficients). Another advantage of neural nets is that the convergence to the answer is independent of the number of local minima in the energy function, thus comparing favorably to other general search techniques. Although the global stability and convergence results have not been extended to the case for nonsymmetric weighing coefficients have been reported.

Conceptually, artificial neural networks are applicable to smart structures for learning spatio-temporal stress patterns associated with an undamaged structure for use in detecting structural damage. The relationship between artificial neural network approach to spatio-temporal pattern recognition and conventional signal processing

structures (i.e., finite impulse filters, correlation detectors, etc.) has been discussed by some researchers. Used in this context for smart structures, neural networks would be the nonalgorithmic counterpart of spatio-temporal filters. It is also conceptually possible to train a neural network representation of a structure with a multitude of damaged structure scenarios isolating a specific damage using the neural net as a classifier. The relative advantages and disadvantages of this approach are discussed on the next section.

The recent interest in artificial neural networks is due to the availability of fast, relatively inexpensive computers made possible by advances in VLSI design for realizing neural network structures. Given that the neurons in the human brain process information in milliseconds while outperforming current serial supercomputers with a processing rate in nanoseconds, there is considerable interest in the new generation neurocomputers and computing environments.

X VIBRATION CHARACTERISTICS OF SMART STRUCTURES

Smart structures typically exploit the dynamically-tunable characteristics of electrorheological fluids and piezoelectric materials by embedding these functional materials into host structural materials which are fabricated in either conventional materials or advanced composite materials.

In order to determine the feasibility of exploiting this class of smart structures for U.S. Army applications the following technical issues were addressed

1. Analytical and experimental investigation of the vibration characteristics of smart beams.

2. Development of a mathematical capability to predict the vibration characteristics of smart structures featuring embedded electrorheological fluids and piezoelectric materials.

The objective of the early experimental programs in the field of smart structural materials featuring ER fluids, was to investigate both the static and the transient response characteristics of various cantilevered beam specimens, fabricated in smart ultra-advanced composite materials in a variety of different operating conditions, in order to provide a basis for evaluating the controllability of these structures in real-time. The transient responses were characterized by the fundamental transverse natural frequencies and the damping ratios. Different classes of beams were fabricated featuring different electrode materials, different fluid volume fractions and different geometrical dimensions. In the first set of tests, specimens were fabricated using graphite prepreg tape AS4/3501-6 manufactured by Hercules, Inc. as the face or electrode material, and each electrode comprised three plies with the lay-ups [90/0/90] for specimen classifications A, B, and C, and [0/90/0] for specimen classification D. The face plates were appropriately configured to provide beams with symmetrical lay-ups and geometry. An RTV silicone rubber adhesive was selected as an insulator in order to provide both excellent bonding between the electrodes and furnish a high dielectric constant.

A schematic diagram of the experimental apparatus employed for evaluating the static and transient responses of cantilevered beams is presented in Figure X.1. Figure X.2 presents the static load-deflection characteristics for the four classes of specimens tested. These nominally linear characteristics clearly demonstrate that the type of ER fluid and

the lay-up of the AS4/3501-6 electrodes have a profound influence upon the response behavior. Moreover, upon carefully scrutinizing the characteristics in the two reference states, it is evident that when a voltage field of 2 kV/mm is generated, all of the specimens become stiffer relative to their reference state of 0 kV/mm. For specimen classification A, the increase in stiffness is negligible, but for specimen classifications B, C, and D the beam stiffness increases by 7%, 10%, and 6%, respectively. Class B and C specimens contain the same ER fluid, and the same electrode lay-up, but class C specimens have an ER fluid volume fraction of 39.4% rather than 36.1%.

The transient vibrational response characteristics of the beam specimens were obtained by imposing an initial tip displacement prior to removing this constraint and subsequently monitoring the resulting transient response. Figure X.3 presents photographs of oscilloscope traces of the transient elastodynamic responses of Class B specimens at room temperature. It is evident from these results that the frequency of the response and also the damping ratio of the signal are strongly dependent upon the voltage applied to the beams. Figure X.4 presents a comparison of the relative frequency and damping ratio increments between Class A and B specimens as a function of the applied voltage. The relative increment in the frequency and damping ratio of each ultra-advanced composite beam specimen in the presence of an electric field, is defined with respect to the corresponding magnitudes in the absence of an electric field, which are employed as datums. Class A and B specimens are identical except for the type of ER fluid filling the beam cavity. Thus, Figure X.4 clearly indicates that the elastodynamic response of specimens featuring ER fluid IMSL-B-88 are much more sensitive to the applied voltage than specimens containing ER fluid IMSL-A-88.

Figure X.5 presents a comparison of the relative frequency and damping ratio increments for Class B specimens with a [90/0/90] lay-up and Class D specimens which feature a [0/90/0] lay-up. In the absence of an electrical field, Class D specimens have a higher natural frequency and a lower damping ratio than Class B specimens. This is to be anticipated because of the different lay-ups of the electrodes which results in different stiffnesses and energy-dissipation characteristics of the electrodes.

Figure X.6 presents the oscilloscope traces of the controlled transient elastodynamic responses of a Class B specimen. The transient response of the specimen for zero applied voltage is presented in the upper photograph, and the transient response of the identical specimen subjected to the same initial conditions for a different electrical field is presented in the lower photograph. This transient response profile was obtained by developing an electrical field corresponding to 0 kV/mm for the first 0.37 seconds of the response profile, prior to simultaneously imposing a voltage corresponding to a field intensity of 2.5 kV/mm. These two piecewise-constant discrete voltage inputs are active-control inputs based on a bang-bang control strategy. A cursory review of the response profiles presented in Figure X.6 clearly demonstrates that the amplitude of the vibrational response in the two profiles is identical for the first 0.37 seconds.

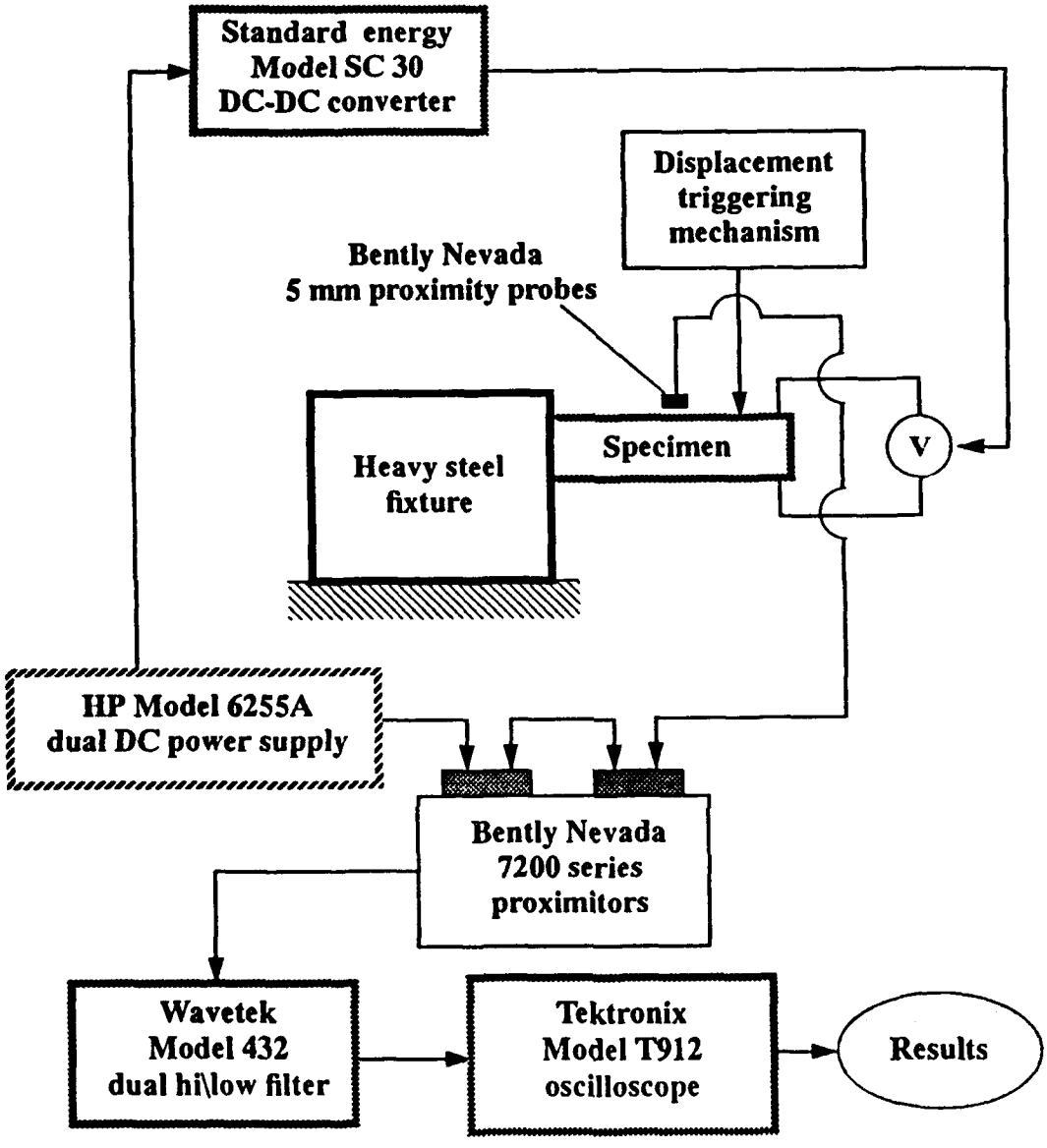

Fig. X.1 A schematic diagram of the experimental apparatus.

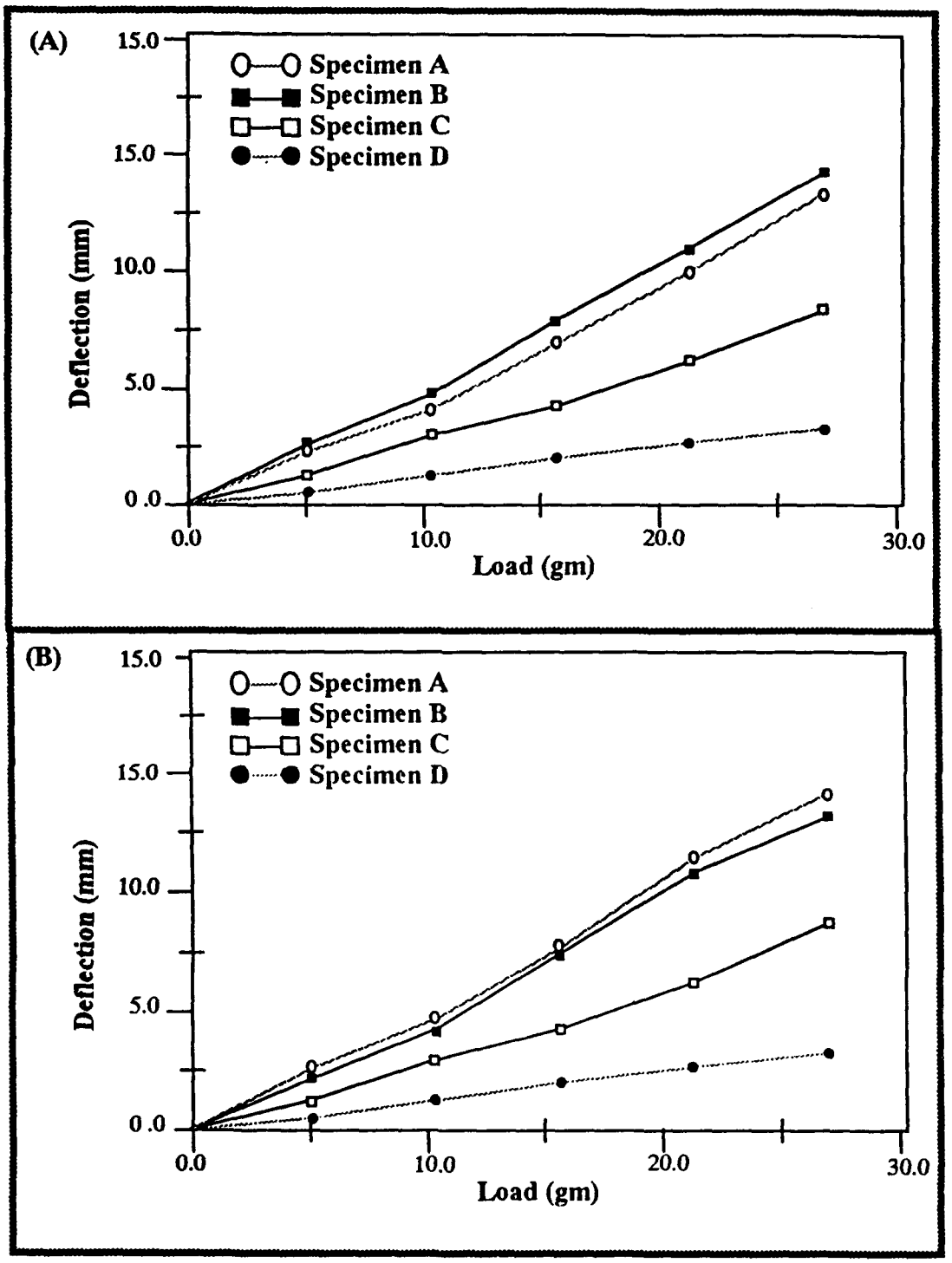

Fig. X.2 Load deflection characteristics for specimen classification A, B, C, and D at (A) 0 kV/mm and 24.5 °C, and (B) 2 kV/mm and 24.5 °C.

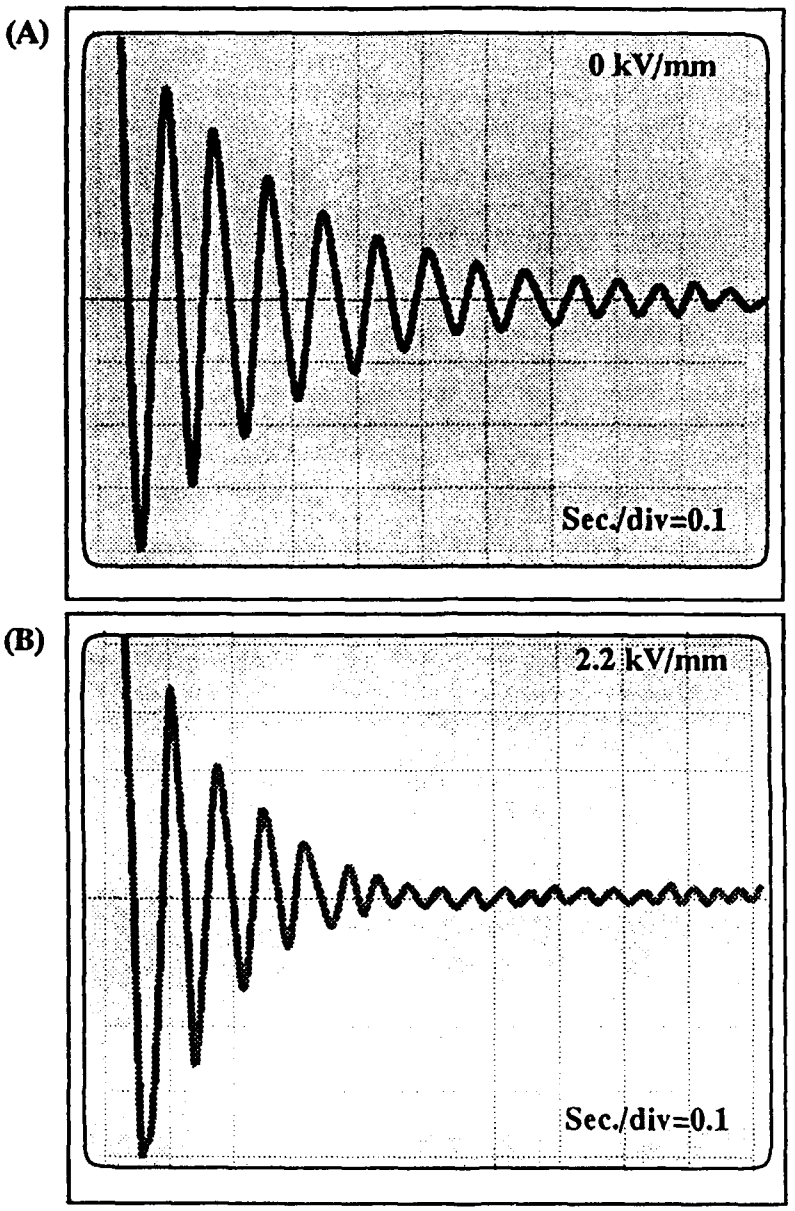

Fig. X.3 Transient response of a Class B specimen at room temperature (A) without and (B) with an electric field imposed on the electrorheological fluid domain

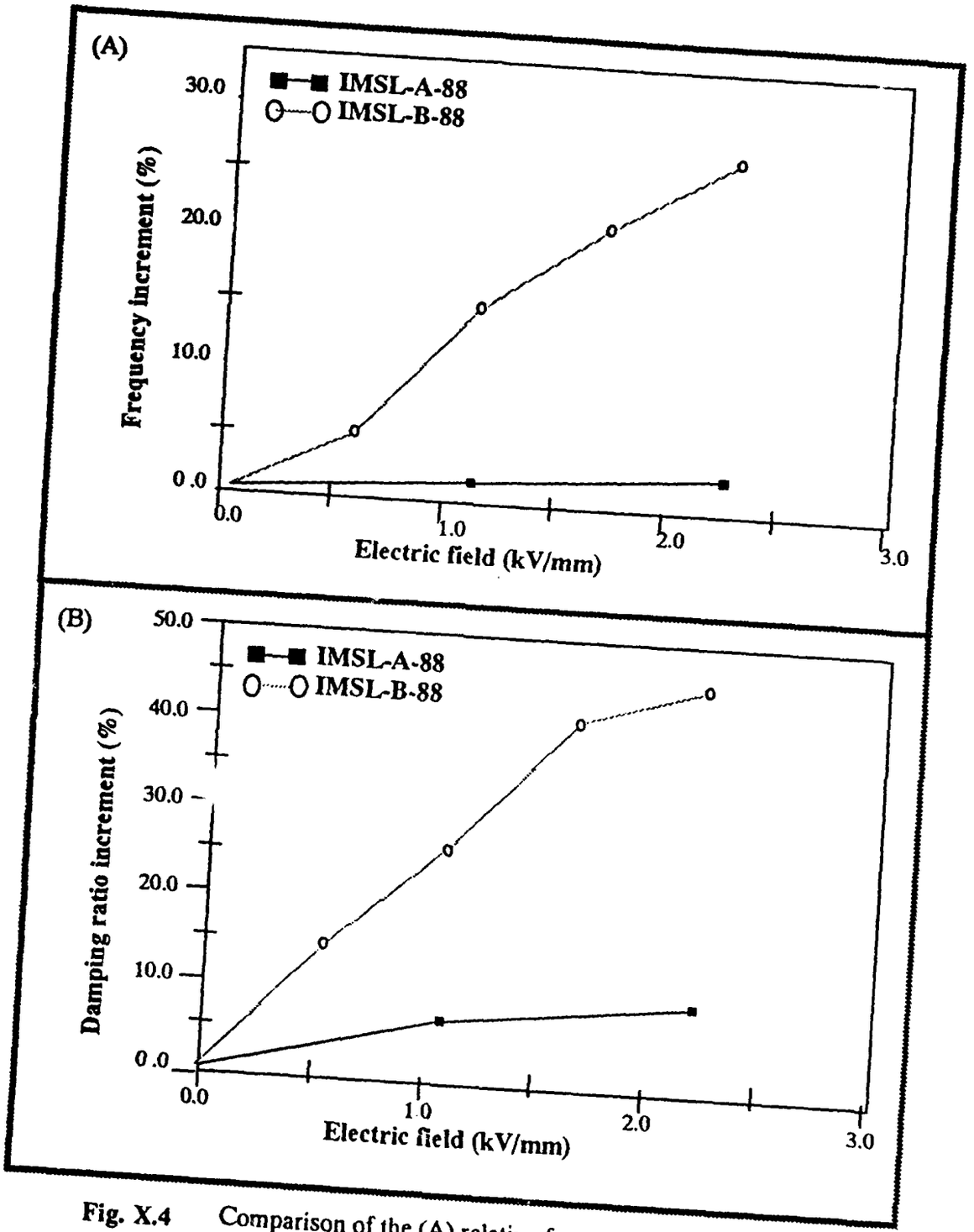

Fig. X.4 Comparison of the (A) relative frequency-increment, and the (B) relative damping-ratio increment, for specimens A and B featuring different ER fluids at room temperature.

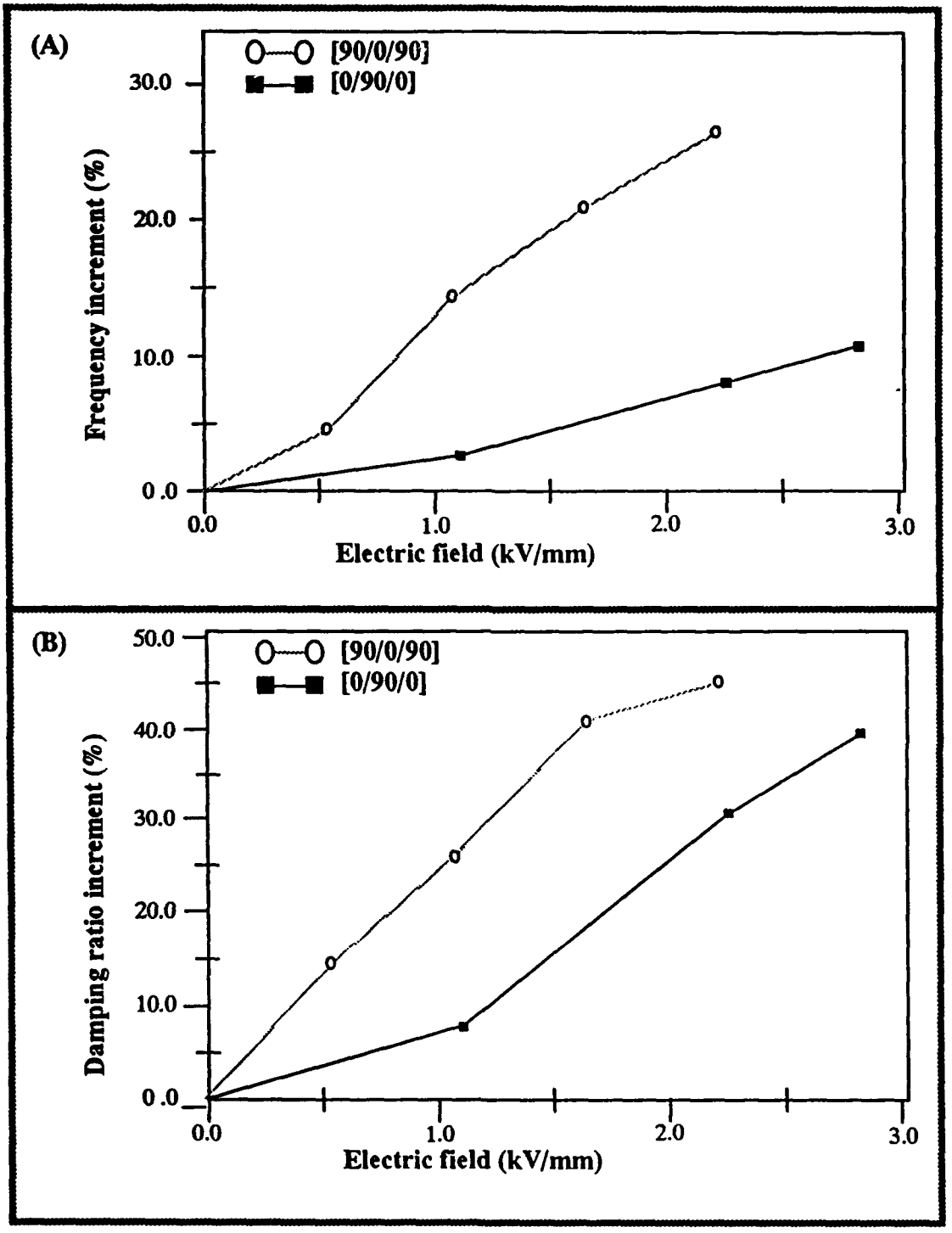

Fig. X.5 Comparison of (A) the relative frequency-increment, and (B) the relative damping-ratio increment between two different lay-ups of face material at room temperature.

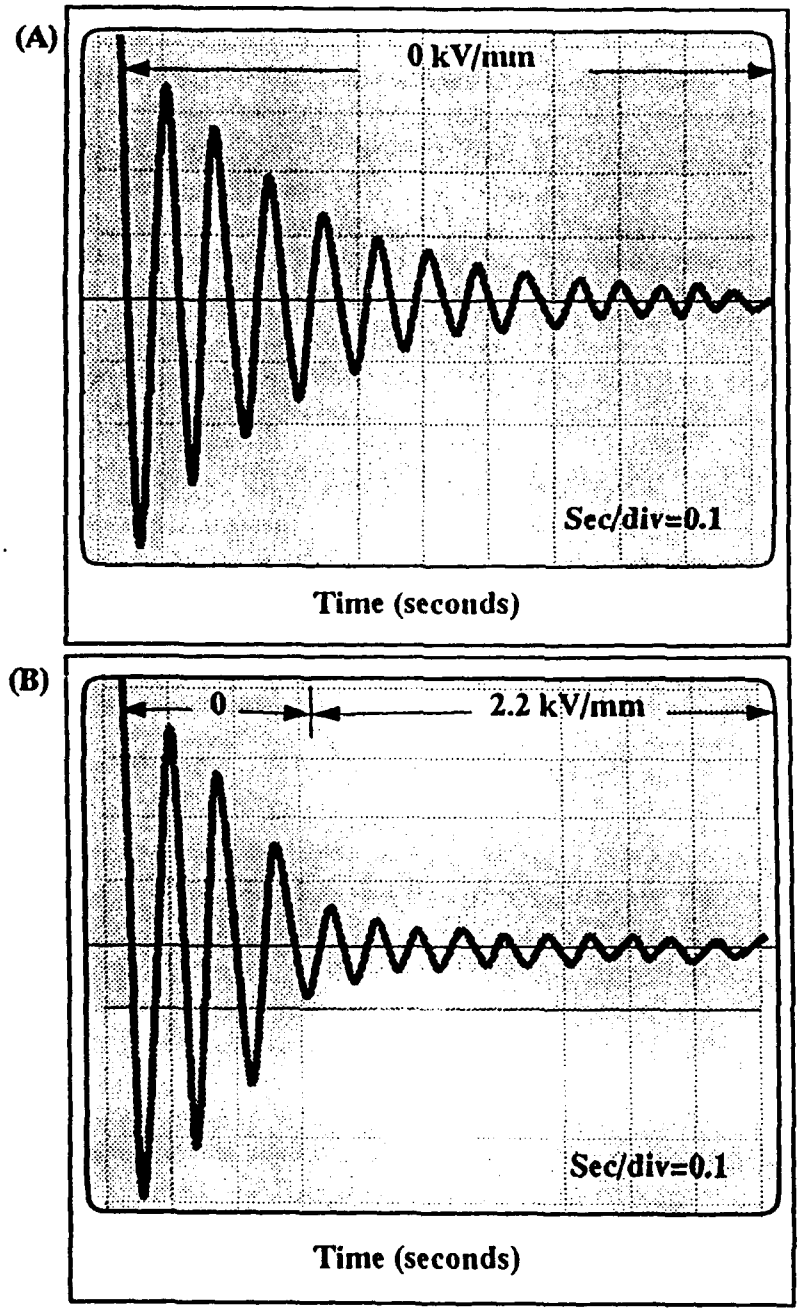

Fig. X.6 Controlled transient response of a class B specimen at room temperature, (A) without control, and (B) with control.

Subsequently, the amplitude of vibration presented in the lower photograph is substantially attenuated upon generating the electrical field strength of 2.5 kV/mm.

A second set of experiments, focused upon evaluating the transient behavior of smart beams featuring aluminum electrodes and various ER fluids, has been reported in the literature. Figure X.7 presents frequency increment and damping data as a function of the electrical field strengths defined with respect to the corresponding magnitudes in the absence of an electrical field. The two classes of beam specimens employed in this study differ only in their respective fluid-solid interface conditions. One set of specimens featured a fluid-solid surface that was subjected to abrasion from carbon sandpaper number A235 manufactured by Norton Corporation. The other set of specimens featured a relatively smooth rolled finish. The smart beams featuring the roughened surface yielded larger in frequency and damping-ratio increments than the unabraded surfaces at the same voltage.

Figure X.8 presents schematically the electrode geometries at the fluid-structural interfaces for class D and class E specimens. These specimens only differed in this feature which involves the bonding of circular and rectangular pieces of polyvinyl sheet of the same total surface area. The results of the transient response studies are presented in Figure X.9 and they indicate that the specimens with the electrodes featuring the rectangular pieces of polyvinyl sheet provided superior response profiles for both frequency and damping than the electrodes featuring the circular polyvinyl disks. Experimental results presented in Figure X.10 demonstrate that both the frequency increment and also the damping-ratio increment increase when the electrode area in contact with the ER fluid domain increases.

The previous discussions have focused upon evaluating the static and transient dynamic response of smart cantilever beams with embedded ER fluid actuators. Subsequently work has been undertaken on evaluating the dynamic response of these systems subjected to forced excitations. Figure X.11 presents a schematic diagram of the apparatus and instrumentation employed in these studies. The smart beam is fixtured to the head of an electrodynamic shaker in a cantilever configuration which enables the beam to be dynamically excited in a controlled manner in order to excite flexural vibrations. The response of the beam at a prescribed sinusoidal excitation can be actively controlled by changing the voltage field imposed upon the ER fluid domain in the beam.

Figure X.12 presents frequency-response results which were obtained by simultaneously exciting the beam with a random noise signal, while the beam was sequentially subjected to two discrete potential differences of 0 kV and 3.42 kV across the upper and lower faces of the beam. In the uncharged state, the first three natural frequencies of the beam in flexure are 20.5 Hz, 79.5 Hz, and 176.0 Hz, while in the charged state of 3.42kV the first three natural frequencies are 35.0 Hz, 135.5 Hz and a value higher than 176.0 Hz which is not observed on the response curve because the upper cut-off frequency was

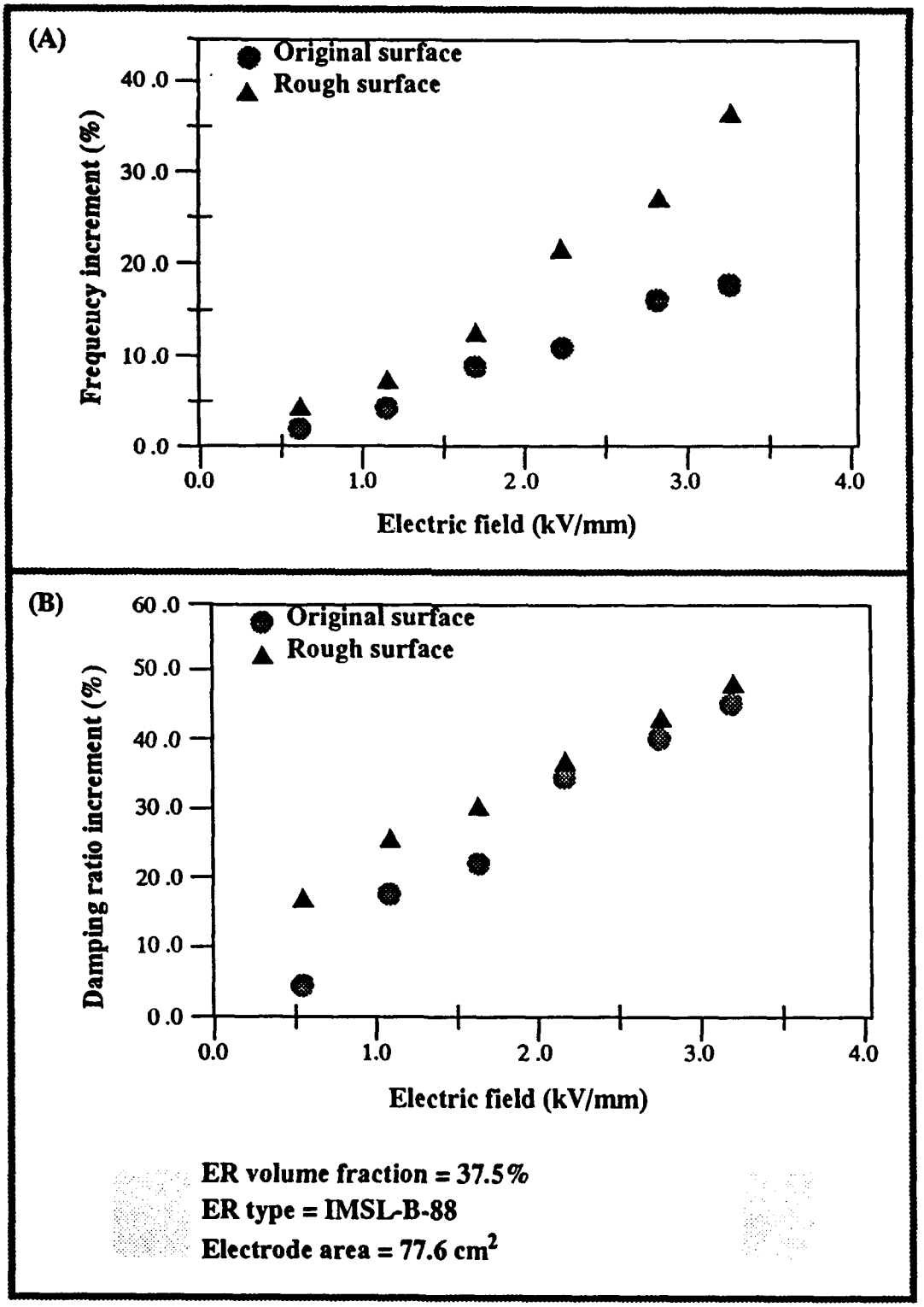

Fig. X.7 (A) Relative frequency-increment, and (B) relative damping-ratio increment of Class A and C specimens.

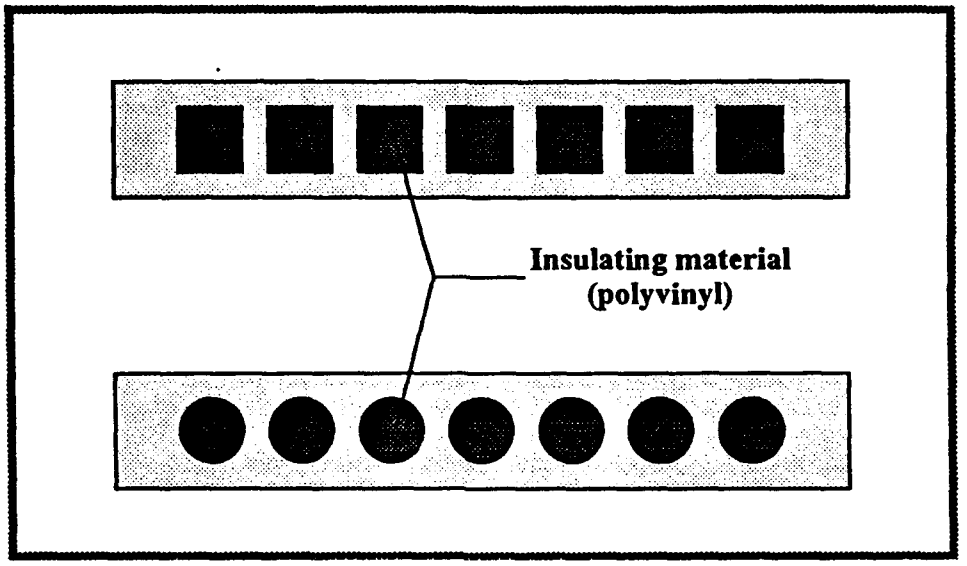

Fig. X.8 Schematic diagram of different electrode surface geometries for Class D and E specimens.

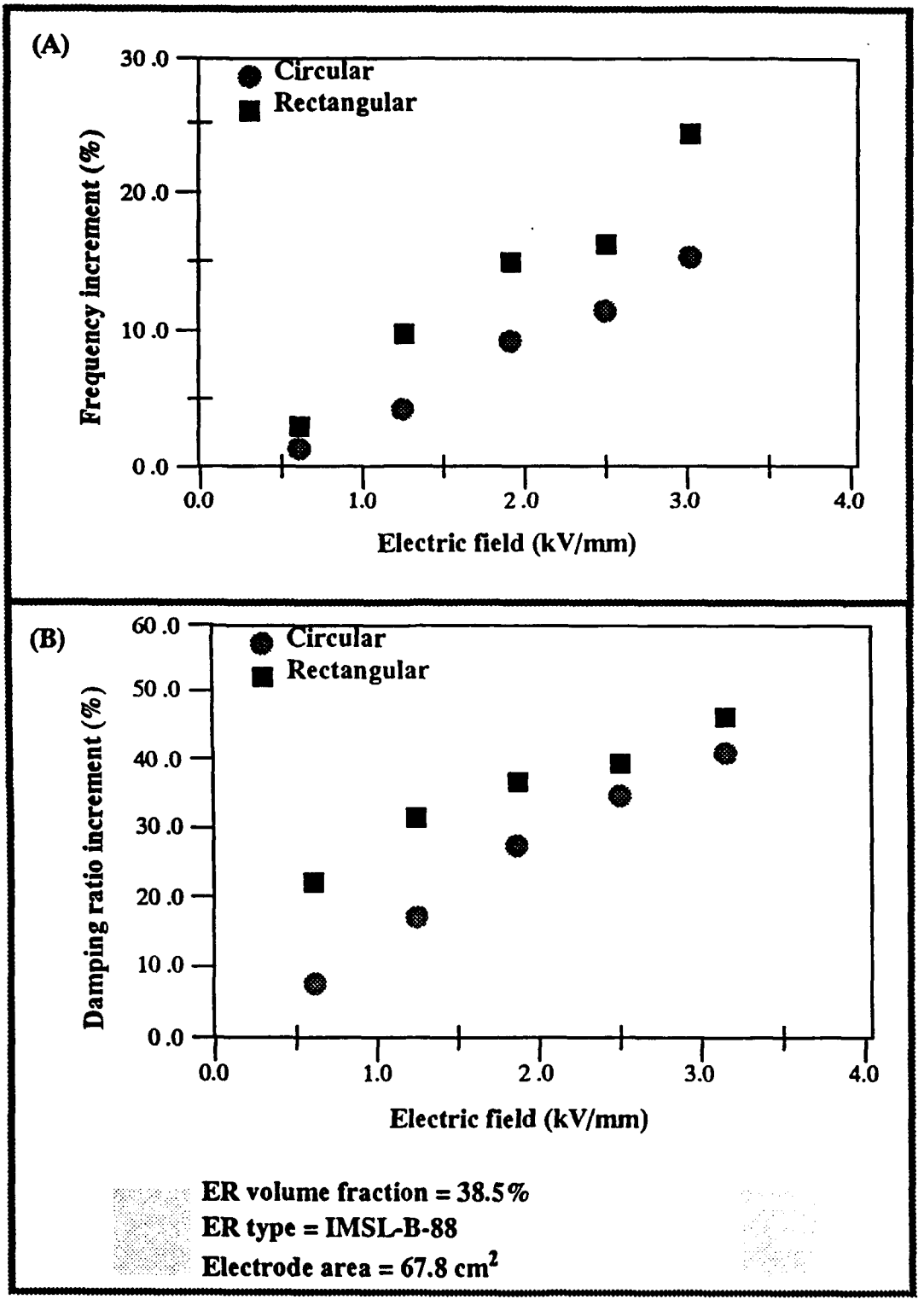

Fig. X.9 (A) Relative frequency-increment, and (B) relative damping-ratio increment of Class D and E specimens.

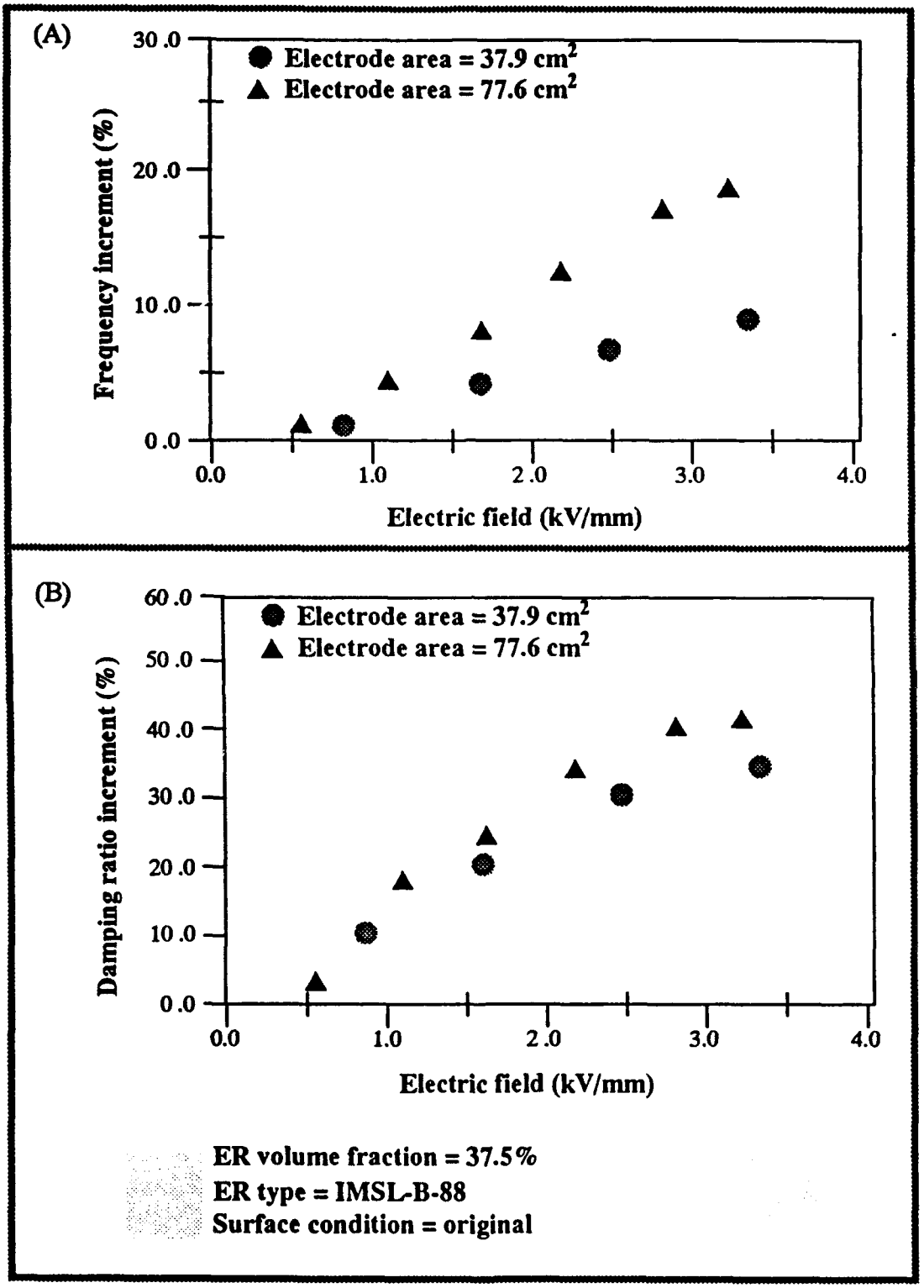

Fig. X.10 (A) Relative frequency-increment, and (B) relative damping-ratio increment of Class A and F specimens.

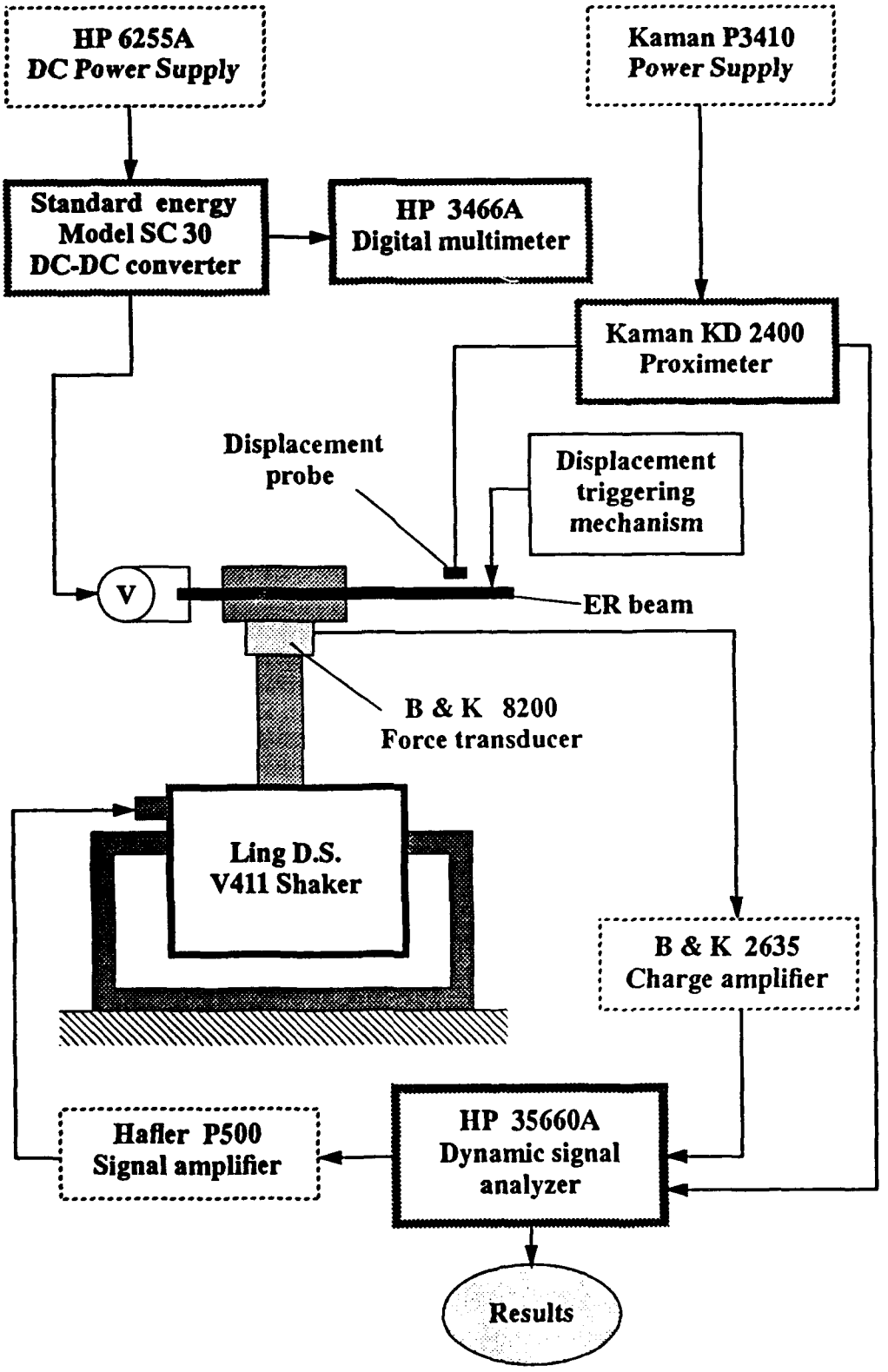

Fig. X.11 Experimental apparatus for dynamically exciting a smart cantilevered beam.

215 Hz. It is, therefore, obvious from the experimental results presented in Figure X.12 that, by controlling the voltage difference between the electrodes of the smart beam, the magnitudes of the individual natural frequencies can be changed or tailored to assume prescribed values.

Thus, for example, the fundamental natural frequency can be changed from 20.5 Hz to 35.0 Hz by changing the intensity of the electrical field imposed on the ER fluid domain, by changing the potential difference across the beam electrodes from 0 kV to 3.42 kV. This ability to increase the fundamental frequency by 15 Hz, or 70% of the original value has broad ramifications. For example, consider the situation in which this beam, which has a fundamental natural frequency of 20.5 Hz is subjected to a forcing frequency of 20.5 Hz in the flexural mode of vibration. The condition of resonance, with the attendant large and potentially dangerous dynamic stress levels, can be avoided by imposing a voltage on the beam to change the magnitude of this fundamental natural frequency to, say, 26 Hz, thereby avoiding resonance. This capability is readily implemented and observable in the laboratory.

Indeed control algorithms have been developed whereby, for the results prescribed in Figure X.12, the voltage imposed on the beam can be tailored to ensure that the magnitude of the maximum beam deflections, is minimized by ensuring that the response is below the lower envelope of the continuous and dotted curves presented in Figure X.12, thereby avoiding the large deflections in the neighborhood of the natural frequencies. Thus for example, if the beam is excited at 79.5 Hz, which is the second fundamental frequency of the uncharged smart beam, then a voltage of 3.42 kV could be imposed on the beam to reduce the response to the magnitude of the chain-dotted line in Figure X.12; whereas if the beam were subjected to a harmonic excitation of 135.5 Hz and the beam was also being subjected to a potential difference of 3.42 kV, then a 0 kV state would be imposed on the beam in order to drastically reduce the amplitude of the response.

The experimental results presented in Figure X.12 indicate that the second natural frequency of the smart beam is much more sensitive to the electrical field imposed on the ER fluid domain than the fundamental frequency. Thus the second natural frequency is increased from 79.5 Hz at 0 kV to 135.5 Hz at 3.42 kV, while the fundamental natural frequency is increased from 20.5 Hz to 35.0 Hz, a change of 70%, when subjected to the same electrical field intensity. A second controllable vibrational characteristic which may be deduced from Figure X.12 is the dependence of damping upon the magnitude of the external voltage field imposed upon the ER fluid actuator in the smart beam. This deduction is based on the shape of the curves in the neighborhood of each natural frequency. Thus, the degree of sharpness of response at 20.5 Hz and 0 kV is much more severe, and hence is characterized by smaller inherent damping, than the response of the fundamental frequency at 35 Hz and 3.42 kV. Similarly, the second natural frequency at 79.5 Hz and 0 kV is much sharper and is characterized by less damping than the response at 135.5 Hz and 3.42 kV.

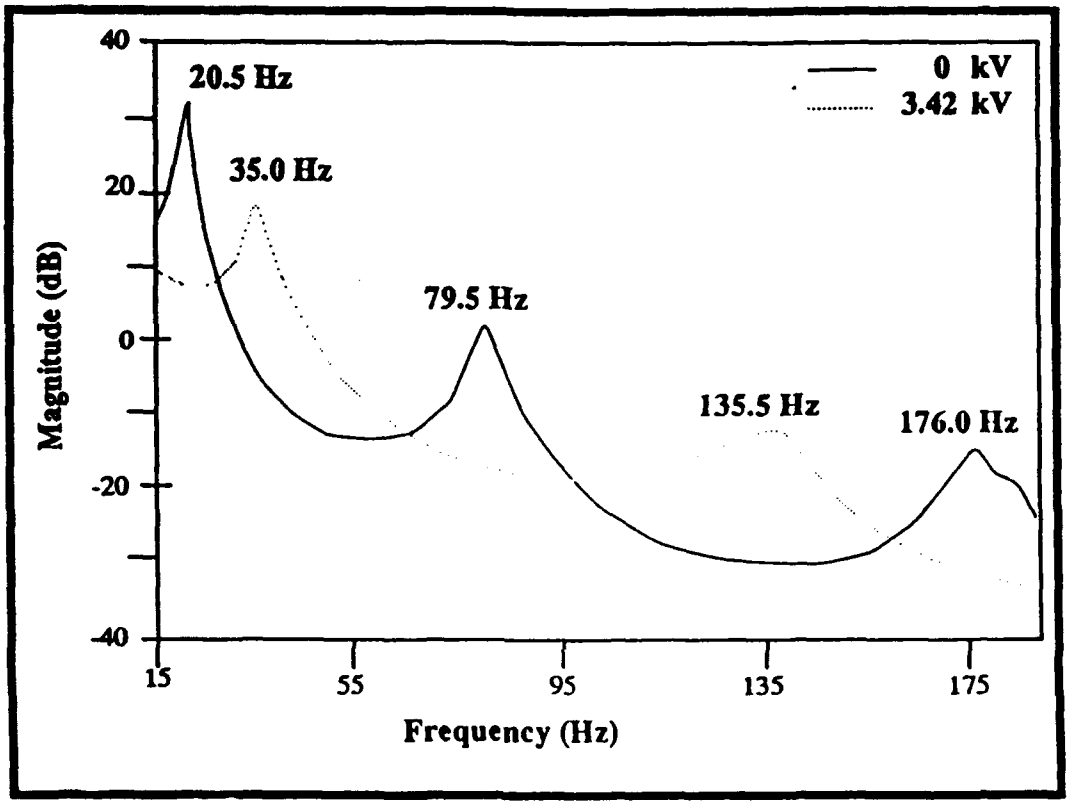

Fig. X.12 Frequency response of a smart cantilevered beam featuring an ER-fluid.

A more comprehensive set of experimental results is presented in Figure X.13 for a similar smart beam with an embedded ER fluid actuator subjected to a number of discrete voltage states with field intensities varying from 0 kV/mm of fluid thickness to 2.09 kV/mm. This data emphasizes and illustrates the ability to tailor the dynamic behavior of this class of smart structural materials by controlling the natural frequencies and the energy-dissipation characteristics. Furthermore, the results indicate that the magnitudes of the natural frequencies will increase from the 0 kV/mm datum as the field intensity increases. This ability to increase the magnitude of the natural frequencies may indeed be advantageous in many industrial applications, where the design engineer is required to synthesize a smart structure in which the natural frequencies must be tailored to yield both higher and also lower natural frequencies. This goal may be accomplished by designing a smart structure with a reference state which is characterized by a non-zero electrical potential. Thus, for example, referring to Figure X.13, an appropriate reference state may be defined as 300 V/mm which enables the magnitudes of the natural frequencies to be either increased or decreased, relative to this value by selecting either larger or smaller electrical field intensities as desired.

Figure X.14 presents a waterfall plot from an experimental study focused upon controlling the chaotic behavior of a smart beam featuring an embedded ER fluid actuator. The experimental apparatus and relevant instrumentation are documented in Figure X.15, from which it is evident that a test fixture, containing an electrically-insulated doubly-encastré beam, was mounted on the head of an electrodynamic shaker. The construction of the 465 mm long beam, which is shown in Figure X.16, comprised two aluminum electrodes each of thickness 0.8 mm which were separated by a silicone rubber insulator of thickness 2 mm. The resulting void contained an inexpensive ER fluid with simple constituents featuring 60% corn starch and 40% silicone oil marketed by Dow Corning as 704 Diffusion Pump Fluid. The beam was sinusoidally excited in a direction perpendicular to the face of the aluminum plate at different frequencies and accelerations, while imposing different discrete electrical field intensities on the ER fluid domain within the beam. The resulting spectra and time responses curve were studied in order to investigate the ability to control the chaotic responses of the smart beam.

Figure X.14 presents a time-frequency amplitude plot of the beam demonstrating how a chaotic response regime ensues when the initial voltage state of 1 kV imposed upon the beam is subsequently reduced to 0 kV. It is evident from the experimental data that upon removing the electrical potential from the ER fluid domain, the somewhat deterministic response is overwhelmed by a chaotic regime with no distinct repetition characteristics. This somewhat preliminary study clearly suggests that the chaotic behavior of certain classes of structures deployed in engineering practice, could conceivably be alleviated by fabricating these structures in smart materials featuring ER fluid actuators. Typical experimental results for the vibration characteristics of a smart plate are presented in Figure X.17.

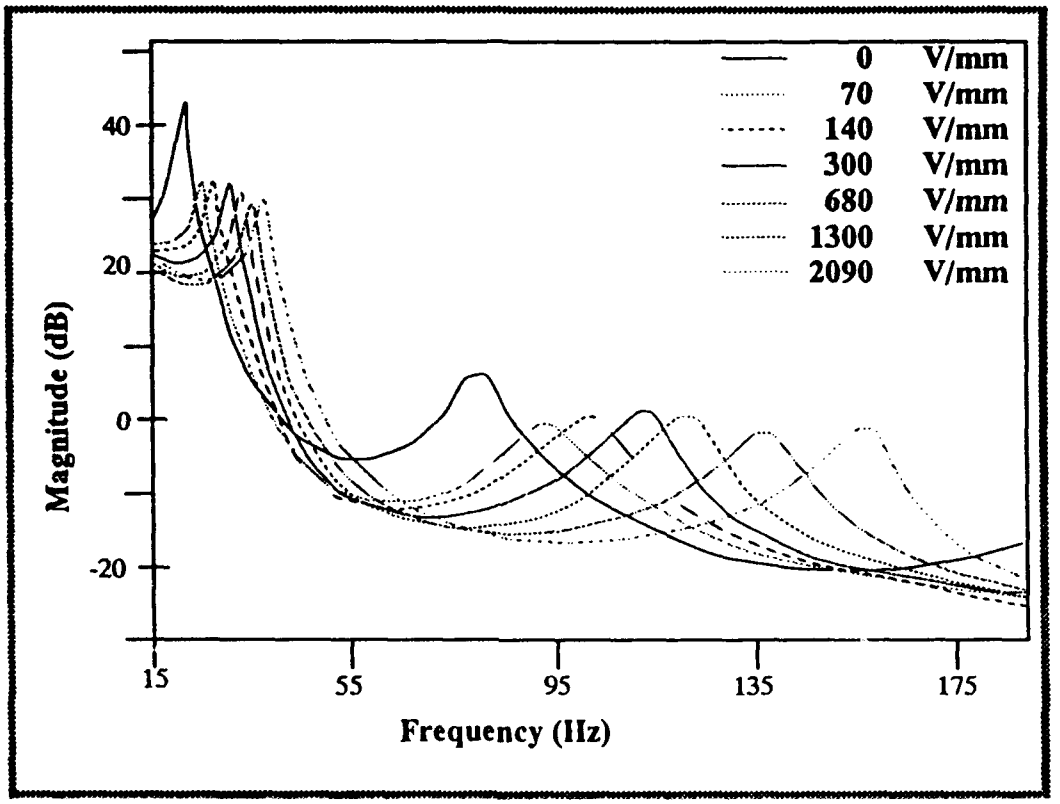

Fig. X.13 Frequency response of a smart cantilevered beam subjected to discrete voltage states.

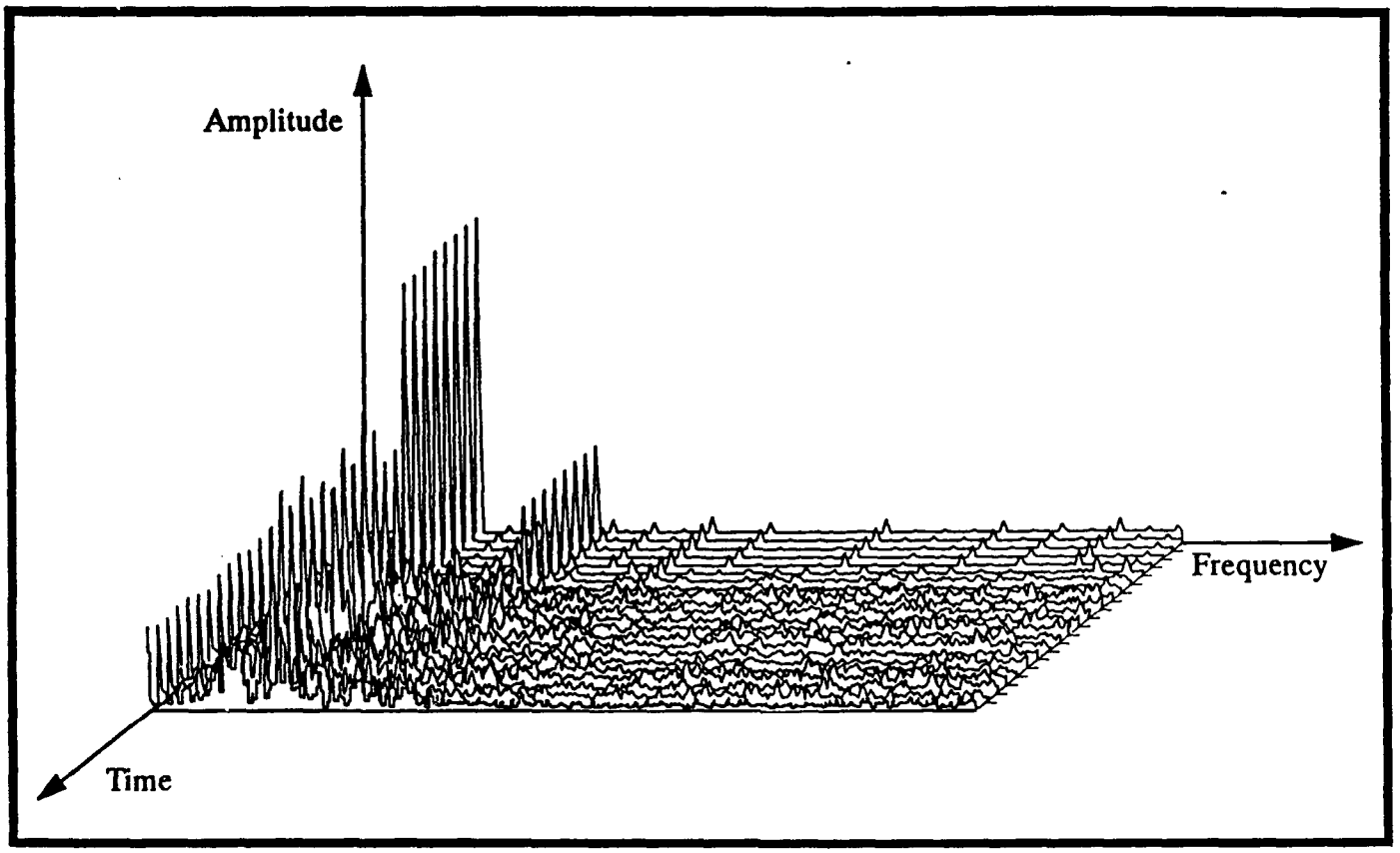

Fig. X.14 Waterfall plot of the elastodynamic response of a doubly encastré beam subjected to dynamical excitation showing that the chaotic response can be controlled by activating the electro-rheological fluid domain within the smart beam.

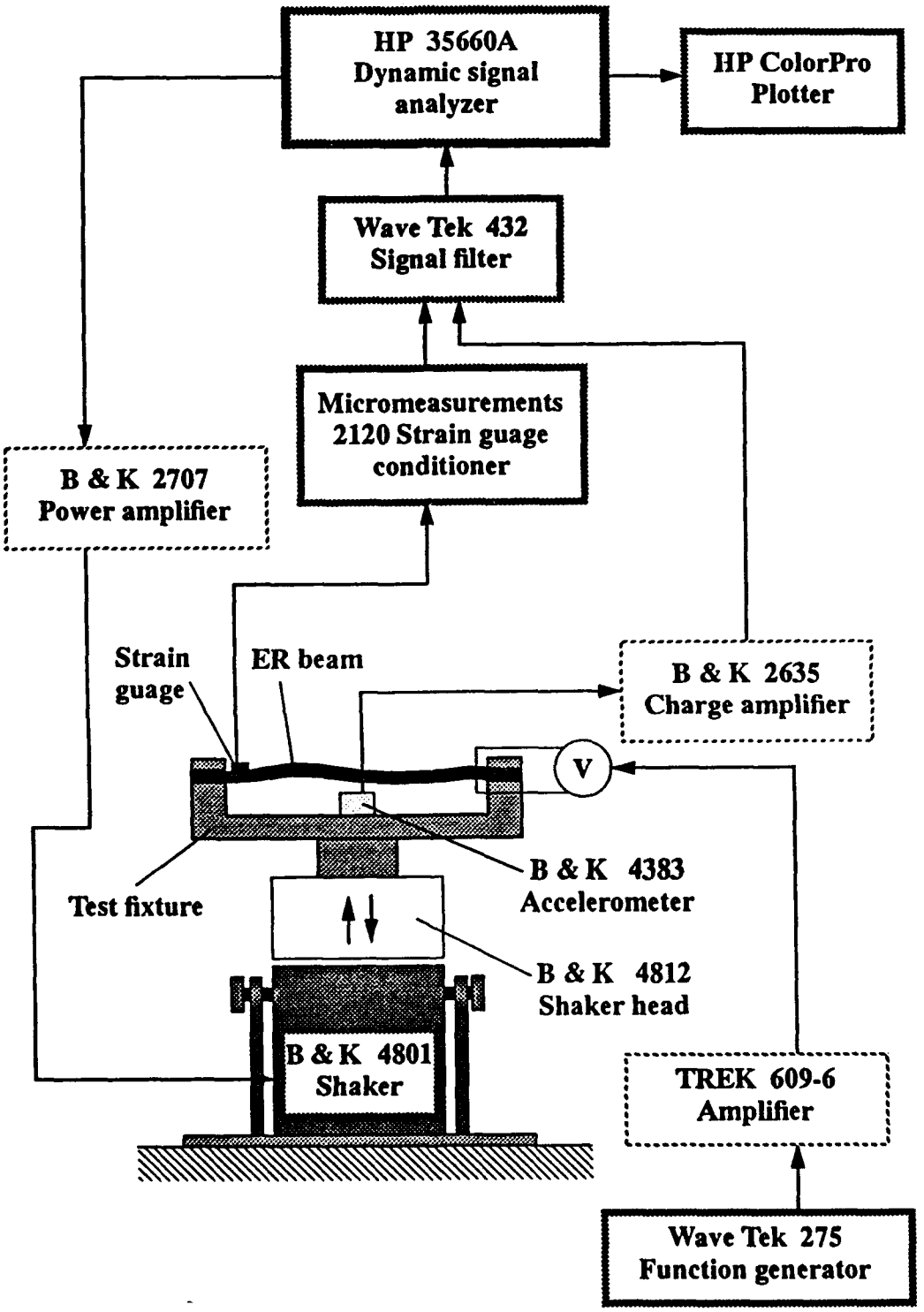

ig. X.15 Apparatus for determining the chaotic response of a preloaded, prebuckeled, doubly-encastre beam subjected to a dynamical excitation.

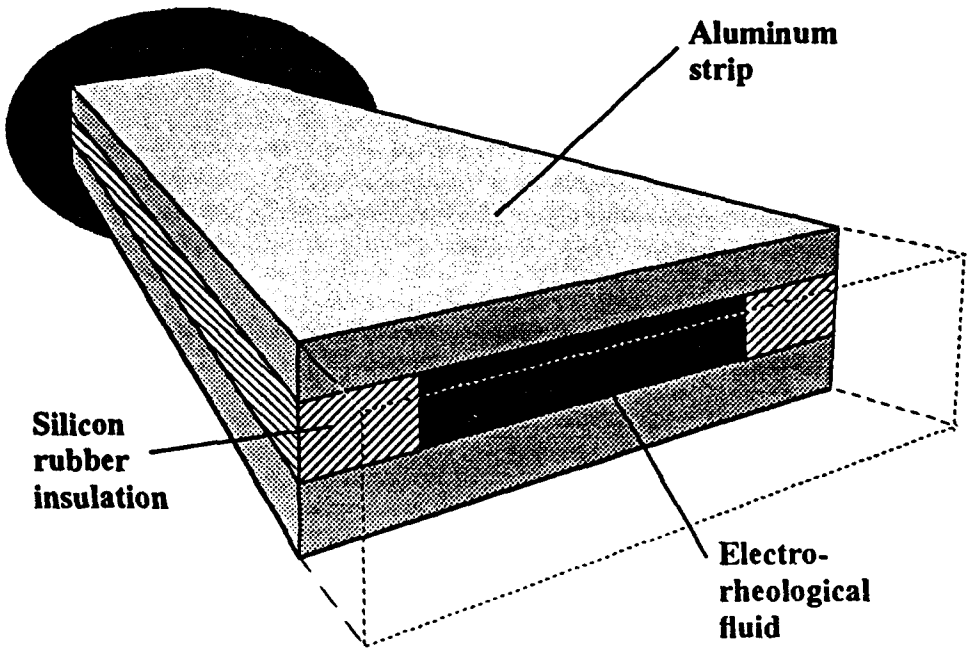

Fig. X.16 A schematic of a smart beam featuring a void filled with an electro-rheological fluid.

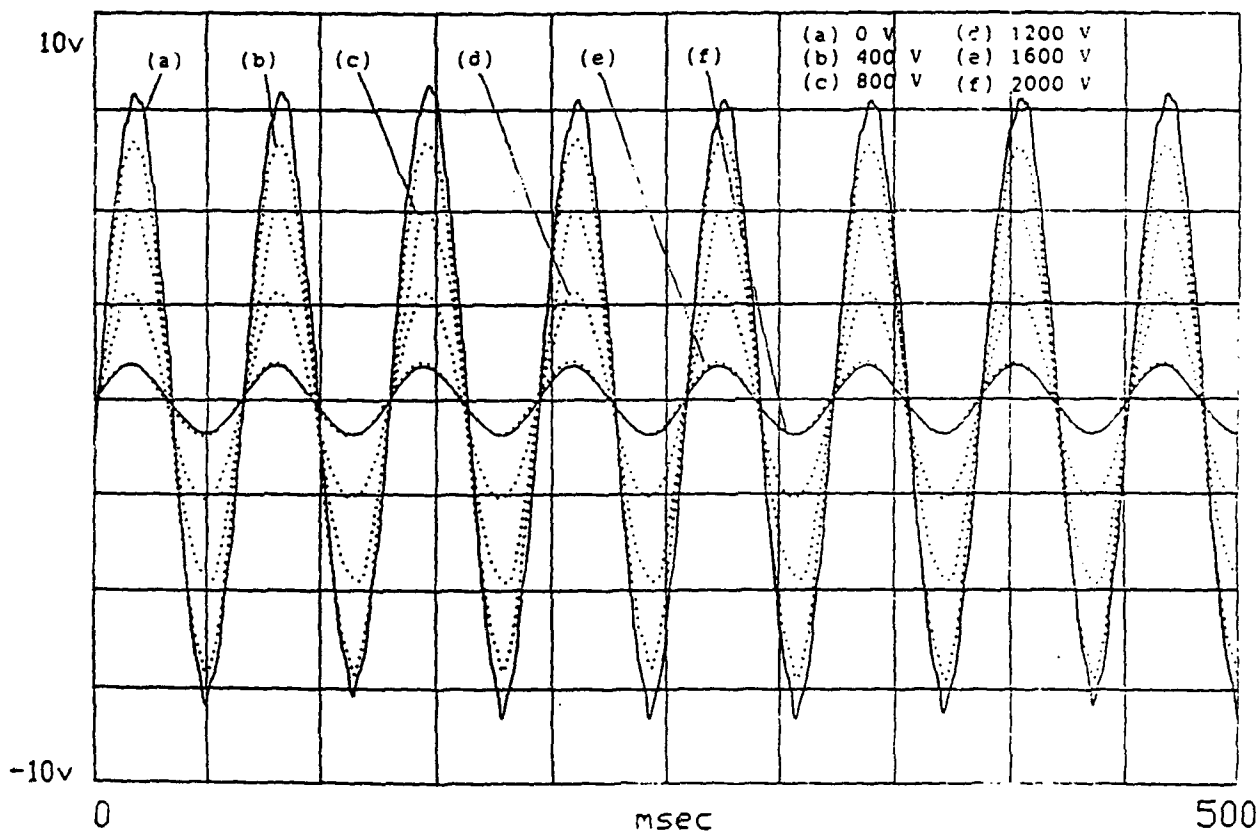

Fig. X.17 Reduction in amplitudes obtained from point 2

The research results distilled from these investigations are summarized succinctly below:

1. Smart beams and plates can change their natural frequencies by several hundred percent when an appropriate external electrical field is employed.

2. Smart beams and plates can change their mode shapes substantially when an appropriate external electrical field is employed.

3. Smart beams and plates can change their damping characteristics significantly when an appropriate external electric field is employed.

4. Typical response times for this class of smart beams and plates is of the order of milliseconds, which is crucial for the control of structural vibrations in real-time.

5. The high voltages mandated by the constitutive characteristics of electrorheological fluids and piezoelectric materials typically mandate the deployment of non-electric sensors, particularly fiber-optic sensors in this class of smart materials because they do not utilize electrical phenomena in the strain detection domain.

6. The research findings indicate that there is an infinite variety of response characteristics for this class of smart beams and plates featuring electrorheological fluid domains and piezoelectric materials because the electrical field imposed upon these domains controls the response of the structure.

10.1 DEVELOPMENT OF A MATHEMATICAL CAPABILITY TO PREDICT AND CONTROL THE VIBRATION CHARACTERISTICS OF SMART STRUCTURES FEATURING EMBEDDED ElectrorheoLOGICAL FLUIDS AND PIEZOELECTRIC MATERIALS

The finite element formulation developed in the previous section is quite general for a broad class of three-dimensional boundary-value problems. In this section, a one-dimensional problem is considered in order to examine the behavior of a beam, and the design of the linear optimal controller will be based on the finite element formulation and modal analysis. Figure 2 presents the proposed one-dimensional smart beam element which comprises piezoelectric films which are bonded to the top and bottom of the original beam. The piezoelectric film on the upper-face plays a role of actuator, while the piezoelectric film on the lower-face has the role of the sensor. Hence, this

configuration can be regarded as a smart beam element with colocated actuator and sensor.

The bending moment produced from the actuator can be obtained by considering force equilibrium in the axial direction. The produced moment $\tilde{M}$ for the proposed symmetric beam with respect to neutral axis is obtained by

$$\tilde{M} = b_2 d_{31} E_2 \left(\frac{h_1+h_2}{2}\right) \tilde{V} \left[h(x-x_1) - h(x-x_2)\right] \qquad (10)$$

Where b_2, h_2, E_2 are the width, thickness, Young's modulus of the piezoelectric film, respectively, d_{31} is the piezoelectric strain constant, h_1 is the thickness of the original beam, $\tilde{V}$ is the applied voltage, x_1 and x_2 are the end positions of piezoelectric element, and $h(\cdot)$ is the Heaviside step function.

On the other hand, the output voltage produced from the sensor is obtained by integrating the electric charge developed at a point on the piezoelectric film along the entire length of the film surface [4]. The produced output voltage $\hat{V}$ for the proposed structure is given by

$$\hat{V} = \frac{Q_o}{C_o}\left(\frac{\partial w(x_1,t)}{\partial x} - \frac{\partial w(x_2,t)}{\partial x}\right) \qquad (11)$$

where C_o is the capacitance of the distributed film sensor, $\frac{\partial w(x_i,t)}{\partial x}$ is the slope at the end location x_i, and Q_o is given by

$$Q_o = \frac{b_2 k_{31}^2}{g_{31}}\left(\frac{h_1}{2} + h_2\right) \qquad (12)$$

In equation (12), k_{31} is the electromechanical coupling factor and g_{31} is the piezoelectric stress constant.

Now, by introducing modal coordinates $\{\eta\}$ and the modal matrix $[\phi]$ associated with the eigenvalues

$$\{U\} = [\phi]\{\eta\} \tag{13}$$

and by incorporating equations (10) and (11), the equation (8) can be decoupled and expressed in the state-space representation as follows,

$$\begin{aligned} \dot{\tilde{x}} &= \tilde{A}\tilde{x} + \tilde{B}\tilde{u} + \tilde{f} \\ \tilde{y} &= \tilde{C}\tilde{x} \end{aligned} \tag{14}$$

where

$$\begin{aligned} \tilde{x} &= [\eta \quad \dot{\eta}]^T \\ \tilde{A} &= \begin{bmatrix} 0 & I \\ -\Omega & -Z \end{bmatrix} \\ \tilde{B} &= [0 \quad \bar{B}]^T \\ \tilde{f} &= [0 \quad \bar{f}]^T \\ C &= [\bar{C} \quad 0] \\ \tilde{u} &= [\bar{V}_1 \ldots \bar{V}_m]^T \end{aligned} \tag{15}$$

$$\tilde{y} = [\hat{V}_1 \ldots \hat{V}_m]^T$$

In equation (15), [I] is the identity matrix, [Ω] (= diag (ω_i^2)) is the modal frequency matrix with the undamped natural frequency ω_i of ith mode, [Z] (= diag $(2\zeta_i\omega_i)$) is the modal damping matrix with the damping ratio ζ_i of ith mode, $(\bar{f})$ is the decoupled external force vector, $\tilde{V}_i$ is the input voltage to the ith piezoelectric element actuator, $\hat{V}_i$ is the output voltage produced from ith piezoelectric element sensor, and input matrix $\bar{B}$ and output matrix $\bar{C}$ is given by

$$\bar{B} = a_1 \begin{bmatrix} \frac{d\phi_1}{dx}(x_1^1) - \frac{d\phi_1}{dx}(x_2^2) & \cdots & \frac{d\phi_1}{dx}(x_1^m) - \frac{d\phi_1}{dx}(x_2^m) \\ \vdots & & \vdots \\ \frac{d\phi_n}{dx}(x_1^1) - \frac{d\phi_n}{dx}(x_2^1) & \cdots & \frac{d\phi_n}{dx}(x_1^m) - \frac{d\phi_n}{dx}(x_2^m) \end{bmatrix}$$

$$\bar{C} = a_2 \begin{bmatrix} \frac{d\phi_1}{dx}(x_1^1) - \frac{d\phi_1}{dx}(x_2^1) & \cdots & \frac{d\phi_n}{dx}(x_1^1) - \frac{d\phi_n}{dx}(x_2^1) \\ \vdots & & \vdots \\ \frac{d\phi_1}{dx}(x_1^m) - \frac{d\phi_1}{dx}(x_2^m) & \cdots & \frac{d\phi_n}{dx}(x_2^m) - \frac{d\phi_n}{dx}(x_2^m) \end{bmatrix} \qquad (16)$$

where $\frac{d\phi_i}{dx}(x_i^j)$ is the modal slope coefficient at the ith end position of the jth element of piezoelectric actuator and sensor, and the constants a_1, a_2 given by

$$a_1 = b_2 d_{31} E_2 \left(\frac{h_1+h_2}{2}\right)$$

$$a_2 = \frac{Q_o}{C_o} \qquad (17)$$

The dynamical behavior described by equation (14) comprises many modes in general, and it is generally impractical to control all of the associated modes. Therefore, the dynamical behavior represented by equation (14) can be decomposed into two sub-dynamics from the practical point of view by considering the first few critical modes as the primary modes and the remaining modes as the residual modes. Hence, the sub-dynamics are

$$\dot{\tilde{x}}_p = \tilde{A}_p \tilde{x}_p + \tilde{B}_p \tilde{u} + \tilde{f}_p \qquad (18)$$

$$\tilde{y}_p = \tilde{C}_p \tilde{x}_p$$

$$\dot{\tilde{x}}_r = \tilde{A}_r \tilde{x}_r + \tilde{B}_r \tilde{u} + \tilde{f}_r \qquad (19)$$

$$\tilde{y}_r = \tilde{C}_r \tilde{x}_r$$

where subscripts (p) and (r) represent primary and residual modes, respectively.

In this study, the linear quadratic gaussian (LQG) controller with a full-order state estimator is formulated by employing the dynamics (18), and the designed control input is applied to the dynamics (19) in order to investigate the control spillover effects of the system which is characterized by the magnitude of excitation from the residual-modal dynamics.

The design of the LQG controller for a linear time-invariant system can be *accomplished independently in two steps; the design of* a full-state feedback regulator and the design of a full-order state estimator by employing so called separation property [22]. Figure 3 represents schematically the block diagram of the closed-loop system which features a constant state feedback with full-order estimator and also the unmodelled dynamics. Thus,

the feedback system with full-order state estimator can be described by the following algebraically equivalent dynamics,

$$\dot{\tilde{x}}_p = (\tilde{A}_p - \tilde{B}_p \tilde{K}_p)\,\tilde{x}_p + \tilde{B}_p \tilde{K}_p \tilde{e}_p + \tilde{B}_p \tilde{r} + \tilde{f}_p \qquad (20)$$

$$\tilde{y}_p = \tilde{C}_p \tilde{x}_p$$

and

$$\dot{\tilde{e}}_p = (\tilde{A}_p - \tilde{L}_p \tilde{C}_p)\,\tilde{e}_p \qquad (21)$$

$$\hat{y}_p = \tilde{C}_p (\tilde{x}_p + \tilde{e}_p)$$

where $\tilde{e}_p$ is the estimation error between the actual state $\tilde{x}_p$ and the estimated state $\hat{x}_p$, L_p is the observer feedback gain and $\hat{y}_p$ is the estimator output. The constant state feedback regulator is designed so as to minimize the following quadratic performance index

$$\pi = \int_0^\infty (\tilde{x}_p^T \tilde{Q}\, \tilde{x}_p + \tilde{u}^T \tilde{R}\, \tilde{u})\, dt \qquad (22)$$

where $\tilde{Q}$ is the state weighting matrix and $\tilde{R}$ is the control weighting matrix. The result of minimization of the equation (22) gives the state feedback control laws

$$\tilde{u}(t) = -\tilde{K}_p \tilde{x}_p, \quad \tilde{K}_p = \tilde{R}^{-1}\, \tilde{B}_p^T\, \tilde{P} \qquad (23)$$

where $\tilde{P}$ is the solution of the steady-state algebraic Riccati equation

$$\tilde{P}\,\tilde{A}_p + \tilde{A}_p^T\,\tilde{P} - \tilde{P}\,\tilde{B}_p\,\tilde{R}^{-1}\,\tilde{B}_p^T\,\tilde{P} + \tilde{Q} = 0 \qquad (24)$$

The observer feedback gain $\tilde{L}_p$ is obtained using pole assignment technique. This technique is one of the most convenient tools for the practical design of an estimator, and the estimator poles which characterize the performance of the overall closed-loop system can be assigned easily after designing feedback gains $\tilde{K}_p$ which will serve as a basis for determining $\tilde{L}_p$.

ILLUSTRATIVE EXAMPLES

In order to demonstrate the viability of the aforementioned control methodology for smart materials featuring piezoelectric actuators and sensors the following two examples will be considered.

Example 1 : Cantilevered-beam

Consider the transverse vibration of the cantilevered-beam shown in Figure 4. The geometrical and material properties of the original beam and the piezoelectric film employed in this simulation are given in Table 1. This piezoelectric film is type PXT7A manufactured by Vernitron Piezoelectric Division. For the determination of the system model parameters such as natural frequencies and modal slope coefficients, a two-node element was employed with two-degrees-of-freedom at each side, and the number of elements was six. Both sides of the first and second elements were bonded with piezoelectric film to provide a pair of colocated actuators and sensors. The damping ratio of each mode is assumed to be $\xi_i = 0.003$.

In this simulation, the first and second modes are considered as the primary modes and it is also assumed that the states $\tilde{x}_p = \hat{x}_p$. In fact, this assumption does not cause significant error so long as the state estimator for $\tilde{x}_p$ is designed in a fashion that the desired observer poles are chosen to be much faster than the closed-loop poles resulting from state feedback gains in order to reduce the transient effect of the state error between actual and estimated states. With arbitrary chosen state weighting matrix $\tilde{Q}$ and control weighting matrix $\tilde{R}$, the feedback gains $\tilde{K}_p$ = [328640 1482740 13712 13753] are obtained and employed for the simulation.

Figure 5 presents a comparison of the transient response of the tip deflection with and without the application of a control voltage. It is remarkable that the transient vibration decays to zero within 0.5 seconds upon applying the control voltage which is presented in Figure 6. Furthermore, it is noted that since there exists a practical limit to the voltage that can be applied to the piezoelectric film (usually ± 200 V ~ ± 300 V), the arbitrary high feedback gains cannot be used.

Example 2: Slider-crank mechanism

Consider the planar motion of the slider-crank mechanism featuring a smart connecting-rod incorporating piezoelectric materials as shown in Figure 7. The slider-crank mechanism consists of a crank length of 5.08 cm and a connecting-rod which has the same geometrical and material properties as used in the Example 1. The crank is assumed rigid and rotating in a constant speed. The connecting-rod is also divided into six elements, and two pairs of piezoelectric films are bonded on the second and fifth element. With arbitrarily chosen state and control weighting matrices, the following feedback gains $\tilde{K}_p$ are obtained and employed for the simulation

$$\tilde{k}_p = \begin{bmatrix} 120 & 50 & 70470 & 70540 \\ 120 & -50 & 70470 & -70540 \end{bmatrix}$$

Table 2 presents the open-loop poles and the closed-loop poles of the control system with the above feedback gains. The data presented in this table permits the damping ratios of first and second modes of the closed-loop system to be distilled. These are 0.255 and 0.425, respectively.

Figure 8 presents a comparison of the midspan transverse deflections of the connecting-rod with and without the imposition of a feedback control voltage at the mechanism operating speed of 250 rpm. The most important and obvious observation from this figure is that the magnitude of the midspan deflection in the absence of control voltage was reduced by 35 percent by invoking the proposed feedback control strategy. Furthermore, it is interesting to observe that the deflection caused by the first and second flexural modes was almost completely eliminated by the imposed feedback control voltage, while the deflection caused by the inertia force of the connecting-rod during high-speed operation was not controlled.

Figure 9 presents the control voltage applied to the second and fifth element actuators. Figure 10 shows the residual midspan transverse deflection of the connecting-rod which is obtained by applying the control voltage given by Figure 5 to the dynamics (18) with third and fourth flexible modes which are defined as residual modes. It is observed that the control spillover effects (excitation magnitude of the residual modes) depend on the crank angle and the magnitude of the vibration is relatively small compared to that of the controlled system in Figure 8. Hence, it may be expected that the instabilities of the closed-loop system with the proposed feedback control law will not occur from the unmodeled modes.

Finally, it should be noted that the control performance can be considerably enhanced by considering the optimal location of actuators or by choosing the appropriate state and control weighting matrices. Furthermore, it is also noted that the stiffer and the thicker piezoelectric film produces the larger control forces with limited applicable voltages.

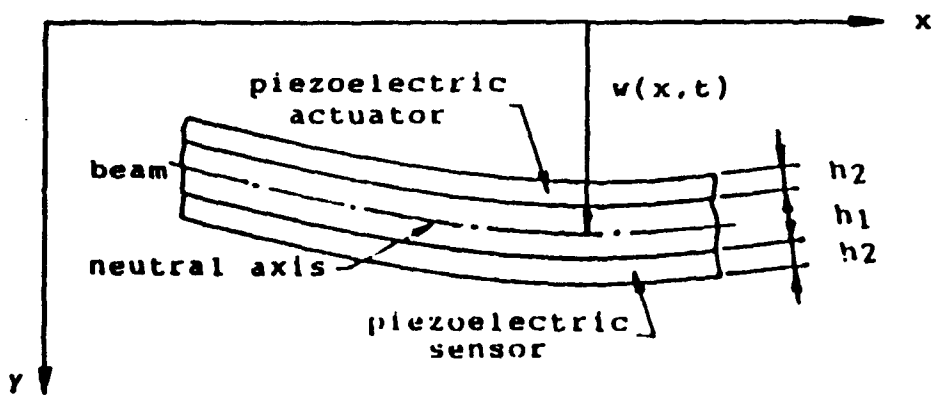

Figure 2. Cross Section of the Proposed Beam with Piezoelectric Film

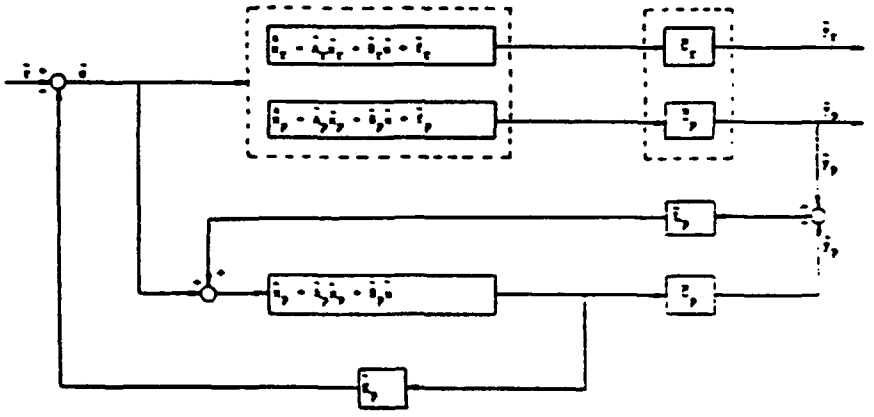

Figure 3. Block-diagram of the Overall Closed-loop System.

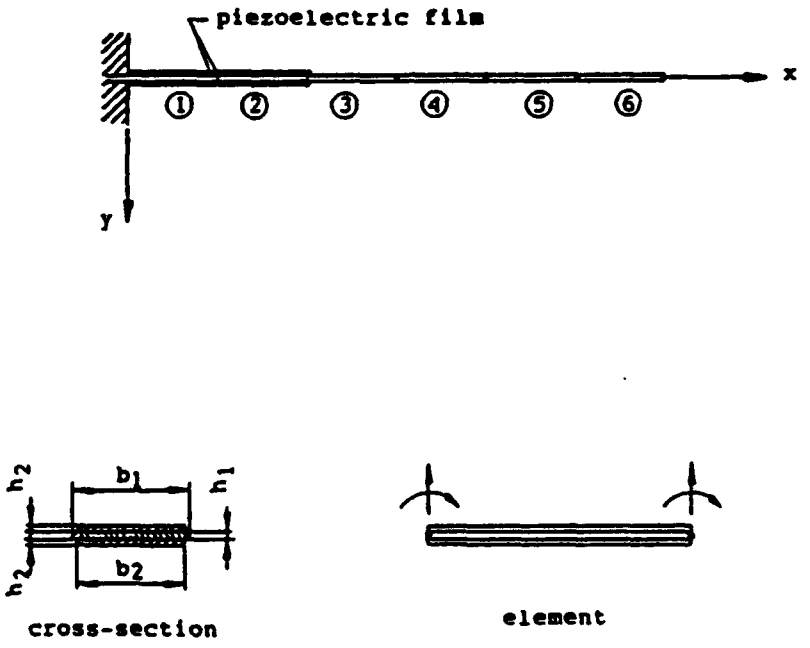

Figure 4. Finite Element Model for the Cantilevered Beam.

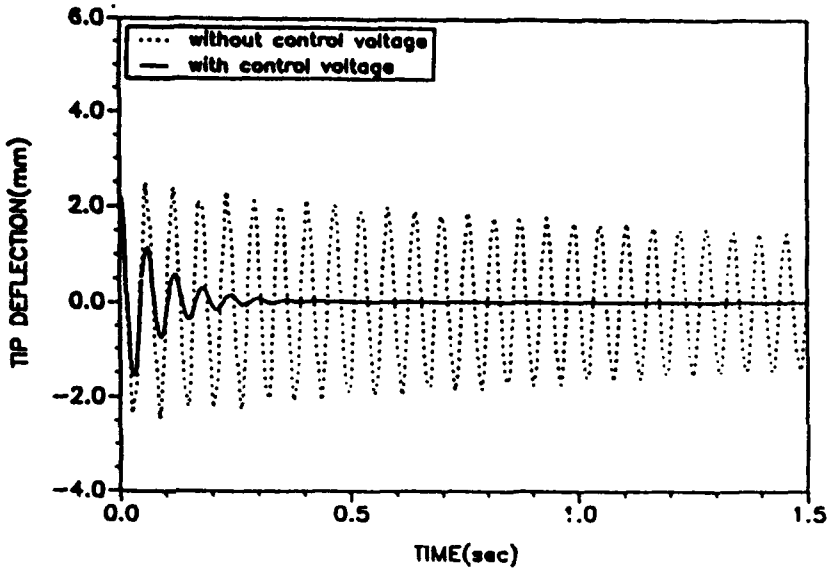

Figure 5. Tip Deflection of the Cantilevered Beam

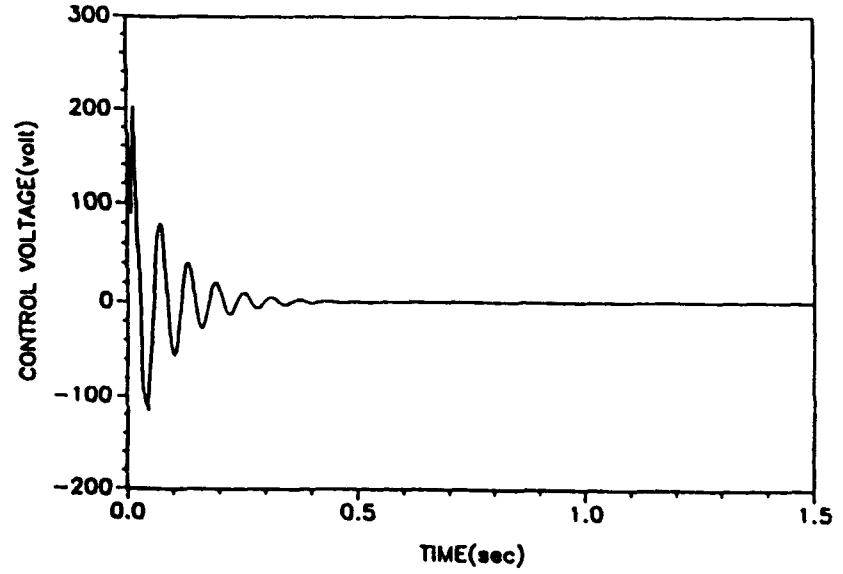

Figure 6. Control Voltage

Table 1. Geometrical and Material Properties of Original Connecting-rod and Piezoelectric Film.

Connecting-rod (aluminum)		Piezoelectric film (ceramic)	
length	29.16 cm	piezoelectric stain constant	60×10^{-12} $\frac{m/m}{v/m}$
width	20 cm	width	20 mm
thickness	1.0 mm	thickness	0.381 mm
density	2740 kg/m^3	density	7700 kg/m^3
Young's modulus	68.95 Gpa	Young's modulus	93.0 Gpa

Table 2. Open-loop and Closed-loop Poles of the System.

Open-loop Poles		Closed-loop Poles	
real	imaginary	real	imaginary
-0.46375	154.58	-39.784	149.38
-0.46375	-154.58	-39.784	-149.38
-1.9845	661.55	-282.38	598.25
-1.9845	-661.55	-282.38	-598.25

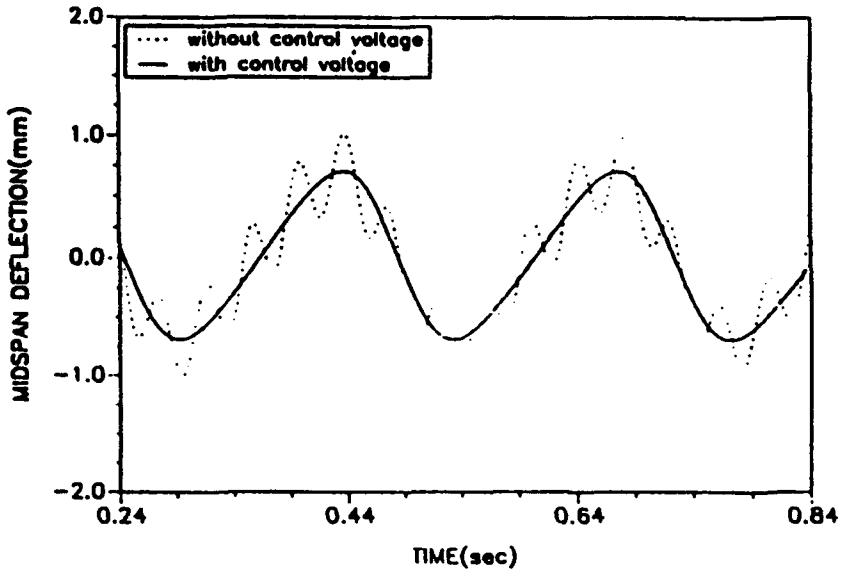

Figure 8. Mid-span Transverse Deflection of the Connecting-rod at Mechanism Operating Speed 250 rpm.

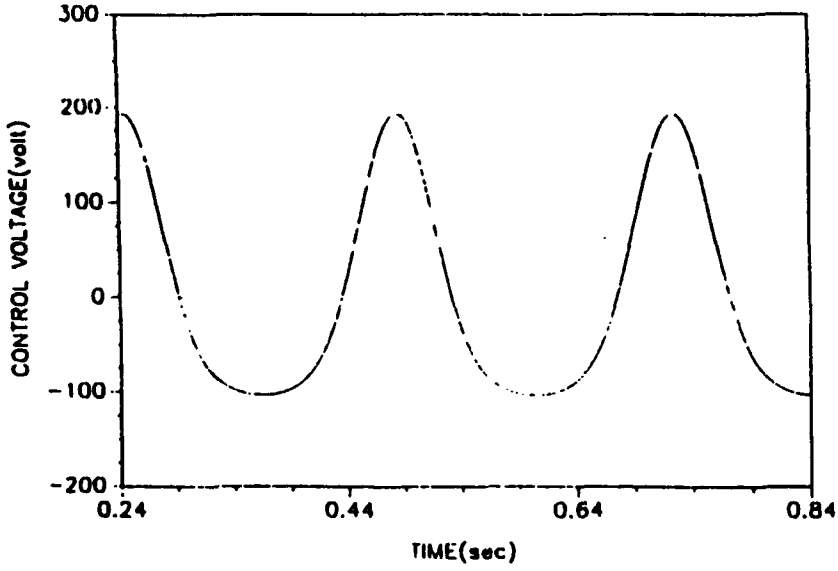

Figure 9. Control Voltage.

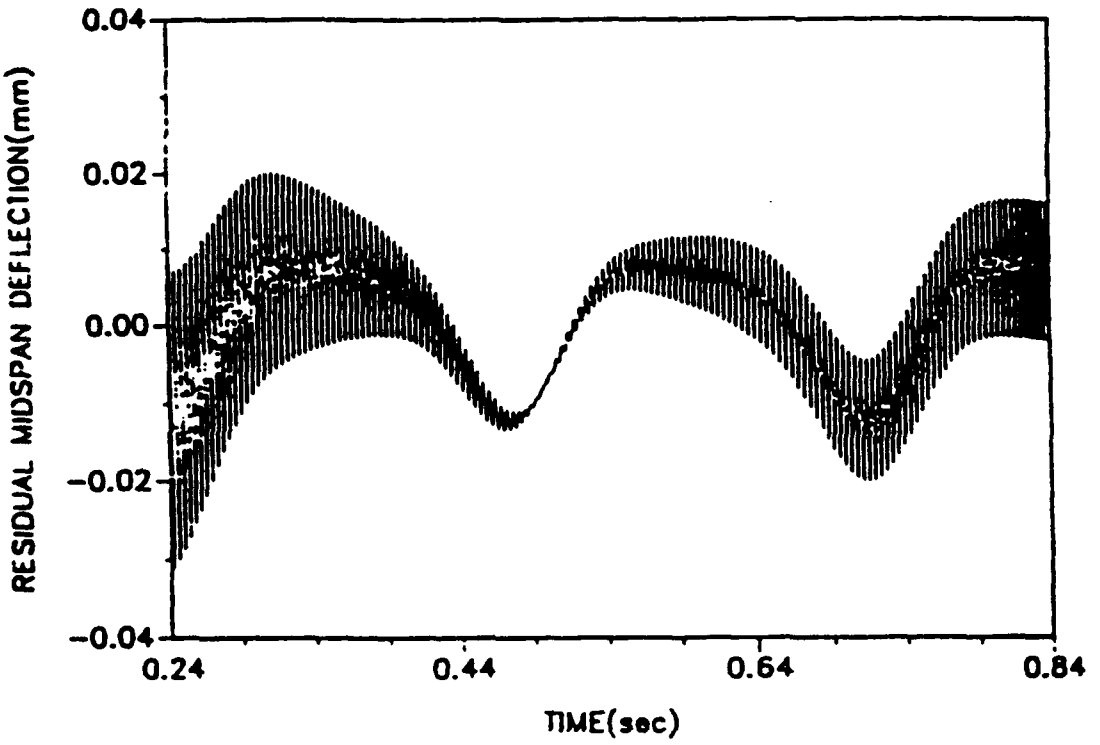

Figure 10. Residue Mid-Span Transverse Deflection of the Connecting-rod.

XI CONTROL STRATEGIES FOR SMART STRUCTURES

The active control of structures for defense systems, aerospace systems, and large flexible space structures in particular, will require the implementation of decentralized control strategies in order for these systems to function effectively when the structure has sustained structural damage. The decentralization constraint enters into the synthesis of large-scale systems because it may be impractical or even impossible to communicate signals from one controller to another for instance, due to data-bandwidth constraints. Moreover, decentralization may be required by the control designer to achieve reliability and survivability with graceful degradation under failures, by imposing a control structure in which control authority is relegated to separate levels. An equally important aspect in synthesizing these systems is the possibility of relief from extreme computational constraints encountered in the design of a centralized controller for the system. Since each control agent is responsible for producing only a subset of the inputs while using restricted information, the overall dynamic system essentially distills to a collection of smaller subsystems for which controllers can be generated with more computational ease than for a single larger-order system.

Early results in optimal decentralized control theory were of a negative nature. The separation of estimation and control is not optimal for linear decentralized control systems with quadratic cost and Gaussian disturbances. In fact the optimal control is not necessarily a linear feedback law; in general, the existence of an optimal law is not guaranteed for decentralized systems, and the optimal linear law can be of infinite dimensions, and hence not realizable in practice. The inevitable probing relevant questions as to the importance of "signalling", "second guessing" and the extent of "cross communication" among decentralized controllers, which of course, do not arise in centralized systems, remain to be answered.

Recently more successful results have been obtained by extending the standard LQG control and estimation algorithms to decentralized systems with fixed information exchange patterns. For instance, the solution to the decentralization LQG control problem without a central supervisor has been obtained by hypothesizing that a network structure consisting of interconnected nodes, where the local filter's estimate at a given node is fused with incoming data from other nodes, in order to compute the globally optimum estimate. The principal benefits of this structure are parallel processing and a minimal required bandwidth for data transmission. Another class of decentralized estimators results from the application of perturbation techniques such as a structure

consisting of a set of locally optimal estimators for the individual subsystems driven by compensatory signals of a global estimator on a higher level to account for the interconnection effects.

In summary, decentralized control using fixed information patterns appear to be the most feasible approach for smart defense structures. The fact that this formation does not address the question of what structure should be assumed may be considered a drawback in general decentralization system applications. However, this aspect would not be a problem in many structural applications because of the large body of knowledge associated with the subsystems.

Since large structures are infinite dimensional distributed parameter systems, their finite order linear system approximations are employed for controller designs. These active shape and vibration control methods, based on modal truncation of the structural modes, naturally suffer due to control and observation spill over effects. Spill over is the coupling between the controller and the unmodeled dynamics within the bandwidth of the controller. The destabilizing effects of spill over are more pronounced at higher modes where the modelling uncertainty is higher for structures with no closed-form solution for the eigenvalue problem. In the last decade, a significant amount of research effort has been expended to address these unique problems associated with the control of large structures and these activities include decentralized control, adaptive control based on identification techniques, and robust reduced order controllers.

In contrast, collocated local direct velocity feedback, has been shown to be unconditionally stable under some assumptions for the actuator dynamics. Recently, positive position feedback has been suggested as an alternative to local velocity feedback. This method is also not sensitive to spillover and it is stable under minimally restrictive conditions. Hence, local velocity and position feedback control algorithms would be ideal for smart structures applications. Again, current methods which may be adequate for low dimensional systems with fairly known parameters, such as a conventional rigid-body aircraft will prove unsuitable for a large structure due to large false alarms caused by parameter modelling errors.

The finite element equation governing the motion of a general arbitrarily-shaped structure fabricated in a smart material and subjected to dynamical loads has the functional form

$$[M]\{\ddot{U}\}+[C(\hat{V})]\{\dot{U}\}+[K(\hat{V})]\{U\}=\{f(t)\} \qquad XI.1$$

where the global mass, damping and stiffness matrices are denoted by [M], [C(V)] and [K(V)] respectively. Clearly the stiffness and damping matrices are functions of the time-dependent external voltage fields V applied to the ER fluid domains within the structure. The deformation field of the smart flexible structure is represented by the

column vector {U} and the forcing function imposed on the structure is denoted by the column vector {f(t)}.

In order to demonstrate how the dynamic response of smart structures featuring embedded ER-fluid domains can be controlled by changing the electrical field intensities imposed on the fluid domains, consider the task of actively controlling the transient response of beam-shaped structures.

For this class of initial-value problems, the equations of motion may be reformulated as follows:

$$[M]\{\ddot{U}\}+([C]+[\Delta C(\hat{V})])\{\dot{U}\}+([K]+[\Delta K(\hat{V})])\{U\}=\{0\} \qquad XI.2$$

where [K] and [C] are the global stiffness and damping matrices associated with a zero electric field strength being imposed on the ER-fluid domains, and [ΔK(V)] and [ΔC(V)] are the incremental global stiffness and damping matrices associated with a change in voltage from zero volts to a general none-zero value of V volts. Consider the modal analysis of a beam fabricated in a smart material featuring an ER-fluid domain, and assume that the ER fluid domains within the beam are not subjected to an external voltage. The governing equation is, from equation (XI.2),

$$[M]\{\ddot{U}\}+[C]\{\dot{U}\}+[K]\{U\}=\{0\} \qquad XI.3$$

Thus, by introducing modal coordinates and the modal matrix [ϕ] associated with the eigenvalues

$$U=[\phi]\{\eta\} \qquad XI.4$$

equation (XI.3) can be decoupled as follows

$$[I]\{\ddot{\eta}\}+[Z]\{\dot{\eta}\}+[\Omega]\{\eta\}=\{0\} \qquad XI.5$$

where [I] is the identity matrix, [Ω] (= diag (ω^2_i)) is the modal frequency matrix with the undamped natural frequency ω_i of each mode, and [Z] (= diag ($2,\zeta_i\omega_i$)) is the modal damping matrix with the damping ratio ζ_i of each mode.

Equation (XI.5) is valid only if the system is subjected to light damping. Under these conditions, modal decoupling is admissible since the off-diagonal terms in the system matrices are very much smaller that the diagonal terms. In order to investigate the viability of this approach when modeling beams fabricated in smart materials, the

transient response for the coupled and uncoupled formulations are presented in Figure XI.1 utilizing data obtained from a complementary program.

Thus Figure XI.1 presents the transient response for the decoupled case which, was obtained by solving the first-mode equation, $\ddot{\eta}_1 + 2\zeta_1\omega_1\dot{\eta}_1 + \omega_1^2 = 0$, and also the transient response for the coupled case which was obtained directly by solving the equation XI.3 using the Newmark method of numerical integration. It is evident form Figure XI.1 that the equation VI.5 may be employed in this study of beams fabricated with smart materials without causing serious error, and generally, the first mode is adequate for developing viable control strategies. Furthermore, the off-diagonal terms of the matrix $\{C\} = [\phi^T][C][\phi]$ is in the order of 10^{-10}, which is very small compared with the values of the diagonal terms which are typically of the magnitude $10^1 \sim 10^3$. Therefore, the modified equations of motion for the system due to the applied electrical field intensity can be expressed in the form

$$[\hat{M}]\{\ddot{\eta}\}+[\hat{C}]\{\dot{\eta}\}+[\hat{K}]\{\eta\}=0 \qquad XI.6$$

where

$$[\hat{M}]=[I] \qquad XI.7$$

$$[\hat{C}]=[Z]+[\phi^T][\Delta C(\hat{V})][\phi] \qquad XI.8$$

and

$$[\hat{K}]=[\Omega]+[\phi^T][\Delta K(\hat{V})][\phi] \qquad XI.9$$

Since the ER fluid layer acts like an infinite number of actuators in the presence of an electric field, each mode is influenced by the applied field. The magnitude of the influence of each mode is relative to the original mode in the absence of the electric field. Thus, the coupling terms of the increased damping and stiffness matrices, [C] and [K] respectively associated the with modal matrix [ϕ]are negligible compared with the diagonal terms, and

$$[\phi^T][\Delta C(\hat{V})][\phi]=[Z(\hat{V})] \qquad XI.10$$

$$[\phi^T][\Delta K(\hat{V})][\phi]=[\Omega(\hat{V})] \qquad XI.11$$

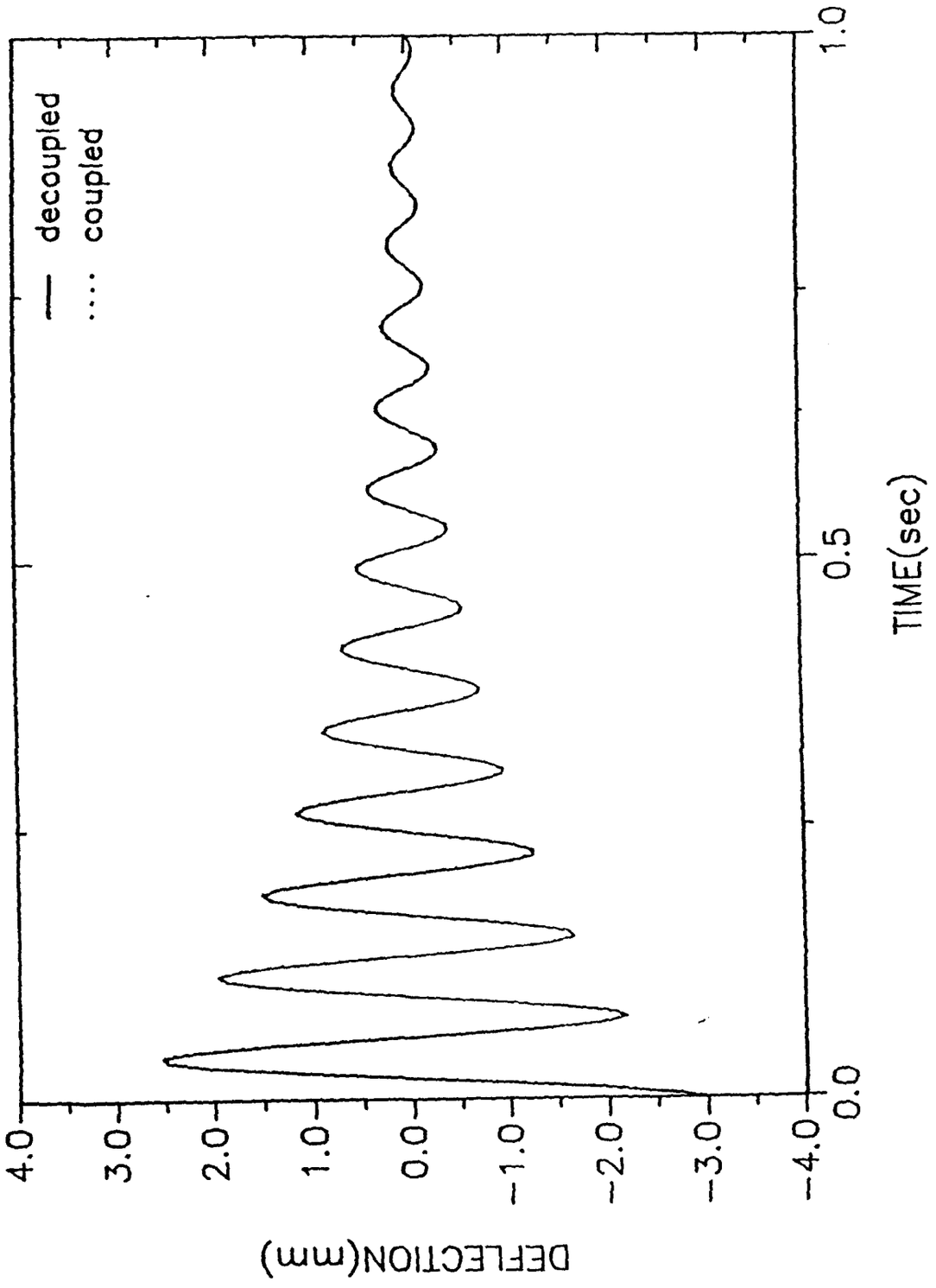
decoupled
coupled
4.0
3.0
2.0
1.0
0.0
-1.0
-2.0
-3.0
-4.0
DEFLECTION(mm)
0.0
0.5
1.0
TIME(sec)

Fig. XI.1

where [Z(V)] (= diag $(2\zeta_i(V)\omega_i(V))$ is the increased modal damping matrix due to the electric field and [Ω(V)] (= diag $(\omega_i^2(V))$ is the matrix containing the increased undamped natural frequencies. Equation VI.6 can therefore be rewritten as

$$[I]\{\ddot{\eta}\}+([Z]+[Z(\hat{V})])\{\dot{\eta}\}+([\Omega]+[\Omega(\hat{V})])\{\eta\}=\{0\} \qquad XI.12$$

or

$$[I]\{\ddot{\eta}\}+[P]\{\dot{\eta}\}+[Q]\{\eta\}=\{0\} \qquad XI.13$$

Experimental observations indicate that both the damping ratio and natural frequency associated with each mode increases as the electric field strength increases. Furthermore, a non-zero dissipation energy function is associated with each of the flexible modes. Since the matrices [P] and [Q] in equation (XI.12) are symmetric and positive definite, the system described by equation (XI.12) is asymptotically stable provided that there is no zero frequency in the original plant described by equation XI.3.

11.1 CONTROLLER DESIGN

The controller design philosophy is motivated by the complimentary experimental program which is focused on studying the free vibration of cantilever beams with an initial prescribed transverse tip deflection. Consequently, the first mode of vibration is assumed to be the dominant mode. Equation XI.12 can, therefore, be reformulated as

$$\ddot{\eta}_1+2\zeta_1\omega_1\dot{\eta}_1+\omega_1^2\eta_1=-2\zeta_1(\hat{V})\omega_1(\hat{V})\dot{\eta}_1-\omega_1^2(\hat{V})\eta_1 \qquad XI.14$$

where subscript 1 refers to the fundamental mode. Clearly equation XI.14 admits the traditional proportional-derivative (PD) state feedback control strategy, which suggests that the proposed smart beam structure can be controlled by applying an imposed external electrical field.

In this preliminary proof-of-concept investigation, it is assumed that the information between the stiffness and energy dissipation increments and the applied voltages is available to the designer. In fact, this assumption can be modified once a viable microstructural-level model of the system is developed. This microstructural-level model would include the interface conditions between the solid and the fluid layers, the conductivity of the face material (electrode), and the dielectric properties of the insulation between the electrodes. The integration of all this information will provide

the basis for establishing a viable model for the actuator dynamics, as a function of the electric field intensity imposed on the ER-fluid domain.

Experimental observations of the response of smart beam-like structures suggest that the characteristics of these structures are governed by relationships of the form

$$\frac{\zeta_1(\hat{V})\omega_1(\hat{V})}{(\zeta_1\omega_1)} - \alpha_1\hat{V} \qquad XI.16$$

$$\frac{\omega_1^2(\hat{V})}{\omega_1^2} - \alpha_2\hat{V} \qquad XI.17$$

where α_1 and α_2 are known constants. Equation XI.14 may be reformulated to incorporate equations XI.16 and XI.17. Thus

$$\ddot{\eta}_1 + 2\zeta_1\omega_1\dot{\eta}_1 + \omega_1^2\eta_1 = -\hat{V}(k_1\dot{\eta}_1 + k_2\eta_1) \qquad XI.18$$

where

$$k_1 = 2\alpha_1\zeta_1\omega_1 \qquad XI.19$$

$$k_2 = \alpha_2\omega_1^2 \qquad XI.20$$

Equation XI.18 can be reformulated as in typical state PD control form, namely,

$$\ddot{\eta}_1 + 2\zeta_1\omega_1\dot{\eta}_1 + \omega_1^2\eta_1 = -K(\dot{\eta}_1 + \beta\eta_1) \qquad XI.21$$

where

$$K = k_1\hat{V} \qquad XI.22$$

and

$$\beta = \frac{k_2}{k_1} \qquad XI.23$$

The ultimate goal for the design of the controller is to achieve the desired time history for the flexural vibrational response by employing a viable control strategy. The control strategy involves the frequency $\omega_{d1}(\tau_i)$ and damping ratio $\zeta_{d1}(\tau_i)$ of the first mode of the beam. Such a control strategy can be easily implemented in practice since the response time of the ER fluid is typically in the order of milliseconds, and a direct current (DC) pulse signal input voltage can be readily imposed on the ER fluid domains of the smart beam. The governing equation for the desired response is given by

$$\ddot{\eta}_{d1}+2\zeta_{d1}(\tau_i)\omega_{d1}(\tau_i)\dot{\eta}_{d1}+\omega^2_{d1}(\tau_i)\eta_{d1}=0 \qquad XI.24$$

where τ_i is a certain period in which the corresponding desired response is maintained. Equation XI.24 serves as the basis for determining the time history of the corresponding feedback gain $K(\tau_i)$. Figure XI.2 presents the relationship between the feedback gain, which is governed by the applied voltages, and time. To validate this relationship herein, an on-off open-loop control strategy was implemented by simply switching on and off the power supply at prescribed times.

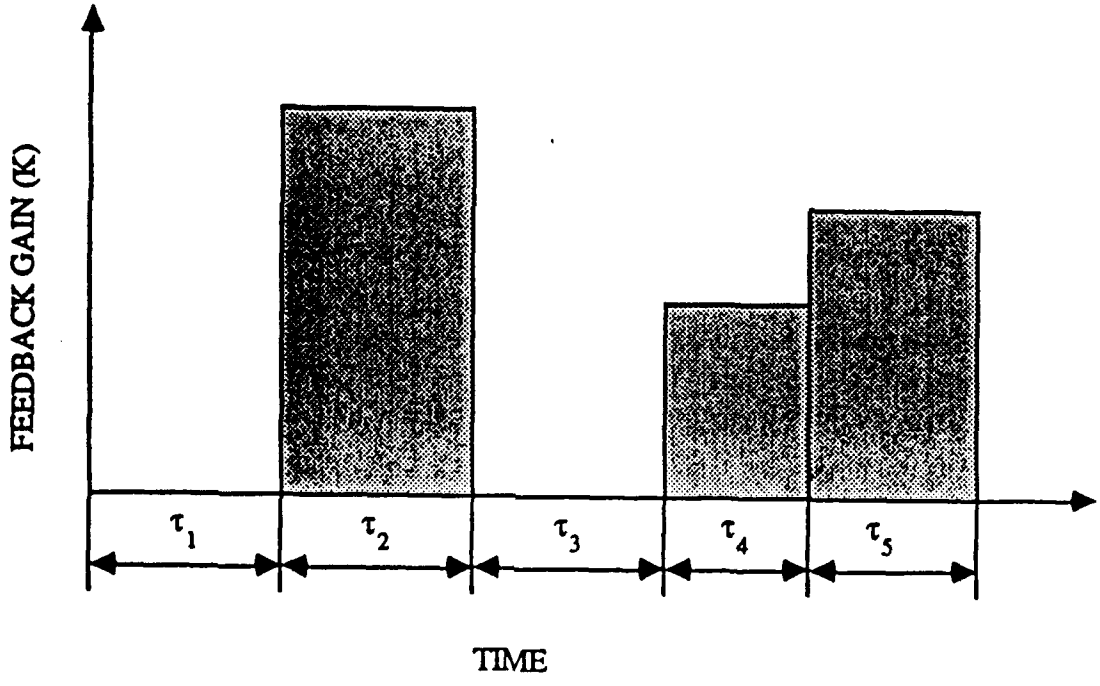

Fig. XI.2

XII PROOF-OF-CONCEPT INVESTIGATIONS OF SMART ARTICULATING MECHANICAL SYSTEMS

Results of investigations focused on evaluating the vibration response characteristics of beam and plate-like structures have been presented in section XI. This section presents preliminary results of proof-of-concept investigations of articulating mechanical systems: slider-crank mechanisms and single-link robots.

Research focused on controlling the dynamic response of articulating machine systems has employed articulating members fabricated in smart structural materials with embedded ER fluid actuators. Figure XII.1 presents the mid-span transverse deflections of the connecting-rod of the planar slider-crank linkage mechanism presented in Figure XII.2 when operating at 95 rpm. The connecting rod was configured to principally deform in flexure in the plane of articulation of the mechanism. It comprised two aluminum electrodes of 0.5 mm thickness and length 265 mm which were separated by a thin layer of silicone rubber adhesive of thickness 1.5 mm in order to insulate the two electrodes and create a uniform void which accommodated the ER fluid. The flexible smart connecting rod was also insulated from the two sets of metallic multi-element bearings at the crank-pin and the gudgeon-pin. It is evident from the two sets of experimental results that the amplitude and frequency of the elastodynamic response of this articulating member, which is being subjected to both parametric and forced excitations, can be controlled by adjusting the external voltage imposed upon the ER fluid domain within the smart structural member.

Figure XII.3 presents a photograph of an experimental robot with a smart arm featuring an embedded ER fluid that is driven by an electrical motor at the hub. Figure XII.4 presents the measured step responses to a commanded step angular position of 7.2 degrees with the compensator zero Z_c = -2. Feedback gains of K_p = 0.5 and K_v = 0.25 were employed. The external input voltage of 2.0 kV/mm and 0 kV/mm were continuously imposed on the ER fluid domain throughout the two manoeuvres. It is clear from the figure that the responses of the robot arm with and without the voltage imposed on the ER fluid domain are dependent upon the magnitude of this voltage. The amplitude of the tip deflection of the robot arm in the absence of the electric field was reduced by approximately 35% when the input voltage of 2.0 kV/mm was imposed on the ER fluid actuator. It is also observed from this response that the settling-time is approximately 1.3 seconds when a voltage is imposed on the fluid domain, while it is approximately 1.6 seconds when an external voltage is not imposed on the ER fluid in

the robot arm. Thus the elastodynamic performance of the robotic system can be greatly enhanced by carefully orchestrating the input signal to the electrical motor and also the electrical signal to the electrorheological fluid actuator embedded within the robot arm.

The research results distilled from these investigations are succinctly summarized below:

1) Smart slider-crank mechanisms can significantly change their characteristics such as amplitudes and frequencies in real-time

2) Smart single-link robots can significantly change their characteristics such as amplitudes and frequencies in real-time

3) These research findings clearly indicate that the smart materials concepts discussed in this report can have a tremendous impact on the evolution of a new generation of smart articulating mechanical systems for the U.S. Army

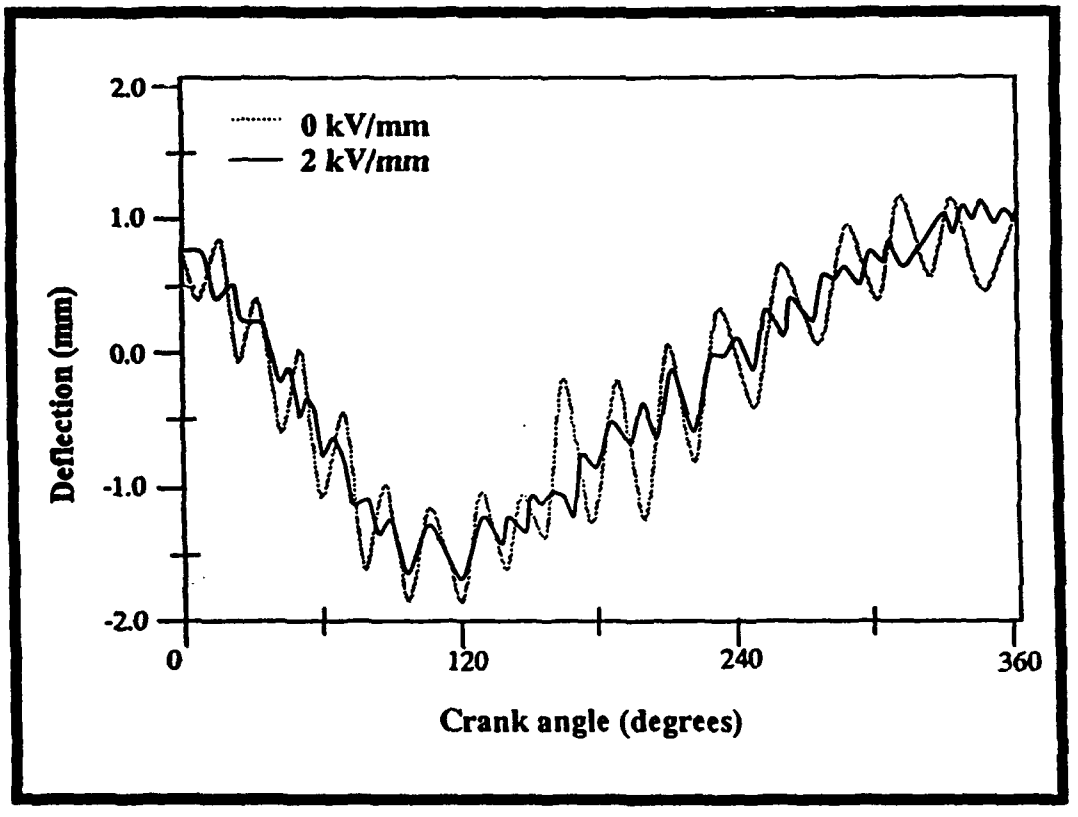

I.1 Midspan transverse deflections of a dynamically tunable connecting rod at an operating speed of 95 rpm.

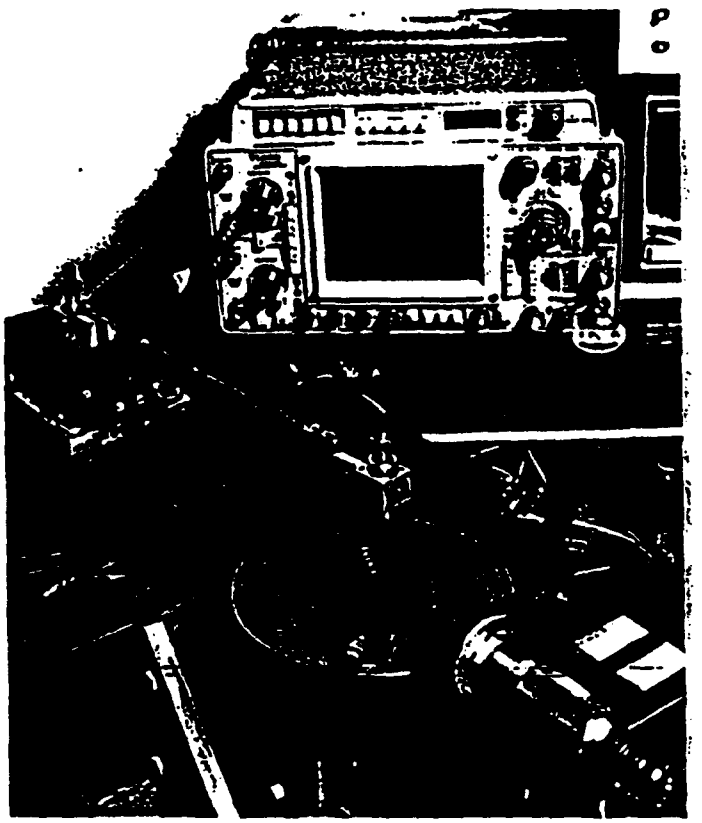

Fig. XII.2 Photograph of an experimental slider-crank mechanism with a smart connecting-rod featuring an embedded electro-rheological fluid domain.

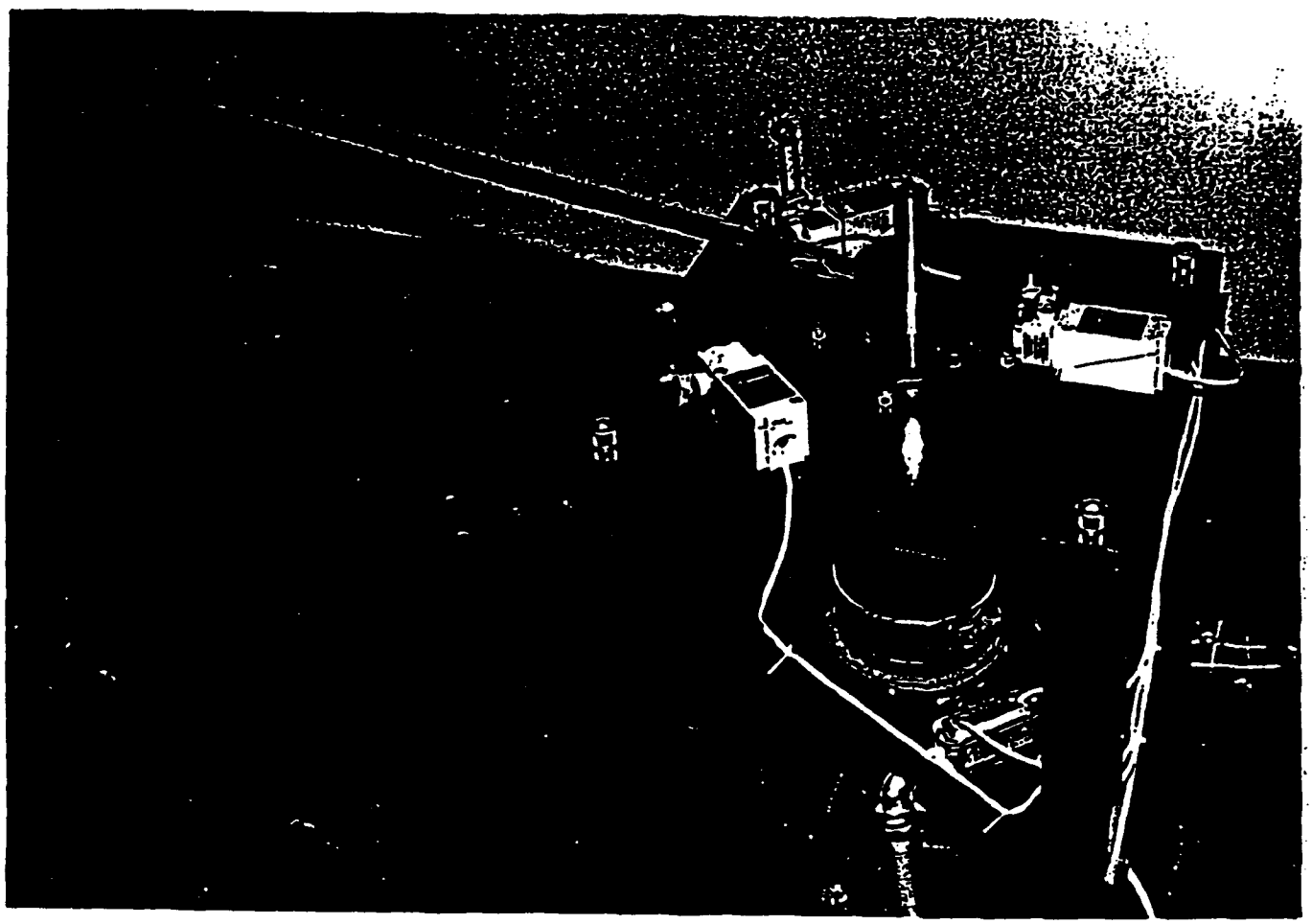

Fig. XII.3 Photograph of a smart robot arm featuring an embedded electro-rheological fluid domain.

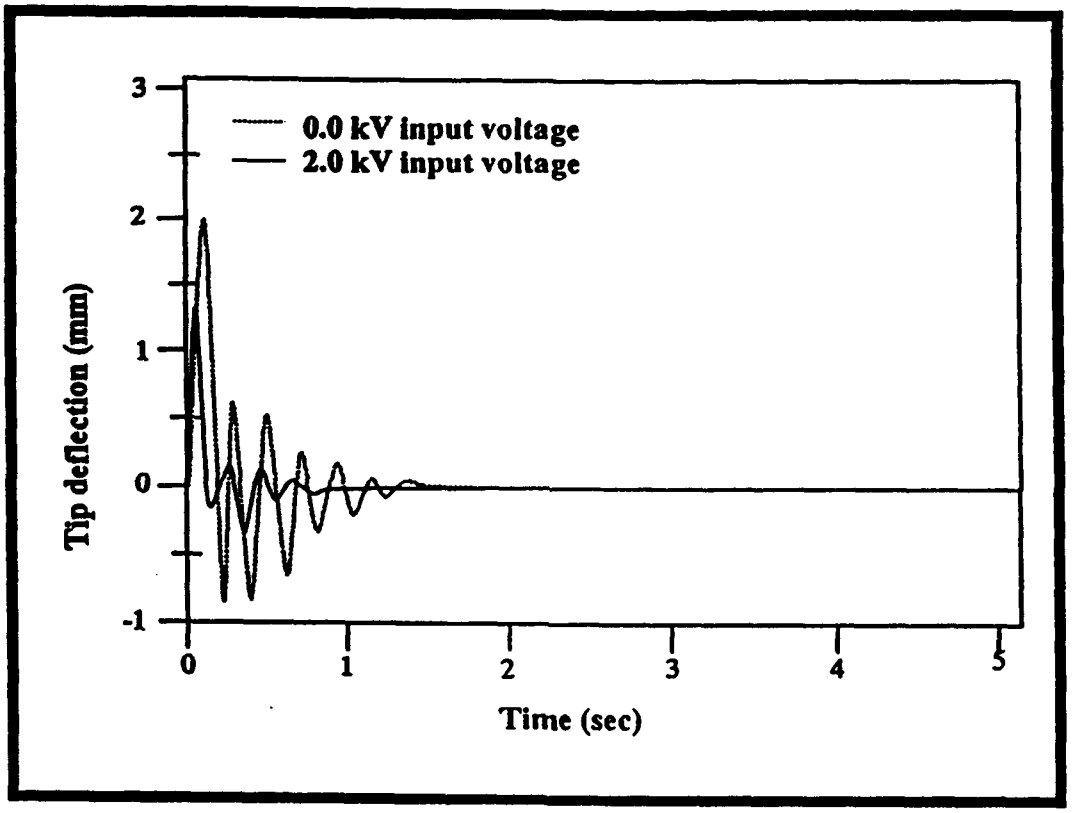

Fig. XII.4 Measured step response with feedback gains of $K_p = 0.5$ and $K_v = 0.25$.

XIII AEROELASTIC TAILORING OF AIRFOILS

Powered high-lift systems such as rotorcraft and other VTOL (vertical take-off and landing) aircraft cannot generate sufficient wing circulation to facilitate take-off, consequently they rely on high ratios of engine thrust to aircraft weight to augment the basic wing lift. In addition to high engine power, however, significant lift augmentation must be obtained by specialized wing design; and this is usually implemented either through the use of boundary-layer control or by the action of a trailing-edge flap. Several derivative designs have evolved from the basic jet flap illustrated in Figure XIII.1(B). Figure XIII.1(A) presents a plot of the variations of coefficient of lift, C_L, for the basic jet flap design, for different values of the angle of attack, α, and the angle of the trailing-edge flap, ^{n}. The deflected flowstream along the flap was found through flow visualization techniques in order to induce an extensive separation bubble on the top surface of the wing, thereby enhancing circulation. The flow visualization produced by the jet flap is depicted in Figure XIII.2. It is sufficient to note here that in level flight the flap would of course be realigned to merge with the leading edge of the wing. The contradictory requirements of high lift and low drag which arise during different stages of flight can be resolved by adjusting the effective camber of the wing. Accomplishing this task will require the development of unique and innovative airfoil designs featuring the appropriate smart materials.

A more subtle adjustment of camber is possible in a lower Reynolds number regime ($\sim 10^6$) that is more characteristic of ultra-light aircraft. A comparison of this lower Reynolds number regime for ultra-light aircraft is illustrated in the Reynolds number spectrum of flight presented in Figure XIII.3. An example of an airfoil which was designed for an ultra-light sailplane of weight 120 kg and 11.5m span is shown in Figure XIII.4. Sufficient lift could be obtained with this airfoil section only by prescribing an under camber of the lower surface of the airfoil, but this shape would induce flow separation near the leading edge during high-speed level flight. Thus the full flight-range requirements could not be met by the highly cambered shape needed for high lift. Low drag could be achieved only by dropping the lower surface to increase the wing thickness and thereby prevent flow separation. This airfoil is intended to change the configuration during flight, activated by command much as by a flap. Clearly, considerable fine-tuning and substantial improvement in the aerodynamic performance of cambered airfoils is possible if smart materials are employed to effect this change in shape and hence, the change in boundary-layer characteristics.

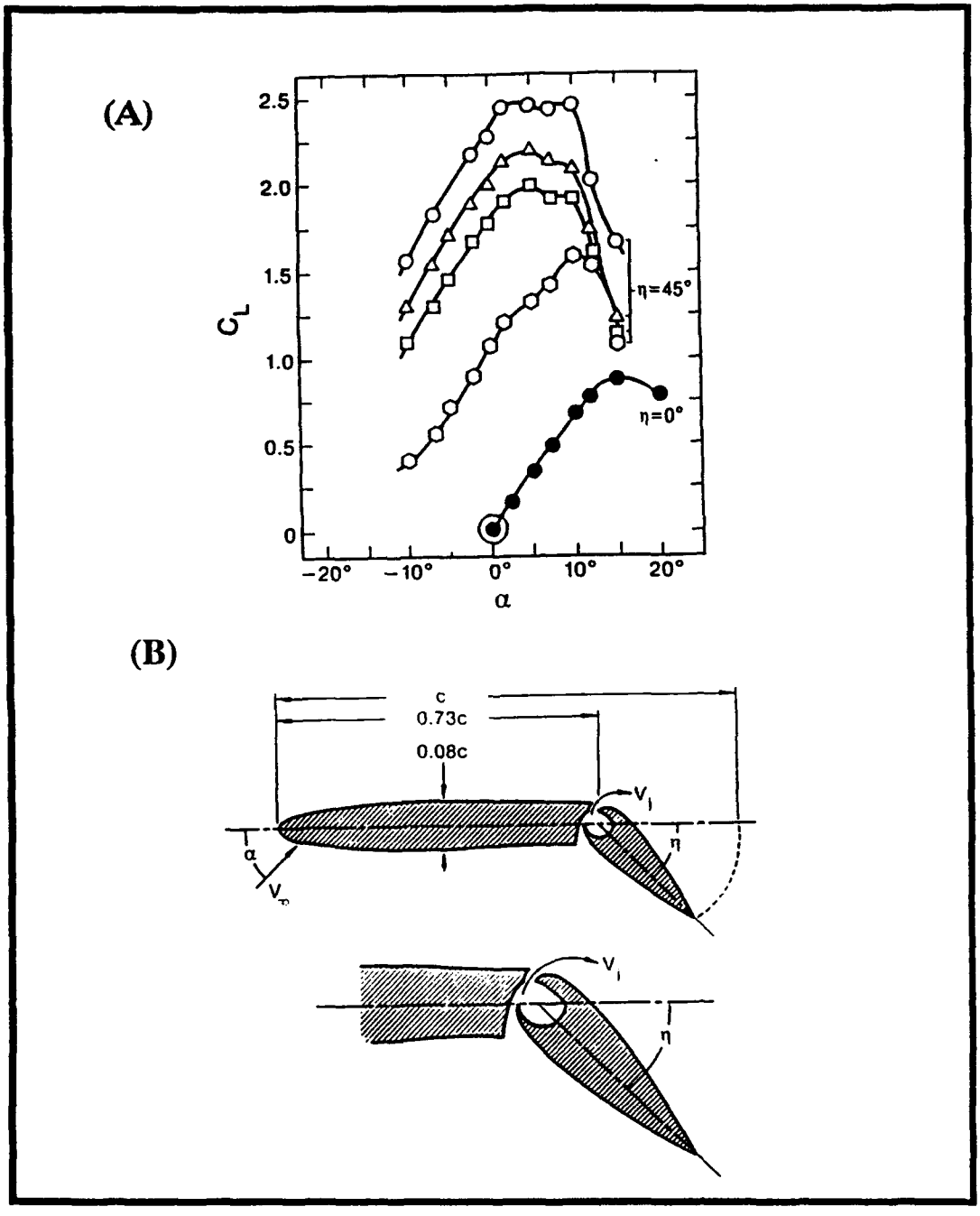

Fig. XIII.1 (A) The variations of the coefficient of lift for different values of the angle of attack and the angle of the trailing-edge.
(B) Basic design of jetf lap, showing lift augmentation obtained by depressing trailing-edge flap.

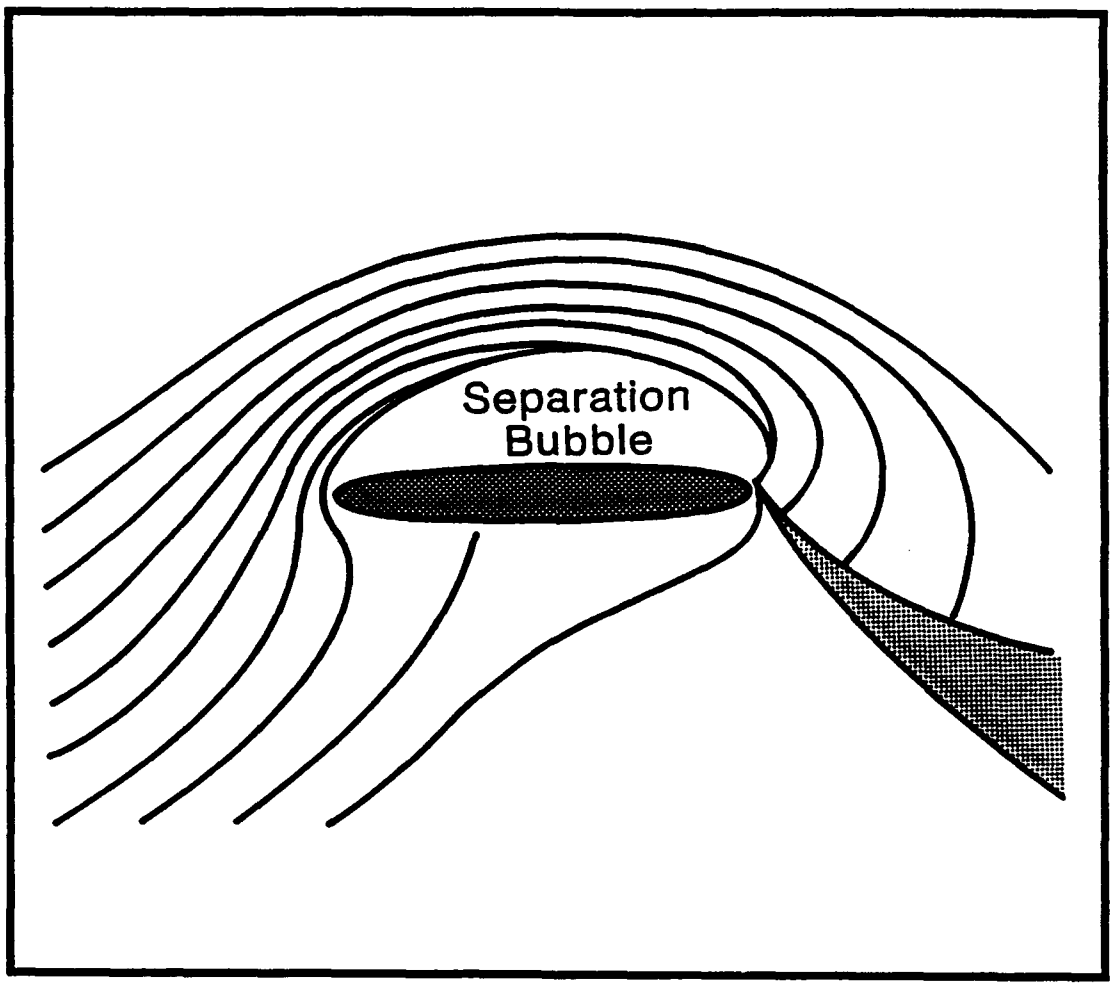

Fig. XIII.2 Flow visualization of the separation bubble produced by a jet flap.

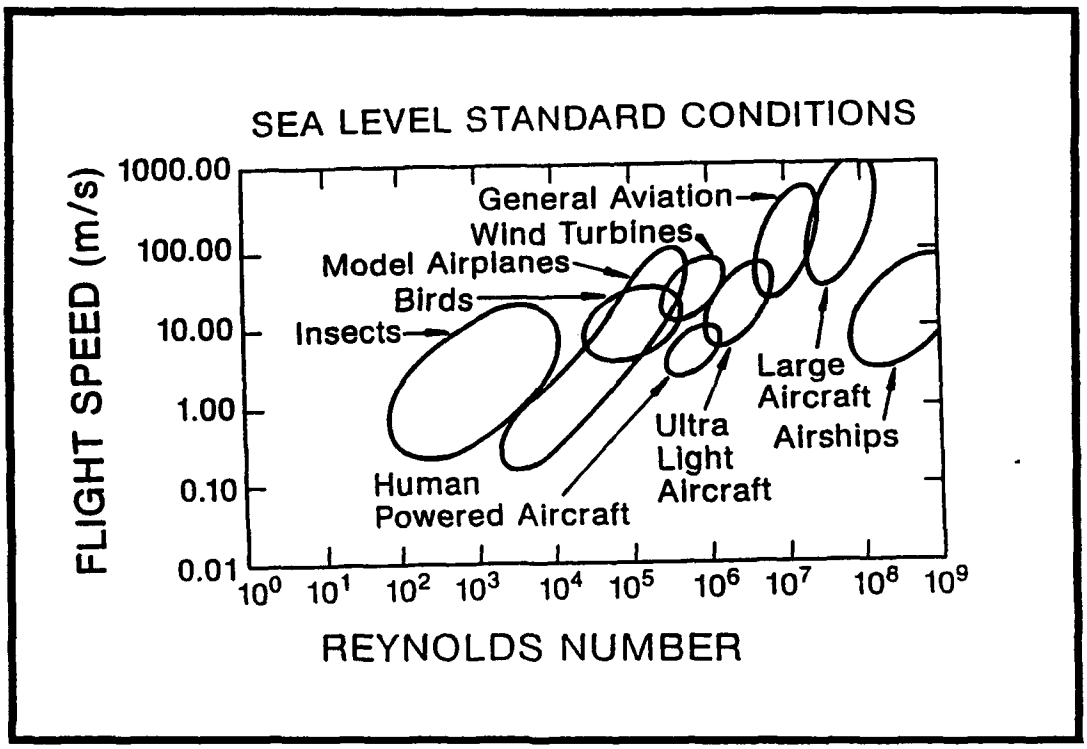

Fig. XIII.3 The Reynolds number-spectrum of flight for various aircraft, airships, and animals.

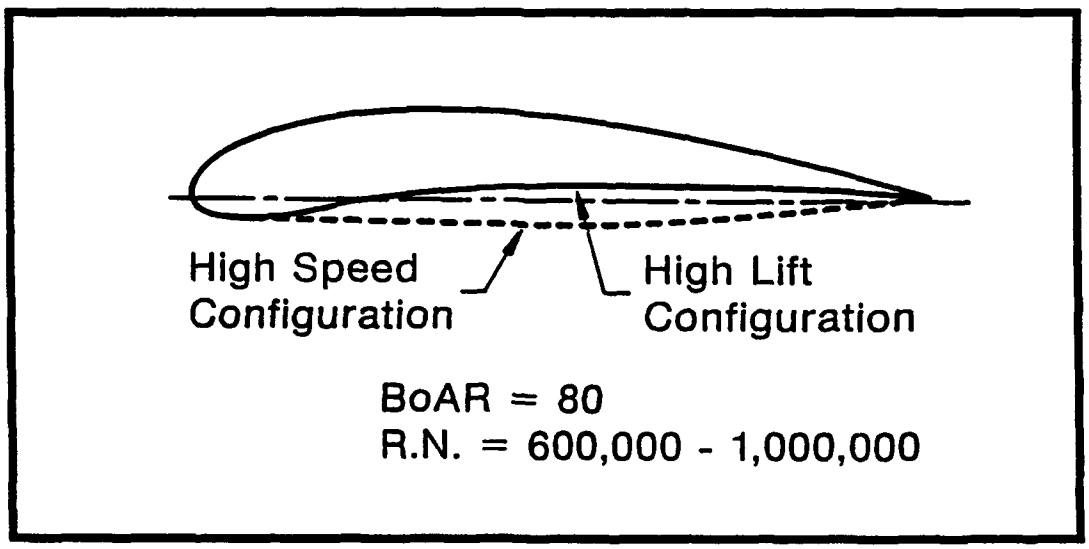

Fig. XIII.4 The proposed BoAR 80 airfoil with adjustable camber.

During prototypical operation, airfoils either encounter or generate unsteady flow at least part of the time. One aim of the aerodynamicist, therefore, is to reduce the undesirable consequences associated with these situations such as flutter, vibration, buffeting, gust response and dynamic stall. Smart materials could play a crucial role in these situations by actively changing the geometrical characteristic of the airfoil in addition to the stiffness and energy dissipation properties. For low Mach-number applications, incompressibility simplifies matters considerably; then thin-airfoil linear theory, suitably modified by superposition of individual corrections for camber, angle of attack and large-amplitude deflections, is often employed to evaluate the effect of oscillating surfaces on lift and drag. Second-order perturbation analyses have been employed to investigate the interaction between thick-cambered airfoils and gust fields. Certain rages of flow conditions, however, cause flow separation leading to effects such as buffeting, flutter and dynamic stall, and all of which exhibit large-scale hysteresis loops. When separation is significant, not even the qualitative behavior of the coefficient of lift, C_L, or the coefficient of drag, C_D, at high angle of attack can be reproduced by neglecting the unsteady motion of the airfoil. This regime of flow-induced vibrations therefore remains largely within the purview of experimentalists.

Autorotation comprises a second category of non-steady flow phenomena pertinent to airfoil design. This phenomenon is exemplified by the Lanchester propeller, illustrated in Figures XIII.5(A),(B), and (C) in simplified form. Any slow rotation produces an opposing force, F, that tends to reduce the motion of the propeller, as shown in Figure XIII.5(B). If, however, the initial rotation, V, is sufficiently high, the net force may reinforce this motion as shown in Figure XIII.5(C).

Under these conditions, the propeller begins to autorotate, and continues to accelerate until a stable equilibrium point is reached, thus, further acceleration reduces the external torque on the blade. This phenomena is depicted in the "Riabouchinsky Curve' shown in Figure XIII.6. The effect of the Reynolds number on the lift to drag ratios, C_L/C_D, for different surface characteristics of airfoils is illustrated in Figure XIII.7. The authors are convinced that significant leads in the aerodynamic performance of rotorcraft and aircraft systems will be accomplished by judiciously employing smart materials.

This phase of the proposed study during Phase II will be focused on the aerodynamic tailoring of smart airfoil sections and also to provide aerodynamic design information pertinent to the construction and operation of the proof-of-concept rotorcraft demonstrator system discussed in section XVI. Therefore the objectives of this investigation are threefold:

1. To conduct subsonic wind-tunnel measurements of lift and drag coefficients on thick-cambered air-foils, to verify the feasibility of transforming high-lift into low-drag configurations simply by altering the material and surface characteristics of the airfoil. Preliminary model selection will be accomplished computationally,

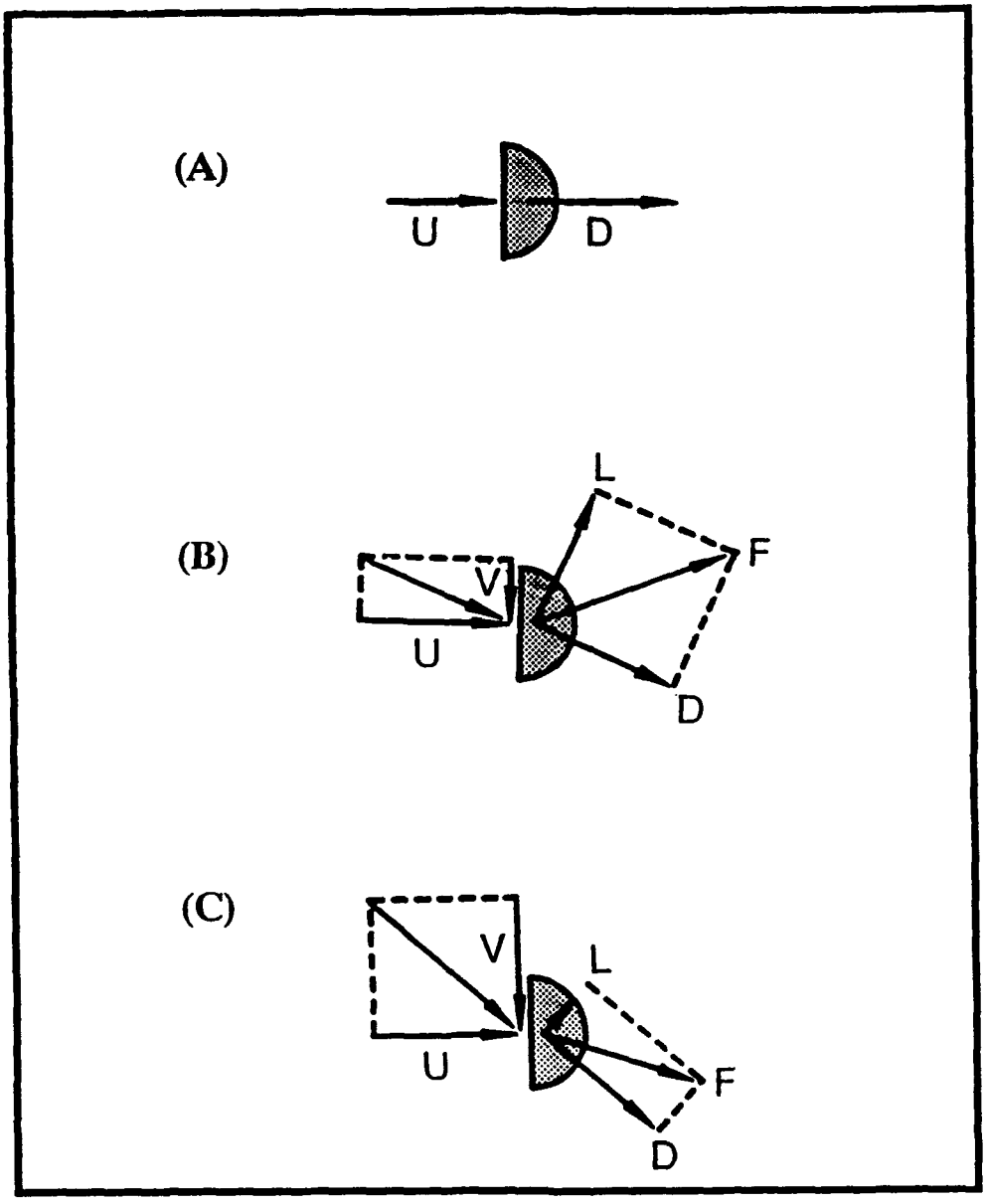

Fig. XIII.5 A demonstration of auto-rotation on a D-shaped blade of a Lanchester propeller.

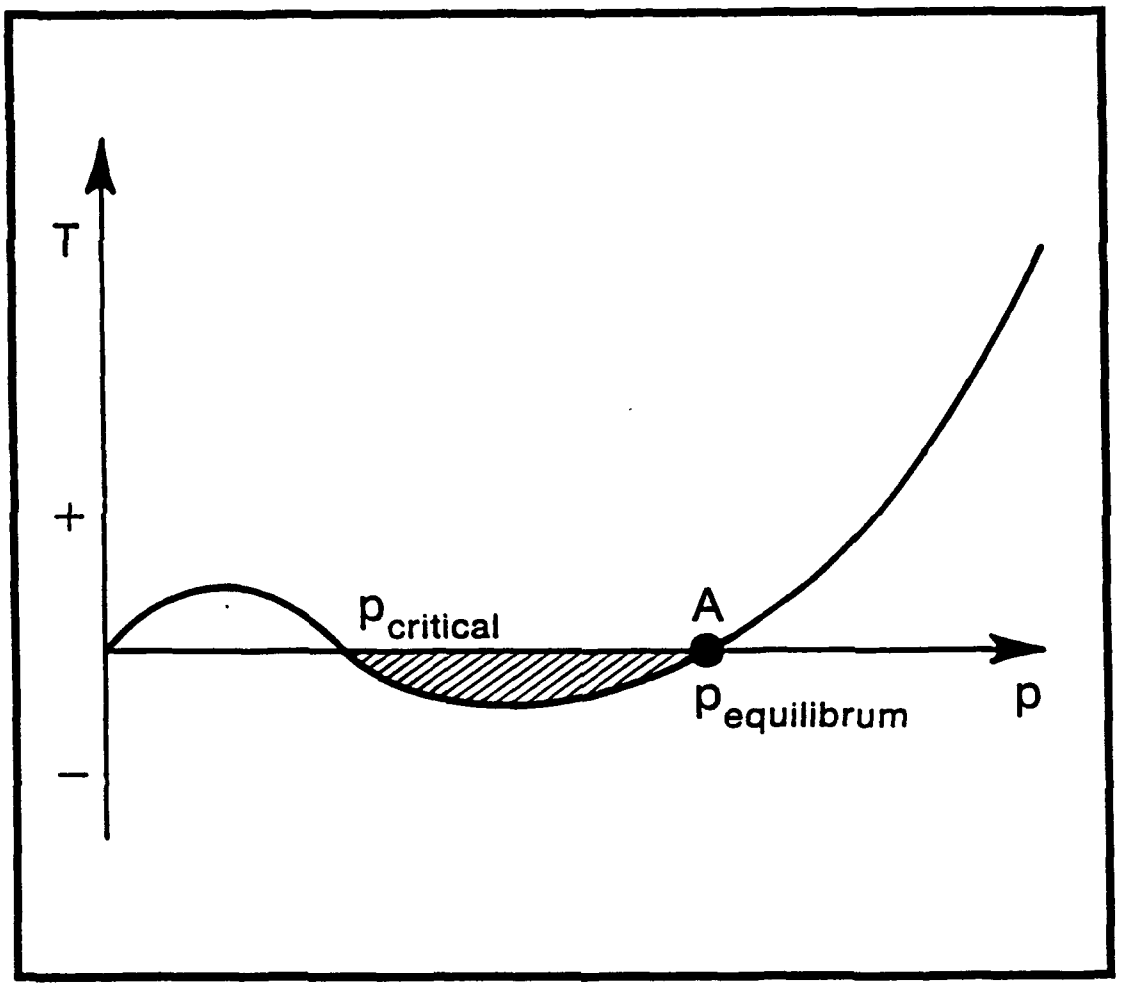

Fig. XIII.6 A "Riabouchinsky curve" which describes the relation between the initial spin, $p_{critical}$, the final spin, $p_{equilibrium}$, and the torque, T, induced on the propeller motion.

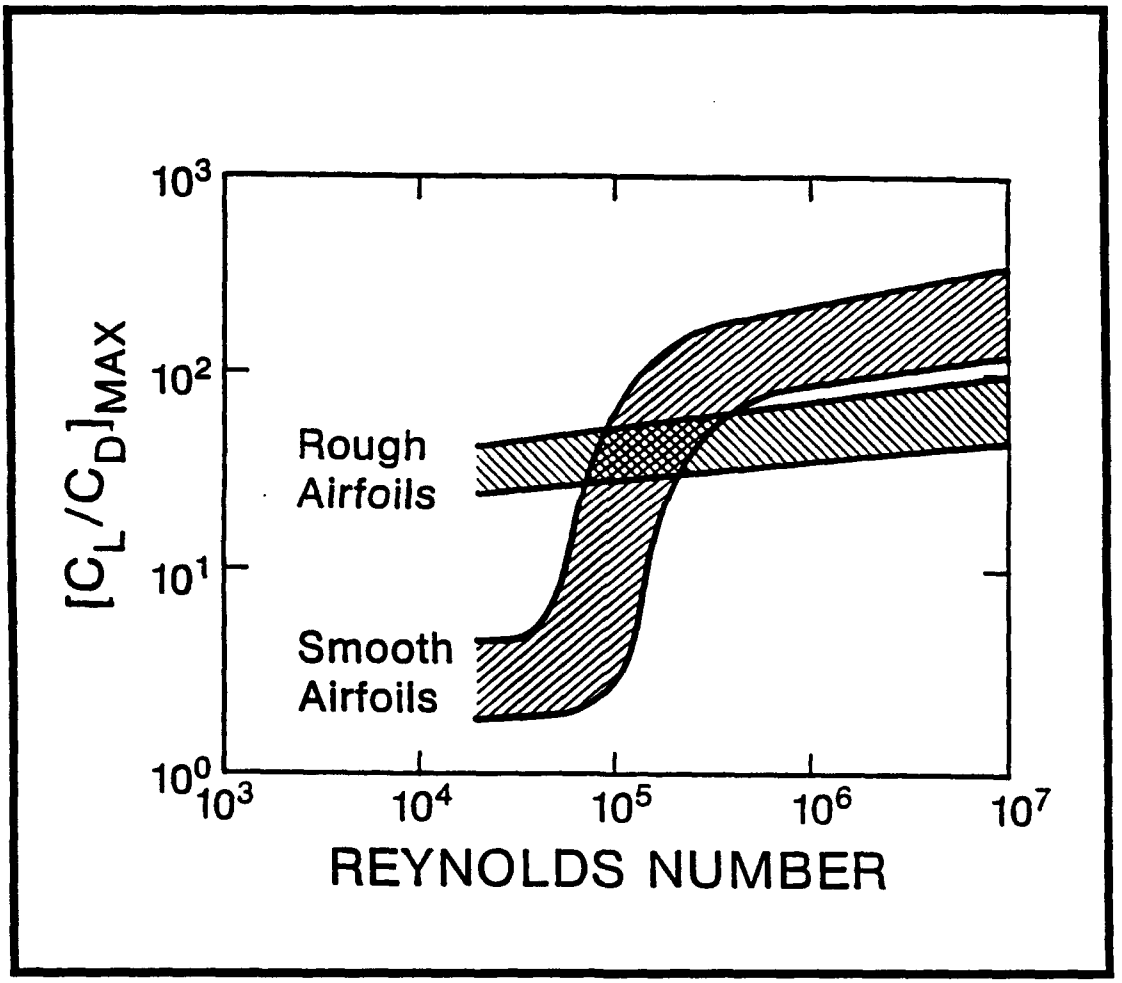

Fig. XIII.7 Low Reynolds number airfoil performance.

using a vortex-panel method. Supplemental three-dimensional velocimetry measurements may be required to evaluate the stability and robustness of flow structures essential to performance, such as the separation bubble on the top surface of the airfoil.

2. To determine experimentally the extent to which autorotation can be suppressed on a thick-cambered blade by altering its configuration.

3. To provide preliminary information regarding airfoil performance during flow transients such as gust fields and/or episodes of flow-induced vibrations.

The procedures used to accomplish these objectives are described below.

13.1 Steady-State Airfoil Performance

Lift and drag coefficients of promising airfoil shapes can be measured in a sub-sonic wind-tunnel facility. It seems preferable, however, to make a prior evaluation of lift computationally, using vortex-panel methods adapted to non-symmetric two-dimensional shapes. Once defined, promising airfoil shapes can then be fabricated.

Simply obtaining lift and drag coefficients of scale models in a specified Reynolds-number range is likely to be insufficient due to a transition in airfoil performance which occurs at Re $\sim 10^5$. Figure XIII.7 shows that the lift-to-drag ratio increases by two orders of magnitude at this point; but conversely, any momentary stall might seriously degrade rotorcraft performance. Several investigators in the literature have emphasized that airfoils which rely on laminar bubbles are especially prone to this instability, so that it seems desirable to explore in some detail the robustness of any particular airfoil design. Three-dimensional velocimetry and/or flow visualization conducted on scale models affords the opportunity for a more fundamental and wider understanding of the mechanisms responsible for measured force coefficients, and therefore is recommended as an integral portion of this study.

13.2 Suppression of Autorotation

A scale-model Lanchester propeller will be mounted on a shaft connected through an automated clutch to a rotary motor, balanced, and driven at critical speed. After spin-up is achieved the clutch will be disengaged to allow coastdown. The subsequent motion will then be monitored by means of a frequency counter which records pulses generated by a piezoelectric/magnetic pickup (the pickup responds to the motion of a permanent magnet imbedded in the shaft, analogous to the operation of a turbine flowmeter).

Substituting blades of different camber will permit an assessment of shape on $p_{critical}$ and p_{equil} defined in Figure XII.6. To ensure safe operation the rotor assembly will, of course, be enclosed entirely within a sturdy containment structure.

13.3 Transient Effects

In the absence of significant flow separation, linear theory provides an appropriate framework to motivate a variety of experimental observations of flow-induced vibrations. Some preliminary estimates of the consequences of large-scale separation to nominal operating values of lift and drag can be made by modifying and extending the planned steady wind-tunnel tests. Altering the angle-of-attack of the scaled rotor blades will produce significant separation, and its consequences on time-dependent lift and drag, including hysteresis, can be monitored using appropriate force transducers at least in a very-low frequency range.

XIV SMART STRUCTURES APPLICATIONS FOR THE U.S. ARMY

14.1 AIRCRAFT

Aircraft continually operate in unstructured environments because of uncertainties in the weather conditions, turbulence, temperatures, payloads, and the duration of the flights. Several smart structures programs have been initiated for both commercial aircraft and also military airplanes. The focus of these "smart skins' programs, so named because of the monocoque design of these structural systems, are dependent upon the specific applications. The commercial aircraft programs focus primarily upon monitoring the health and flight worthiness of aircraft. Arrays of sensors throughout the wings, control surfaces and the fuselage will monitor the structural properties in the context of fatigue cracks and incipient failures. Other types of sensors will monitor the ice build up on wings and control surfaces which can adversely affect aerodynamic performance at take-off and also the controllability of the machine.

While the above programs are largely sensor-based, other efforts are focused on the synthesis of smart structures featuring both sensors and actuators. Some of these programs are directed towards the design of aircraft with non-articulating control surfaces, where the appropriate regions at the edges of the relevant airfoil sections would deform in order to provide the aerodynamic control required. Another program is focused on the development of smart wings whose dynamical response can be automatically adjusted in order to provide smooth flight by tailoring the stiffness and damping properties in discrete sections of the wings.

This philosophy, featuring finite element control segments incorporates sensors, actuators and microprocessing capabilities. Thus as the mass of the wing is reduced by the consumption of aviation fuel from the fuel tanks in the wings, the natural frequencies of the wing structure will also change. An application of this approach is schematically presented in Figure XIV.1. The sensors will monitor the relevant characteristics of the smart structure, and the signals from the sensors will be fed to the appropriate microprocessors which will evaluate the characteristics of the signals, prior to determining an appropriate control strategy in order to synthesize the desired response characteristics. This will typically be accomplished by controlling the material characteristics of the actuators in the specific finite element segments. The material

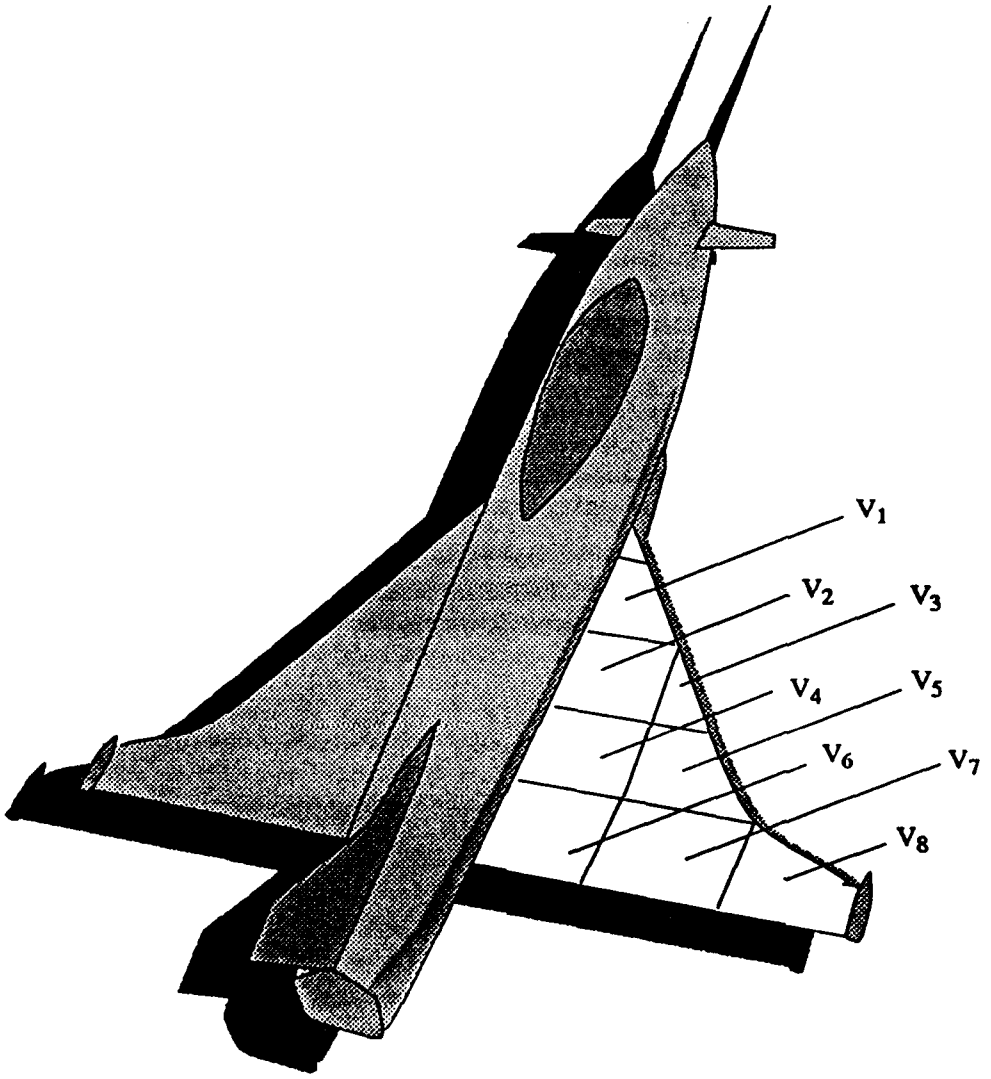

Fig. XIV.1 A strategy for controlling the dynamic response of an aircraft wing fabricated in smart materials.

changes in a typical finite element control segment will in turn alter the global stiffness, and damping characteristics of the smart structure in order to achieve the desired response.

14.2 HELICOPTERS

The dynamic behavior and performance of state-of-the-art helicopter rotors fabricated in advanced polymeric fibrous composite materials are dependent upon the speed of rotation, the speed of the machine, aerodynamic loads and also the ambient environmental conditions of temperature and relative humidity. The rotor is typically designed for a worst-case scenario, which results in a state of over-design for all other operating conditions because the rotor is a passive system. A consequence of this design philosophy is inferior performance at other operating conditions, because of the attendant design-cascading effects associated with the heavier design.

A rotor designed and fabricated in a smart material would be able to detect changes in temperature and moisture associated with operating in the cold dry Arctic regions, or alternatively in the hot, humid equational climates, in addition to detecting dynamic strains associated with wind gusts for example. These data could be monitored and processed by a microprocessor system in a smart rotor, prior to dictating the appropriate corrective actions to be implemented by a network of embedded actuator systems in the structure, in order to ensure optimal performance under all service conditions.

Consider a smart rotorcraft system which capitalizes on the knowledge-base in the area of smart materials and exploits the unique capability of smart materials to interface with solid-state electronics, by the successful incorporation of intelligent sensor technologies and modern control strategies. This innovative rotorcraft system could have the capacity to truly integrate sensing, processing, and actuator functions in order to respond autonomously to flutter, buffeting, gust fields, and dynamic stall, all of which exhibit large scale hysteresis loops, Furthermore, this system could exploit hybrid optimal control strategies in order to tailor the aerodynamic and elastodynamic performance characteristics of the rotorcraft system, which typically is subjected to variable service conditions while operating in unstructured environments in service.

In such a smart rotorcraft system, the fiber-optic sensing system will instantaneously sense the resulting vibrations and changes in temperature, for example, which will permit the microprocessors to optimally actuate the electrorheological fluid, magnetostrictive, SMA and piezo-electric domains in the rotor blades as shown in Figure XIV.2, thereby tailoring the aero-elasto-dynamic performance of the rotor with a pre-defined performance criterion. The rotorcraft system would typically feature SMA actuators for generating large changes in camber, piezo-electric actuators to provide a capability for changing the surface geometrical characteristics, in order to substantially improve the

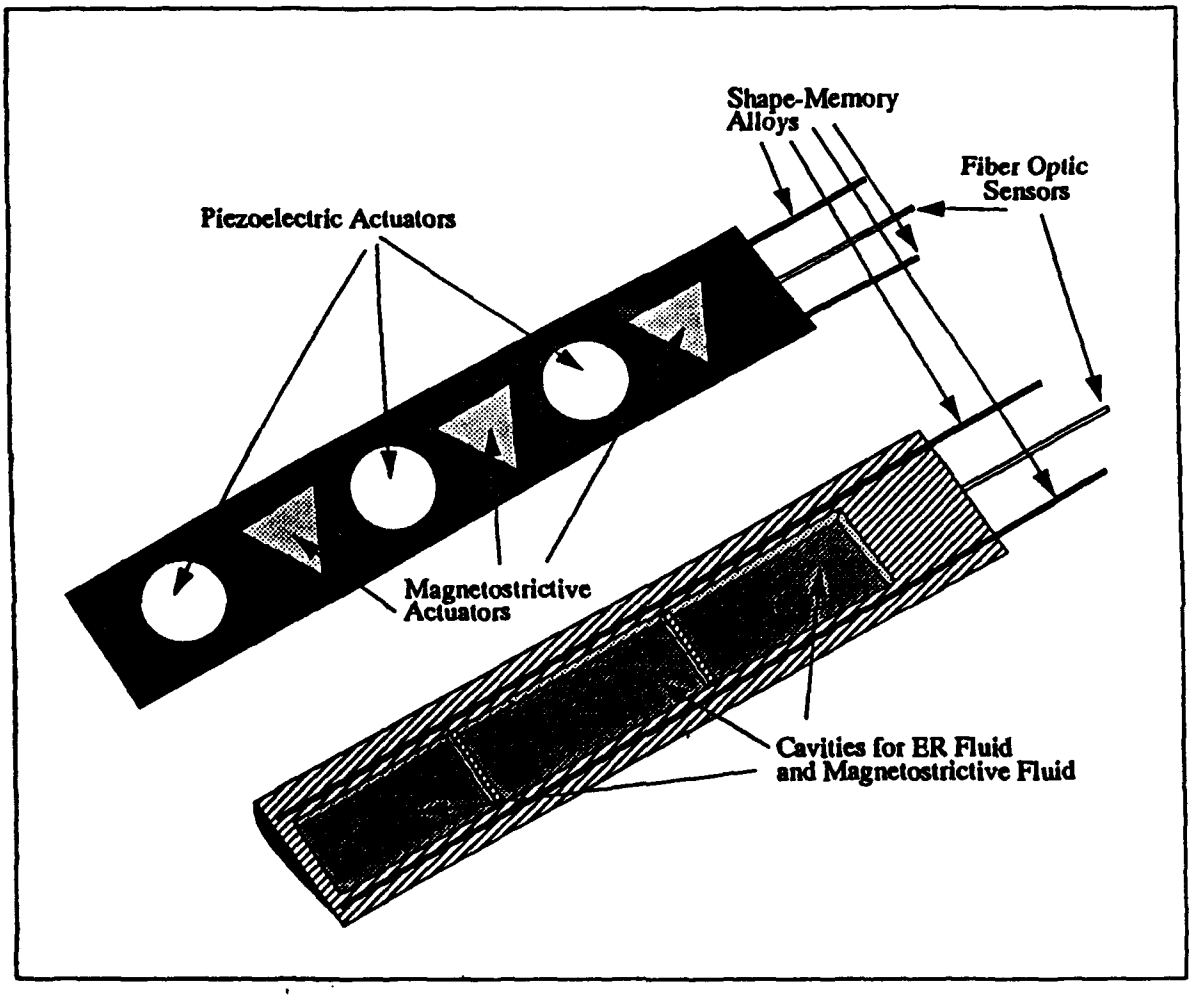

Fig. XIV.2 Conceptual rotor blade featuring smart materials.

aerodynamic performance of cambered airfoil section, ER fluids and magnetostrictive materials to control the vibrational response of the structure, for example. Furthermore, SMAs will allow large changes in the geometry of a structure to be readily accomplished. The hybridization of these distinct classes of actuator systems will permit a dramatic alteration in the microstructural characteristics of the smart actuators, which will permit the global geometrical configuration, and surface geometrical characteristics to be changed, and also the global mass, stiffness, dissipative, and aerodynamic characteristics of the ultra-advanced composite rotor structure to be changed. These accomplishments will be achieved by changing the electric field imposed upon the ER fluid and piezoelectric domains, the magnetic field imposed upon the magnetostrictive domains and the thermal field imposed upon the SMA domains.

Military programs for both helicopters and aircraft are not only focused upon the above objectives but also a number of other aspects too. For example, if the aircraft is damaged by enemy action, then what are the consequences, and how does this event affect the original scope of the mission? Smart structures will be developed which will quickly assess the state of the airframe prior to advising the pilot of limitations in the flight envelope and also the degree of severity of the maneuvers that the plane can safely withstand without catastrophic failure, or else automatically adjusting the controls to ensure stable operation of the aircraft. Stealth technologies are also being incorporated in the smart skins of these shell-like aerospace vehicles. The goal is to be able to actively change or reduce the radar signature of the vehicle by controlling the absorbtivity of the skin or else changing the local geometry of the skin. The U.S. Air Force claim that the radar image of the 172-foot wide, 370 000 pound, $815 million B-2 stealth bomber is in the insect category when viewed by enemy ground or airborne radar. The generic research associated with these programs which focuses on coupled field phenomena is also relevant to submarines, and their interactions with sonar waves, and also the acoustical noise radiated from military, commercial and domestic products.

The "smart-materials tool-kit' of diverse classes of actuators, sensors, microprocessors, and data-links available to design engineers can be readily employed to synthesize a new generation of superior products for the sporting goods industries. Typically, the superior performance would be achieved by exploiting the superior dynamic response characteristics of smart materials which would be achieved by actively changing the mass, stiffness, and energy-dissipation characteristics of the smart structure. This technology could revolutionize the sporting goods industry as dramatically as the current generation of equipment fabricated in polymeric advanced composite materials, which have been a major factor in the establishment of numerous records in many different sporting events.

14.3 DEFENSE INDUSTRY

- Hydraulic valves, actuators and pumps

- Switches
- Variable radar and acoustical signature
- Smart skins (life through death health monitoring capabilities: manufacturing, service, battlefield damage)
- Ammunition supply systems
- Materials handling equipment
- Smart armor
- SDI (space structures supporting weapons and antenna for retargetting maneuvers without detrimental jitter and thermo-flutter)
- Stealth technologies (to evade enemy emitter and platform identifications to make more specific threat determinations_
- Field-repairable airframe structures (Innovative high-lift rotors for helicopter super-maneuverability)
- Acoustically-damped propellers and fans
- Smart skins containing phased-arrays (to permit aircraft to sense and communicate in various frequency bands and in any direction)
- Smart wings (improve manufacturing quality and productivity, improve aerodynamics and system performance in service, detect damage and impending failure)
- Smart control surfaces
- Smart rotor-craft systems (minimize vibrations, improve system performance under variable service conditions)
- Vibration suppression systems
- Instrument panels (improved design for strategic and tactical systems)
- Undercarriage, shock absorbers, landing gear
- Hydraulic pumps, actuators and valves

- Missile actuator systems
- Large space structures (improve performance in unstructured environments)
- Space robots
- Self-deploying space structures

14.4 MILITARY VEHICLE APPLICATIONS

- Engine mounts (minimize vibration and noise)
- Active suspensions (improve ride and handling)
- Steering systems (improve system performance)
- Shock absorbers
- Smart windshields
- Smart bumpers (improve crashworthiness)
- Pumps, valves and actuators (improve system performance)
- Clutches and transmission systems (smooth start-up and improved performance)
- Anti-lock braking systems
- New generation of engines
- Automotive springs

14.5 BIOMEDICAL DEVICES

- Prostheses: artificial limbs, hands and joints
- Orthodontic braces
- Sclerosis

- Wheelchairs
- Treatment of supporting injuries (fractures)
- Implants

14.6 ADVANCED MACHINERY APPLICATIONS

- Active balancing
- Dynamically-tunable robot arms
- Vibration control of machine-tool structures (improve quality and productivity)
- Hydraulic actuators, valves and pumps
- Joint actuators for articulating robotic systems
- Robotic end-effectors
- Smart flexible fixtures and grippers (to handle workpieces of various shapes and sizes)
- Material handling
- Oil drilling and mining equipment (improved performance in unstructured environments)

14.7 HIGHWAYS, BUILDINGS AND BRIDGES

- Smart foundations
- Smart skins
- Dynamically tunable optical and thermal characteristics for doors and windows (energy efficiency and comfort)
- Smart structures, bridges, buildings (minimize vulnerability to damage)
- Building elevators

14.8 IMPACT ON OTHER CONSUMER PRODUCTS AND SPORTING GOODS

- Skis
- Tennis rackets
- Golf clubs
- Fishing poles
- Baseball bats
- Snowmobiles
- Bicycle industry
- Switches
- Washing machines
- Household dryers
- Vacuum cleaners
- Lawn mowers
- Snow blowers

14.9 HIGH PRECISION INSTRUMENTS, ELECTRONIC PCB'S AND PACKAGING

- Advanced vibration isolation concepts
- Dynamically-tunable optical characteristics
- Dynamically-tunable thermal characteristics

XV RESEARCH FINDINGS AND RECOMMENDATIONS

15.1 RESEARCH FINDINGS

15.1.1 Electrorheological Fluids

The research results distilled from undertaking combined experimental and analytical investigations on electrorheological fluids are succinctly summarized below:

1. Electrorheological fluids are characterized by non-Newtonian constitutive behavior.
2. Electrorheological fluids sometimes exhibit shear thinning.
3. There is a large change in the non-Newtonian viscosity in the presence of an electric field for a prescribed shear rate.
4. As the concentration of the particulate phase of an electrorheological fluid decreases, the electrorheological effect also decreases.
5. The yield stress of electrorheological fluids increases monotonically with the magnitude of the electrical field intensity.
6. A first-order model for electrorheological fluids has been proposed.

15.1.2 Piezoelectric Materials

The research results distilled from undertaking experimental and analytical investigations on piezoelectric materials are summarized succinctly below:

1. The constitutive characteristics of commercially available piezoelectric ceramics and polymers are adequately modeled by linear constitutive relations.

2. Distinct classes of piezoelectric ceramic (PZTs) materials are more appropriate for actuators while piezoelectric polymeric materials (PVDF) are more appropriate for sensors in smart material applications.

3. Piezoelectric actuators have capabilities superior to the electrorheological fluids for imposing higher magnitude bending moments and other classes of loading characteristics on smart structures. However, their dissipative characteristics are substantially inferior to these exhibited to these exhibited by electrorheological fluids.

4. The response characteristics of piezoelectric actuators are infinitely variable through the selection of appropriate excitation voltages which permit amplitudes and frequencies of smart structures to be controlled in real-time. Non-harmonic and harmonic excitation voltages can also be employed to tailor the response characteristics of this class of smart structures.

15.1.3 Fiber-Optic Sensing Systems

A variety of fiber-optic materials and sensing strategies for several applications were comprehensively evaluated. The research results are highlighted below.

1. Fiber-optic sensing systems are able to monitor the state of cure during the manufacture of a composite structural component and this information can provide the basis for on-line closed loop control during manufacture in an autoclave process, for example.

2. Fiber-optic sensing systems possess the ability to rapidly transfer high volumes of data, and in addition photonic phenomena permit a diverse group of parameters to be measured such as pressure, force, strain, magnetic fields, damage, and temperature, for example.

3. Typical fiber-optic systems are Mach-Zehnder interferometers, Michelson interferometers and several polarimetric devices.

4. Fiber-optic strain sensors have been developed for measuring strain at a point and they have also been employed for damage detection associated with impact and delamination phenomena.

5. The embedding of optical fibers in polymeric laminates does *not* significantly adversely affect the interlaminar toughness of the structure, or the strength of the structure provided empirical guidelines are complied with.

6. Damage detection in polymeric composites can be accomplished by the utilization of an array of optical wave guides that are severed by cracks propagating through the structure, thereby severing the optical path and reducing the intensity of light at the photodetector.

15.1.4 Smart Structures and Articulating Mechanical Systems

The research results distilled from investigations on smart structures and articulating mechanical systems are succinctly summarized below:

1. Smart beams and plates can change their natural frequencies by several hundred percent when an appropriate external electrical field is employed.

2. Smart beams and plates can change their mode shapes substantially when an appropriate external electrical field is employed.

3. Smart beams and plates can change their damping characteristics significantly when an appropriate external electric field is employed.

4. Typical response times for this class of smart beams and plates is of the order of milliseconds, which is crucial for the control of structural vibrations in real-time.

5. The high voltages mandated by the constitutive characteristics of electrorheological fluids and piezoelectric materials typically mandate the deployment of non-electric sensors, particularly fiber-optic sensors in this class of smart materials because they do not utilize electrical phenomena in the strain detection domain.

6. The research findings indicate that there is an infinite variety of response characteristics for this class of smart beams and plates featuring electrorheological fluid domains and piezoelectric materials because the electrical field imposed upon these domains controls the response of the structure.

7. Design tools for smart materials and structures applications will typically involve the integration of concepts from continuum mechanics, such as field equations and boundary conditions, and computational techniques such as finite element methods. In order to develop these computational tools, two variational theorems were established for smart structures featuring firstly an elastic body with embedded electrorheological fluid domains. Subsequently,

finite element formulations were systematically developed for these two classes of smart structural systems.

8. Appropriate control strategies for smart structures have also been developed and presented.

9. Innovative concepts on smart structures utilizing hybrid actuator materials have been presented and preliminary results of experimental investigations focused on hybrid smart structures have clearly demonstrated the feasibility of exploiting hybrid actuator systems in practice.

10. Proof-of-concept investigations focused on slider-crank mechanisms and single-link robots have clearly demonstrated the feasibility of deploying smart material concepts for both structural and mechanical system applications.

11. Innovative concepts on the development of smart airfoils which can tailor their aeroelastic characteristics in real-time have also been presented.

12. A comprehensive library of smart structures applications has been developed in addition to a library of applications of articulating mechanical systems featuring smart materials.

15.2 RECOMMENDATIONS

Preliminary proof-of-concept investigations have been undertaken, and also the appropriate mathematical and computational tools for the development and deployment of a smart demonstrator system have been successfully established in Phase I. A comprehensive library of smart structures and articulating mechanical system applications has been developed and documented.

The principal research findings distilled from these comprehensive set of investigations clearly indicate that it is possible to significantly tailor the vibrational and aeroelastic characteristics of structural and mechanical systems for US Army applications. It is, therefore, recommended that Phase II be focused on the development of a US Army smart rotorcraft demonstrator system which will have the ability to autonomously tailor its vibrational and aeroelastic characteristics in response to variable service conditions while operating in unstructured environments. The rotorcraft system will also feature capabilities to detect and appropriately respond to routine service damage and/or battlefield damage by employing state-of-the-art optronic systems. Preliminary concepts for the design, development, fabrication, and testing of a smart US Army rotorcraft demonstrator have also been presented.

XVI PHASE II : PRELIMINARY CONCEPTS FOR THE DESIGN, DEVELOPMENT, FABRICATION, AND TESTING OF A SMART U.S. ARMY ROTORCRAFT DEMONSTRATOR

A multi-disciplinary inter-institutional research program is proposed herein which focuses on the development of innovative self-adapting smart materials, whose unique capabilities can be exploited in the development of a new generation of U.S. Army systems mandating *active continuum vibration control* and *aerodynamic tailoring* capabilities. These smart systems will feature embedded hybrid multi-functional actuation systems which capitalize on the diverse strengths of electro-rheological (ER) fluids, magnetostrictive materials, shape-memory alloys (SMAs) and piezoelectric materials, and which operate in conjunction with fiber-optic sensing systems. This class of smart structures will accelerate the development of a new generation of advanced helicopter and rotorcraft systems, battlefield ammunition-supply systems, and matériel handling systems, for example. Typical national defense programs which will also significantly benefit from the research proposed herein include the Strategic Defense Initiative, the National Aerospace Plane, and self-adaptive stealth submarine skins. *The market for these applications which are crucial to the national defense mission, has been estimated to be $65 billion a year by 2010.*

This proposal builds upon the seven years experience of the *Quantum* Team in the area of smart materials which has culminated in the award of three DoD contracts in 1988-1991. The *Quantum* Team has already successfully undertaken pioneering proof-of-concept studies, and also combined experimental and analytical investigations which clearly demonstrate, the ability to dramatically change the vibrational characteristics of mechanical systems fabricated in smart composites featuring ER fluids, piezoelectric materials, SMAs and magnetostrictive materials by controlling the external stimuli imposed upon them. This work has provided first-order analytical tools for the design of a variety of prototype laboratory platforms including robotic systems, linkage mechanisms and a first generation rotorcraft system.

The proposed research program, led by a *multi-disciplinary team of research physicists, chemists and engineers at Quantum Consultants, Inc.*, will permit viable analytical tools to be established for deploying smart rotorcraft system with optimally adaptive mass, stiffness, dissipative, and also aero-elastic characteristics. The capabilities developed through this program will permit engineers to actively-tune natural frequencies and geometric configurations, amplitudes of vibration, damping properties, sub-harmonic

resonances, and lift/drag ratios of cambered airfoils, for example, in a wide variety of engineering systems subjected to diverse forced, transient and parametric excitations.

The knowledge-base developed through this research program will be crucial in exploiting the unique capabilities of smart materials for developing an innovative rotorcraft demonstrator system which will be the first of its kind to truly integrate sensing, processing, and actuation functions in order to autonomously respond to simulated flutter, buffeting, gust fields and dynamic stall. It is anticipated that this demonstrator will catalyze the evolution of a new generation of high-performance military systems.

By judicious selection, the smart-materials designer can synthesize numerous classes of hybrid actuation systems from these principal classes of actuators to satisfy a broad range of performance specifications than can not be satisfied by employing a single class of actuator systems alone. *The proposed research program is focussed on tailoring the geometric configurations and the elastodynamic and aerodynamic characteristics of US Army rotorcraft systems, therefore, the hybridization of ER fluids, magnetostrictive materials, shape memory alloys and piezoelectric actuator systems is proposed herein. This hybridization philosophy will enable geometrical configuration tailoring, and continuum vibration and aerodynamic tailoring capabilities to be accomplished with a high level of reliability.* The commercial and economic significance of these smart-materials technologies will be evident once these materials are adequately modeled so that design engineers can capitalize on their unique, adaptive capabilities.

16.1 INTRODUCTION

The insatiable demand in the international marketplace for high-performance structural and mechanical systems for the aerospace, defense, and advanced manufacturing industries has triggered the evolution of advanced composite materials. These diverse high-performance applications have mandated that designers tailor both the materials and the material microstructural characteristics in order to ensure optimal performance of mechanical and structural systems under variable service conditions and unstructured environments. Designers have responded to these challenges by developing optimal design methodologies for a broad class of composite materials. Typically, these methodologies have been employed to optimally select the individual constituents, their micromechanical characteristics, and the spatial distribution of these constituents in order to synthesize a viable structure or subsystem with the desired mass, stiffness, and damping properties, for example.

However, these optimization strategies for traditional advanced composite materials yield an optimal design which is passive in nature. This situation can be readily illustrated by considering the response of an optimally-designed helicopter rotor fabricated in a conventional advanced composite material, which cannot respond to unstructured

environments, and changes in the rotational speed, aerodynamic loading, payload, and the ambient hygrothermal environment, for example. Therefore, even an optimally-tailored rotor designed in a traditional advanced composite material is clearly sub-optimal for all service conditions except the one for which the rotor was "optimally designed". *In sharp contrast to this undesirable scenario, if the rotor were fabricated in one of the smart ultra-advanced composite materials proposed herein, then the performance of the rotor could be dynamically-tuned in real-time to ensure optimal performance under all service conditions and in all unstructured environments. Therefore, the technology on smart materials and structures proposed in this document represents a revolutionary quantum jump in the technology-base relative to the current generation of advanced composite materials in the marketplace at this time.*

A multi-disciplinary research program focused on the development of a new generation of self-adapting mechanical and structural systems featuring embedded hybrid multiple multifunctional actuation systems which capitalize on the diverse strengths of electrorheological fluids, magnetostrictive materials, shape-memory alloys and piezoelectric materials, and operate in conjunction with hybrid fiber-optic sensing systems is proposed herein for *active continuum vibration* and *aerodynamic tailoring* applications. These ultra-advanced, smart composite structures feature hybrid fiber-optic sensing systems and dynamically-tunable embedded ER fluids, magnetostrictive materials, shape-memory alloys and piezoelectric materials, which are interfaced with the advanced composite structures.

The almost instantaneous response-time of the magnetostrictive materials, ER fluids, and piezoelectric materials, and the inherent ability of these materials to interface with solid-state electronics and modern control systems provides designers, for the first time, with a unique capability to synthesize ultra-advanced smart composite structures whose continuum elastodynamic response characteristics can be actively controlled in real-time. Small and moderate changes in the surface geometrical characteristics can be accomplished in real-time by employing piezoelectric ceramic materials in order to substantially improve the aerodynamic performance of thick cambered airfoils, for example. Furthermore, shape-memory alloys will allow large changes in the geometry of a structure to be readily accomplished. The hybridization of these distinct classes of actuator systems proposed in this document will permit a dramatic alteration in the microstructural characteristics of the smart actuators, and hence the global geometrical configuration, and surface geometrical characteristics, and also global mass, stiffness, dissipative, and aerodynamic characteristics of the smart ultra-advanced composite structure by changing the electric field imposed upon the ER fluid and piezoelectric domains, the magnetic field imposed upon the magnetostrictive domains and the thermal field imposed upon the SMA domains. An application of this hybridization philosophy to control the vibrational and aerodynamic response characteristics of an aircraft wing is schematically presented in Figure XVI.1.

This class of innovative materials derive their intelligence from the merger of sensors, built into the finite element control segments of the ultra-advanced composite material continuum, microprocessors, and dynamically-tunable electro-rheological fluids, magnetostrictive materials, shape-memory alloys and piezoelectric materials as shown in Figure XVI.3. The sensors monitor the elastodynamic behavior of the ultra-advanced composite structure, and the signals from the sensors are fed to the appropriate microprocessor which evaluates the signals prior to determining appropriate control strategies in order to synthesize the desired elastodynamic and aerodynamic response characteristics, for example. This is typically accomplished by controlling the geometrical constitutive characteristics of the smart actuators embedded in the finite element segment associated with the particular sensor. This change in the microstructural characteristics of the smart material in a typical finite element control segment in turn alters the global geometrical configuration and surface geometrical characteristics, and also the global mass, stiffness, and dissipative characteristics of the ultra-advanced composite structure in order to achieve the desired aerodynamic and vibrational response.

The knowledge-base developed through this research program will be crucial in exploiting the unique capability of smart materials to interface with solid-state electronics by the successful incorporation of intelligent sensor technologies and modern control strategies in order to develop a smart rotorcraft demonstrator system. This innovative rotorcraft system will be the first of its kind to truly integrate sensing, processing, and actuator functions in order to autonomously respond to simulated flutter, buffeting, gust fields and dynamic stall, all of which exhibit large scale hysteresis loops. Furthermore, this demonstrator will exploit hybrid optimal control strategies in order to tailor the aerodynamic and elastodynamic performance characteristics of the rotorcraft system by integrating the diverse fundamental research studies undertaken in the previous phases of the research program.

A schematic diagram of the rotorcraft demonstrator system is presented in Figure XVI.2. The rotorcraft system will be dynamically excited by two or more computationally orchestrated electro-dynamic shaker systems in order to replicate the excitations experienced by military rotorcraft systems subjected to variable service conditions while operating in unstructured environments in practice. These dynamic excitations will typically simulate wind gusts, dynamic stall, speed variations, and flutter, for example.

The rotorcraft system will be tested at various speeds of operation, with different blade geometries and orientations. The fiber-optic sensing system will interactively sense the resulting vibrations and changes in temperature, for example, which will permit the microprocessors to instantaneously optimally actuate the ER fluid, magnetostrictive, shape-memory alloy and piezoelectric domains in the rotor blades as shown in Figure XVI.3, thereby tailoring the aero-elasto-dynamic performance of the rotor with a pre-defined performance criterion.

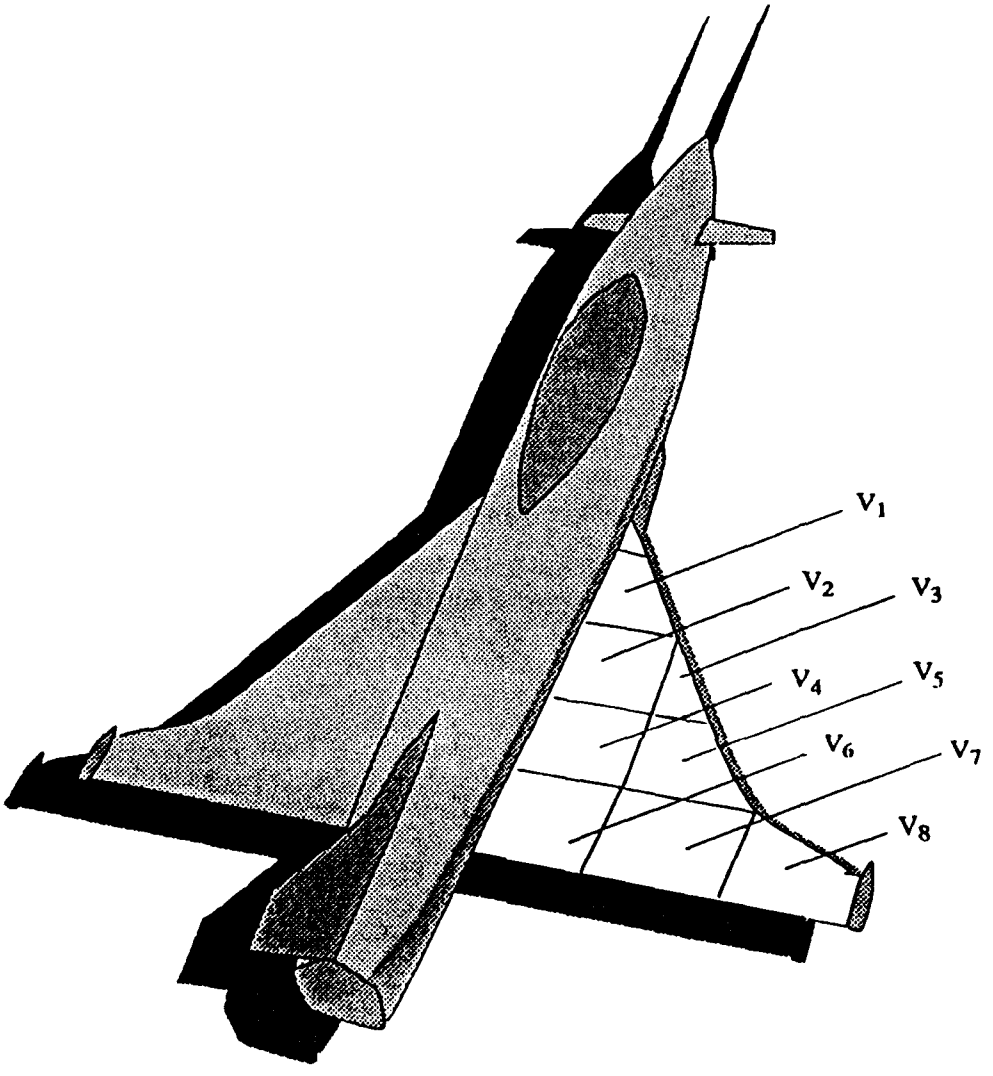

Fig. XVI.1 A strategy for controlling the dynamic response of an aircraft wing fabricated in smart materials

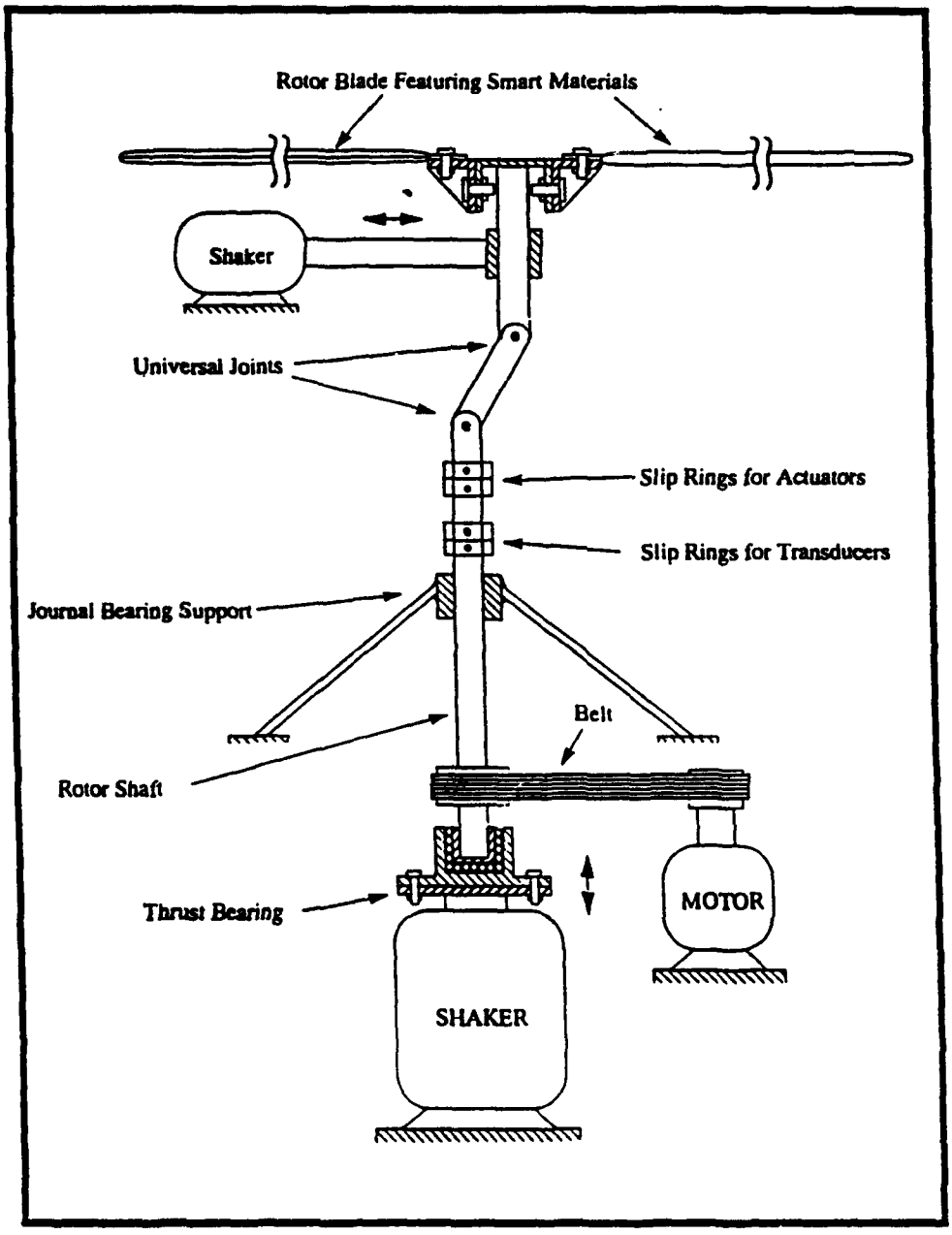

Fig. XVI.2 Schematic of Smart Rotorcraft System Demonstrator

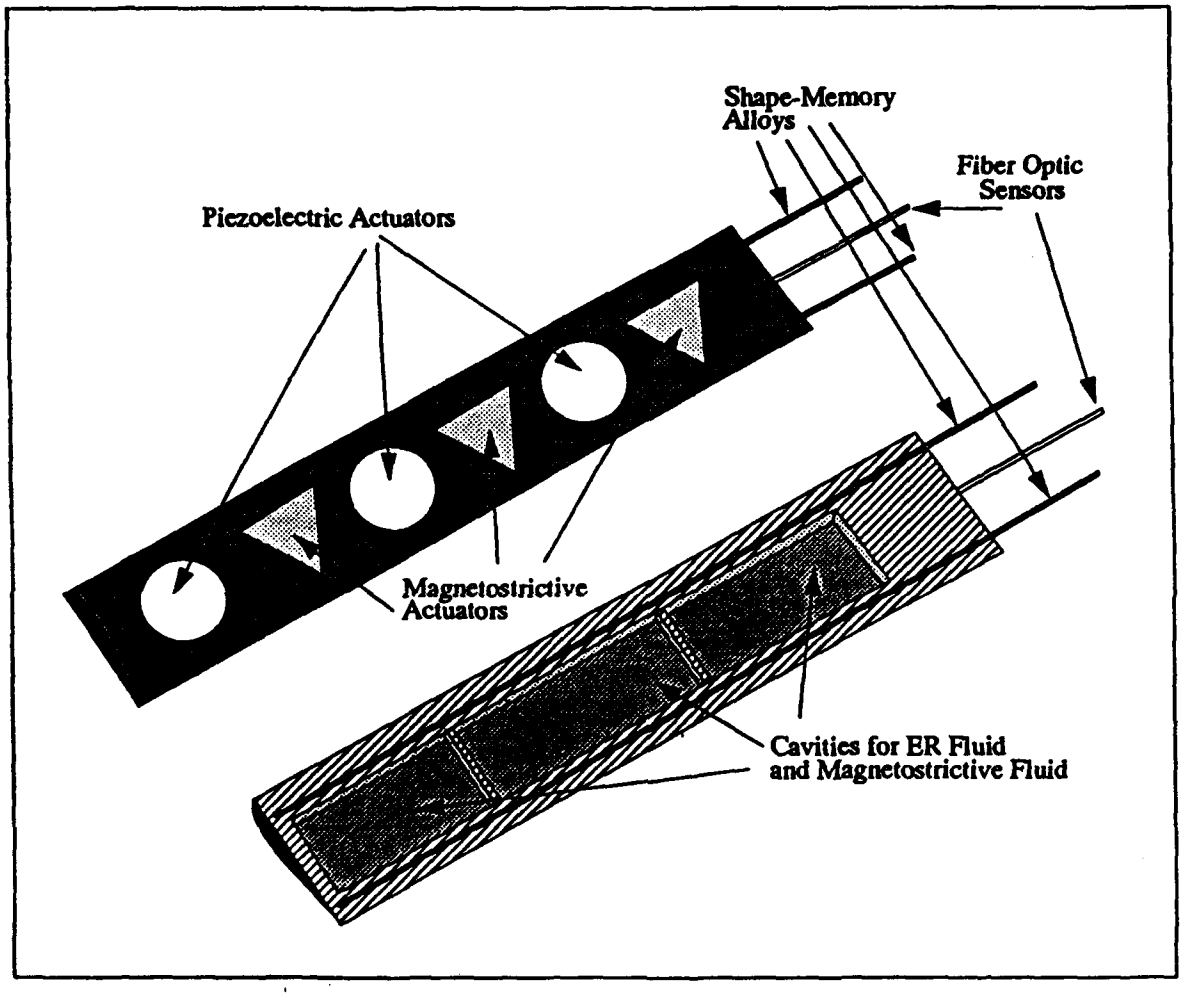

Fig. XVI.3 Conceptual rotor blade featuring smart materials.

The Quantum Team wishes to emphasize the fact that the schematic diagrams presented in Figures XVI.2 and XVI.3 are strictly conceptual in nature. This phase of the proposed program will be undertaken during the Phase III research program will capitalize on the significant analytical and computational predictive capabilities developed during Phase I for the selection and location of appropriate sensors, actuators, microprocessors, and optimal control strategies. It is anticipated that the final configuration of the rotorcraft system will feature shape-memory alloy actuators for generating large changes in camber, piezoelectric actuators to provide a capability for changing the surface geometries, electrorheological fluids and magnetostrictive materials to control the vibrational response of the structure, for example. Furthermore, wind tunnel experiments will also be undertaken to demonstrate aerodynamic tailoring capabilities.

XVII BIBLIOGRAPHY

B1: Electrorheological Fluids

Adamson, A.W., *Physical Chemistry of Surfaces*, John Wiley and Sons, New York, 1976.

Adriani, P.M. and A.P. Gast, "A Microscopic Model of Electrorheology,' *Physics of Fluids*, Vol. 31, No. 10, October 1988, pp. 2757-68.

Anaskin, I.F., V.K. Gleb, and E.V. Korobko, Khizhinskii, B.P. and Khusid, B.M., "Effect of External Electric Field on Amplitude-Frequency Characteristics of Electo--Rheological Damper,' *Inzhenerno-Fizicheskii Zhurnal*, Vol. 46, No. 2, 1984, pp. 309-315.

Andrade, E.N. and C. Dodd, "The effect of an electric field on the viscosity of liquids. Part I,' *Proceedings of the Royal Society*, Vol. 187A, 1946, pp. 296-306.

Andrade, E.N. and C. Dodd, "The effect of an electric field on the viscosity of liquids. Part II,' *Proceedings of the Royal Society*, Vol. 204A, 1951, pp. 449-464.

Andrade, E.N. and J. Hart, "The effect of an electric field on the viscosity of liquids. Part III,' *Proceedings of the Royal Society*, Vol. 225A, 1954, pp. 463-472.

Arguelles, J., H.R. Martin, and R. Pick, "A Theoretical Model for Steady Electroviscous Flow Between Parallel Plates,' *Journal Mechanical Engineering Science*, Vol. 16, No. 4, 1974, pp. 232-239.

Batchelor, G.K., "The Stress System in a Suspension of Force-free Particles,' *Journal of Fluid Mechanics*, Vol. 41, April 1970, pp. 545-570.

Bird, R.B., R.C. Armstrong, and O. Hassager, *Dynamics of Polymeric Liquids: Volume I. Fluid Mechanics*, Wiley, New York, 1977.

Block, H. and J.P. Kelly, "Electrorheology,' *Journal Physics D. Applied Physics*, Vol. 21, 1988, pp. 1661-76.

Block, H. and J.P. Kelly, U.K. Patent Application 8,503,581, 1986 and U.S. Patent Specification 4,687,589, 1987.

Booth, F., "The electroviscous effect for suspensions of solid spherical particles,' *Proceedings of the Royal Society,* Vol. A203, 1950, pp. 533-551.

Brooks, D.A., "Electrorheological Effect Adds Muscle,' *Control & Instrumentation*, October 1982, pp. 57-59.

Brooks, D.A., "Electrorheological Devices,' *Chartered Mechanical Engineer*, London, September 1982, pp. 81-93.

Bullough, W.A. and Peel, D.J., "Electro-Rheological Oil Hydraulics,' *Proceedings*

of Japan Society for Hydraulics and Pneumatics, Vol. 61, No. 17, November 1986, pp. 520-526.

Bullough, W.A. and J.D. Stringer, "The Utilization of the Electroviscous Effect in a Fluid Power System,' *3rd International Fluid Power Symposium*, Turin, May 1973, Paper # F3-37.

Bullough, W.A., D.J. Peel, and R. Firoozian, "Electrical Characteristics and other Considerations for Electro-Rheological Fluids,' *Proceedings of the First International Symposium on ER Fluids, 18th Annual Meeting of the Fine Particle Society*, Boston 1987.

Buscall, R., J.W. Goodwin, and R.H. Ottewill, "The Settling of Particles through Newtonian and Non-Newtonian Media,' *Journal of Colloid and Interface Sciences*, Vol. 85, No. 1, 1982, pp. 78-86.

Canby, T.Y., "Reshaping our Lives,' *National Geographic Magazine*, December 1989, pp. 746-781.

Carlson, J.D., A.F. Sprecher, and H. Conrad, (ed.), *2nd International Conference on Electrorheological Fluids*, Raleigh, NC, August 1989.

Carlson, J.D., A.F. Sprecher, and H. Conrad, "Electrorheology at Small Strains and Strain Rates of Suspensions of Silica Particles in Silicone Oil,' *Materials Science and Engineering*, Vol. 95, 1987, pp. 187-197.

Choi, S.B., B.S. Thompson, and M.V. Gandhi, "An Experimental Investigation on the Active-Damping Characteristics of a Class of Ultra-advanced Intelligent Composite Materials Featuring Electro-Rheological Fluids,' *Proceedings of the Damping '89 Conference*, West Palm Beach, February 1989, organized by the Flight Dynamics Laboratory of the Air Force Wright Aeronautical Laboratories, Wright Patterson Air Base, Ohio, WRDC-TR-89-3116, Vol. 1, pp. CAC-1 to CAC-14.

Choi, S.B., M.V. Gandhi, and B.S. Thompson, "Control of Smart Flexible Structures Incorporating Electrorheological Fluids: A Proof-of-Concept Investigation,' *1989 Automatic Control Conference, Pittsburgh*, June 1989.

Choi, S.B., M.V. Gandhi, and B.S. Thompson, "An Experimental Investigation of the Elastodynamic Response of a Slider-Crank Mechanism Featuring a Smart Connecting Rod Incorporating Embedded Electro-Rheological Fluid Domains,' *Proceedings of the 1st National Mechanisms Conference*, Cincinnati, Ohio, Vol. II, Nov. 1989, 9B-3.1 to 9B-3.7.

Choi, S.B., B.S. Thompson, and M.V. Gandhi, "Smart Structures Incorporating Electrorheological Fluids for Vibration-control and Active-Damping Applications: An Experimental Investigation,' 12th Biennial ASME Conference on Mechanical Vibration and Noise, Montreal, Sept. 1989, published in *Machine Dynamics-Applications and Vibration Control Problems*, T.S. Sankar, V. Kamala, P. Kim and D.K. Rao, eds., DE Vol. 18-2, ASME Book H00508B, pp. 229-236.

Choi, S.B., B.S Thompson, and M.V. Gandhi, "Electrorheological Fluids Technology Stimulates a New Generation of Robotic and Machine Systems,' *Proceedings of the Tenth OSU Applied Mechanisms Conference*, New Orleans, Vol. I., December 1987, pp. 3B.2-1 to 3B.2-8.

Choi, Y., A.F. Spencer, and H. Conrad, "Vibration Characteristics of a Composite Beam Containing an Electrorheological Fluid,' *Journal of Intelligent Material*

Systems and Structures, Vol. 1, January 1990, pp. 91-104.
DeLang, R.G., C.A. Verbraak, and J.A. Zijderveld, U.S. Patent 3,450,372.
Deinega, Y.F., "Some Problems of the Electrorheology of Dispersed Systems,' *Royal Aircraft Establishment*, Farnborough, England, HC A02/MP A01, 1982.
Dirty Oil: The Discovery and Application of the Winslow Effect, *Hydraulics and Pneumatics*, Vol. 19, 1962, pp. 144-147.
Duclos, T.G., "Design of Devices Using Electrorheological Fluids,' SAE paper #881134, 1988.
Duclos, T.G., D.N. Acker, and J.D. Carlson, "Fluids that Thicken Electrically,' *Machine Design*, January 1988, pp. 42-46.
Elton, G.A.H. and F.G. Hirschler, "Electroviscosity: Vol. I and II,' *Proceedings of the Royal Society*, 1948 v.194, pp. 259-288, 275-288.
Elton, G.A.H. and F.G. Hirschler, "Electroviscosity: Vol. III,' *Proceedings of the Royal Society*, 1949 v.197, pp. 568-572.
Elton, G.A.H. and F.G. Hirschler, "Electroviscosity: Vol. IV,' *Proceedings of the Royal Society*, 1949 v.198, pp. 581-590.
Filisko, F.E. and W.E. Armstrong, Electric Field Dependent Fluids, U.S. Patent 4,744,914, May 1988.
Freundlich, H., *Colloid & Capillary Chemistry*, Methuen, London, 1926, (First published in German, 1909).
Gast, A.P. and C.F. Zukowski, "Electrorheological Fluids as Colloidal Suspensions,' *Advances in Colloid and Interface Science*, Vol. 30, 1989, pp. 153-202.
Gandhi, M.V., B.S. Thompson, S.B. Choi, and S. Shakir, "Electro-Rheological-Fluid-Based Articulating Robotic Systems,' *ASME Journal of Mechanisms, Transmissions and Automation in Design*, Vol. 111, 1989, pp. 328-336.
Gandhi, M.V. and B.S. Thompson, "An Innovative Class of Revolutionary Articulating Mechanism and Robotic Systems Exploiting Smart Materials and Structures: Fiber-optics, Shape-Memory Metals, Piezoelectric Materials and Electrorheological Fluids,' *Proceedings of the 1st National Mechanisms Conference*, Cincinnati, Ohio, Vol. II, Nov. 1989, 7C-2.1 to 7C-2.7.
Gandhi, M.V., B.S. Thompson, and S.B. Choi, "A New Generation of Innovative Ultra-Advanced Intelligent Composite Materials Featuring Electro-Rheological Fluids: An Experimental Investigation,' *Journal of Composite Materials*, Vol. 23, 1989, pp. 1232-55.
Gandhi, M.V., B.S. Thompson, and S.B. Choi, "A Note on an Experimental Investigation of a Slider-Crank Mechanism Featuring a Smart Dynamically-Tunable Connecting-Rod Incorporating and Electro-Rheological Fluid,' *Journal of Sound and Vibration*, Vol. 135, 1989, pp. 511-515.
Gandhi, M.V., B.S. Thompson, and S.B. Choi, "Smart Ultra-Advanced Composite Materials Incorporating Electro-Rheological Fluids for Military, Aerospace and Automated Manufacturing Applications,' SME/ESD Advanced Composites Conference and Exposition, published in *Advanced Composites III: Expanding the Technology*, Detroit, MI, September 1987, pp. 23-30.

Gandhi, M.V., B.S. Thompson, and S.B. Choi "Ultra-Advanced Composite Materials Incorporating Electro-Rheological Fluids,' *Proceedings of the 4th Japan-U.S. Conference on Composite Materials*, Washington, DC, June 1988, pp. 875-884.

Gandhi, M.V. and B.S. Thompson, "A New Generation of Revolutionary Intelligent Composite Materials Featuring Electro-Rheological Fluids,' *Proceedings of the ARO Workshop on Smart Materials, Structures and Mathematical Issues*, Blacksburg, VA, September, 1988, pp. 63-68.

Gandhi, M.V. and B.S. Thompson, "Dynamically-tunable Smart Composites Featuring Electrorheological Fluids,' *Proceedings of the SPIE 1989 Boston Symposium OE/FIBERS '89 Optoelectronics and Fiber-optic Devices and Applications*, Boston, MA, Vol. 1170, September 1989, pp. 294-304.

Gandhi, M.V. and B.S. Thompson, "A New Generation of Revolutionary Ultra-Advanced Intelligent Composite Materials Featuring Electrorheological Fluids *Smart Materials, Structures and Mathematical Issues*, C.A. Rogers, (ed.), Lancaster, PA: Technomic Publishing Company, Inc., 1988, pp. 63-68.

Goodwin, J.W., R.W. Hughes, S.J. Partridge, and C.F. Zukoski, "The Elasticity of Weakly Flocculated Suspensions,' *Journal of Chemical Physics*, Vol. 85, No. 1, July 1986, pp. 559-566.

Goodwin, J.W., R.H. Ottewill, and A. Parentich, "Optical Examination of Structured Colloidal Dispersions,' *Journal of Physical Chemistry*, Vol. 84, 1980, pp. 1580-86.

Gorodkin, R.G., Y.V. Kovobko, G.M. Blokh, V.K. Gleb, G.I. Sidorova, and M. Ragother, "Applications of the Electro-Rheological Effect in Engineering Practice,' *Fluid Mechanics-Soviet Research*, Vol. 8, No. 4, 1979, pp. 48-61.

Gorodkin, R.G., I.V. Bukovich, M.B. Smolskii, and M.M. Ragotner, "The effect of vibration on structure formation in ER-suspensions,' *Applied Mechanics and Rheophysics*, Minsk, 1983, pp. 75-79.

Hinch, E.J. and J.D. Sherwood, "The Primary Electroviscous Effect in a Suspension of Spheres with Thin Double Layers,' *Journal of Fluid Mechanics*, Vol. 132, 1983, pp. 337-347.

Honda, T. and T. Sasada, "Electroviscous Effect in Liquids of Low Permittivity,' *Japanese Journal of Applied Physics*, Vol. 18, No. 8, 1979, pp. 1605-06.

Honda, T. and T. Sasada, "The Mechanism of Electroviscosity. I. Electrohydrodynamic Effect on Polar Liquids,' *Japanese Journal of Applied Physics*, Vol. 16, No. 10, October 1977, pp. 1775-83.

Honda, T. and T. Sasada, "The Mechanism of Electroviscosity.II.Conductivity Effect of Dielectric Liquids on Electroviscosity,' *Japanese Journal of Applied Physics*, Vol. 16, No. 10, October 1977, pp. 1785-91.

Honda, T., K. Kurosawa, and T. Sasada, "Transient Pressure-Drop Fluctuations in Electroviscous Effect,' *Japanese Journal of Applied Physics*, Vol. 18, No. 11, November 1979, pp. 2059-63.

Honda, T. and T. Sasada, "The Electroviscous Effect of Water,' *Japanese Journal of Applied Physics*, Vol. 18, No. 3, 1979, pp. 675-676.

Honda, T., K. Kurosawa, and T. Sasada, "A.C. Characteristics of the Electroviscous Effect,' *Japanese Journal of Applied Physics*, Vol. 19, No. 8, 1980, pp. 1463-66.

Hunter, R.J., *Foundations of Colloid Science, Vol. I and Vol. II*, Oxford Science Publications, Clarendon Press, Oxford, England, 1989.

Klass, D.L. and T.W. Martinek, "Electroviscous Fluids No. I. Rheological Properties,' *Journal of Applied Physics*, Vol. 38, 1967, pp. 67-74.

Klass, D.L. and T.W. Martinek, "Electroviscous Fluids No. II. Electrical Properties,' *Journal of Applied Physics*, Vol. 38, 1967, pp. 75-80.

Konig, W., "Bestimmung einiger Reibungsco-efficienten und versuche iber den Einfluss der Magnetisitung und Electrisinung auf die Reibungder Flussigleuten,' *Annals of Physics*, Vol. 25, 1885, pp. 618-624.

Korobko, E.V. and I.A. Chernobal, "Influence of an External Electric Field on the Propagation of Ultrasound in Electrorheological Suspension,' Inzhenerno-Fizicheskii Zhurnal, Vol. 48, No. 2, 1985, pp. 219-224.

Lever, D.A., "Large Distortion of the Electric Double Layer around a Charged Particle by a Shear Flow,' *Journal of Fluid Mechanics*, June 1979, Vol. 92, Part 3, pp. 421-433.

Mandell, M., "Smart Fluids: Wavelet of the Future?,' *High Technology Business*, July-August 1989, pp. 20-23.

Mullins, J.P., "Fluid Powerful!,' *Automotive Industries*, September 1988, pp. 68-69.

Peel, D.J., R. Firoozian, and W.A. Bullough, "Deviation of the Electrical Characteristics of an Electrorheological Fluid from Biased Sine Wave Excitation Tests,' *Proceeding of the First International Symposium on ER Fluids, 18th Annual Meeting of the Fine Particle Society*, Boston 1987.

Reiner, M.A. "Lectures in Theoretical Rheology,' North Holland, Amsterdam, 1960 [Russian Translation] as Reologiya (Rheology), 1965.

Reiner, M.A. "Mathematical Theory of Dilatancy,' *American Journal of Mathematics*, Vol. 67, 1945, pp. 350-362.

Rosen, M.J., *Surfactants and Interfacial Phenomena*, John Wiley, Inc.: New York, New York, 1978.

Russel, W.B. and A.P. Gast, "Non-equilibrium Statistical Mechanics of Concentrated Colloidal Dispersions: Hard Spheres in Weak Flows,' *Journal Chemical Physics*, Vol. 84, No. 3, February 1986, pp. 1815-26.

Russel, W.B., "The Rheology of Suspensions of Charged Rigid Spheres,' March 1978 *Journal of Fluid Mechanics*, Vol. 85, Part 2, pp. 209-232.

Saitoh, S., T. Sakai, and H. Kusama, "Fluidic electro-fluid converter by use of electro-viscous fluid,' *Second International JSME Symposium*, September 1972 (Tokyo).

Schmerling, M.A., M.A. Wilkov, A.E. Sanders, and J.E. Woosley, *Journal of Biomedical Materials Research*, Vol. 10, 1976, pp. 879-902.

Scott, D. and J. Yamaguchi, "ER fluid devices near commercial stage,' *Automotive Engineering*, Vol. 93, No. 11, November 1985, pp. 75-79.

Sherwood, J.D., "The primary electroviscous effect in a suspension of spheres,' *Journal of Fluid Mechanics*, Vol. 101, December 1980, pp. 609-630.
Shul'man, Z.P., "Utilization of Electric and Magnetic Fields for Control of Heat and Mass Transfer in Dispersed Systems (Suspensions),' *Heat Transfer-Soviet Research*, Vol. 14, No. 5, September-October 1982, pp. 1-23.
Shul'man, Z.P. et al, *Elektroreologicheskiy Effekt* (The Electrorheological Effect), Nauka i Tekhnika Press, Minsk, 1972.
Shul'man, Z.P., B.M. Khusid, E.V. Korobko, and E.P. Khizhinsky, "Damping of Mechanical Systems Oscillation by a Non-Newtonian Fluid with Electric-Field Dependent Parameters,' *Journal of Non-Newtonian Fluid Mechanics*, Vol 25, 1987, pp. 329-346.
Shul'man, Z.P., A.D. Matespuro, and B.M. Khusid,"Structurization of electro-Rheological suspensions in electric field, Part 1: Qualitative analysis,' Vestsi Akademii Navuk Belaruskai SSR, *Seryya Fizika Energetychnykh Navuk*, No. 3, 1977, pp. 116-121.
Shul'man, Z.P., A.D. Matsepuro, and B.M. Khusid, "Structurization of electro-rheological suspensions in electric field, Part 2: Quantitative estimates,' Vestsi Akademii Navuk Belarskai SSR, *Seryya Fizika Energetychnykh Navuk*, No. 3, 1977, pp. 122-127.
Shul'man, Z.P., R.G. Gorodkin, V.K. Gleb, and E.V. Korobko, "The electro-Rheological effect and its possible uses,' *Journal of Non-Newtonian Fluid Mechanics*, No. 8, 1981, pp. 29-41.
Simon, M., R. Kaplow, E. Salzman, and D. Freiman, *Radiology*, Vol. 125, No. 1, 1977, p.92.
Snyder, B., "Application of Electrorheological Fluids to Hydrodynamic Lubrication,' UNR Report # ME-BS-900507, 1990, (proprietary).
Sprecher, A.F., J.D. Carlson, and M. Conrad, "Electrorheology at small strains and strain rates of suspensions of silicon particles in silicone oil,' *Material Science and Engineering*, Vol. 95, 1987, pp. 187-197.
Stangroom, J.E., UK Patent Specification 1501635, 1978.
Stangroom, J.E., "Electrorheological Fluids,' *Physics in Technology*, Vol. 14, 1983, pp. 290-296.
Stanway, R., J.L. Sproston, and R. Firoozian, "Identification of the Damping Law of an Electro-Rheological Fluid in Vibration,' ASME Winter Annual Meeting, Anaheim, California, December 1986, paper 86-WA/DSC-6.
Stevens, N.G., J.L. Sproston, and R. Stanway, "On the Mechanical Properties of Electrorheological Fluids,' *ASME Journal of Applied Mechanics*, Vol. 54, June 1987, pp. 456-458.
Stevens, N.G., J.L. Sproston, and R. Stanway, "The Influence of Pulsed D.C. Input Signals on Electrorheological Fluids,' *Journal of Electrostatics*, Vol. 17, 1985, pp. 181-191.
Strandrud, H.T., "Electric-Field Valves Inside Cylinder Control Vibrator,' *Hydraulics and Pneumatics*, September 1966, pp. 132-143.
Thompson, B.S. and M.V. Gandhi, "A Commentary of Flexible Fixturing,' *ASME Applied Mechanics Reviews*, Vol. 39, No.9, 1986, pp. 1365-69.

Thompson, B.S., M.V. Gandhi, and C.Y. Lee, "A Variational Formulation for Smart Structural Members of Robotic Systems Featuring Embedded Electro--Rheological Fluids,' *Proceedings of the 1st National Mechanisms Conference*, Cincinnati, Ohio, Vol. I, Nov. 1989, 2C-2.1 to 2C-2.7.

Treasure, U.Y., F.E. Filisko, and L.H. Radzilowski, "Polyelectrolytes as Inclusions in Electrorheologically Active Materials: Effect of chemical characteristics on ER activity,' *Journal of Rheology*, Vol. 35, No. 6, August 1991, pp. 1051-69.

Uejima, H., "Dielectric Mechanism and Rheological Properties of Electro-Fluids", *Japanese Journal of Applied Physics*, Vol. 11, No. 3, 1972, pp. 319-325.

Viongradov, G.V., Z.P. Shul'man, Yu. G. Yanovskii, V.V. Barancheeva, E.V. Korobko, and I.V. Bukovich, "Shear Viscoelastic Behavior of Electrorheological Suspensions,' *Inzhenerno-Fizicheskii Zhurnal*, Vol. 50, No. 4, April 1986, pp. 429-432.

Willson, J.R. and K.T. Krueger, U.S. Patent 3,645,443.

Winslow, W.M., "Induced Vibration of Suspensions,' *Journal of Applied Physics*, Vol. 20, 1949, pp. 1137-40.

Winslow, W.M., "Method and Means for Translating Electrical Impulses into Mechanical Forces,' *U.S. Patent 2,417,850*, 1947.

B2: Shape-Memory-Alloys

Achenbach, M., T. Atanackovic, and I. Muller, "A Model for Memory Alloys in Plane Strain,' *International Journal of Solids and Structures*, Vol. 22, No. 2, 1986, pp. 171-219.

Achenbach, M. and I. Muller, "Creep and Yield in Martensitic Transformation,' *Ingenieur-Archiv*, Vol. 53, 1983, pp. 73-83.

Aifantis, E.C. and J. Gittus, *Phase Transformations*, 1986, Elsevier, Amsterdam.

Baz, A., K. Inman, and J. McCoy, "Active Vibration Control of Flexible Beams Using Shape Memory Actuators,' *Journal of Sound and Vibration*, Vol. 140, 1990, pp.437-456.

Baz, A., K. Inman, and J. McCoy, "The Dynamics of Helical Shape Memory Actuators,' *Journal of Intelligent Material Systems and Structures*, Vol. 1, 1990, pp. 105-133.

Banks, R., *Phase Transitions in Shape Memory Alloys and Implications for Thermal Energy Conversion*, Elsevier Applied Science Publishers Ltd.: Essex, UK, 1986, Phase Transformations 77-96.

Buehler, W.J. and R.C. Wiley, "Nickel-Base Alloys,' U.S. Patent 3,174,851, 1965.

Claus, R.O., "Optical Fiber Sensors and Single Processing for Smart Materials and Structures Applications,' *Proceedings of the U.S. Army Research Office Workshop*, September 15-16, 1988, Blacksburg, Virginia.

Collins, C. and M. Luskin, "The Computation of the Austenitic-Martensitic Phase Transition,' *Partial differential Equations and Continuum Models of Phase Transitions, Lecture Notes in Physics 344*, eds. M. Rascle, D.Serre and M. Slemrod, Springer Verlag, 1989, pp. 34-50.

Cross, W.B., A.H. Kariotis, and F.J. Stimler, "Nitinol Characterization Study,' NASA CR-1433, September 1969.

Delaey, R.V., H. Tas Krishnan, and H. Warlimont, "Thermoelasticity, Pseudo-elasticity, and the Shape-Memory-Effects Associated with Martensitic Transformations,' *Journal of Material Science*, Vol. 9, 1974, pp. 1521-45.

Duerig, T.W., Melton, K.N., Stockel, D. and Wayman, C.M., *Engineering Aspects of Shape Memory Alloys*, Butterworth-Heinemann, 1990.

Efsic, E., K. Mukherjee, and C.M. Wayman, "Observations on the Phase Transition in NH_4Cl Single Crystals at Subzero Temperatures,' *Journal of Metals*, Vol. 16, p. 120.

Funakubo, H.(translated by J.B. Kennedy), *Shape-Memory-Alloys*, 1987, Gordon and Breach Science Publishers, New York.

Goldstein, D., "A Source Manual for Information on Nitinol and NiTi,' Naval Surface Weapons Center, Silver Spring, Maryland, Report NSWC/WOL TR 73-26, 1978.

Harrison, J.D. and D.E. Hodgson, *Shape-Memory Effects in Alloys*, p. 517, Plenum Press, 1975.

Hashimoto, M., M. Takeda, H. Sagawa, I. Chiba, and K. Sato, "Application of Shape Memory Alloy to Robotic Actuators,' *Journal of Robotic Systems*, Vol. 2, No. 1, 1985, pp. 3-25.

Hirose, S., K. Ikutra, M. Tsukamoto, K. Sato, Y. Umetani, "Several Considerations on Design of SMA Actuators,' *Proceedings of the International Conference on Martensitic Transformations*, ICOMAT-86, Nara, Japan, August 1986.

Hoffman, K.H. and M. Niezgodka, "Mathematical Models of Dynamical Martensitic Transformations in Shape Memory Alloys,' *Journal of Intelligent Material Systems and Structures*, Vol. 1, No. 3, July 1990, pp. 335-374.

Honma, D., Y. Miwa, and N. Iguchi, "Application of Shape Memory Effect to Digital Control S Actuator,' *Bulletin of Suspense Society of Mechanical Engineers*, Vol. 27, 1984, pp. 1737-42.

Horbogen, E., "Alloys with Shape Memory-New Materials for Future Technology?" *Metallurgy*, Vol. 41, No. 5, May 1987, pp. 488-493.

Jackson, C.M., H.J. Wagner, and R.J. Wasilewski, "55-Nitinol - The Alloy with a Memory, Its Physical Metallurgy, Properties, and Applications,' NASA-SP-5110, 1972, p. 91.

Likhachev, V.A., S.L. Kuzmin, and Z.L. Kamenceva, *Shape Memory Effect*, Leningrad: Leningrad University Press, (in Russian).

Miwa, Y. "Shape memory alloy application for sequential operation control,' *System and Control*, Vol. 29, No. 5, May 1985, pp. 303-310.

Muller, I., "A Model for a Body with Shape-Memory,' *Archives of Rational Mechanics and Analysis*, Vol. 70, 1979, pp. 61-77.

Niezgodka, M. and J. Sprekels, "Existence of Solutions for a Mathematical Model of Structural Phase Transitions in Shape Memory Alloys,' *Mathematical Methods in the Applied Sciences*, Vol. 10, 1988, pp. 197-223.

Nishiyama, Z., *Martensitic Transformation*, 1978, Academic Press, New York, NY.

Nakai, K., T. Okuda, H. Tanaka, and Sharp, "Heat Conduction in Ni-Ti Shape Memory Alloy in the Presence of Phase Transformation Under Stress,' *Proceedings of the International Conference on Martensitic Transformations*, ICOMAT-86, Nara, Japan, August 1986.

Oonishi, H., *Artificial Organs*, Vol. 12, No. 4, p. 871, 1983, (in Japanese).

Oonishi, H., M. Miyagi, T. Hamada, E. Tsuji, Y. Suzuki, T. Hamaguchi, N. Okabe, and T. Nabeshima, "Application of the Memory Alloy TiNi an implant material,' *Proceedings of the 4th European Conference on Biomaterials*, 1983, p 149-154.

Oonishi, H., T. Hamaguchi, T. Nabeshima, M. Miyagi, E. Tsuji, T. Hamada, Y. Suzuki, and Shikida, "Studies on the Development of a high frequency Induction Heating Apparatus to Heat a Shape Memory TiNi Alloy Implanted in a Living Body,' *Proceedings of the 3rd Conference of the Japanese Society for Biomaterials*, 1982, p. 155-161, (in Japanese).

Perkins, J., ed., *Shape Memory Effects in Alloys*, Plenum Press, New York, 1975.

Rogers, C.A., and H.H. Robertshaw, "Shape Memory Alloy Reinforced Composites,' *Engineering Science Preprints 25*, ESP25.88027, Society of Engineering Sciences, Inc., June 1988.

Rogers, C.A., "Dynamic Control Concepts Using Shape Memory Alloy Reinforced Plates,' *Proceedings of the U.S. Army Research Office Workshop*, September 15-16, 1988, Blacksburg, Virginia.

Rogers, C.A., C. Liang, and J. Jia, "Behavior of Shape Memory Alloy Reinforced Composite Plates,' AIAA Paper 89-1389, 1989.

Saburi, T., and C.M. Wayman, "Crystallographic Similarities in Shape-Memory Martensites,' *Acta Metallurgica*, Vol. 27, 1979, pp. 979-995.

Schetky, L.M., and J. Perkins, "The Quiet Alloys,' *Machine Design*, Vol. 50, No. 8, 1978, pp. 202-206.

Schetky, L.M., "Shape Memory Alloys,' *Scientific American*, Vol. 241, 1979, p.74.

Shimizu, K. and K. Otsuka, "Pseudo-elasticity and Shape Memory Effects,' *International Metals Review*, Vol. 31, No. 3, 1986, pp. 93-114.

Thumann, M., B. Velten, E. Hornbogen, "Composites Containing Shape Memory Fibers,' *Proceedings of the International Conference on Martensitic Transformations*, ICOMAT0-86, Nara, Japan, August 1986.

Wayman, C.M., and K. Shimizu, "The Shape Memory ('Marmem') Effect in Alloys,' *Metal Science Journal*, Vol. 6, 1972, pp. 175-183.

Wayman, C.M., "Some Applications of Shape-Memory-Alloys,' *Journal of Metals*, June 1980, pp. 129-137.

Wille, J., B. Hansknecht, M.V. Gandhi, and B.S. Thompson, "A Proof-of-Concept Experimental Investigation on a Four-Bar Linkage with a Smart Rocker Link Featuring a Shape-Memory-Alloy,' *Proceedings 1st National Mechanisms Conference*, Cincinnati, Ohio, Vol. II, Nov. 1989, pp. 9B-4.1 to 9B-4.4.

Yeager, J., "A Practical Shape-Memory Electro-Mechanical Actuator,' *Mechanical Engineering*, Vol. 106, 1984, pp. 52-55.

B3: Piezoelectric Actuators

Allik, H. and T.J. Hughes, "Finite Element Method for Piezoelectric Vibration,' *International Journal of Numerical Methods in Engineering*, Vol. 2, 1979, pp. 151-168.

Bailey, T., and J.E. Hubbard. "Distributed Piezoelectric-Polymer Active Vibration Control of a Cantilever Beam,' *AIAA Journal of Guidance, Control, Dynamics*, Vol. 8, No. 5, September-October, 1985, pp. 605-611.

Baz, A. and S. Poh, "Performance of an Active Control System with Piezoelectric Actuators,' *Journal of Sound and Vibration*, Vol. 126, No. 2, 1988, pp. 327-343.

Bleustein, J.L. and H.F. Tiersten, "Forced Thickness-Shear Vibrations of Discontinuously Plated Piezoelectric Plates,' *The Journal of the Acoustical Society of America*, Vol. 43, No. 6, 1968, pp. 1311-18.

Bondarenko, A.A., N.I. Karas, and A.F. Ulitko, "Methods for Determining the Vibrational Dissipation Characteristics of Piezoceramic Structural Elements,' *Soviet Applied Mechanics*, 1982, pp. 175-179.

Bryant, M.D. and R.F. Keltie, "A Characterization of the Linear and Nonlinear Dynamic Performance of a Practical Piezoelectric Actuator,' *Sensors and Actuators*, Vol. 9, 1986, pp. 95-114.

Burke, S.E. and J.E. Hubbard, "Active Vibration Control of a Simply-Supported Beam Using a Spatially-Distributed Actuator,' *IEEE Control Systems Magazine*, Vol. 7, No. 4, August 1987, pp. 25-30.

Burke, S.E. and J.E. Hubbard, "Distributed Parameter Control Design for Vibrating Beams Using Generalized Functions,' *1986 IFAC Symposium on Distributed Parameter Systems*, June 1986, Los Angeles, CA.

Burke, S.E. and J.E.Hubbard Jr., "Performance Measures for Distributed Parameter Control Systems,' *Proceedings of IMACS/IFAC International Symposium on Modeling and Simulation of Distributed Parameter Systems*, October 1987, Hiroshima, Japan.

Cady, W.G. *Piezoelectricity*, 1964, Dover, New York.

Connally, J.A. and J.E. Hubbard, Jr., "Low Authority Control of a Composite Cantilever Beam in Two Dimensions,' *Proceedings of American Control Conference*, August 1988, pp. 1903-08.

Crawley, E.F. and J. de Luis, "Use of Piezo-Ceramics as Distributed Actuators in Large Space Structures,' *Proceedings of 26th Structures, Structural Dynamics and Materials Conference*, 1985, pp. 126-133.

Crawley, E.F. and J. de Luis, "Use of piezoelectric Actuators as Elements of Intelligent Structures,' *American Institute of Aeronautical Astronautics Journal*, Vol. 25, No. 10, 1987, pp. 1373-85.

Crawley, E.F., J. de Luis, N.W. Hagwood, and E.H. Anderson, "Development of Piezoelectric Technology for Applications in Control of Intelligent Structures,' *Proceedings of American Control Conference*, 1988, pp. 1890-96.

Crawley, E.F. and E.H. Anderson, "Detailed Models of Piezoceramic Actuation of Beams,' *Journal of Intelligent Materials and Structures*, Vol. I, 1990, pp. 4-25.

Cudney, H.H., D.J. Inman, and Y. Oshman, "Distributed Structural Control Using Multilayered Piezoelectric Actuators,' *Proceedings of the 7th VPI & SU/AIAA Symposium on Dynamics and Control of Large Structures*, 1987.

Hagood, N.W., W.H. Chung, and A. von Flotow, "Modelling of Piezoelectric Actuator Dynamics for Active Structural Control,' *Journal of Intelligent Material Systems and Structures*, Vol. 1, No. 3, July 1990, pp. 327-334.

Hanagud, S., C.C. Won, and M.W. Obal, "Optimal Placement of Piezoceramic Sensors and Actuators,' *Proceedings of American Control Conference*, August 1988, pp. 1884-89.

Hanagud, S., M.W. Obal, and M. Meyyappa, "Electronic Damping Techniques and Active Vibration Control,' *Proceedings of 26th Structures, Structural Dynamics and Materials Conference*, 1985, pp. 443-453.

Haun, M.J. and Newnham, R.E., "Experimental and Theoretical Study of 1-3 and 1-3-0 Piezoelectric PZT-Polymer Composites for Hydrophone Applications,' *Ferroelectrics* 68, pp. 123-139 (1986).

Haun, M.J., Moses, P., Gururaja, T.R., Schulze, W.A. and Newnhawn, R.E., "Transversely Reinforced 1-3 and 1-3-0 Piezoelectric Composites,' *Ferroelectrics* 49, pp. 259-264 (1983).

Hubbard, Jr., J.E., "Distributed Sensors and Actuators for Vibration Control in Elastic Components,' *Proceedings of Noise-Conf 87*, 1987, pp. 407-412.

Ikegami, R., D.G. Wilson, J.R. Anderson, and G.J. Julien, "Active Vibration Control Using NiTiNOL and Piezoelectric Ceramics,' *Journal of Intelligent Materials Systems and Structures*, Vol. 1, April 1990, pp. 189-206.

Im, S. and S.N. Atluri, "Effects of a Piezo-Actuator on a Finitely Deformed Beam subjected to General Loading,' *AIAA Journal*, Vol. 27, No. 12, 1989, pp. 1801-07.

Jaffe, B., R. Cook, and H. Jaffe, *Piezoelectric Ceramics*, 1971, Academic Press: New York, NY.

Kawai, H., "The Piezoelectricity of Poly(vinylidene fluoride),' *Japanese Journal of Applied Physics*, Vol. 8, No. 7, 1969, pp. 975-978.

Kynar Piezo Film Technical Manual, Pennwalt Corporation, Valley Forge, Pennsylvania, 1987.

Lawson, A.W., "The Vibration of Piezoelectric Plates,' *Physical Review*, Vol. 62, July 1942, pp. 71-76.

Lee, C.Y., S.B. Choi, B.S. Thompson, and M.V. Gandhi, "A Variational Formulation for the Finite Element Analysis of Linkage and Robotic Systems Featuring Smart Links Incorporating Piezoelectric Materials,' *Proceedings 1st National Mechanisms Conference*, Cincinnati, Ohio, Vol. I, Nov. 1989, 2C-1.1 to 2C-1.10.

Liao, C.Y. and C.K. Sung, "An Elastodynamic Analysis of Flexible Linkages using Piezoceramic Sensors and Actuators,' *Flexible Mechanisms, Dynamics and Robot Trajectories*, DE-Vol. 24, ASME Book H00623, edited by S. Derby, M. McCarthy, A. Pisano, 1990, pp. 503-510.

Mason, W.P., "Piezoelectricity its History and Applications,' *Journal of the Acoustical Society of America*, Vol. 70, No. 6, 1981, pp. 1561-66.
Miller, S.E. and J.E. Hubbard, Jr., "Observability of a Bernoulli-Euler Beam Using PVF_2 as a Distributed Sensor,' *Proceedings of 6th VPI & SU/AIAA Symposium on Dynamic and Control of Large Structures*, June 1987.
Miller, S.E. and J.E. Hubbard, Jr., "Smart Components for Structural Vibration Control,' *Proceedings of American Control Conference*, 1988, pp. 1897-02.
Mindlin, R.D., "Thickness-shear and Flexural Vibrations of Crystal Plate,' *Journal of Applied Physics*, Vol. 22, No. 3, 1951, pp. 316-323.
Mindlin, R.D., "Forced Thickness-Shear and Flexural Vibrations of Piezoelectric Crystal Plates,' *Journal of Applied Physics*, Vol. 23, No. 1, 1952, pp. 83-88.
Mindlin, R.D., "High Frequency Vibrations of Crystal Plates,' *Quarterly of Applied Mathematics*, Vol. 19, 1961, pp. 51-61.
Mindlin, R.D., "High Frequency Vibrations of Piezoelectric Crystal Plates,' *International Journal of Solids and Structures*, Vol. 8, 1972, pp. 895-906.
Mindlin, R.D., "Coupled Piezoelectric Vibrations of Quartz Plates,' *International Journal of Solids and Structures*, Vol. 10, 1974, pp. 453-459.
Mindlin, R.D, "Equations of High Frequency Vibrations of Thermo Piezoelectric Crystal Plates,' *International Journal of Solids and Structures*, Vol. 10, 1974, pp. 625-637.
Newcomb, C.V. and I. Flinn, "Improving the Linearity of Piezoelectric Ceramic Actuators,' *Electronics Letters*, Vol. 18, No. 11, 1982, pp. 442-444.
Piezoelectric Ceramics, edited by J. Van Randeraat and R.E. Setterington, N.V. Philips, Eindhoven, 1974.
Piezoelectric Products Company Literature, Piezoelectric Products Inc., Metuchen, NJ, 1984.
Plump, J.M., J.E. Hubbard, Jr., and T. Bailey, "Nonlinear Control of a Distributed System: Simulation and Experimental Results,' *ASME Journal of Dynamic Systems, Measurement, and Control*, Vol. 109, June 1987, pp. 133-139.
Procopio, G.M. and J.E. Hubbard, Jr., "Active Damping of a Bernoulli-Euler Beam via End Point Independence Control Using Distributed Parameter Techniques,' *Proceedings of 1987 ASME Vibration Conference.*
Seo, I., "Application of piezoelectric polymer to actuator,' *Journal of the Japanese Society of Precision Engineers*, Vol. 52, No. 5, May 1987, pp. 689-691.
Sessler, G.M., "Piezoelectricity in Polyvinylidene Fluoride,' *Journal of the Acoustical Society of America*, Vol. 70, No. 6, 1981, pp. 1596-08.
Smith, W.A. and Auld, B.A., "Modeling 1-3 Composite Piezoelectrics: Thickness-Mode Oscillations' *IEEE Transactions on Ultrasonics, Ferroelectrics, and Frequency Control*, Vol. 38, pp. 40-47, 1991.
Takahashi, S., "Piezoelectric actuators and their applications,' *Journal Institute of Electronic Information and Communication Engineering*, Vol. 70, No. 3, March 1987, pp. 295-297.
Tamaru, N., "Piezoelectric bimorph actuator control using a Kalman filter,' *Transactions of the Society of Instrumentation and Control Engineering*, Vol. 23, No. 8, August 1987, pp. 873-875.

Tzou, H.S. and M. Gadre., "Active Vibration Isolation by Piezoelectric Polymer with Variable Feedback Gain,' *American Institute of Aeronautics and Astronautics Journal*, Vol. 26, No. 8, 1988, pp. 1014-17.

Tzou, H.S. and M. Gadre, "Theoretical Analysis of a Multi-layered Thin Shell Coupled with Piezoelectric Shell Actuators for Distributed Vibration Controls,' *Journal of Sound and Vibration*, Vol. 132, 1989, pp. 433-450.

Tzou, H.S. and M. Gadre,"Active Vibration Isolation and Excitation by Piezoelectric Slab with Constant Feedback Gains,' *Journal of Sound and Vibration*, Vol. 136, No. 3, 1989, pp. 477-490.

Tzou, H.S. and C.I. Tseng, "Distributed Piezoelectric Sensor/Actuator Design for Dynamic Measurement/Control of Distributed Parameter Systems: A Piezoelectric Finite Element Approach,' *Journal of Sound and Vibration*, 1990, Vol. 138, No. 1, pp. 17-34.

Uchino, K., "Actuator applications of piezoelectric/electrostrictive ceramics,' *Journal of the Japanese Society of Precision Engineers*, Vol. 53, No. 5, May 1987, pp. 686-688.

B4: Piezoelectric Sensors

Barsky, M.F., D.K. Linder, R.O. Claus, "Robot gripper control system demonstrating PVDF piezoelectric sensors,' *IEEE 1986 Ultrasonics Symposium Proceedings*, pp. 545-548, Vol. 1, November 1986, Williamsburg, VA, USA.

Barsky, M.F., D.K. Lindner, R.O. Claus, "Active damping of a robotic gripper PVDF piezoelectric sensor,' *Proceedings of the Eighteenth Southeastern Symposium on System Theory*, April 1986, Knoxville, TN, USA.

Carey, W.P., B.R. Kowalski,"Chemical piezoelectric sensor and sensor array characterization,' *Analytical Chemistry*, Vol. 58, No. 14, December 1986, pp. 3077-84.

Carlisle, B.H., "Piezoelectric plastics promise new sensors,' *Machine Design*, Vol. 58, No. 25, October 1986, pp. 105-110.

Crawley, E.F., J. de Luis, H.W. Hagood, and E.H. Anderson, "Development of Piezoelectric Technology for Applications in Control of Intelligent Structures,' *Proceedings of the 1988 American Control Conference*, Atlanta, GA, Vol. 3, 1988, pp. 1897-02.

Dong Tai-Huo, Pao Cheng-Kang, Kin Dan, "Accurate measurement of the voltage micro-displacement correlation of piezoelectric sensor with a fiber-optic interferometer,' *Proceedings SPIE - International Society Optical Engineers (USA)*, Vol. 798, pp. 304-306, 1987, Fiber-optic Sensors II, March/April 1987, The Hague, The Netherlands.

Hanagud, S., "Piezoceramic Devices and PVDF Films as Sensors and Actuators for Intelligent Structures,' *Proceedings of the 1988 U.S. Army Research Office Workshop*, Blacksburg, Virginia, September 1988.

Leaver, P., M.J. Cunningham, B.E. Jones,"Piezoelectric polymer pressure sensors,' *Sensors and Actuators*, Vol. 12, No. 3, pp. 225-233, October 1987.

Miller, S.E. and J.E. Hubbard Jr., "Smart Components for Structural Vibration Control,' *Proceedings of the 1988 American Control Conference,* Atlanta, GA, Vol. 3, 1988, pp. 1897-1902.

Measures, R.M., "Fiber-optic Sensors-the Key to Smart Structures,' *Fiber-optics 89*, SPIE, Vol. 1120, pp. 1120-32.

Measures, R.M., "Fiber-optic Smart Structures Program at UTIAS,' *Fiber-optic Smart Structures and Skins II*, E. Udd (ed.), SPIE, 1989, Vol. 1170, pp. 92-108.

Motghare, S.J., A.M. Kolte, C.V. Dhuley, A.G. Karpatal, "Samariaum doped potassium-niobate-a new piezoelectric sensor,' ISAF '86. *Proceedings of the Sixth IEEE International Symposium on Applications of Ferroelectrics*, June 1986, Bethlehem, PA, USA, pp. 472-475.

Newham, R.E., "Smart Ceramics,' *Proceedings of the 1988 U.S. Army Research Office Workshop*, Blacksburg, Virginia, September 1988.

Plump, J.M., J.E. Hubbard Jr., and Baily, "Nonlinear Control of a Distributed System: Simulation and Experimental Results,' *ASME Journal of Dynamic Systems,*

Measurements, and Control, Vol. 109, 1987, pp. 133-139.
Safari, A., G. Sa-gong, J. Giniewicz, R.E. Newnham, Composite piezoelectric sensors, Tressler, R.E., Mesing, G.L., Pantano, C.G., Newnham, R.E. (Editors) Tailoring Multiphase and Composite Ceramics, Proceedings of the Twenty-First University Conference on Ceramic Science, pp. 445-454, July 1985, University Park, PA, USA.
Wilkes, G.L., "Materials Issues for Smart Structures,' *Proceedings of the 1988 U.S. Army Research Office Workshop*, Blacksburg, Virginia, September 1988.

B5: Fiber-Optic Sensors

Allard, F.C., ed., *Fiber-optics Handbook for Engineers and Scientists*, McGraw-Hill Publishing Co.: New York, 1990.

Auch, W., E. Schlemper, W. Wenzel, "Fiber-optic gyroscope: an advanced rotation rate sensor,' *Electronic Communications*, Vol. 61, No. 4, 1987, pp. 372-378.

Batchellor, C.R., J.P. Dakin, D.A.J. Pearce, "Fiber-optic mechanical sensors for aerospace applications,' *International Journal of Optic Sensors*, Vol. 2, No. 5-6, October-December 1987, pp. 407-411.

Bennett, K.D., R.O. Claus, "Analysis of composite structures using optical fiber modal sensing techniques,' *Proceedings IEEE SOUTHEASTCON '86*, pp. 95-98, March 1986, Richmond, VA, USA.

Bennett, K.D., S.J. Hanna, R.O. Claus, "Monitoring of strain in layered media using clad rod acoustic waveguides,' McAvoy, B.R. (Editor), *IEEE 1985 Ultrasonics Symposium Proceedings*, pp. 1064-1067, Vol. 2, October 1985, San Francisco, CA, USA.

Blake, J.N., S.Y. Huang, B.Y. Kim, "Elliptical core two-mode fiber strain gauge,' *Proceedings SPIE - International Society Optical Engineers (USA)*, Vol. 838, pp. 332-339, 1988, Fiber-optic and Laser Sensors V, August 1987, San Diego, CA, USA.

Bucholtz, F., A.D. Kersey, A. Dandridge. "DC fiber-optic accelerometer with sub-μg sensitivity,' *Electronic Letter*, Vol. 22, No. 9, April 1986, pp. 451-453.

Butler, C.D. and G.B. Hocker, "Fiber-optics Strain Gauge,' *Applied Optics*, Vol. 17, 1978, pp. 2867-69.

Claus, R.O., B.S. Jackson, and R.G. May, "Nondestructive evaluation of composites by optical time domain reflectometry in embedded optical fibers,' *Proceedings IEEE SOUTHEASTCON '85*, Raleigh, NC, USA, March 1985, pp. 241-245.

Claus, R.O., B.S. Jackson, K.D. Bennett, "Nondestructive testing of composite materials by OTDR in imbedded optical fibers,' Proceedings SPIE International Society Optical Engineers, Vol. 566, 1985, pp. 243-248.

Cusworth, D.S., J.M. Senior, "Optical fiber sensing using GRIN rod lenses,' *International Journal of Optic Sensors*, Vol. 2, No. 5-6, October-December 1987 pp. 421-436.

Dakin, J.P., "Optical Fiber Sensors-Principles and Applications,' *Proceedings: Fiber-optics '83*, SPIE, Vol. 374, 1983, pp. 172-182.

DeHart, D.W., "Air Force Astronautics Laboratory Smart Structures and Skins Program Overview,' SPIE, Vol. 1170, *Fiber-optics Smart Structures and Skins II*, E. Udd, ed., 1989, pp. 11-18.

Farahi, F., T.P. Newson, J.D.C. Jones, D.A. Jackson, "Coherence multiplexing of remote fiber-optic Fabry--Perot sensing system,' *Optical Communications*, Vol. 65, No. 5, March 1988, pp. 319-321.

Field, S.Y. and K.H.G. Ashbee, "Weathering of Fiber Reinforced Plastics: Progress of Debonding Detected in Model Systems by Using Fibers as Light Pipes,' *Polymeric Engineering and Science*, Vol. 12, 1972, pp. 30-33.

Flax, A., C. Pennington, R.O. Claus, "Single mode optical fiber vibration sensor,' *Proceedings IEEE SOUTHEASTCON '87*, pp. 553-555, Vol. 2, April 1987, Tampa, FL, USA.

Freidah, J.T., R.E. Wagoner, T.J. Cash, N.H. Safar, "Long-lead cable effects on interferometric sensors,' *Proceedings SPIE-International Society Optical Engineers*, Vol. 838, 1988, Fiber-optic and Laser Sensors V, August 1987, San Diego, CA, USA, pp. 372-378.

Hattori, H., "Development of intelligent optical fiber sensors,' *Instrumentation* Vol. 30, No. 12, December 1987, pp. 25-28.

Higley, S.E., E. Udd, R.J. Michal, J.P. Theriault, D.A. Jolin, "Fiber-optic spectrometer,' *Proceedings SPIE-International Society Optical Engineers*, Vol. 838, 1988, pp. 318-324.

Kist, R., "Line Independence of Optical Fiber Sensors,' *Technica* (Switzerland) Vol. 37, No. 4, March 1988, pp. 13-16.

Kuhlman, R., B. Duncan, R.O. Claus, "Fiber-optic composite impact monitor,' *Proceedings IEEE SOUTHEASTOCON '87*, Vol. 2, April 1987, Tampa, FL,USA, pp. 414-417.

Leka, L.G. and E. Bayo, "A Close Look at the Embedment of Optical Fibers into Composite Structures,' *Journal of Composites Technology & Research*, Vol. 11, No. 3, 1989, pp. 106-112.

Liu, K., S.M. Ferguson, and R.M. Measures, "Damage Detection in Composites with Embedded Fiber-optic Interferometric Sensors,' *Proceedings: Fiber-optic Smart Structures and Skins II, SPIE Vol. 1170*, Boston, paper 1170-1122, (to be published 1989).

Main, R.P. "Fiber-optic sensors-future light,' *Sensor Review*, Vol. 5, No. 3, July, 1985, pp. 133-139.

Mann, R. "So what future do you see in fiber-optics?,' *Process Engineering (GB)*, Vol. 66, No. 6, June 1985, pp. 79-81.

Martinelli, M. "Fiber-optic sensors,' *Elettron Oggi.*, No. 4, April 1984, pp. 115-124.

Mazus, C.J., G.P. Sendeckyj, and D.M. Stevens, "Air Force Smart Structures/Skins Program Overview,' SPIE, Vol. 986, *Fiber-optic Smart Structures and Skins*, E. Udd, ed., 1988, pp. 19-29.

Measures, R.M., D. Hogg, R.D. Turner, T. Valis, and M.J. Giliberto, "Structurally Integrated Fiber-optic Strain Rosette,' *Proceedings: Fiber Optic Smart Structures and Skins I, SPIE Vol. 986*, Boston, paper 986-07, 1988, pp. 32-42.

O'Conner, W.T., R.O. Claus, "Optical Fiber Sensor Application in a Simple Robotic Gripper,' *Proceedings of IEEE SOUTHEASTCON '84*, April 1984, Louisville, KY, USA, pp. 295-297.

Rogers, A.J., "Distributed Optical-Fiber Sensors,' *Journal of Physics D: Applied Physics*, Vol. 19, 1986, pp. 2237-55.

Saleh, B.E.A. and Teich, M.C., *Fundamentals of Photonics*, John Wiley & Sons, 1991.
Shahriari, M.R., G.H. Sigel, Quan Zhou, "Porous glass fibers for high sensitivity chemical and biomedical sensors,' *Proceedings SPIE--International Society Optical Engineers*, Vol. 838, 1988, Fiber-optic and Laser Sensors V, August 1987, San Diego, CA, USA, pp. 348-352,
Shankaranarayanan, N.K., K.T. Srinivas, R.O. Claus, "Mode-mode interference effects in axially strained few-mode optical fibers,' *Proceedings SPIE--International Society Optical Engineers*, Vol. 838, 1988, pp. 385-388.
Shankaranarayanan, N.K., K.D. Bennett, R.O. Claus, "Optical fiber modal domain detection of stress waves,' McAvoy, B.R., editor, *IEEE 1986 Ultrasonics Symposium Proceedings*, Vol. 2, 1986, November 1986, Williamsburg, VA.
Shih, J.C., R.O. Claus, "Concentric Core Optical Fiber Strain Sensor,' *Proceedings IEEE SOUTHEASTOCON '86*, March 1986, Richmond, VA, pp. 91-94.
Spillman W.B., and B.R. Kline, "Fiber-optic Vibration Sensors for Structural Control Applications' *Proceedings of Damping '89*, West Palm Beach, FL, 1989, published by Flightdynamics Laboratory, Wright-Patterson Air Force Base, Ohio.
Su, S.F. "Fiber-optic electric field sensors utilizing electro-absorption,' *Proceedings IEEE SOUTHEASTCON '85*, Raleigh, NC, USA, March/April 1985, pp. 241-245.
Tsutsui, T., S. Yamamoto, "Optical fiber sensor,' *Journal of the Japanese Society Precision Engineers*, Vol. 53, No. 12, pp. 1847-51, Dec. 1987.
Turner, R.D., T. Valis, W.D. Hogg, and R.M. Measures, "Fiber-Optic Strain Sensors for Smart Structures,' *Journal of Intelligent Material Systems* and Structures, Vol. 1, January 1990, pp. 26-49.
Valis, T., E. Tapanes, and R.M. Measures, "Localized Fiber-optic Strain Sensors Embedded in Composite Materials,' *Proceedings: Fiber-optic Smart Structures and Skins II, SPIE Vol. 1170*, Boston, paper 1170-53, (to be published 1989).
Wade, J.C., R.O. Claus, "Interferometric Techniques Using Embedded Optical Fibers for the Quantitative NDE of Composites,' Thompson, D.O., Chimenti, D.E. Editors, *Review of Progress in Quantitative Nondestructive Evaluation*, Vol. 2, August 1982, San Diego, CA, pp. 1731-38.
Waite, S.R., R.P. Tatam, and A. Jackson, "Use of optical fiber for damage and strain detection in composite materials,' *Composites*, Vol. 19, No. 6, November 1988, pp. 435-442.
Waite, S.R. and G.N. Sage, "The failure of optical fibers embedded in composite materials,' *Composites*, Vol. 19, No. 4, July 1988, pp. 288-294.
Wiencko, J.A., R.O. Claus, R.E. Rogers, "Embedded optical fiber sensors for intelligent aerospace structures,' *Proceedings of SENSORS EXPO, September 1987*, Detroit, MI, USA, pp. 257-262.
Zhipeng Zhand, Qin Zhang, "Magnetic field sensitivity analysis of an optical fiber with metallic glass strips,' *International Journal of Optic Sensors*, Vol. 2, No. 5-6, pp. 341-347, October-December 1987.

B6: Smart Sensors and Actuators

"Adjustment of intelligent sensors with a low-cost function tester,' *Elektronik* (West Germany) Vol. 37, No. 6, March 1988, pp. 134-138.

Alba, M., "Tradeoffs in automotive smart sensors system partitioning,' *Proceedings of SENSORS EXPO*, 401, September 1987, Detroit, MI, USA.

Brignell, J.E., J.K. Atkinson, "Sensors, Intelligence, and Networks,'*IEE Colloquium on 'Solid State and Smart Sensors'*, Digest No. 39, March 1988, London, UK.

Caro, J., "Using numerical processors for intelligent sensor design,' P. Albertos, De La Puente, J.A., Editors, Components, Instruments and Techniques for Low Cost Automation and Applications. *IFAC Symposium*, 1988, November 1986, Valencia, Spain, Pergamon, Oxford, UK, pp. 61-65.

De Rossi, D., A. Nannini, and C. Domenici, "Biomimetic Tactile Sensor With Stress-Component Discrimination capability,' *Journal of Molecular Electronics*, Vol. 3, 1987, p. 173.

De Rossi, D., A. Nannini, and C. Domenici, "Artificial Sensing Skin Mimicking Mecho-electrical Conversion Properties of Human Dermis,' *IEEE Transactions of Biomedical Engineering*, BME-35, 1988, p. 83.

De Rossi, D., L. Lazzeri, C. Domenici, A. Nannini, and P. Basser , "Tactile Sensing by an Electromechanochemical Skin Analog,' *Sensors and Actuators*, Vol. 17, 1989, p. 107.

Favennec, J.-M., "Smart sensors in industry,' *Journal of Physics E.*, Vol. 20, No. 9, pp. 1087-90, September 1987.

"Future-generation Smart Field Sensor and Smart Field Network,' *Instrumentation*, Vol. 30, No. 11, pp. 52-53, November 1987.

Giachino, J.M., "Smart sensors,' *Sensors & Actuators,* Vol. 10, No. 3-4, November-December 1986, pp. 239-248.

Hanneborg, A., P. Ohlckers, "SI's Smart Silicon Sensor,' *Elektro*, Vol. 98, No. 15, September 1985, pp. 8-10.

Hattori, H., "Development of Intelligent Optical Fiber Sensors,' *Instrumentation*, Vol. 30, No. 12, December 1987, pp. 25-28.

Hester, C.F., H.F. Caulfield, "Optical AI Architectures for Intelligent Sensors,' *Proceedings SPIE-International Society Optical Engineers, Vol. 754, Optical and Digital Pattern Recognition*, January 1987, Los Angeles, CA, USA, pp. 185-192.

Hockaday, B., J. Waters, "Opto-Mechanical Smart Actuator,' *Proceedings of the 1987 American Control Conference*, Vol. 1, June 1987, Minneapolis, MN.

"Intelligent Sensors: One Must First be Convinced,' *Measures*, Vol. 52, No. 7, May 1987, pp. 61-67.

Jayawant, B.V., J.D.M. Watson, "Array Sensor for Tactile Sensing in Robotic Applications,' *IEE Colloquium on 'Solid State and Smart Sensors'*, Digest

No. 39, March 1988, London, UK.
Legras, J.C., M. Priel, C. Ranson, "Application of Multiple Regression Methods and Automatic Testing Equipment to the Characterization of 'Smart' Sensors,' *Sensors and Actuators*, Vol. 12, No. 3, October 1987, 2nd International Meeting on Chemical Sensors, July 1986, Bordaux, France, pp. 235-243.
Middelhoek, S. and A.C. Hoogerwerf, "Smart Sensors: When and Where?,' *Sensors and Actuators*, Vol. 8, No. 1, September 1985, pp. 39-48.
Montgomery, R.C. and J.P. Williams, "The Use of Distributed Microcomputers in the Control of Structural Dynamics Systems,' Hamza, M.H. (Editor), Mini and Microcomputers in Control, Filtering and Signal Processing, *Proceedings of the ISMM International Symposium*, December 1984, Las Vegas, NV, USA, pp. 140-144.
Seo, I., "Development of Intelligent Sensors Using Polymer Materials,' *Instrumentation*, Vol. 30, No. 12, December 1987, pp. 32-35.
Stojilikovic, Z. and J. Clot, "Integrated behavior of Artificial Skin,' *IEEE Transactions for Biomedical Engineering*, BME-24, 1977, p.396.
Takahashi, K., "Sensor Materials For the Future: Intelligent Materials,' *Sensors & Actuators*, Vol. 13, No. 1, January 1988.
Tinham, B., "Micros and Sensors Make Smart Transmitters,' *Control & Instrumentation*, Vol. 18, No. 9, September 1986, pp. 55-57.
Trontelj, J., L. Trontelj, V. Kunc, M. Stiglic, "Generalized Smart Sensor Array Electronics,' *Proceedings of the IEEE 1987 Custom Integrated Circuits Conference*, May 1987, Portland, OR, USA, pp. 708-711.
Udd, Eric (ed.), *Fiber-optic Sensors: An Introduction for Engineers and Scientists*. New Jersey, John Wiley & Sons, 1991.
Ushikubo, S., "Field Network of Intelligent Sensors,' *Instrumentation*, Vol. 30, No. 12, December 1987, pp. 40-44.

B7: Magneto-Rheological Suspensions

Kordonskii, V.I., M.Z. Shul'man, and T.V. Kunevich, "Investigation of the Magneto-Rheological Effect' in: *Rheology of Polymeric and Disperse Systems and Rheophysics* [in Russian], Part 2, Minsk, 1975, pp. 79-82.

Martinet, A., "Experimental Evidence of Static and Dynamic Anisotropies of Magnetic Colloids,' in: *Thermomechanics of Magnetic Fluids*, Hemisphere, Washington, D.C., 1978, pp. 96-114.

Mikelson, A.E., "Effect of Magnetic Fields and Thermoelectromotive Force on the Kinetics of the Formation of the Solid Phase,' *Magnitnaya Gidrodinamika*, No. 1, January-March 1981, pp. 66-69.

Sahu, M.D. and V.A. Gadgil, "Effects of Electromagnetic Fields on Solidification of some Aluminum Alloys,' *British Foundryman*, No. 3, 1977, pp. 89-92.

Shul'man, Z.P., V.I. Kordonskii, and E.A. Zaltsgendler, "Measurement of the Magneto-rheological Characteristics of Ferrosuspensions,' *Magnitnaya Gidrodinamika*, No. 1, January-March 1979, pp. 39-43.

Shul'man, Z.P., V.I. Kordonskii, I.V. Prokhorov, and M.B. Smolskii, "Experimental Investigation of the Magnetic Characteristics of Magneto-Rheological Suspensions,' *Magnitnaya Gidrodinamika*, No. 3, July-September 1980, pp. 31-37.

Shul'man, Z.P., V.I. Kordonskii, and S.A. Demchuk, Demchuk, "Electrical Conductivity of Magneto-rheological Suspensions,' *Kolloidn. Zhurnal*, No. 1, 1979, pp. 193-195.

Uhlmann, D.R., T.P. Seward, and B. Chalmers, "The Effect of Magnetic Fields on the Structure of Metal Alloy Castings,' *Transactions of the Metallurgical Society AIME*, Vol. 236, 1966, pp. 527-531.

B8: Neural Networks

Amit, D.J., *Modelling Brain Function*, Cambridge University Press, 1989.

Grossberg, S., "Nonlinear Neural Networks, Principles, mechanisms and architectures,' *Neural Networks*, Vol. 1, 1988, pp. 17-61.

Hirsch, M., "Convergent Activation Dynamics in Continuous Time Networks,' *Neural Networks*, Vol. 2, 1989, pp. 341-349.

McCullough, W.S. and W. Pitts, "A Logical Calculus od the Ideas Immanent in Nervous Activity,' *Bulletin of Mathematical Biophysics*, Vol. 3, 1943, pp. 115-133.

Mead, C.A., *Analog VLSI and Neural Systems*, Addison-Wesley, 1988.

Minsky, M. and S. Pappert, *Perceptrons*, Cambridge, MA. MIT Press, 1986.

Murray, A.F. and L. Tarassenko, "Programmable Analog Pulse-Firing Neural Networks,' Oxford University Preprint, 1990.

Rosenblatt, F., *Principles of Neurodynamics*, New York, Spartan, 1962.

Sheperd, G.H., *Neurobiology*, Oxford University Press, 1988.

B9: General Publications Relevant to Smart Materials

Abela, G.S., "Laser Re-canalization: Preliminary Clinical Experience,' *Cardiovascular Disease Chest Pain*, Vol. 3, 1987, p. 3.

Advanced Materials by Design, U.S. Congress Office of Technological Assessment Report OTA-E-358, June 1988.

Allen, S.M. and J.W. Cahn, "A Macroscopic Theory for Antiphase Boundary Motion and its Application to Antiphase Domain coarsening,' *Acta Metallurgica*, Vol. 27, 1979, pp. 1085-98.

Ball, J. and R. James, "Fine Phase Mixtures as Minimizers of Energy,' *Archives Rational Mechanical Analysis*, Vol. 100, 1987, pp. 13-52.

Bassett, C.A.L., "Biophysical Principles Affecting Bone Structure,' in *The Biochemistry and Physiology of Bone*, (ed. G.H. Bourne) (2nd Edition), Vol. 3, 1971, Academic Press, New York, pp. 1-76.

Bassett, C.A.L., "Current Concepts of Bone Formation,' *Journal of Bone Jt. Surg.*, Vol. 44, 1962, p. 1217.

Bassett, C.A.L., "Electrical Effects in Bone,' *Scientific American*, Vol. 213, No. 4, 1965, pp. 18-25.

Bassett, C.A.L. and Becker, R.O., "Generation of Electric Potentials by Bone in Response to Mechanical Stress,' *Science*, Vol. 137, pp. 1063-64.

Bassett, C.A.L., Pawluk, R.J. and Becker, R.O., "Effects of Electric Currents on Bone In Vivo,' *Nature*, 1964, Vol. 204, pp. 652-654.

Becker, R.D., C.A.L. Bassett, and C.H. Bachman, "Bioelectrical Factors Controlling Bone Structure,' in *Bone Biodynamics*, (ed. H.M. Frost), 1964, Little-Brown, Boston, pp. 209-232.

Bendsoe, M. and N. Kikuchi, "Generating Optimal Topologies in a Structural Design Using a Homogenization Method,' *Computational Methods Applied Mechanical Engineering*, Vol. 71, 1988, pp. 197-224.

Brighton, C.T., J. Black, and S.R. Pollack, *Electrical Properties of Bone and Cartilage: Experimental Effects and Clinical Applications*, 1979, Grune & Stratton, New York.

Bronowicki, A.J., T.L. Mendenhall, and R.M. Manning, *Advanced Composites with Embedded Sensors and Actuators (ACESA)*, AL-TR-90-022, Astronautics Laboratory, Air Force Space Technology Center, April 1990, Report F04611-88-C-0054.

Brown, W.F., *Magnetostatic Principles in Ferromagnetism*, Vol. 1 of Selected Topics in Solid State Physics, ed. E.P. Wohlfarth, North-Holland, 1962.

Brown, W.F., *Micromagnetics*, John Wiley and Sons, New York, 1963.

Burstall, A.F., *A History of Mechanical Engineering*, Faber and Faber, London, 1963.

Butler, J.L., *Application Manual for the Design of ETREMA Terfenol-D Magnetostrictive Transducers, Edge Technologies*, Inc., N. Marshfield, 1988.

Calvert, P., "Biomimetic Processing of Ceramics and Composites,' *Proceedings of*

the International Workshop on Intelligent Materials, The Society of Non-Traditional Technology, March 1989, Tsukuba Science City, Japan, pp. 63-72.
Chopra, D., *Quantum Healing*, Bantam Books, New York, 1989.
Clark, A.E., "Chapter 7-Magnetostrictive Rare Earth Fe_2 Compounds,' *Ferromagnetic Materials, Vol. I*, Edited by E.P. Wohlfarth, North-Holland Publishing Co., 1980, pp. 531-589.
Clark, A.E., J.P. Teter, and M. Wun-Fogle, "Magnetomechanical Coupling in Bridgman-Grown $Tb_{0.3}Dy_{0.7}Fe_{1.9}$ at High Drive Levels,' presented at the *34th Conference on Magnetism and Magnetic Materials*, Boston, November 1989.
Clark, J.P. and M.C. Flemings, "Advanced Materials and the Economy,' *Scientific American*, Vol. 255, No. 4, 1986, pp 43-49.
Clark, W.W., H.H. Robertshaw, and T.J. Warrington, "A Comparison of Actuators for Vibration Control of the Planar Vibrations of a Flexible Cantilevered Beam,' *Journal of Intelligent Material Systems and Structures*, Vol. 1, No. 3, July 1990, pp. 289-308.
Collins, C., D. Kinderlehrer, and M. Luskin, "Numerical Approximation of the Solution of a Variational Problem with a Double Well Potential' *IMA Preprint 605, SIAM Journal of Numerical Analysis* (to appear).
The Concept of Intelligent Materials and the Guidelines on R&D Promotion, Japanese Science and Technology Agency, November 1989.
Confino, E., I. Tur-Kaspa, A. DeCherney, R. Corfman, C. Coulam, E. Robinson, G. Haas, E. Katz, M. Vermesh, N. Gleicher, "Transcervical Balloon Tuboplasty-A Multicenter Study,' *Journal of the American Medical Association*, Vol. 264, No. 16, October 1990, pp. 2079-82.
Edberg, D.L., "Control of Flexible Structures by Applied Thermal Gradients,' *AIAA Journal*, Vol. 25, No. 6, June 1987.
The Encyclopaedia Britannica, Encyclopaedia Britannica Inc., Chicago IL, 1989.
Eringen, A.C., *Mechanics of Continua*, R.E. Krieger Publishing Company, Malabar, FL, USA, 1980.
Eringen, A.C. and G.A. Maugin, *Electrodynamics of Continua I: Foundations and Solid Media*, Springer Verlag, New York, 1989.
Eringen, A.C. and G.A. Maugin, *Electrodynamics of Continua II: Fluids and Complex Media*, Springer Verlag, New York, 1989.
First Joint U.S./Japan Conference on Adaptive Structures, edited by B.K. Wada, J.L. Fanson, and K. Miura, *Proceedings of the First Joint U.S./Japan Conference on Adaptive Structures*, November 13-15 1990, Maui, Hawaii, Technomic Publishing Company.
Fischer, G., "Strategies Emerge for Advanced Ceramic Business,' *American Ceramic Society Bulletin*, Vol. 65, No. 1,1986, pp. 39-42.
Forester T., ed., *The Materials Revolution*, MIT Press, Cambridge, MA, 1988.
Forward, R.L., "Electronic Damping of Vibrations in Optical Structures,' *Journal of Applied Optics*, Vol. 18, No. 5, pp. 690-697.
Gandhi, M.V., B.S. Thompson, and F. Fischer, "Manufacturing-Process-Driven Methodologies for Composites Materials,' *Composite Manufacturing*, Vol. 1, No. 1, March 1990, pp. 32-40.

Gerardi, T., "Health-Monitoring Aircraft,' *Journal of Intelligent Material Systems and Structures*, Vol. 1, No. 3, July 1990, pp. 375-385.
Gerardi, A.G., "Health-Monitoring Aircraft,' *Proceedings of ARO/NASA/AFOSR/NASA/ONR, US-Japan Workshop*, Smart Intelligent Materials and Systems, Honolulu, Hawaii, March 1990.
Grippo, P.M., B.S. Thompson, and M.V. Gandhi, "Flexible Fixturing Systems for CIM Environments,' *International Journal of Computer Integrated Manufacturing*, Vol. 1, No. 2, 1988, pp. 124-135.
Gandhi, M.V. and M. Usman, "Equilibrium Characterization of Fluid-Saturated Continua, and an Interpretation of the Saturation Boundary Condition Assumption for Solid-Fluid Mixtures,' *International Journal of Engineering Science*, Vol. 27, No. 5, 1989, pp. 539-548.
Gandhi, M.V., M. Usman, A.S. Wineman and K.R. Rajagopal, "Combined Extension and Torsion of a Swollen Cylinder within the Context of Mixture Theory,' *Acta Mechanica*, Vol. 79, 1989, pp. 81-95.
Gazes, P.C., *Clinical Cardiology*, 3rd Edition, Lea & Febiger, Philadelphia, 1990, pp. 95-98.
Gurtin, M.E., "On the Two-Phase Stefan Problem with Interfacial Energy and Entropy,' *Archives Rational Mech. Analysis*, Vol. 96, 1986, pp. 199-241.
Gurtin, M.E., "Multi-Phase Thermomechanics with Interfacial Structure. 1. Heat Conduction and the Capillary Balance Law,' *Archive Rational Mechanical Analysis*, Vol. 104, 1988, pp. 195-221.
Hall, D.P. and A.R. Gruentzig, "Chapter 117: Technique of Percutaneous Transluminal Angioplasty,' *The Heart*, Hurst, J.W., Editor-in-Chief, Logue, R.B., Rackley, C.E., Schlant, R.C., Sonnenblick, E.H., Wallace, A.G., and Wenger, N.K., eds., 6th Edition, McGraw Hill, New York, 1985, pp. 1901-15.
Hiller, M.W., M.D. Bryant, and J. Umegaki, "Attenuation and Transformation of Vibration through Active Control of Magnetostrictive Terfenol,' *Journal of Sound and Vibration*, Vol. 133, No. 3, 1989, pp. 1-13.
Ikegami, R., D.G. Wilson, and J.H. Laakso, *Advanced Composites with Embedded Sensors and Actuators (ACESA)*, AL-TR-90-022, Astronautics Laboratory, Air Force Space Technology Center, June 1990, Report F04611-88-C-0053.
Jennings, J.S. and N.H. Macmillan, "On the Architecture and function of Cuttle-fish Bone,' *Journal of Materials Science*, Vol. 18, 1983, pp. 2081-86.
Kohn, R., "Recent Progress in the Mathematical Modelling of Composite Materials,' *Composite Material Response: Constitutive Relations and Damage Mechanisms*, G. Sih *et al.* eds., 1988, pp. 155-177.
Kohn, R. and G. Strang, "Optimal Design and Relaxation of Variational Problems I-III,' *Communications in Pure Applied Mathematics*, Vol. 39, 1987, pp. 113-137, 139-182, 353-377.
Kranzberg, M. and C.S. Smith, "Materials Science and Engineering: Its Evolution, Practice and Prospects,' *Material Science and Engineering*, Vol 37, No 1., 1979.
Lemonick M.D., T. McCarroll, J.M. Nash, and D. Wyss, "Superconductors! The Startling Breakthrough That Could Change Our World,' *Time*, May 11, 1987.
Lubin, G., *Handbook of Composites*, Van Nostrand Reinhold Inc., 1982.

Lurie, K., A. Cherkaev, and A. Fedorov, "Regularization of Optimal Design Problems for Bars and Plates I, II,' *Journal Optics, Theory, and Applications*, Vol. 37, 1982, pp. 499-522, 523-543.
Mahanti, S.D., and S. Tang, "Vortices and Strings: Phase Transition in Anisotropic Planar-Rotor Systems,' *Physical Review*, Vol B 33, 1986, pp. 3419.
Mahanti, S.D., S. Tang, and R.K. Kalia, "Ferroelastic Phase Transitions in Two-Dimensional Molecular Solids,' *Physics Review Letters*, Vol. 56, 1986, p. 484.
Mahanti, S.D., G. Kemeny, and J. Kales, "Generalized Non-linear Langevin Equation for a Rotor,' *Physical Review*, Vol. B 33, 1986, p. 3512.
Mahanti, S.D., and S. Tang, "Phase Transitions in Diatomic Molecular Monolayers,' *Superlattices and Microstructure*, Vol. 1, 1986, p. 517.
Mahanti, S.D., G. Kemeny, and G. Zhang, "Dynamics of Strongly Coupled Model Rotational-Transitional Systems,' *Physical Review*, Vol. B 35, 1987, p. 8551.
Mahanti, S.D., W. Jin, and S. Tang, "Dynamics of a Two-Dimensional Diatomic Molecular Monolayer-a Molecular Dynamics Study,' *Solid State Communications*, Vol. 66, 1988, p. 877.
Mahanti, S.D., W. Jin, S. Tang, and R. Kalia, "Ferroelastic Phase Transition and Phonons in a Diatomic Molecular Monolayer,' *Physical Review*, Vol. B 39, 1989, p. 1989.
Mahanti, S.D., W. Jin, and S.Y. Tang, "Internal Stress Tensor in Constant-Pressure Molecular Dynamics of Anisotropic Molecular Solids,' *Physical Review*, Vol. B 39, 1989, p. 11928.
Margolis, J.M., *Conductive Polymers and Plastics*, Chapman and Hall, 1989.
Margolis, J.M., "Composites Challenge Metals for Aircraft/Auto Panel Applications,' *Machine and Tool Blue Book*, February 1987, pp 45-48.
Moon, F.C., *Magneto-solid Mechanics*, Wiley Interscience, NY 1984.
Moulson, A.J. and Herbert, J.M., *Electroceramics-Materials, Properties, Applications*, Chapman and Hall, 1990.
Mullins, W.W., "Two-dimensional motion of idealized grain boundaries,' *Journal of Applied Physics*, Vol. 27, 1956, pp. 900-904.
Murat, F. and L. Tartar, "Calcul des variations et homogenization,' *Les Methodes de l'Homogenization: Theorie et Applications en Physique*, Collection de la Dir. des Etudes et Recherche d'Electricite de France, Eyrolles, 1985, pp. 319-369.
Negahban, M., and A.S. Wineman, "Material Symmetry and the Evolution of Anisotropies in a Simple Material: II. The Evolution of Symmetry,' *International Journal of Nonlinear Mechanics*, Vol. 24, No. 6, 1989, pp. 537-549.
Negahban, M., and A.S. Wineman, "The Evolution of Anisotropies in the Elastic Response of an Elastic-Plastic Material,' *International Journal of Plasticity*, (to appear).
Negahban, M., and A.S. Wineman, "Following the Mechanical Response in Phase Transitions: Elastic Solid to Elastic Solid Transitions,' *Proceedings of the Twelfth Canadian Congress of Applied Mechanics*, Ottawa, Ontario, 1989, pp. 840-841.

Negahban, M., "The Effect of Continuous Phase Transition on a Torsional Oscillator,' *62nd Annual meeting of the Society of Rheology*, Santa Fe, New Mexico, October 1990.
Negahban, M., "Constitutive Modeling of Phase Transition in Smart materials, *ADPA/AIAA/ASME/SPIE Conference on Active Materials and Adaptive Structures*, Alexandria, Virginia, November 1991.
Olson, D.E., and B. Snyder, "The Growth of Swirl in Curved Circular Pipes,' *Physics of Fluids*, Vol. 26, No. 2, 1983, pp. 347-349.
Olson, D.E., and B. Snyder, "The Upstream Scale of Flow Development in Curved Circular Pipes,' *Journal of Fluid Mechanics*, Vol. 150, 1986, pp. 139-158.
Osada, Y., R. Kishi, K. Umezawa, and H. Yasunaga, "Mechochemical devices using polymer gels,' *Proceedings of International Workshop on Intelligent Materials*, published by the Society of Non-Traditional Technology, Tokyo 105, Japan, March 1989, pp. 297-302.
Prasad, P.N., "Multifunctional Molecular and Polymeric Materials for Nonlinear Optics and Photonics,' *Materials Research Society Symposium Proceedings*, Vol. 175, 1990, pp. 79-87.
Prasad, P.N. and D.R. Ulrich, *Nonlinear Optical and Electroactive Polymers*, Plenum Press, New York, 1988.
Purna, S., *The Truth Will Set You Free*, Element Books, New York, 1987.
Rogers, C.A., ed., "Smart Materials, Structures and Mathematical Issues,' selected papers presented at the *U.S. Army Research Office Workshop on Smart Materials, Structures and Mathematical Issues*, VPI, September 1988, Technomic Publishing, Lancaster, PA, 1989.
Rosato, D., Di Mattia, D. and Rosato, D., *Designing with Plastics and Composites-A Handbook*, Van Nostrand Reinhold Inc., 1991.
Rosenweig, R.E., *Ferrohydrodynamics*, Cambridge University Press, New York, 1985.
Rozvany, G., T. Ong, W. Szeto, R. Sandler, N. Olhoff, and M. Bendsoe, "Least-weight design of perfurated elastic plates I and II,' *International Journal of Solids and Structures*, Vol. 23, 1987, pp. 521-536, 537-550.
Rudd, J.L., "Air Force Damage Tolerance Design Philosophy,' *ASTM STP 842 on Damage Tolerance of Metallic Structures: Analysis Methods and Applications*, pp. 134-141.
Shipman, P., A. Walker, and D. Bichell, *The Human Skeleton*, Harvard University Press, Cambridge, MA, 1985, pp. 53-63.
Snyder, B., "A New Class of Fluid Instabilities: Vorticity-Induced Waveforms on Falling Parabolic Jets,' *Physics of Fluids*, Vol. 25, No. 5, 1982, pp. 905-907.
Snyder, B., J.R. Hammersley, and D.E. Olson, "The axial Skew of Flow in Curved Pipes,' *Journal of Fluid Mechanics*, Vol. 161, 1985, pp. 281-294.
Snyder, B., and D.E. Olson, "Entrance-Flow Invariance in a Tapering Elliptical Slit,' *Physics of Fluids*, Vol. 29, 1986, pp. 2341-2343.
Snyder, B., D.E. Olson, J.R. Hammersley, C.V. Peterson, and M.J. Jaeger, "Reversible and Irreversible Components of Central Airway Flow Resistance,' *ASME Journal of Biomechanics Engineering*, Vol. 109, 1987, pp. 154-159.

Snyder, B., and C. Lovely, "A Computational Study of Developing 2-D Laminar Flow in Curved Channels,' *Physics of Fluids A*, Vol. 2, 1990, pp. 1808-1816.
Snyder, B., K.T. Li, and R.A. Wirtz, "Secondary Goertler Vortices in a Serpentine Duct,' Bulletin of American Physical Society, Series II, Vol. 35, 1990, p. 2331.
Snyder, "Spatially-Periodic Motion in a Curved Ducts,' *Bulletin of American Physical Society*, Series II, Vol. 36, 1991.
Sung, C.K. and B.S. Thompson, "A Methodology for Synthesizing High-Performance Robots Fabricated in Optimally-Tailored Composite Laminates,' *ASME Journal of Mechanisms, Transmissions, and Automation in Design*, Vol. 109, No. 1, March 1987, pp. 74-86.
Suzuki, A. and T. Tanaka, "Phase Transition in Polymer Gels Induced by Visible Light,' *Nature*, Vol. 346, No. 6282, July 1990, pp. 345-347.
Takahashi, K., "Intelligent Materials for Future Electronics,' *Journal of Intelligent Material Systems and Structures*, Vol. 1, No. 2, April 1990 pp. 248-258.
The Concept of Intelligent Materials and Guidelines on their R&D Promotion, Science and Technology Agency in Japan, November 1989, (published in English in January 1990).
Thompson, B.S. and M.V. Gandhi, "Smart Materials,' in *Encyclopaedia Britannica Science and the Future 1991 Year Book*, Encyclopaedia Britannica, Chicago, IL, July 1990, pp. 162-171.
Thompson, B.S. and M.V. Gandhi, "A Commentary on Flexible Fixturing,' *ASME Applied Mechanics Review*, Vol. 39, No. 9, 1986, pp. 1365-69.
Thompson, B.S., "Composite Laminate Components for Robotic and Machine Systems: Research Issues in Design,' *ASME Applied Mechanical Reviews*, Vol. 40, No. 11, November 1987, pp. 1545-52.
Uchino, K., "Electrostrictive Actuators: Materials and Applications,' *American Ceramic Society Bulletin*, Vol. 65, No. 4, April 1986, pp. 647-652.
Udd, E., "Embedded Sensors make Structures Smart,' *Laser Focus/Electro--Optics*, May 1988, pp. 135-139.
Vaughan, J., *The Physiology of Bone*, 3rd Edition, Clarendon Press, Oxford, 1981, pp. 22-25.
Vincent, J.F.V., *Structural Biomaterials*, Macmillan Press, London, 1982.
Vincent, J.F.V, "Toughness in Biological Materials,' *Proceedings of International Workshop on Intelligent Materials*, published by the Society of Non-Traditional Technology, Toyko, Japan, March 1989, pp. 131-138.
Vogel, S., "Smart Skin,' *Discover*, April, 1990, p.26.
Wada, B.K., editor, *Adaptive Structures*, ASME Book AD-Vol. 15, 1989.
Wildey, J.F. II, "Aging Aircraft,' National Association of Corrosion Engineers, NACE.
Wildey, J.F. II, "Aloha 737,' *ASTM*, November 1989.
The World Book Encyclopedia, World Book Inc., Chicago, IL, Vol. 1-25, 1988.
Yamauchi, A. H. Okihiko, S. Fujishige, S. Ito, and H. Ichijo, "Heat Sensitive and Responsible Polymer Gels,' *Proceedings of International Workshop on Intelligent*

Materials, published by the Society of Non-Traditional Technology, Tokyo 105, Japan, March 1989, pp. 303-313.

Zhao, M.T., M. Samoc, B.P. Singh, and P.N. Prasad, "Study of Third-Order Microscopic Optical Nonlinearities in Sequentially Built and Systematically Derivatized Structures,' *Journal of Physical Chemistry*, Vol. 93, 1989, pp. 7916-20.

DISTRIBUTION LIST

No. of Copies	To
1	Office of the Under Secretary of Defense for Research and Engineering, The Pentagon, Washington, DC 20301
	Commander, U.S. Army Laboratory Command, 2800 Powder Mill Road, Adelphi, MD 20783-1145
1	ATTN: AMSLC-IM-TL
1	AMSLC-CT
	Commander, Defense Technical Information Center, Cameron Station, Building 5, 5010 Duke Street, Alexandria, VA 22304-6145
2	ATTN: DTIC-FDAC
	Commander, Army Research Office, P.O. Box 12211, Research Triangle Park, NC 27709-2211
1	ATTN: Information Processing Office
	Commander, U.S. Army Materiel Command, 5001 Eisenhower Avenue, Alexandria, VA 22333
1	ATTN: AMCSCI
	Commander, U.S. Army Materiel Systems Analysis Activity, Aberdeen Proving Ground, MD 21005
1	ATTN: AMXSY-MP, H. Cohen
	Commander, U.S. Army Missile Command, Redstone Scientific Information Center, Redstone Arsenal, AL 35898-5241
1	ATTN: AMSMI-RD-CS-R/Doc
	Commander, U.S. Army Armament, Munitions and Chemical Command, Dover, NJ 07801
1	ATTN: Technical Library
	Commander, U.S. Army Natick Research, Development and Engineering Center, Natick, MA 01760-5010
1	ATTN: Technical Library
	Commander, U.S. Army Tank-Automotive Command, Warren, MI 48397-5000
1	ATTN: AMSTA-TSL, Technical Library
	Director, U.S. Army Ballistic Research Laboratory, Aberdeen Proving Ground, MD 21005
1	ATTN: SLCBR-TSB-S (STINFO)
	Commander, Harry Diamond Laboratories, 2800 Powder Mill Road, Adelphi, MD 20783
1	ATTN: Technical Information Office
	Director, Benet Weapons Laboratory, LCWSL, USA AMCCOM, Watervliet, NY 12189
1	ATTN: AMSMC-LCB-TL
1	AMSMC-LCB-R
1	AMSMC-LCB-RM
	Commander, U.S. Army Foreign Science and Technology Center, 220 7th Street, N.E., Charlottesville, VA 22901-5396
1	ATTN: AIFRTC, Applied Technologies Branch, Gerald Schlesinger
	Commander, U.S. Army Aviation Systems Command, Aviation Research and Technology Activity, Aviation Applied Technology Directorate, Fort Eustis, VA 23604-5577
1	ATTN: SAVDL-E-MOS
1	SAVRT-TY-ATS
	Commander, U.S. Army Agency for Aviation Safety, Fort Rucker, AL 36362
1	ATTN: Technical Library
1	Clarke Engineer School Library, 3202 Nebraska Ave. North, Ft. Leonard Wood, MO 65473-5000

No. of Copies	To
	Naval Research Laboratory, Washington, DC 20375
1	ATTN: Code 5830
	Chief of Naval Research, Arlington, VA 22217
1	ATTN: Code 471
1	Edward J. Morrissey, WRDC/MLTE, Wright-Patterson Air Force, Base, OH 45433-6523
	Commander, U.S. Air Force Wright Research & Development Center, Wright-Patterson Air Force Base, OH 45433-6523
1	ATTN: WRDC/MLLP, M. Forney, Jr.
1	WRDC/MLBC, Mr. Stanley Schulman
	NASA - Marshall Space Flight Center, MSFC, AL 35812
1	ATTN: Mr. Paul Schuerer/EH01
	U.S. Department of Commerce, National Institute of Standards and Technology, Gaithersburg, MD 20899
1	ATTN: Stephen M. Hsu, Chief, Ceramics Division, Institute for Materials Science and Engineering
1	Committee on Marine Structures, Marine Board, National Research Council, 2101 Constitution Ave., N.W., Washington, DC 20418
1	The Charles Stark Draper Laboratory, 68 Albany Street, Cambridge, MA 02139
	General Dynamics, Convair Aerospace Division, P.O. Box 748, Fort Worth, TX 76101
1	ATTN: Mfg. Engineering Technical Library
1	Department of the Army, Aerostructures Directorate, MS-266, U.S. Army Aviation R&T Activity - AVSCOM, Langley Research Center, Hampton, VA 23665-5225
1	NASA - Langley Research Center, Hampton, VA 23665-5225
1	Plastics Technical Evaluation Center, (PLASTEC), ARDEC, Bldg. 355N, Picatinny Arsenal, NJ 07806-5000
	Director, U.S. Army Materials Technology Laboratory, Watertown, MA 02172-0001
2	ATTN: SLCMT-TML
1	SLCMT-IMA-V
1	SLCMT-PR
11	SLCMT-MEC, P. Blanas (COR)

U.S. Army Materials Technology Laboratory
Watertown, Massachusetts 02172-0001
SMART MATERIALS FOR ARMY STRUCTURES

Subramaniam Rammamurthy, Mukesh V. Gandhi
and Brian S. Thompson
Quantum Consultants, Inc.
Hannah Technology and Research Center
East Lansing, MI 48823

Technical Report MTL TR 92-29, April 1992, 197 pp
illus-tables, Contract DAAL04-91-C-0033,
Final Report

AD
UNCLASSIFIED
UNLIMITED DISTRIBUTION

Key Words

Composite materials
Smart materials
Electrorheological fluids
Fiber-optic sensors
Vibration
Piezoelectric materials

This final report documents the results of the research and development activities focused on the development of a new generation of smart structures incorporating embedded hybrid multiple actuation systems which capitalize on the diverse strengths of both electrorheological fluids and piezoelectric materials, and employ fiber-optic sensing systems. A state-of-the-art review of smart materials and structures technologies has been undertaken, and an in-depth critique of the current generation of actuators and sensors for smart structures applications has also been presented. An in-depth review of analytical, computational and experimental investigations on controlling the vibrational characteristics of beams, plates and a variety of prototype structural systems has also been undertaken. Furthermore, variational formulations for predicting the performance characteristics of smart structures featuring hybrid embedded piezoelectric and electrorheological domains have been successfully developed. These formulations will form viable bases for the development of finite element design tools for Phase II. A comprehensive library of smart structures and articulating mechanical systems applications has been developed and documented. The principal research findings distilled from these comprehensive set of investigations clearly indicate that it is possible to significantly tailor the vibrational and aeroelastic characteristics of structural and mechanical systems for US Army applications. Phase II will, therefore, be focused on the development of a US Army smart rotorcraft demonstrator system which will have the ability to autonomously tailor its vibrational and aeroelastic characteristics in response to variable service conditions while operating in unstructured environments. The rotorcraft system will also feature capabilities to detect and appropriately respond to routine service damage and/or battlefield damage by employing state-of-the-art optronic systems. Preliminary concepts for the design, development, fabrication, and testing of a smart US Army rotorcraft demonstrator have also been presented.

U.S. Army Materials Technology Laboratory
Watertown, Massachusetts 02172-0001
SMART MATERIALS FOR ARMY STRUCTURES

Subramaniam Rammamurthy, Mukesh V. Gandhi
and Brian S. Thompson
Quantum Consultants, Inc.
Hannah Technology and Research Center
East Lansing, MI 48823

Technical Report MTL TR 92-29, April 1992, 197 pp
illus-tables, Contract DAAL04-91-C-0033,
Final Report

AD
UNCLASSIFIED
UNLIMITED DISTRIBUTION

Key Words

Composite materials
Smart materials
Electrorheological fluids
Fiber-optic sensors
Vibration
Piezoelectric materials

This final report documents the results of the research and development activities focused on the development of a new generation of smart structures incorporating embedded hybrid multiple actuation systems which capitalize on the diverse strengths of both electrorheological fluids and piezoelectric materials, and employ fiber-optic sensing systems. A state-of-the-art review of smart materials and structures technologies has been undertaken, and an in-depth critique of the current generation of actuators and sensors for smart structures applications has also been presented. An in-depth review of analytical, computational and experimental investigations on controlling the vibrational characteristics of beams, plates and a variety of prototype structural systems has also been undertaken. Furthermore, variational formulations for predicting the performance characteristics of smart structures featuring hybrid embedded piezoelectric and electrorheological domains have been successfully developed. These formulations will form viable bases for the development of finite element design tools for Phase II. A comprehensive library of smart structures and articulating mechanical systems applications has been developed and documented. The principal research findings distilled from these comprehensive set of investigations clearly indicate that it is possible to significantly tailor the vibrational and aeroelastic characteristics of structural and mechanical systems for US Army applications. Phase II will, therefore, be focused on the development of a US Army smart rotorcraft demonstrator system which will have the ability to autonomously tailor its vibrational and aeroelastic characteristics in response to variable service conditions while operating in unstructured environments. The rotorcraft system will also feature capabilities to detect and appropriately respond to routine service damage and/or battlefield damage by employing state-of-the-art optronic systems. Preliminary concepts for the design, development, fabrication, and testing of a smart US Army rotorcraft demonstrator have also been presented.

U.S. Army Materials Technology Laboratory
Watertown, Massachusetts 02172-0001
SMART MATERIALS FOR ARMY STRUCTURES

Subramaniam Rammamurthy, Mukesh V. Gandhi
and Brian S. Thompson
Quantum Consultants, Inc.
Hannah Technology and Research Center
East Lansing, MI 48823

Technical Report MTL TR 92-29, April 1992, 197 pp
illus-tables, Contract DAAL04-91-C-0033,
Final Report

AD
UNCLASSIFIED
UNLIMITED DISTRIBUTION

Key Words

Composite materials
Smart materials
Electrorheological fluids
Fiber-optic sensors
Vibration
Piezoelectric materials

This final report documents the results of the research and development activities focused on the development of a new generation of smart structures incorporating embedded hybrid multiple actuation systems which capitalize on the diverse strengths of both electrorheological fluids and piezoelectric materials, and employ fiber-optic sensing systems. A state-of-the-art review of smart materials and structures technologies has been undertaken, and an in-depth critique of the current generation of actuators and sensors for smart structures applications has also been presented. An in-depth review of analytical, computational and experimental investigations on controlling the vibrational characteristics of beams, plates and a variety of prototype structural systems has also been undertaken. Furthermore, variational formulations for predicting the performance characteristics of smart structures featuring hybrid embedded piezoelectric and electrorheological domains have been successfully developed. These formulations will form viable bases for the development of finite element design tools for Phase II. A comprehensive library of smart structures and articulating mechanical systems applications has been developed and documented. The principal research findings distilled from these comprehensive set of investigations clearly indicate that it is possible to significantly tailor the vibrational and aeroelastic characteristics of structural and mechanical systems for US Army applications. Phase II will, therefore, be focused on the development of a US Army smart rotorcraft demonstrator system which will have the ability to autonomously tailor its vibrational and aeroelastic characteristics in response to variable service conditions while operating in unstructured environments. The rotorcraft system will also feature capabilities to detect and appropriately respond to routine service damage and/or battlefield damage by employing state-of-the-art optronic systems. Preliminary concepts for the design, development, fabrication, and testing of a smart US Army rotorcraft demonstrator have also been presented.

U.S. Army Materials Technology Laboratory
Watertown, Massachusetts 02172-0001
SMART MATERIALS FOR ARMY STRUCTURES

Subramaniam Rammamurthy, Mukesh V. Gandhi
and Brian S. Thompson
Quantum Consultants, Inc.
Hannah Technology and Research Center
East Lansing, MI 48823

Technical Report MTL TR 92-29, April 1992, 197 pp
illus-tables, Contract DAAL04-91-C-0033,
Final Report

AD
UNCLASSIFIED
UNLIMITED DISTRIBUTION

Key Words

Composite materials
Smart materials
Electrorheological fluids
Fiber-optic sensors
Vibration
Piezoelectric materials

This final report documents the results of the research and development activities focused on the development of a new generation of smart structures incorporating embedded hybrid multiple actuation systems which capitalize on the diverse strengths of both electrorheological fluids and piezoelectric materials, and employ fiber-optic sensing systems. A state-of-the-art review of smart materials and structures technologies has been undertaken, and an in-depth critique of the current generation of actuators and sensors for smart structures applications has also been presented. An in-depth review of analytical, computational and experimental investigations on controlling the vibrational characteristics of beams, plates and a variety of prototype structural systems has also been undertaken. Furthermore, variational formulations for predicting the performance characteristics of smart structures featuring hybrid embedded piezoelectric and electrorheological domains have been successfully developed. These formulations will form viable bases for the development of finite element design tools for Phase II. A comprehensive library of smart structures and articulating mechanical systems applications has been developed and documented. The principal research findings distilled from these comprehensive set of investigations clearly indicate that it is possible to significantly tailor the vibrational and aeroelastic characteristics of structural and mechanical systems for US Army applications. Phase II will, therefore, be focused on the development of a US Army smart rotorcraft demonstrator system which will have the ability to autonomously tailor its vibrational and aeroelastic characteristics in response to variable service conditions while operating in unstructured environments. The rotorcraft system will also feature capabilities to detect and appropriately respond to routine service damage and/or battlefield damage by employing state-of-the-art optronic systems. Preliminary concepts for the design, development, fabrication, and testing of a smart US Army rotorcraft demonstrator have also been presented.